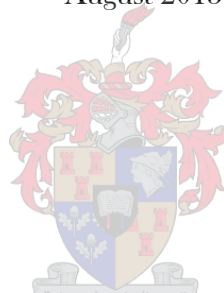


The role of ergothioneine in mycobacteria

CARINE SAO EMANI

Dissertation presented for the degree of Doctor of Philosophy in the department of
Biomedical Sciences, Division of Molecular Biology and Human Genetics, Faculty of
Medicine and Health Sciences of Stellenbosch University
August 2015



Promoter: Dr Bienyameen Baker

Co-promoters: Dr Monique Joy Williams and Prof Ian Johannes Wiid

Declaration

By submitting this dissertation electronically, I declare that the entirety of the work contained therein is my own, original work, that I am the sole author thereof (save to the extent explicitly otherwise stated), that reproduction and publication thereof by Stellenbosch University will not infringe any third party rights and that I have not previously in its entirety or in part submitted it for obtaining any qualification.

I declare that the experiments performed in this study have been ethically approved. Ethical number: N07/09/195

Summary

Glutathione (GSH) is a well-known anti-oxidant that prevents cellular damage caused by oxidative stress. It is synthesized by most eukaryotes but not by actinomycetes amongst which mycobacteria. However, mycobacteria synthesize two other thiols namely Mycothiol (MSH) and Ergothioneine (ERG). The role of MSH has been extensively investigated in mycobacteria and it has been shown that it protects mycobacteria from oxidative stress. However, MSH-deficient *M. tuberculosis* mutants have no growth defect *ex vivo* neither *in vivo* which indicates that MSH deficiency is compensated for. On the other hand, many studies have demonstrated the anti-oxidative role of ERG in eukaryotes but little is known of the role of ERG in mycobacteria. Recently, the enzymes involved in ERG biosynthesis have been identified. This enabled us to investigate the role of ERG in mycobacteria specifically *M. tuberculosis*. To achieve that we first generated an ERG deficient single mutant and an ERG/MSH deficient double mutant in *M. smegmatis*, a non-pathogenic fast growing mycobacteria used as a surrogate for *M. tuberculosis*. This was achieved by deleting the gene coding for the first enzyme involved in ERG biosynthesis (EgtD) in a wild type strain of *M. smegmatis* and a related MSH-deficient strain of *M. smegmatis*. Then we tested the susceptibility of the resulting mutants to oxidative stress, nitrosative stress and anti-tuberculosis drugs. We could show that ERG protects *M. smegmatis* from oxidative stress and that it compensates for MSH-deficiency in *M. smegmatis*. Then we investigated the role of ERG in *M. tuberculosis*. To achieve that, we generated mutants deficient in ERG biosynthetic enzymes, namely EgtA, EgtB, EgtC, EgtD and EgtE, a MSH-deficient single mutant and a MSH/ERG-deficient double mutant. Ergothioneine quantification in these mutants revealed that EgtE is not essential for ERG biosynthesis and may not be the only enzyme that catalyses the last step of ERG biosynthesis. On the other hand, though EgtB is essential for ERG biosynthesis, it may not be an ideal drug target since the loss of EgtB caused the accumulation of gamma glutamyl cysteine which potentially protected the mycobacteria from oxidative and nitrosative stress. The enzyme EgtC as well may not be an ideal drug target since the mutant deficient in this grew slightly better than the wild type during the exponential phase. The enzymes EgtA and EgtD could be the ideal drug targets since deleting the gene coding for these enzymes did not favour the survival of the resulting mutants under stress conditions. In addition, we were able to show that every CDC1551 ERG-deficient mutant generated in this study grew poorly during stationary phase. This indicates the

potential protective role of ERG in dormant mycobacteria during latent tuberculosis. In addition; we have shown that ERG is secreted by mycobacteria (*M.smegmatis*, *M.bovis* and *M.tuberculosis*). This finding is an indication of the imperative role of ERG during infection. Taking into account the ability of ERG to modulate immune responses, it is possible that *M.tuberculosis* secretes it during infection to suits its survival and proliferation within the host.

Opsomming

Glutatioon (GSH) is 'n welbekende antioksidant en beskerm teen radikaal selskade as gevolg van oksidatiewe stres. Dit word in die meeste eukariote vervaardig maar nie deur aktinomyces nie en waaronder mycobakterieë ook resorteer. Mycobakterieë vervaardig egter twee ander tione naamlik mycothiol (MSH) en ergothioneine (ERG). Die rol wat MSH in mycobakterieë speel is reeds goed bestudeer waar dit bewys is dat MSH mycobakterieë beskerm teen oksidatiewe stres. MSH tekort *M.tuberculosis* (*M. tuberculosis*) mutante toon geen groei afwykings ex vivo of in vivo nie wat daarop dui dat die MSH tekort op 'n ander manier voor gekompenseer word. In vele studies is dit reeds aangetoon dat ERG 'n antioksidatiewe rol speel in eukariote maar baie min is bekend omtrent ERG se rol in mycobakterieë. Onlangs is die ensiemstelsel betrokke by die biosintese van ERG geïdentifiseer wat ons in staat gestel het om die rol van ERG in mycobakterieë en spesifiek *M. tuberculosis* te ondersoek. Om dit te kon bereik is eerstens 'n ERG enkelmutant in *M.smegmatis* geskep, gevolg deur 'n ERG/MSH dubbelmutant. Mutante is eers in *M.smegmatis* geskep en daarna in *M. tuberculosis* om tegnieke te standardiseer en ook omdat *M.smegmatis* 'n nie-patogeniese model is vir *M.tuberculosis* studies. Mutante is geskep deur die uitskakeling van die geen wat vir die eerste stap van ERG biosintese verantwoordelik is (EgtD) in *M.smegmatis* en ook in 'n MSH tekort mutant van *M.smegmatis*. Hierna is die mutante geëvalueer vir vatbaarheid vir oksidatiewe stres, stikstofradikaal stres en anti-tuberkulose middels. Ons kon aantoon dat ERG in *M.smegmatis* 'n beskermingsfunksie het teen oksidatiewe stres en dat ERG kompenseer vir MSH tekort in *M.smegmatis*. Om die rol van ERG in *M.tuberculosis* te bestudeer is mutante geskep wat 'n tekort het aan ensieme in die ERG biosintese pad nl. EgtA, EgtB, EgtC, EgtD, EgtE, 'n MSH tekort en 'n MSH/ERG dubbelmutant. Kwantifisering van ERG in hierdie mutante het getoon dat EgtE nie belangrik

is vir ERG biosintese nie en is moontlik dat dit deur n ander ensiem vervang word vir die finale stap in ERG biosintese in *M. tuberculosis*. Alhoewel EgtB essensieel is vir ERG biosintese sal dit nie 'n goeie middekteiken wees nie aangesien die verlies aan EgtB die akkumulاسie van gamma-glutamiel sisteien tot gevolg het wat op sy beurt weer mycobakterieë teen oksidatiewe stres beskerm. Die ensiem EgtC is moontlik ook nie 'n goeie middekteiken nie omdat *M. tuberculosis* mutante van EgtC effens beter gegroei het in die eksponensiële fase in vergelyking met die intakte kontrolestam. Daarteenoor sal EgtA en EgtD beter middekteikens wees omdat *M. tuberculosis* mutante wat tekorte het aan hierdie ensieme baie sensitief was vir en moeilik oorleef het onder oksidatiewe toestande. Ons kon ook aantoon dat elke CDC1551 ERG mutant, wat in hierdie studie gegenereer is, baie swak groei getoon het in die stasionêre groeifase. Dit is 'n sterk aanduiding van die potensiële beskermings rol wat ERG kan speel in dormante *M. tuberculosis* gedurende sluimerende tuberkulose.

Presentations and Publications

Poster presentation at Stellenbosch University Faculty of Health Sciences Annual Academic

Day 2011: **Generation of *Mycobacterium smegmatis* and *Mycobacterium tuberculosis* single mutants deficient in ergothioneine and double mutants deficient in both mycothiol and ergothioneine.** C SAO EMANI, B BAKER, I WIID, MJ WILLIAMS

Oral presentation at Stellenbosch University Faculty of Health Sciences Annual Academic

Day 2012: **The role of Ergothioneine in Mycobacteria.** C SAO EMANI, MJ WILLIAMS, IJ WIID, B BAKER

Poster presentation at the EMBO Tuberculosis 2012: Biology, Pathogenesis, Intervention Strategies Conference held at the Pasteur Institute, Paris, France, 11-15 September 2012

The role of ergothioneine in the physiology of *Mycobacterium smegmatis*

C SAO EMANI, MJ WILLIAMS, IJ. WIID, B. BAKER

Poster presentation at Stellenbosch University Faculty of Health Sciences Annual Academic

Day 2014: **Ergothioneine is secreted by slow growing mycobacteria**

C SAO EMANI, MJ WILLIAMS, IJ. WIID, B. BAKER

Oral/Poster to be presented in August 2015 at the Annual Academic Day of Stellenbosch University:

Investigation of the role of Ergothioneine in *Mycobacterium tuberculosis*

C SAO EMANI, MJ WILLIAMS, I. WIID, B. BAKER

PUBLICATION:

Ergothioneine is a secreted antioxidant in *Mycobacterium smegmatis*

Antimicrobial Agents Chemotherapy. 2013, 57(7):3202. DOI: 10.1128/AAC.02572-12.

CARINE SAO EMANI, MONIQUE J. WILLIAMS, IAN J. WIID, NICHOLAS F. HITEN, ALBERTUS J. VILJOEN, RAY-DEAN D. PIETERSEN, PAUL D. VAN HELDEN, BIENYAMEEN BAKER

POTENTIAL PULICATIONS:

1. The role of ergothioneine biosynthetic enzymes in the production of ergothioneine and in the physiology of *Mycobacterium tuberculosis*
2. The role of ergothioneine in relation to mycothiol in *Mycobacterium tuberculosis*

Acknowledgement

Thank you Lord **JESUS CHRIST**, you have been my strength even when I was weak, exhausted or overwhelmed; my hope when I was in despair. My guide, when I did not know what to do. I kept going because of you JESUS, thank you Lord for always being there for me, even when no one else was. Let your name be glorified in all my achievements. Thank you Lord

Thank you Mum (**Marie Sao**) and Dad (**Clement Sao**) for been the best parents one ever needs to succeed. Thank you Dad for bringing me up in a very strict and disciplinary manner, you made me believe in hard work and discipline which made who I am today. Thank you Mum for been that caring, lovely, mother that supports the dreams of her children at all cost. For all your prayers and fasting for me. You made lots of sacrifices to get me where I am. For that I will be forever grateful

Thank you **Arnold Sao**, my only brother for always being by my side, for always supporting me morally in everything I do and for believing in me, for always seeing me through a magnifying glass. Thank you for all the love and respect

Thank you, **Sylvie Sao** and **Chantal Sao** (my little sisters) for all your prayers and moral supports. Thank you **Sylvie** for your listening ears, for all the effort you took to understand my study in order to provide advice though you are not a scientist

Thank you **Tata Patience** (my lovely aunt) for believing in me. Every time I was at life's edge, I remembered your words "Carine, you will struggle yes; but you will make it". That kept me going. Thank you, Tata

Thank you, **Olive Dziko** and **Olivier Ngalieu** (my cousins) for your prayers for me. Yes the Lord has been taking good care of me in this foreign land

Thank you **Saskia Soysal** my dearest friend for always being the shoulder I could cry on when life was hitting me hard, when my experiments were frustrating. You've always been there for me in spite of the distance between us, even though you don't understand how this whole "research thing" works

Thank you dear **Katie Schoemann**, for all your spiritual, financial, moral support, for all these days where you had to sit to listen to my groan, prayed for me, and encouraged me. You are a blessing in my life. You fuel my life through your prayers. In line with that, I will love to thank every member of the **Belville Presbyterian Church** and especially **Patrick**

Dunn, Mandy Botsis and **Deirdre Hewett**, for your fervent prayers, your listening ears and encouraging words

Thank you **Marieta McGrath, Kennedy Tawanda Zvinairo** and **Caroline Pule** for all your moral supports

Thank you **Zenda Cuvillier** my friend, for those days you had to cook for me, just to make sure I had something to eat when I was completely plunged in my lab work, and for your listening ears and encouragements when I complained of the challenges I face on campus

Thank you **Roxanne Reed** and **Daniel Sauer** my friends; for bringing the fun in my monotonous research life, for making me realise that recreation is a good brain stimulant. Amazingly, it contributed a lot to my success

Thank you **Claudia Ntsapi** my friend, for always being that source of encouragement. You believed in me more than I did in myself. Knowing that, someone out there believes that I beat all odds kept me going

Thank you **Marvin Theys** and **Jonathan Brown** for being the friends I needed to share my last minutes PhD submission stress, fears and anxieties with; thank you for your listening ears, and sympathy

Thank you dear **Glenda Durrheim**, I felt welcome from the first day I ever stepped in this department and this was because of you. You are not only a well-organized co-ordinator, you are that lovely, caring mother who makes every student feel welcome, irrespective of their background, gender or race. You are the main reason I decided to further my studies in this department

Thank you **Pedro Fernandez** for all your encouragements, for believing that I could achieve great things, for believing that I could make it with flying colours. Thank you my mentor and friend

Thank you **William Haylett** for all the support we had for each other, all the experience we shared during this race, thank you for being my race buddy, thank you for all the encouragements and supports you gave me even when you reached the finishing line and I was still running. You inspired me to know that I can also make it, no matter what

Thank you **Melanie Grobbelaar**; you came in my life towards the end of my PhD. However, the gesture of kindness you showed to me will be forever engraved in my heart. Knowing that someone is willing to sacrifice the comfort of her bed any time at night just to give me a lift home when I work late in the lab; means a lot to me

Thank you **Danicke Willemse** and **Lynthia Paul** for being my troubleshooting buddies and for supporting me morally when experiments drove me insane

Thank you **Noorjahn Rawoot** for always giving me the opportunity to do my experiments in your laminar Flow cabinet when I was restricted to use the others

Thank you, **Vuyiseka Mpongoshe** and most especially **James Galant** for all the tricky scientific questions that stimulated my brain and pushed me to think like a scientist and be able to explain scientific knowledge; the fact that you came to me; to help you understand some scientific knowledge, meant a lot to me. It meant you believed in me, so I had to work very hard not to disappoint you. Even when I did not have an accurate answer, I had to keep searching and that made me a rational thinker. I would also want to thank you James, for the thesis writing tricks that you gave me

Thank you **Ray-Dean** for always being not only a moral support but a financial support when I'm financially low

Thank you **Albertus Viljoen** for being patient enough to teach me the basis of cloning.

Thank you dear **Paul Van Helden**, for always being my financial support without which I would not have had a place to stay, food to eat, in fact I would not have been able to further my studies. Thank you for making every student welcome to study in this department. Thank you too for all your encouragements, motivations, open-mindedness, and sincerity. You are the reason why I'm still in this department. You are an inspiration

Thank you to the **postgraduate office of Stellenbosch University** who supported me with a merit bursary to pay my fees during the last 3 years of my PhD

Thank you **Ian Wiid** for always being that father of the lab, who makes sure his children (students) have all they need to succeed. You spontaneously provide every possible means that will enable your students to succeed; I'm very grateful

Thank you **Bienyameen Baker** for your intellectual input in this study, encouragements and for believing in me, I'm very grateful

Thank you **Monique Williams** for making me a scientist, for framing and directing my reasoning and thinking to that of a scientist; I'm very grateful. Thank you also for your immense intellectual input in this study

Thank you **Gustav Styger** for believing that I can make it big, you inspired me when I had a low self-confidence, thank you as well for your technical help during the Southern blot analysis of the *M. tuberculosis* mutants and your intellectual input

Thank you **Leanie Kleynhans**, **Nelita Du Plessis** and **Lance Lucas** for your help in providing an alternative during the BSL3 crisis

Thank you to every other member of the **TBDrug lab**, to **Anwar Jardine**, **Peguy Lutete**, **Marianna De Kock** and **Irene Mardarowicz** (in the BSL3) for all your intellectual and technical support

Thank you **Nicholas F. Hiten** for your assistance in the LC-MS analyses; I'm very grateful for all the efforts you made to optimize the quantification of all the analytes, and for your patience and perseverance to make the analyses work. For going beyond working hours when you handled my samples

Thank you **Ronald Dreyer** for your assistance in the use of the BD FACSJazz,

Thank you **Andrea Gutschmidt** for your assistance in the use of the BD FACSCalibur

Thank you, **John Michie** for your teaching me the science of flow cytometry

Thank you **Ruzayda van Aarde** and **Victoria Pichler** for your technical support with genomic DNA extraction and Southern blotting

Thank you **Suereta Fortuin** and **Dominique Anderson** for your technical support with SDS-PAGE analysis

Thank you, **Yossef Av-Gay** and **Adrie Jc Steyn** for kindly donating the $\Delta mshA$ *M. smegmatis* mutant and the *CDC1551* strain.

Thank you to the **BEI resources**, who kindly donated the *CDC1551* transposon mutants, and to **Miracle** more particularly for her patience and kind collaboration during the shipment of the strains.

Thank you **Joey Gouws** and **Lineo Motopi** for your guide and help during the application of the mycobacteria import permit

Thank you **Rika van Dyk**; for all your assistance and guide during purchase of products and import of specimens

Thank you **Johan Coetzer** (Postgraduate coordinator); for all your encouragements, it meant a lot to me because it came from someone who does not know me personally

Thank you **Nico van Pittius** for all your help and guide during the registration on the ATTC website and application for mycobacterial strains import

Thank you **Gian Van der Spuy**; for your guide on how to use the program Prism for statistical analyses and your immense help when my referencing software crashed

Thank you **Frank Peiser** for making sure our computer is functioning properly

Thank you **Louise Botha** for the last minute thesis advice

Thank you **Tanya Parish**; for your valuable advice and guidance during the cloning process and the generation of the *M. tuberculosis* mutants

Thank you, **Catherine Vilchèze** and **William R. Jacobs, Jr** for kindly donating the *M. tuberculosis* wild type H37Rv and its $\Delta mshA$ mutant strain

Thank you **Rybniiker Jan Lars** and **Sala Claudia** for kindly donating the $\Delta iscS$ mutant

Thank you to the founders of Google (**Larry Page** and **Sergey Brin**) and the founders of Wikipedia (**Jimmy Wales** and **Larry Sanger**); these are helpful sources of information

Thank you to the **DST/NRF** Centre of Excellence for Biomedical Tuberculosis Research and the MRC Centre for Molecular and Cellular Biology for funding this study

“Don’t just do what you have to do to get by, but work heartily, as Christ’s servants doing what God wants you to do”. (Eph 6:6)

‘’But those who trust in the LORD will find new strength. They will soar high on wings like eagles. They will run and not grow weary. They will walk and not faint’’. (Is40:31)

ABBREVIATIONS

- ACN: Acetonitrile
- AR: Auramine-rhodamine
- AIDS: acquired immunodeficiency syndrome
- ADP: adenosine diphosphate
- AMP: adenosine monophosphate
- ATP: adenosine triphosphate
- BCG: Bacille Calmette-Guérin
- CFUs: colony forming units
- CuOOH: cumene hydroperoxide
- CBB: coomassie brilliant blue
- CFP-10: culture filtrate protein 10
- BLAST: Basic Local Alignment Search Tool
- DMNQ: dimethoxy-1, 4-naphthoquinone
- DNA: deoxynucleic acid
- DTT: dithiothreitol
- DEAE: diethylaminoethyl
- DETA/NO: Diethylaminetriamine nitric oxide adduct
- DCO: Double cross over
- EDTA: Ethylenediaminetetraacetic acid
- ERG: ergothioneine
- ETB: ethambutol
- ESAT6: early secretory antigen target 6
- ELISPOT: Enzyme-Linked ImmunoSpot
- g: gram(s)
- GGC: γ -glutamyl cysteine
- Grxs: glutaredoxins
- GSH: glutathione
- GS: glucose salt
- HIV: human immunodeficiency virus
- HPLC: high performance liquid chromatography
- IE: Intracellular ERG
- EE: Extracellular ERG
- IFN- γ : interferon-gamma
- IGRA: interferon gamma release assay
- IMP: inosine monophosphate
- INH: isoniazid
- Kan: kanamycin
- kd: kilodalton
- LB: Lurea-Bertani
- LC: liquid chromatography
- LC-MS: liquid chromatography tandem mass spectrometry
- MDR: multi-drug resistant
- MGIT: Mycobacteria growth indicator tube

- MIC: minimum inhibiting concentration
- mA: milliamperes
- ml: millilitre
- mm: millimetre
- M: molar
- mM: millimolar
- MS: mass spectrometry
- MSH: mycothiol
- MSSM mycothiol disulphide / oxidized mycothiol
- *M. tuberculosis*: *Mycobacterium tuberculosis* (*M. tuberculosis*)
- MW: molecular weight marker
- NADP: nicotinamide adenine dinucleotide phosphate
- NADPH: reduced nicotinamide adenine dinucleotide phosphate
- NNRTI: non-nucleoside-reverse-transcriptase-inhibitors
- nm: nanometre(s)
- NaCl: sodium chloride
- NO: nitric oxide
- OADC: Oleic acid Dextrose Catalase
- OD₆₀₀: optical density at 600nm path length
- PAGE: polyacrylamide gel electrophoresis
- PA: perchloric acid
- PI: propidium iodide
- PCR: polymerase chain reaction
- Pi: phosphate
- PRG: pyrogallol
- PZA: pyrazinamide
- RNA: ribonucleic acid
- RNS: reactive nitrogen species
- ROS: reactive oxygen species
- rpm: revolutions per minute
- RT: room temperature
- SAM: S-adenosylmethionine
- SDS: sodium dodecyl sulphate
- SCO: single cross over
- TAE: Tris acetate EDTA
- TBHP: Tert-butyl hydroperoxide
- TB7: Rv2654c
- TE: Tris-EDTA
- TEMED: N, N, N', N' -tetramethyl ethylene diamine
- TFA: trifluoroacetic acid
- TNF: tumour neucrosis factor
- Tris: 2-amino-2-(hydroxymethyl)-1,3-propandiol
- Trx: thioredoxin
- TST: Tuberculin skin test
- TDR-TB: totally drug resistant TB
- µl: micolitre
- µg: microgram

- μF : micofaraday
- US: upstream
- DS: downstream
- UV: ultraviolet
- w/v: weight per volume
- XDR-TB: extensively drug resistant TB
- X-gal: X-gal: 5-bromo-4-chloro-3-indolyl- β -D-galactopyranoside
- ZN: Ziehl-Neelsen

Table of content

CHAPTER 1: INTRODUCTION (LITERATURE REVIEW).....	19
1.1 Tuberculosis infection and transmission	19
1.2 Tuberculosis currently and treatment	20
1.3 Basic factors of tuberculosis control and eradication.....	21
<input type="checkbox"/> Diagnostic factors.....	21
<input type="checkbox"/> Therapeutic factors	22
1.4 The survival of Mycobacterium tuberculosis in adverse conditions	24
1.5 The protective role of thiols	26
<input type="checkbox"/> Thiols with cysteine as their core amino acid	26
<input type="checkbox"/> Thiols with histidine as their core amino acid.....	32
1.6 Rational of this study	36
CHAPTER 2: METHODOLOGY	39
2.1 Investigation of ERG secretion in <i>M. smegmatis</i> and <i>M.tuberculosis</i>	39
<input type="checkbox"/> ERG and MSH extraction and quantification in <i>M. smegmatis</i>	39
<input type="checkbox"/> Extraction and quantification of ERG, MSH, cysteine and hercynine in <i>M.tuberculosis</i>	39
<input type="checkbox"/> Mass spectrometry analysis of samples	40
<input type="checkbox"/> Evaluation mycobacteria membrane integrity	41
<input type="checkbox"/> Investigation of ERG transporter	43
2.2 Generation of <i>M. smegmatis</i> and <i>M.tuberculosis</i> mutants	43
<input type="checkbox"/> Methods used to mutate genes	43
<input type="checkbox"/> Generation the $\Delta egtD$ and the $\Delta mshA/egtD$ <i>M. smegmatis</i> mutant strains	46
<input type="checkbox"/> Generation of <i>M.tuberculosis</i> mutants	48
<input type="checkbox"/> Generation of complementation strains	53
<input type="checkbox"/> -Generation of the genetically complemented $\Delta egtD attB::pMV306D$ and $\Delta mshA/egtD attB::pMV306D$	53
<input type="checkbox"/> -Generation of <i>M.tuberculosis</i> complemented strains	53
2.3 Genotyping of the mutants.....	56
<input type="checkbox"/> Genotyping of <i>M.smegmatis</i> mutants	56
<input type="checkbox"/> Genotyping of <i>M.tuberculosis</i> mutants.....	58
2.4 Drug susceptibility testing of mutants.....	59
2.5 Growth curve of mutants	60
<input type="checkbox"/> Growth curve of <i>M.smegmatis</i> mutants	60
<input type="checkbox"/> Growth curve of <i>M. tuberculosis</i> mutants.....	60
2.6 Oxidative, acidic and nitrosative stress susceptibility testing of mutants.....	60
<input type="checkbox"/> Testing of <i>M.smegmatis</i> mutants	60
<input type="checkbox"/> Testing of <i>M. tuberculosis</i> mutants.....	61
2.7 SDS-PAGE analysis of the mutants	61
CHAPTER 3: THE ROLE OF ERGOTHIONEINE IN <i>Mycobacterium smegmatis</i>	64
3.1 <i>M. smegmatis</i> secretes ERG	65
3.2 EgtD is essential for ERG biosynthesis	68
3.3 ERG does not protect <i>M. smegmatis</i> from antibiotics.....	72
3.4 ERG protects <i>M. smegmatis</i> from oxidative stress	73

3.5 ERG does not protect <i>M. smegmatis</i> from nitrosative stress	76
3.6 Conclusion	76
CHAPTER 4: THE ROLE OF ERGOTHIONEINE IN <i>M.tuberculosis</i>	79
4.1 Slow growing mycobacteria secrete ERG	80
4.2 Ergothioneine biosynthetic genes are not essential in vitro	84
4.3 Deletion of ERG biosynthetic genes does not affect <i>M. tuberculosis</i> susceptibility to current anti-tuberculosis drugs	96
4.4 The enzyme EgtE is not essential for ERG biosynthesis	96
4.5 ERG is necessary for growth during the stationary phase	101
4.6 ERG deficiency does not affect <i>M. tuberculosis</i> susceptibility to in vitro stress ...	108
4.7 Conclusion	119
CHAPTER 5: FUTURE/CURRENT STUDIES	122
5.1 Final conclusion	122
5.2 Future studies: Quantification of ERG in the $\Delta iscS$ (<i>Rv3025c</i>) mutant	123
5.3 Future studies: Investigation of the role of ERG during dormancy	123
5.4 Future studies: Generation and characterization of $\Delta egtA$-<i>mshA</i>, $\Delta egtC$-<i>mshA</i> and $\Delta egtD$-<i>mshA</i> <i>M. tuberculosis</i> CDC1551 mutants	123
5.5 Future studies: Cytokine expression profile determination upon infection with ERG-deficient mutants	123
5.6 Future studies: Investigation of ERG transporter	124
5.7 Future studies: Investigation of ERG import	124
5.8 Future studies: Investigation of the role of EgtE in the metabolism of Tween80	124
5.9 Future studies: Deletion of <i>egtA</i>, <i>egtC</i> and <i>egtD</i> in H37Rv and characterization of the mutants	124
5.10 Future studies: Generation of $\Delta mshA$, $\Delta egtA$-<i>mshA</i>, $\Delta egtB$-<i>mshA</i>, $\Delta egtC$-<i>mshA</i> and $\Delta egtD$-<i>mshA</i> in H37Rv and characterization of the mutants	125
5.11 Future studies: Evaluation of total thiols content of ERG single and ERG/MSH double deficient mutants	125
5.12 Future studies: Measurement of the oxidative stress level of ERG single and ERG/MSH double deficient mutants by flow cytometry	125
5.13 Future studies: Investigation of the susceptibility of ERG and ERG/MSH deficient mutants to vitamin C	125
Appendix: Additional information and references	126
ADDITIONAL INFORMATION.....	126
References	130
Table of Figures	
Figure 1.1. Tuberculosis disease progression upon exposure.....	20
Figure 1.2 AhpC enzymatic detoxification of ROS and RNS in <i>M. tuberculosis</i> [57].....	26
Figure 1.3 Thiols with cysteine in their core	27
Figure 1.4 Mycothiol biosynthesis [90]	28
Figure 1.5 Mycothiol metabolism [97]	29
Figure 1.6 Thiols with histidine in their core.....	32
Figure 1. 7 Ergothioneine biosynthesis pathway suggested in 1962 [147].....	34
Figure 1. 8 Ergothioneine biosynthesis [149]	35

Figure 2.1 Two step homologous recombination event.....	45
Table 2.6 Primers used to generate the suicide plasmid and the complementation vector.....	46
Figure 2.2 Genomic alignment of the operon of genes coding for enzymes involved in ERG biosynthesis.....	48
Figure 2.3 Illustration of the Joint PCR technique used to design the complementation constructs	55
Figure 2.4 Illustration of broth micro-dilution.....	59
Figure 3.1 Characterization of <i>M. smegmatis</i> membrane integrity by flow cytometry	65
Figure 3.2 Detection of mycothiol in <i>M. smegmatis</i>	67
Figure 3.3 Colony PCR of the $\Delta egtD$ mutant.....	69
Figure 3.4 Validation of <i>egtD</i> deletion by Southern blotting	70
Figure 3.5 Growth curves of <i>M. smegmatis</i> strains	71
Figure 3.6 Relative quantification of mycothiol by LC-ESI-HRMS	72
Table 3.5 Anti-tuberculosis drugs MIC ($\mu\text{g/ml}$) of <i>M. smegmatis</i> strains.....	73
Figure 3.7 Survival of <i>M. smegmatis</i> mutants during in vitro oxidative stress	74
Figure 3.8 SDS PAGE of <i>M. smegmatis</i> cell extract	75
Figure 3.9 Survival of <i>M. smegmatis</i> strains to nitrosative stress generated by DETA/NO.....	76
Figure 4.1 Population distribution of <i>M. bovis</i> (first row), <i>M. tuberculosis</i> H37Rv (2 nd row) and <i>M. tuberculosis</i> CDC 1551 culture (3 rd row)	81
Figure 4.2 Restriction map of <i>M. tuberculosis</i> deletion constructs generated in this study	84
Figure 4.3 Screening PCR design of the unmarked mutants	85
Figure 4.4 Screening PCR of <i>egtA</i> mutant generated in CDC1551	86
Figure 4.5 Screening PCR of <i>egtB</i> mutant generated in CDC155 and H37Rv.....	86
Figure 4.6 Screening PCR of <i>egtC</i> mutant generated in CDC155.....	87
Figure 4.7 Screening PCR of <i>egtD</i> mutant generated in CDC155	87
Figure 4.8 Screening PCR of <i>egtE</i> mutant generated in H37Rv and CDC155.....	88
Figure 4.9 Screening PCR design of the marked mutants	88
Figure 4.10 Screening PCR of $\Delta mshA$, $\Delta egtB/mshA$ mutant generated in CDC1551	89
Figure 4.11 Southern blotting analysis of the CDC1551 $\Delta egtA$ mutant.....	90
Figure 4.12 Southern blotting analysis of <i>egtB</i> deletion in H37Rv $\Delta egtB$, CDC1551 $\Delta egtB$ and the <i>mshA/egtB</i> mutants.....	91
Figure 4.13 Southern blotting analysis of <i>egtC</i> deletion in the CDC1551 $\Delta egtC$ mutant.....	92
Figure 4.14 Southern blotting analysis of <i>egtD</i> deletion in the CDC1551 $\Delta egtD$ mutant.....	93
Figure 4.15 Southern blotting analysis of <i>egtE</i> deletion in H37Rv $\Delta egtE$ and CDC1551 $\Delta egtE$	94
Figure 4.16 Southern blotting analysis of <i>mshA</i> deletion in CDC1551 $\Delta mshA$ and the <i>mshA/egtB</i> mutant	95
Figure 4.17 Growth curve of CDC1551 <i>M. tuberculosis</i> mutants.....	103
Figure 4.18 Evaluation of the mutants' viability when grown without Tween80	108
Figure 4.19 Susceptibility of <i>M. tuberculosis</i> mutants to nitrosative stress generated by DETA-NO.....	110
Figure 4.20 Susceptibility of <i>M. tuberculosis</i> mutants to oxidative stress generated by CuOOH	112
Figure 4.21 Susceptibility of <i>M. tuberculosis</i> mutants to oxidative stress generated by PRG	113
Figure 4.22 Susceptibility of <i>M. tuberculosis</i> mutants to acidic stress (pH~4.5).....	114
Figure S 1 Gene deletion process.....	129

CHAPTER 1:
INTRODUCTION
(LITERATURE REVIEW)

CHAPTER 1: INTRODUCTION (LITERATURE REVIEW)

1.1 Tuberculosis infection and transmission

Tuberculosis (TB) is an infectious disease caused by *Mycobacterium tuberculosis* (*M. tuberculosis*) that was discovered in 1882 by Robert Koch. Around 460 BC, this disease was described by Hippocrates as the most common of the time [1]. *M.tuberculosis*, *M. bovis*, *M. Africanum*, *M. macroti*, *M. pinnipedii*, *M. caprae* and *M. canetti* are members of the *M. tuberculosis* complex and are all pathogenic [2]. Active TB is primarily manifested by a cough, loss of appetite, fever and chest abnormalities (observed by X-ray) in case of pulmonary TB. Extra-pulmonary TB develops when mycobacteria spread to other parts of the body such as the abdominal cavity, bladder, bones, pericardium, kidneys, brain, lymph nodes, spine, joints and reproductive system [3]. This may lead to fatigue, swelling, painful urination, brain damage, sterility etc. TB is transmitted either through inhalation of the bacilli from cough aerosols, ingestion of bacilli from milk of diseased cows, inoculation through the skin (very rare) or through the placenta from a diseased pregnant woman to the foetus. Some studies indicate that TB transmission is more likely to occur after a prolonged repeated exposure. Using a model they indicated that constant travelling in minibuses (usually poorly ventilated), or long flights contribute enormously to the spread of pulmonary TB [4-6]. But this remains to be shown in other settings. It has been speculated using a model that transmission may also depend on the environment, type of activity (usually the commuter population), and also on the size of the household [7]. Approximately 30% of individuals get infected after exposure (depending on the inhaled bacillary load, the competency of the immune system, the state of the inhaled mycobacteria) [8], then 5 to 10 % of these develop disease (primary TB). In the remaining 90%, in 10% the immune system eradicates the mycobacteria, and the remaining 90% of cases, the mycobacteria may escape the host defence activities and remain dormant in old lesions. In this latter case, some develop disease after 5 years, some during their life time (HIV co-infection) and others when they age (≥ 65), this is known as post-primary TB (latent TB) and occurs in low endemic countries (figure 1.1). Post primary TB is usually caused by re-infection of individuals by a new strain or reactivation of the dormant bacilli due to immune suppression [9, 10]. Primary TB occurs as

a result of either HIV co-infection or immune suppression by medications, other diseases, renal dysfunction, stress, malnutrition or cancer.

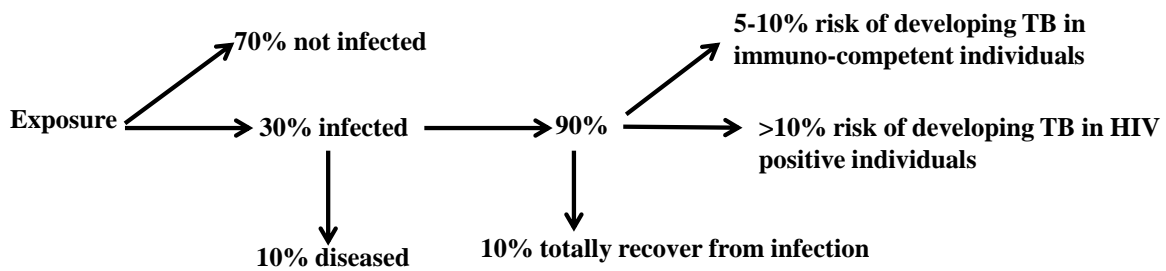


Figure 1.1. Tuberculosis disease progression upon exposure
Seventy percent of individuals are usually not infected upon exposure

1.2 Tuberculosis currently and treatment

Today, TB cases are increasing, with an average of 2 million deaths annually. The current drug regimen consists of combination of Isoniazid and Rifampicin which last to 6 months. In 2010, the highest rate of multidrug-resistant tuberculosis (MDR-TB, resistance to at least 2 first line drugs namely rifampicin and isoniazid) was recorded and extensive drug resistant tuberculosis (XDR-TB, which are MDR that are resistant to the most effective second line drugs (fluoroquinolones) and at least one injectable second line drug (capreomycin, amikacin or kanamycin, [11]) cases were detected in 58 countries [12]. There are 27 high burden countries for MDR-TB. These are countries with at least 4000 MDR cases a year and/or where MDR constitute at least 10% of newly registered TB cases. In 2011, there was an estimate of 10085 notified cases of MDR TB in South Africa. In 2012, there was an estimate of about 170000 deaths from MDR TB and 450000 new cases of MDR-TB worldwide. More than 10 million children were orphaned due to TB. In 2013, there were an estimated 9 million new cases of TB and 1.5 million deaths amongst which 1.14 million were HIV negative while 360 000 were HIV positive people. Most of the new cases occurred in Asia (56%) and the African Region (29%) amongst which 0.55 million were children and 3.3 million women, while 1million were co-infected with HIV. An estimated 480 000 people had developed MDR-TB while an estimated 9% of these had XDR-TB. South Africa is amongst the six countries with the largest numbers of newly reported TB cases in 2013 (~0.45 million) and is the country with the largest numbers of new TB cases per 100 000 population (860) [13]. Amongst children there were an estimated 550 000 cases and 80 000 deaths of HIV negative children. An estimate of TB deaths in HIV positive children is not yet available [14]. Totally

drug resistant tuberculosis (TDR) for which no effective treatments are available is becoming a major threat [15].

1.3 Basic factors of tuberculosis control and eradication

HIV co-infection, the rapid emergence of MDR-TB, overcrowded hospitals in the third world, rapid increase of population density, drug abuse, destructive life styles, inaccurate or delayed diagnoses are the main hindrances of TB control. A few of these factors are discussed below.

- **Diagnostic factors**

Diagnosis of TB plays an essential role in its transmission and spread [7]. An inappropriate diagnosis of tuberculosis, will lead to a wrong prescription of the drug combination regimen and consequently acquisition of drug resistance. A diagnostic test that will be very quick (to minimize transmission, disease spread), determine the type of infection (active or latent), the drug resistance pattern of the patient strain (to enable the right drug regimen) will be ideal. The current diagnostic tools are: microscopy detection of the mycobacteria in sputum samples, solid culture of the specimen, tuberculin skin test (TST), molecular based techniques and interferon gamma release assays.

There are two main microscopy tools that enable detection of acid fast bacilli such as *M. tuberculosis* in sputum. These are based on two staining methods: the ziehl-neelsen (ZN) method and the auramine-rhodamine (AR) method.

The ziehl-Neelsen principle is based on counter staining the sample with carbol fuchsin and methylene blue. This will enable distinction between the pink acid fast bacilli from the blue non-acid fast bacilli under the microscope. Because of the low sensitivity of the ZN based microscopy, it was subsequently replaced by the AR based fluorescence microscopy. AR was shown to be less specific than ZN, however it is more sensitive. Acid fast bacilli fluoresce red-yellow under microscopy. However, microscopy based diagnosis is less sensitive in case of HIV co-infection, and is not appropriate in paediatric diagnosis due to the fact that children can't expel sputum [16, 17].

The original culture based diagnosis involves plating the samples on solid media containing selective reagents such as malachite green and antibiotics such as ampicillin and nalixidic acid that prevent the growth of bacteria other than *M. tuberculosis*. It is a slow technique as it takes 8 weeks for visible growth of the bacteria [18, 19]. However, faster technologies have

been developed. These include the BATEC system (quick automated radiometric detection of *M. tuberculosis* in a liquid medium) [20] and the MGIT system (quick automated fluorescence based detection of *M. tuberculosis*) [21]. However, the equipment used in these techniques is very expensive and therefore not readily available in developing countries.

The tuberculin skin test (TST) (Mantoux test, heaf test, tine test) involves injecting intradermally a purified protein derivative tuberculin (glycerol extract of tubercle bacillus) that will cause an immune reaction displayed as an induration on the site of injection of the skin of the patient. Diagnosis is based on the size and diameter of the induration. TST reliability is affected by infection by other mycobacteria or by calmette Guerin vaccine with *Mycobacterium bovis*, (in this case, false TB positive results are predominant) [22-24]. Radiographic examinations of the chest to detect visible lesions are used for the diagnosis of TB as well. However, diseases such as sarcoidosis that affect lungs and HIV co-infection make chest radiography not reliable [25]. Interferon gamma release assay (IGRA) (QuantiFERON-TB Gold, T-SPOT.TB and ELISPOT (Immunotec, UK)) measures the quantity of interferon gamma produced in the serum of the patient as a result of stimulation with ESAT 6 and CFP 10 antigens. However, members of the *M. tuberculosis* complex such as *Mycobacterium marinum*, or *Mycobacterium szulgai*, or *Mycobacterium kansasii* share 3 common proteins: CFP10, TB7 and ESAT6. Therefore the specificity of IGRA is questionable.

Molecular based diagnoses involve the detection the *M. tuberculosis* DNA molecule in the patient sample. There are several molecular based diagnostic methods available currently with the new rapid fully automated test known as GeneXpert MTB/RIF which enable the detection of rifampicin resistant strains [26, 27]. However, no molecular tests are able to differentiate DNA molecules from dead mycobacteria (or from latent mycobacteria) from DNA of actively growing mycobacteria. Therefore they are usually performed only on TST positive patient samples [28, 29].

- **Therapeutic factors**

A combination of isoniazid (INH), rifampicin (RIF), pyrazinamide (PZN), streptomycin, and ethambutol (ETB) is the current standard regimen for active cases of drug susceptible TB [30]. This treatment is cumbersome and lengthy (6 to 9 months) increasing the probability of poor compliance and consequently, rapid emergence of drug resistant TB cases. Therefore, there is a need for drugs that could be taken in lower quantities and which can efficiently

achieve TB treatment within a shorter period. This could be preferably drugs that can destroy latent bacilli since it was shown that dormant bacilli were less sensitive to some drugs like isoniazid [31, 32].

On the other hand, toxicity of the second line drugs considerably impedes the eradication of MDR and XDR TB, Aminoglycosides are nephrotoxics and ototoxics, while ethionamide is hepatotoxic and gatifloxacin may cause dysglycemia [11, 33].

HIV co-infection is another factor. In this case, the patient's immune system is not only compromised and therefore favours the spread of the infection throughout the body, but also the TB therapy may interfere with the antiretroviral therapy. One common case is the decrease of therapeutic concentration in the body of any drugs (including HIV protease inhibitors) co-medicated with Rifampicin. This is because Rifampicin causes an up-regulation of hepatic cytochrome (CYP) p450 oxidase system expression which as a result induces a higher metabolism [34]. On the other hand, retonavir is usually administered to inhibit CYP450, in order to increase the intracellular level of the antiretroviral drug to meet the therapeutic dose. However, when taken with rifampicin in case of TB co-infection, it would favour the increase of Rifampicin beyond the therapeutic dose and therefore expose the patient to Rifampicin toxicity [35]. Diabetes has become another major factor. Diabetes does not only promote the development of active TB [36], but also increases the risk of MDR development because it slows the response to TB treatments [37, 38]. Though it is well known that diabetes suppresses the cell-mediated immunity, no biological link has been established between diabetes and TB. It was proposed that this results from the effect hyperglycaemia and cellular insulinopenia on macrophages; leading to a diminish capacity of containing mycobacteria. This speculation was supported by the finding showing that 90% diabetic's mice relatively to 10% of normal mice died after challenging with tuberculosis. To support this finding, it was shown that aveolar macrophage of diabetic patient were less activated and produced less hydrogen peoxide [39]. Therefore further investigation into this peculiar effect of diabetes on TB disease progression is required, and in so doing enabling the development of new drugs for these cases.

In view of all these, there is an urgent need for the development of new anti-TB drugs. An ideal regimen would enable a brief therapy, decreased dosage, would target dormant bacilli, and would be effective in TB in diabetic patient cases and in HIV-co-infected individuals without interfering with their HIV regimen. But since RIF was approved, only 2 anti-TB

drugs (Rifanbutin and Rifapentine) were approved in the USA and other countries 38 years later [40, 41]. The inability to find a suitable inhibitor once a target has been validated; to convert any target inhibitor into a stable derivative able to cross the complex mycobacterial cell wall is one of the many obstacles in drug development.

1.4 The survival of *Mycobacterium tuberculosis* in adverse conditions

As mycobacteria enter the alveolar space, the immune system reacts through two main defensive mechanisms. In an oxygen dependent mechanism, upon phagocytosis of mycobacteria by macrophages, the oxygen intake of macrophages generate a respiratory burst leading to the formation of oxidants (superoxide, hydrogen peroxide, free radicals) toxic to both the macrophages and the mycobacteria [42, 43]. In addition, Interferon gamma induces the production of nitric oxide by macrophages which is highly toxic to the mycobacteria [44]. In an oxygen-independent mechanism, lysozymes breakdown the cell wall, lactoferrin removes essential iron or charged proteins from the bacteria to damage it and hydrolytic enzymes and proteases digest the proteins [45, 46]. The myeloperoxidase enzyme secreted by neutrophil granules in the phagolysosome catalyses the reaction between chlorine and hydrogen peroxide (from the respiratory burst) to form hypochlorite, a very toxic compound to the cell [42, 47, 48]

In spite of the harsh conditions generated by the host immune system to kill invading mycobacteria, some do survive and multiply causing active disease (primary TB) or become dormant for several years (latent TB) in lesions known as granulomas [31, 49, 50]. However, these granulomas are composed of dead macrophages surrounded by fibroblasts. The dormant mycobacteria reside at the centre of the granuloma which is known to be hypoxic, containing nitric oxide, carbon monoxide and other toxic substances [51]. On the other hand, it was shown that the intracellular ATP levels were 5-6 times lower in dormant bacilli than in actively growing bacilli. In addition, these bacilli can use the anaerobic electron transport chain to generate proton motive force while *ndh-2* is responsible for the turnover of NAD^+ [52].

The host susceptibility to TB depends largely on its ability to destroy invading mycobacteria with ROS and RNS. This was proven when it was observed that NADPH oxidase deficient (NOX2) mice and iNOS (nitric oxide synthase) deficient mice were more susceptible to invading mycobacteria [53, 54]. Furthermore, children with chronic granulomatous disease (a disorder characterized by phagocytic oxidative bursts causing recurrent pyogenic infections)

are highly susceptible to TB and present complications during BCG vaccination [55] which further support the imperative role of ROS released by phagocytes to destroy *M. tuberculosis*. Therefore, investigating the mechanisms that enable *M. tuberculosis* to survive in harsh, adverse host conditions has been important. A clear understanding of the physiological elements that enable *M. tuberculosis* survival will be an avenue for the development of new drug targets against tuberculosis. Few studies have identified enzymes that may enable the mycobacteria to resist the oxidative burst generated by the macrophages during their first encounter. There are two families of enzymes associated with the detoxification of ROS in bacteria; the peroxiredoxin family and the Ohr/OsmC superfamily. Alkyl hydroperoxide reductase AhpC belongs to the peroxiredoxin family. It exists as two subunits AhpC and AhpF that are co-transcribed in some bacterial species[56]. While AhpC metabolises peroxynitrite, reduces hydrogen peroxide, alkyl hydroperoxides and organic peroxides into their corresponding alcohol, AhpF is a flavoprotein that reduces the oxidized AhpC at its NH₂-terminal cysteine residue using NADPH or preferably NADH [56, 57]. However, thioredoxin, or thioredoxin reductase/trypanredoxin, or trypanothione/trypanothione reductase or cyclophilin reduce the oxidized AhpC in bacteria lacking AhpF [58]. *M. tuberculosis* does not have any AhpF-like proteins[59] and neither does it use its thioredoxin/thioredoxin reductase to support the activity of AhpC. Instead, AhpD, coded by *ahpD* which is located 11 base pairs downstream of *ahpC* and contributes to the reduction of the oxidized AhpC in *M. tuberculosis*. Oxidized AhpD in turn reduced by SucB (dihydrolipoamide succinyltransferase) that is in turn reduced by Lpd (dihydrolipoamide dehydrogenase) using NADH [57] (Figure 1.2). There are three main classes of peroxide-sensing regulators, OxyR, PerR and Ohr. AhpC are regulated by a member of the LysR family of the OxyR sensing regulators [60]. The OxyR gene is inactivated in *M. tuberculosis* by multiple lesions conferring its sensitivity to INH [61].

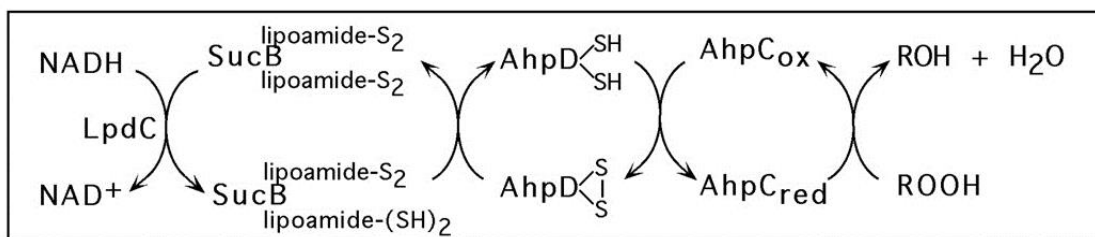


Figure 1.2 AhpC enzymatic detoxification of ROS and RNS in *M. tuberculosis* [57]

The ROS detoxifying enzyme AhpC can be reduced by AhpD which is dependent on SucB and NADH

The second ROS detoxification enzyme family Ohr/OsmC, constitute of organic hydroperoxide reductase (Ohr) first identified in *Xanthomas campestris* [62] and the osmotically inducible protein (OsmC) first identified in *E.coli* [63]. OsmC and Ohr are structurally and functionally similar [64-66]. They both are implicated in the protection of bacteria against organic peroxides [67-70]. However, OsmC is induced by ethanol and sodium chloride while Ohr is induced by organic peroxides [64, 71]. Ohr expression is regulated by the ohr regulator OhrR (suppressor) [60, 71]. *M. tuberculosis* on the other hand does not have Ohr but OsmC. The regulator of OsmC is not known and OsmC deficient *M. tuberculosis* mutants have not yet been characterized [67].

On the other hand, few proteins have been speculated to play a protective role in the dormant mycobacteria that reside in the hypoxic granuloma causing latent TB. *Rv3133 (devR)* was shown to be up-regulated in dormant mycobacteria and this gene is implicated in the induction of three other dormancy proteins namely, α -crystallin, *Rv2626c (hrp1)* and *Rv2623 (TB31.7)* known as the dosR (dormancy survival and regulation) which are able to regulate the expression of many other dormancy proteins in latent bacilli [72-77]. There are ten proteins shown to be up-regulated during dormancy known as the universal stress proteins (USP). Three are regulated by the dosR. However, mutants deficient in most of these proteins present no growth defect under in vitro stress conditions representing the macrophage environment, neither in mouse nor in human derived macrophage cell lines [78]. This is an indication that *M. tuberculosis* acquires a wide range of compensatory mechanisms in response to the host defence conditions.

1.5 The protective role of thiols

Thiols are compounds with a sulfhydryl group and their function is to maintain the redox balance of biological systems. There are two main types of thiols: Thiols with cysteine as their core amino acid and thiols with histidine as their core amino acid. However, it is worth mentioning the intracellular thiol 2-mercapto-ethanesulfonate (Coenzyme M).

- **Thiols with cysteine as their core amino acid**

Thiols with cysteine as their core amino acid are: the tripeptide glutathione (γ -L-Glutamyl-L-cysteinylglycine), the pseudoglucosaminidiasaccharide mycothiol (1-D-myo-inosityl-2-(N-acetyl-L-cysteinyl) amino-2-deoxy- R -D-glucopyranoside) and the bis-glutathionyl conjugate of spermidine trypanothione (Figure 1.3).

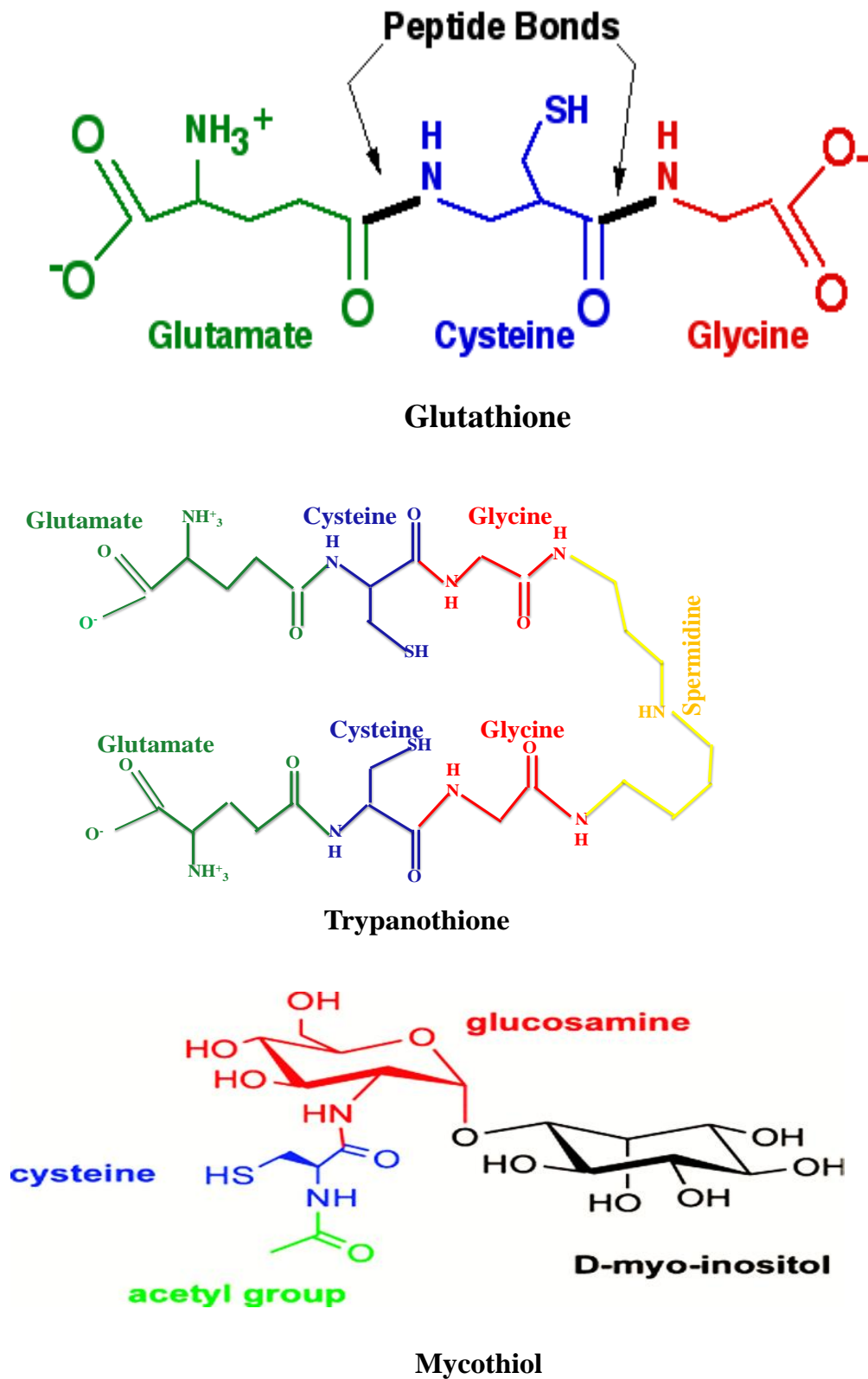


Figure 1.3 Thiols with cysteine in their core

Glutathione (GSH) is found in eukaryotes, gram negative bacteria, but not in gram positive bacteria [79, 80]. Elaborate studies of the role of glutathione have demonstrated the anti-oxidative role of GSH, its ability to function as a cofactor, and its involvement in the cellular maintenance of the redox system [81]. Trypanothione (TSH) is predominantly found in protozoa of the genera *Trypanosoma* and *Leishmania* the causative agents of trypanomiasis [82] and leishmaniasis respectively [83]. The inhibition of the biosynthesis of TSH or the reduction of the intracellular level of TSH affects the viability, virulence and the susceptibility to oxidative stress of protozoa, making trypanothione biosynthesis a potent drug target against Trypanomiasis and Leshmianiasis [84, 85]. On the other hand, mycothiol (MSH) is synthesized and abundant in streptomycetes and mycobacteria [80]. Glucose-6-phosphate (Glc-6-p) is the precursor of MSH biosynthesis. It is generated by myo-Inositol-1-phosphate synthase (Ino1). Then four other enzymes are involved in MSH biosynthesis: N-acetylglucosamine transferase (MshA) transfers N-acetylglucosamine (GlcNAc) from uridine diphosphate (UDP)-GlcNAc to myo-inositol to form GlcNAc-inositol [86], which is deacetylated by deacetylase (MshB) [87] and the resulting GlcN-inositol (GlcN-INS) is ligated by a ligase (MshC) [88] to cysteine and then acetylated by acetylase (MshD) [89] to form MSH (Figure 1.4).

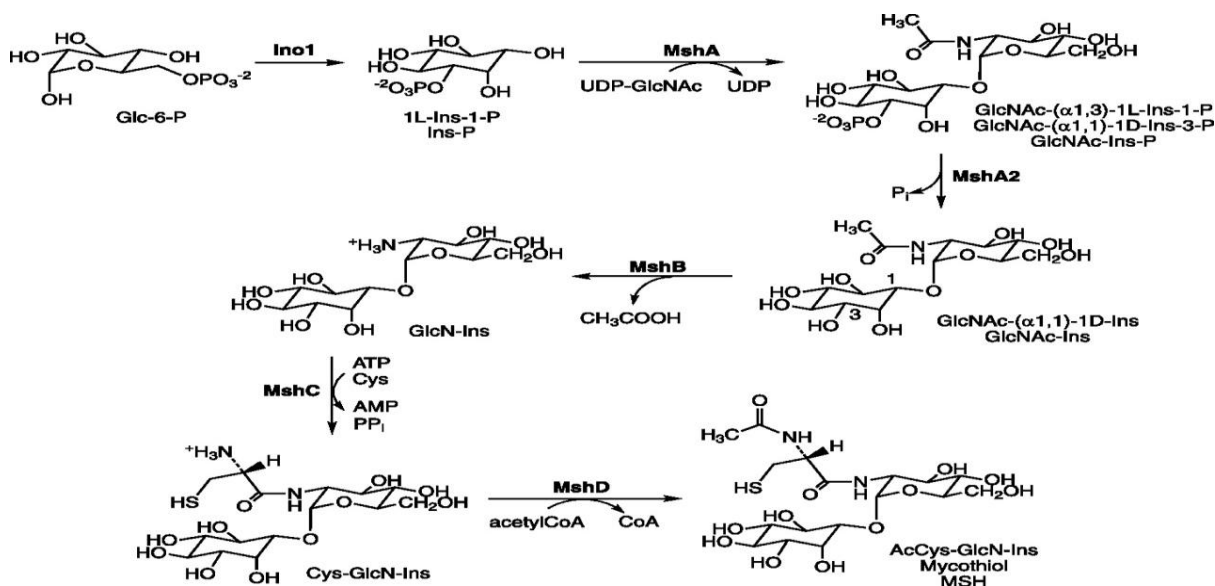


Figure 1.4 Mycothiol biosynthesis [90]

Glucose-6-phosphate (Glc-6-p) is the precursor of MSH biosynthesis. It is generated by myo-Inositol-1-phosphate synthase (Ino1). The enzyme MshA catalyses the transfer of GlcNAc and the dephosphorylation of GlcNAc-Ins-P

Then, in the presence of NAD/mycothiol-dependent formaldehyde dehydrogenase, MSH will detoxify formaldehyde resulting in an oxidized MSH known as mycothioldisulfide (MSSM)

which can be reduced by MSSM reductase (MTR) to MSH. Mycothiol can also form a conjugate (MSX) with toxic substances which will be degraded by MSH conjugate amidase (Mca) to glucosamine-myo-inositol (GlcN-Ins) and mercapturic acid derivatives (AcCysSR) which are excreted from the cell [91, 92]. In addition it was shown that MSH is involved in the biosynthesis of the antibiotic lincomycin A by *Streptomyces lincolnensis* where it serves as the sulphur donor involving the Mca-homologs LmbT, LmbV and LmbE [93]. In the detoxification of arsenate, MSH forms an arseno-MSH conjugate by the MSH-dependent arsenate reductase (ArsC1/C2) reduced in the mycoredoxin -1 (Mrx-1) /MSH/Mtr pathway [94]. In contrast, it can use another arsenate reductase (Cg_ArsC1) to detoxify arsenate through the thioredoxin (Trx) [95] pathway. Mycothiol can form a conjugate with monochlorobimane catalysed by MSH S-transferase (Mst) in *M. smegmatis*[96]. Mycothiol serves as a cofactor of enzymes involved in the detoxification of peroxides, electrophiles, nitric oxide and aromatic compounds (maleylpyruvate) such as MSH peroxidase (MpX), thiol peroxidase (Tpx) and one-cyst peroxidoxin (AhpE) [97]. It was shown that the formaldehyde dehydrogenase AdhE/FadH depends on MSH to detoxify formaldehyde. The mycothiol-dependent alcohol dehydrogenase (MscR), catalyses the detoxification of S-nitrosyl-mycothiol (MSNO) and formaldehyde as well [90]. Protein S-mycothiolation (of Tpx and Mpx) is induced under hypochlorite NaOCl stress [98]. The S-mycothiolated proteins are involved in carbohydrate metabolism, amino acid biosynthesis and nucleotides biosynthesis [97] (Figure 1.5).

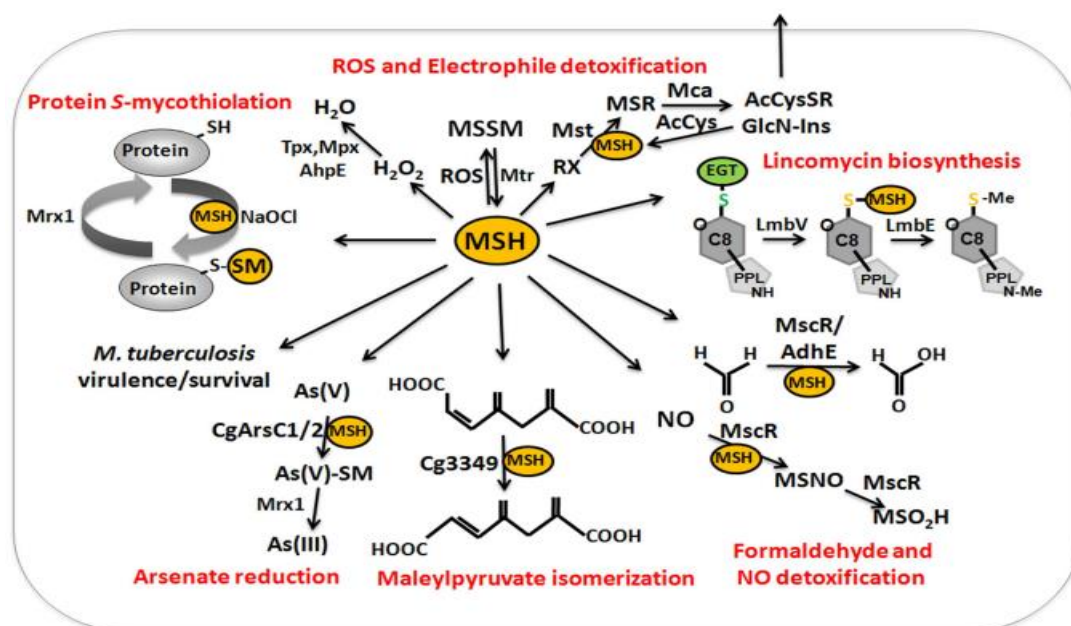


Figure 1.5 Mycothiol metabolism [97]

Mycothiols are involved in protein S-mycothiolation, in ROS and electrophile detoxification, in lincomycin biosynthesis, in maleylpyruvate isomerization and in arsenate reduction.

It has been shown that MSH-deficient *M. smegmatis* mutants produce a high level of Ohr [99, 100] indicating the role of Ohr in the protection of *M. smegmatis* from organic peroxides, this finding was supported when OhR (Ohr suppressor) deficient *M. smegmatis* were shown to be very sensitive to oxidative stress generated by organic peroxides [67]. Since *M. tuberculosis* does not have any homolog of Ohr, it is not known if MSH-deficient *M. tuberculosis* mutants produce a high level of OsmC, however studies indicate that mycobacteria acquire a wide range of compensatory protective mechanisms against oxidative stress in-vivo. An example is the Ohr-deficient *M. smegmatis* mutants which are highly susceptible to oxidative stress in vitro but had no growth defect ex-vivo [67]. While it was shown that *mshC* is essential in *M. tuberculosis* [101], *mshA*, *mshB*, *mshD* have been successfully deleted in *M. tuberculosis* [102, 103]. *M. tuberculosis* $\Delta mshA$ mutants are MSH-deficient [102] while $\Delta mshB$ and $\Delta mshD$ *M. tuberculosis* mutants produce a low but detectable level of MSH which indicates the possibility of compensatory enzymes with low activities [103, 104]. On the other hand, *M. bovis* $\Delta mshC$ and $\Delta mshA$ mutants produce no detectable level of MSH [105]. Mycothiol protects mycobacteria from oxidative stress and acidic stress making it a potent drug target against tuberculosis [104, 106, 107]. Though it was previously shown that $\Delta mshD$ Erdman mutant strain grew poorly within macrophages [103], it was however reported that H37Rv mutants $\Delta mshA$ mutants had no growth defect in immuno-competent mice neither in immuno-deficient [102] mice. *M. smegmatis* $\Delta mshA$ and $\Delta mshD$ mutants are sensitive to RIF but resistant to INH and ETH (Table 1.1). The *M. smegmatis* $\Delta mshC$ is susceptible to RIF, INH and ETH. The *M. smegmatis* $\Delta mshB$ is resistant to ETH and susceptibility to INH and RIF [108]. The $\Delta mshA$ and $\Delta mshC$ *M. bovis* mutants are resistant to INH and ETH [105]. The H37Rv frame shift spontaneous $\Delta mshA$ mutants are ETH and INH resistant. The CDC1551 $\Delta mshA$ deletion mutants are ETH and INH resistant. The H37Rv and Erdman strain $\Delta mshA$ deletion mutants are ETH resistant only [102]. The H37Rv $\Delta mshB$ mutants are sensitive to RIF and resistant to INH but their susceptibility to ETH has not been determined [104] (summary in Table 1.1). Therefore drugs targeting mycothiol may not be used in combination with INH.

Table 1.1 First line drug resistance profile of MSH-deficient mutants

Strains	<i>M. smegmatis</i>	<i>M. bovis</i>	<i>M. tuberculosis</i> (H37Rv)	<i>M. tuberculosis</i> (CDC1551)	<i>M. tuberculosis</i> (Erdman strain)
<i>mshA</i>	RIF-S*	ETH-R	ETH-R	ETH-R	ETH-R
	ETH-R*	INH-R	INH-R	INH-R	INH-S
	INH-R				
<i>mshB</i>	ETH-R	ND	INH-R	ND	ND
	RIF-S		RIF-S		
	INH-S				
<i>mshC</i>	RIF-S	ND	ND	ND	ND
	ETH-S				
	INH-S				
<i>mshD</i>	RIF-S	ND	ND	ND	ND
	ETH-R				
	INH-R				

***S: sensitive, R: resistant**

In contrast, it was shown that ETH hypersensitivity results from a gain of function mutation of the mono-oxygenase gene (*etaA*) (coding for an antioxidant) while ethionamide resistance resulted from an overproduction of the regulatory protein *EtaR* (which affects *EtaA* by down regulating its expression) [109]. But the level of *EtaR* has not been investigated in MSH deficient mutants, so it is not sure if MSH deficiency affects the production of *EtaR*. On the other hand it was shown that a mutation in the catalase-peroxidase gene (*KatG*) is associated with INH resistance [110]. The drugs INH and ETH are activated by *KatG* and *EthA* respectively but they both target the NADH-dependent enoyl-ACP reductase *InhA* [111]. Therefore it is expected that mycobacterial strains that are co-resistant to INH and ETH should harbour mutations in *inh* and or *ndh* (NADH dehydrogenase that indirectly affects *InhA* since it is NADH-dependent). On the contrary, it was shown that INH and ETH co-resistance could be associated with a mutation in *mshA* or *mshC* in *M. bovis*, *M. tuberculosis* and *M. smegmatis* [102, 105, 108]. In vitro experiments showed that MSH is involved in the activation of ETH by *EthA* but the exact mechanism is still unclear [102]. On the other hand, it was proven that INH resistance is observed in MSH-deficient mutants because of the increased production of *Ohr* since the *ohrR*-deficient *M. smegmatis* mutants are resistant to INH as well. Therefore INH resistance is observed in *M. smegmatis* because of the absence of the antioxidant that causes an increase of intracellular organic peroxides leading to an overproduction of *Ohr* which in turn inhibits INH activity [67]. It is not known if *Ohr* is

directly involved in the INH mode of action or if INH action is dependent on the regulation of enzymes that can reduce ROS. Because it was also observed that *M. smegmatis ahpC* mutants were sensitive to INH which may be due to an elevated expression of KatG in these strains [112]. This is an indication that drugs targeting MSH biosynthesis should not be used in combination with ETH or INH.

- **Thiols with histidine as their core amino acid**

The second group of thiols have a histidine core. These include Ovothiol (OSH) and ergothioneine (ERG) (Figure 1.6).

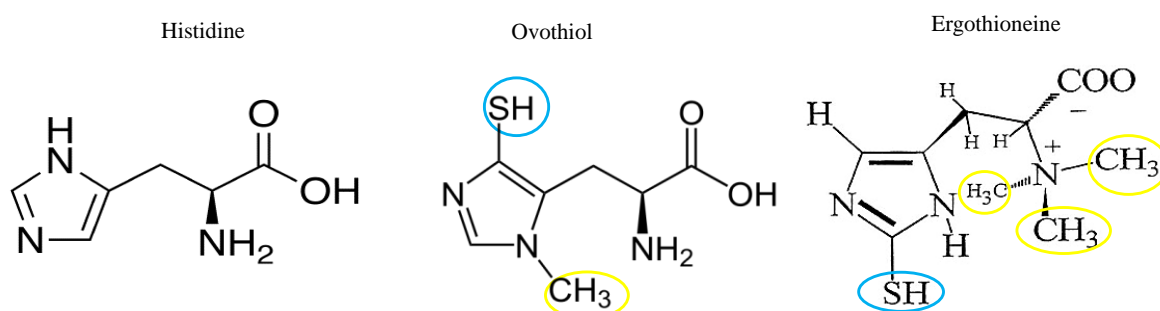


Figure 1.6 Thiols with histidine in their core

On the left is histidine; in the middle is ovothiol that differs from histidine by the extra sulphhydryl group (SH) (blue) and the methyl group (CH₃) (yellow) and on the right is ergothioneine that has the SH-group (blue), and three extra methyl groups (yellow).

Ovothiol has been identified in sea urchins [113], marine invertebrates [114] and the pathogenic Trypanosome and Leishmania [115]. There are 3 derivatives of OSH: OSH A, B and C. These are all π -N-methyl-5-thiohistidines and their highly acidic sulphhydryl group make them potent anti-oxidants [116]. Ergothioneine (2-mercapto histidine trimethyl betaine) was first identified in the ergot fungus in 1909 [117]. Plants absorb ERG through their roots from microorganisms in the soil. Ergothioneine is abundant in mushrooms, black beans, red beans and oat bran [118]. Ergothioneine is synthesized by fungi and actinomycetes but not in animals. Ergothioneine is ingested from food by animals; and is distributed in various tissues [119-121]. Ergothioneine is found in the seminal fluid [122], ocular tissues [123], in the plasma (where it is bound to specific proteins) [121], brain [124, 125], fibroblasts [126], myocardiocytes [127], bone marrow, cord blood, foetal liver, trachea ileum, kidney and peripheral leukocytes [128]. Ergothioneine is transported into these cells via An organic cation transporter known as OCTN1 or ETT [127][128][129]. Ergothioneine import efficiency is enhanced when co-transported with sodium ions. OCTN1 can only import ERG into the cells but can't export it. On the other hand, ERG does not easily diffuse across the

membrane. Consequently, cells lacking the OCTN1 transporter do not contain ERG [128]. Ergothioneine is a zwitterion, prevailing in its thione form more than its thiol form and it has a high redox potential at physiological pH ($E_0 = -60\text{mV}$) and is able to chelate divalent metals [130, 131]; that makes it very stable, and less susceptible to auto-oxidation than other thiols [132]. It is worth noting that the redox potential of GSH is -250mV while that of OSHA is 170mV making ERG more stable in its reduced form than GSH while is more stable in its reduced form than OSHA [133]. In addition, as opposed to other thiols ERG is not consumed and can accumulate in cells throughout their lifespan [128, 134]. Ergothioneine is sub-cellularly located in the cytoplasm, microsomes and in mitochondria but not in the nucleus [121, 127]. The role of ERG in eukaryotes has been extensively studied. It inhibits the copper induced oxidation of protein and DNA in the serum [135] electrically stimulate the cerebellum [125], prevents neuronal injury [136], protects skin cells against UV irradiation effects [137], protect the eye and protozoa against damage caused by oxidative stress and prevent the formation of cataract [123, 138-140] and is able to suppress inflammatory responses by indirectly suppressing IL-8 via TNF- α mediated activation of NF-kappa β [141]. Ergothioneine can also be a potential diagnostic marker. Patients with autoimmune disorders have a high level of ERG in their erythrocytes [142]. The OCTN1 gene variant 503F is associated to Crohn's disease and the transport efficiency of ERG is high in patients suffering from this disease [143]. The role of ERG in microorganisms is still under investigation. It was shown that it is a potent anti-oxidant in bacteria [144], in fungi [145] and in *M. smegmatis* [99]. In addition it has been shown that ERG is involved in the biosynthesis of the antibiotic lincomycin A by *Streptomyces lincolnensis* where it serves as a sulphur carrier [93] (Figure 1.5) and was found to be a moiety of Spithioneines A and B implicating the implication of ERG in the synthesis of these polyketides in *Streptomyces spinoverrucosus* [146].

Histidine has been suggested to be a precursor of ERG in previous studies when ^{14}C labelled histidine was shown to be converted to ERG in *Neurospora crassa* cultures, then it was speculated that thiohistidine could be an intermediate of ERG biosynthesis which was disproved later since ERG production did not result from the in ^{14}C labelled thiohistidine introduced in the *Neurospora crassa* culture [119]. However, it was shown that hercynine was a precursor of ERG. Chemically synthesized ^{14}C labelled hercynine was added in *Neurospora crassa* cultures which resulted ^{14}C labelled ERG [147] (Figure 1.7).

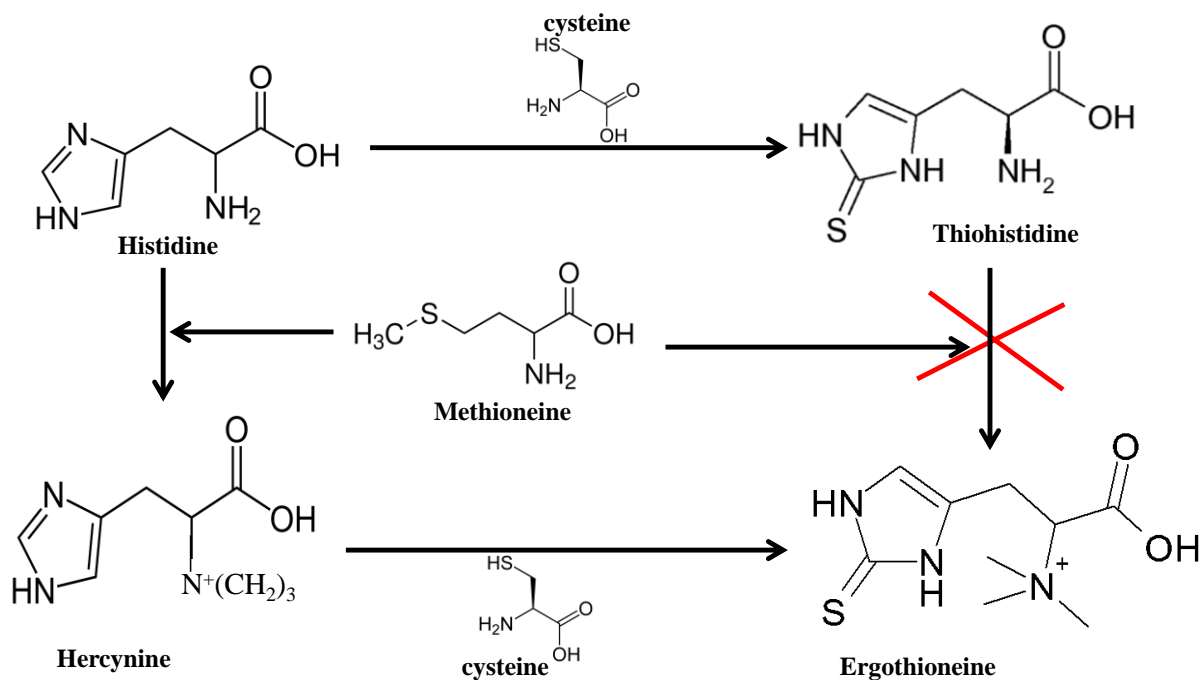


Figure 1.7 Ergothioneine biosynthesis pathway suggested in 1962 [147].

It was speculated that thiohistidine could be converted to ERG or hercynine could be converted to ERG in the presence of cysteine. The second speculation is true, but however involves more intermediates.

But the enzymes catalysing the reactions were unknown until EgtA, EgtB, EgtC, EgtD and EgtE were identified as the enzymes catalysing ERG biosynthesis in mycobacteria [148]. The biosynthesis was expounded as follows: Histidine is methylated in the presence of S-adenosylmethionine (SAM) by the methyltransferase EgtD to yield trimethylhistidine (hercynine) which will react with γ -glutamylcysteine (γ -GC) (synthesized in a reaction catalysed by γ -GC synthetase (EgtA)) catalysed by an FGE-like protein (EgtB) to form a compound from which glutamine will be cleaved by glutamine amido transferase (EgtC) to yield S-(β -amino- β -carboxyethyl)-ergothioneine sulfoxide from which pyruvate and ammonia will be released catalysed by a pyridoxal phosphate (PLP) dependant β -liase (EgtE)) to yield ERG (Figure 1.8).

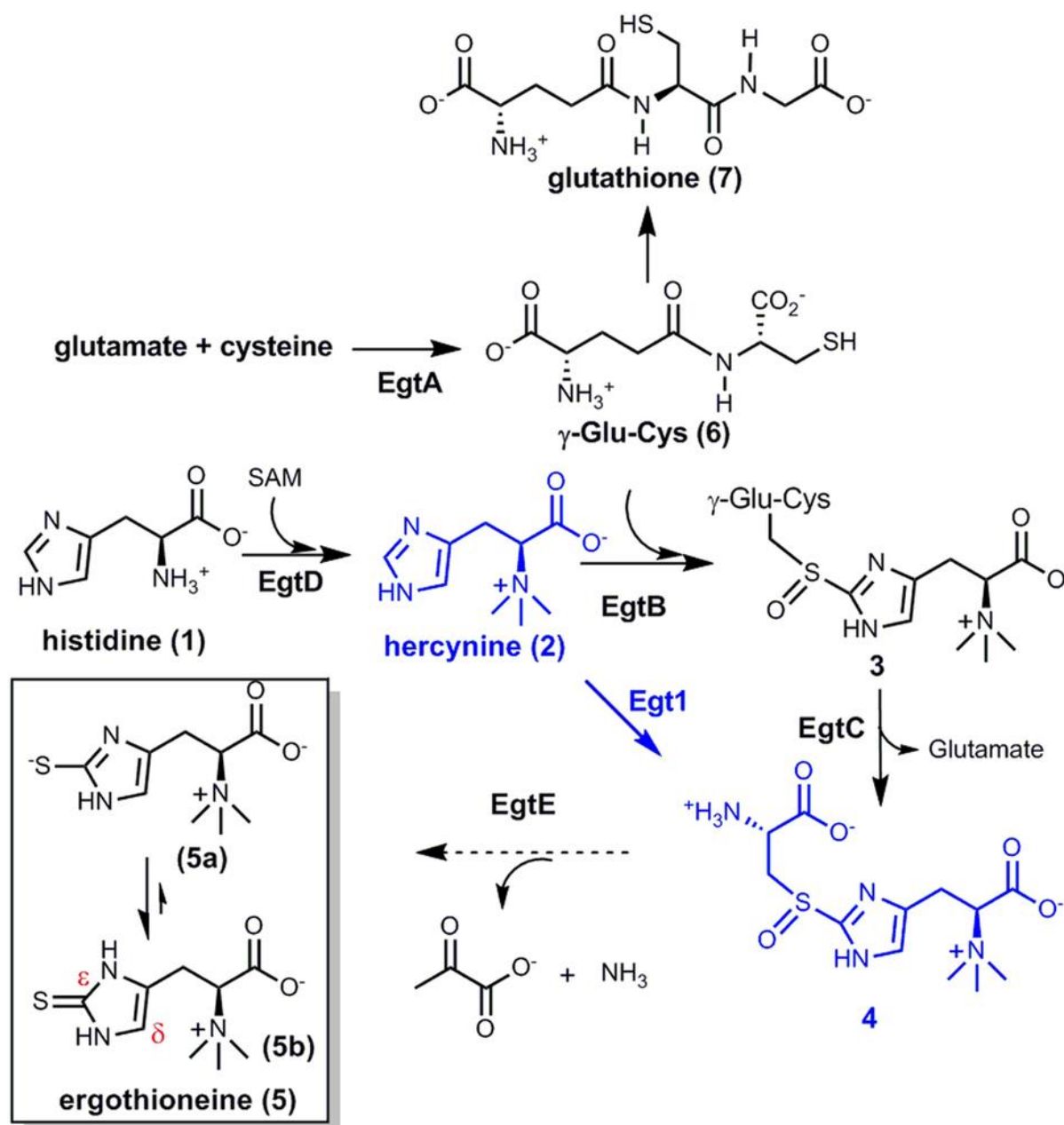


Figure 1. 8 Ergothioneine biosynthesis [149]

The enzyme EgtA catalyses the formation of γ -glutamyl cysteine (6), EgtD catalyses the methylation of histidine (2), EgtB catalyses the ligation of 6 to 2, EgtC catalyses the cleavage of glutamate to form 4 and EgtE catalyses the cleavage of pyruvate and NH₃ to form ERG (5) (indicated in black). However, in *N. crassa* only one enzyme involved in ERG biosynthesis has been identified so far (Egt1) which catalyses the conversion of 2 to 4 (indicated in blue). γ -glutamyl cysteine (6) formed by EgtA can also be used in the synthesis of glutathione in organisms that synthesized glutathione as well. Ergothioneine can exist either in a thiol configuration (5a) or a thione configuration (5b) but exist more predominantly at physiological pH in the thione configuration, conferring its stability [150].

In this new reaction scheme, thiohistidine is not an intermediate confirming what was shown in previous studies that the sulphur atom is incorporated through a more complex intermediate (S-(β -amino- β -carboxyethyl)-ergothioneine sulfoxide; 4 in Figure 1.8). However the gene cluster coding for enzymes involved in ERG biosynthesis is found mainly in

actinomycetes, most organisms lack orthologs of EgtA, EgtC and EgtE [151]. There are bacterial species lacking EgtA, EgtC, and EgtE that still produce ERG [152], indicating that they may not be universal ERG essential enzymes or may be compensated for by other enzymes or by spontaneous chemical reactions. In addition, the expression of *egtB* and *egtD* is positively correlated while there is no evidence that the expression of either *egtC*, or *egtA*, or *egtE* is positively correlated with that of *egtB* or *egtD* [153]. The first two steps of ERG biosynthesis in *N. crassa* is catalysed by NcEgt-1 (Figure 1.8). This enzyme contains domains found in EgtD and EgtB, thereby playing the catalytic role of both enzymes in the fungus *N. crassa* [145]. However, the enzymes catalysing the downstream reaction have not yet been identified. On the other hand it has been shown that EgtB binding is specific to γ – GC. However, any mutation on its residue (D416) may affect its sulphur donor specificity [154]. The enzyme EgtD on the other hand, catalyses methylation of histidine by a proximity and orientation effect in a successive reaction. It consists of two domains, the methyltransferase domain and the substrate binding domain. The histidine binding pocket primarily recognises the imidazole ring and carboxylate group of histidine accounting for its methylation selectivity and specificity. In other words EgtD can only methylate histidine and/or mono, di methyl histidine [155].

1.6 Rational of this study

It is known that eukaryotic cells import ERG via the OCTN1 transporter [127, 129, 156], and ERG was observed in the buffer of resting *M. smegmatis* pellicle [157], leading to the hypothesis that ERG is secreted by mycobacteria.

The anti-oxidative role of ERG in eukaryotes is well documented [150]. In addition to that, MSH-deficient *M. smegmatis* mutants produce more ERG than the wild type [100]. Leading to our second hypothesis that ERG plays a protective anti-oxidative role in mycobacteria.

Therefore, our first aim is to prove that ERG as opposed to MSH is secreted by mycobacteria. This aim can be achieved by quantifying ERG in the extracellular medium of mycobacteria culture, and proving that the ERG detected in that culture does not result from dead cells or a leakage through the mycobacterial membrane.

The second aim is to prove that ERG protects mycobacteria against oxidative stress and may complement MSH in that regard. To prove this, we must first generate an ERG-deficient mycobacteria mutant, then an ERG/MSH-deficient double mutant and investigate their survival under in vitro stress conditions.

Further, the objective of this study is to validate ERG biosynthesis as a potential drug target.

CHAPTER 2: METHODOLOGY

CHAPTER 2: METHODOLOGY

2.1 Investigation of ERG secretion in *M. smegmatis* and *M.tuberculosis*

- **ERG and MSH extraction and quantification in *M. smegmatis***

Approximately 50µl of *M. smegmatis* frozen stock ($OD_{600} \sim 1$) was used to inoculate 10 ml of Difco™ middlebrook 7H9 broth (Becton Dickinson South Africa) supplemented with 1% Glucose salt (GS) solution (5% Tween 80, 8.5% NaCl, 20% glucose). This was grown in a 100ml Erlenmeyer flask overnight at 37°C in a shaking incubator set to 200-250 rpm. The next day, a sterile, autoclaved Erlenmeyer flask containing 200 ml of 7H9 was inoculated with the starter culture to an $OD_{600} \sim 0.0025$ for the wild type and $OD_{600} \sim 0.005$ for the $\Delta mshA$ mutant and allowed to grow to the desired OD_{600} .

A serial dilution of each culture was performed and a 100µl aliquot was plated on Luria-Bertani (LB) agar (Merck or Sigma Aldrich) to determine colony forming units (CFUs)/ml. Cultures were harvested for extracellular and intracellular ERG (EE and IE) extractions. For EE, 10 ml of culture was pelleted at 4000rpm, and the supernatant was filtered sterilized (0.22µm diameter, PVDF membrane), snapped frozen in liquid nitrogen and lyophilised overnight in a vacuum pump (Labconco; 8811 Prospect Avenue Kansas City, MO 64132-2696; USA). For IE, 150 ml of culture was pelleted by centrifugation, and the pellet was re-suspended in the lysis buffer (2mM EDTA (pH ~8)+0.25M perchloric acid (PA) + 40% acetonitrile (ACN)). All chemicals used in the lysis buffer were supplied by Sigma Aldrich (St. Louis, MO, USA). In case of stationary phase cultures, the volume of the lysis buffer was doubled. The suspension was sonicated using a probe sonicator (Qsonica, LLC. 53 Church Hill Rd; Newtown, CT 06470) for 5 mins for exponential cultures and for 10 mins for stationary cultures at 25-50 pulses/s. The cell lysate was collected by centrifugation at 4°C for 10 mins (4000rpm), the pH of the supernatant was adjusted to between 8 and 10 with potassium carbonate (Sigma-Aldrich) and lyophilised overnight (26, 27). The lyophilised extracellular and intracellular portions were re-dissolved in a solution containing 25% acetonitrile and 0.05% formic acid and analysed by ultraperformance liquid chromatography-electrospray ionization-tandem mass spectrometry (UPLC-ESI-MS/MS) [118, 137]

- **Extraction and quantification of ERG, MSH, cysteine and hercynine in *M.tuberculosis***

Ergothioneine was extracted as previously described [99] with slight modifications. Approximately 35 ml or 15 ml of actively growing exponential or stationary liquid cultures respectively, (middlebrook 7H9 (Difco) broth supplemented with 10% Middlebrook OADC (Becton Dickenson, USA) and 0.05% Tween 80 (Sigma Aldrich) and 0.2% (v/v) glycerol grown in tissue culture flasks without shaking) was pelleted for IE extraction. The pellet was re-suspended in the lysis buffer (40% ACN+0.25 M PA+ 2mM EDTA) and cells were lysed in tubes containing 0.1mm beads (Biospec Products Inc., Bartlesville, United Kingdom) using FastPrep-24 (MP Biomedicals) (5 m/s) 5 times for 50 s with 1-min intermittent cooling steps on ice. The cell extract was clarified by centrifugation, and the pH equilibrated to between 8 and 9 using potassium carbonate. The precipitate was removed by centrifugation and the supernatant was filtered, lyophilised and re-suspended in the running buffer. This was subsequently analysed for ERG content using UPLC-ESI-MS/MS as previously described [99]. For extracellular ERG quantification, 1ml of the supernatant was filtered twice using 13mm PVDF 0.2um membrane filter or 13mm PTFE 0.2um membrane filters (SIGMA ALDRICH), lyophilised (Concentrator plus / Vacufuge® plus; Eppendorf, Becton Dickinson, Franklin lakes, NJ, USA) re-dissolved in 400µl of the running solvent (25% acetonitrile, 0.05% formic acid) and analysed for ERG concentration by ultra-performance liquid chromatography-electrospray ionization-tandem mass spectrometry (UPLC-ESI-MS/MS). For every extraction, serial dilutions of every culture were plated on 7H11 media for CFU counts. ERG concentration was expressed as pg/10⁵ CFU_s. Results are representative of the mean value of at least 3 biological replicates.

- **Mass spectrometry analysis of samples**

UPLC-ESI-MS/MS analysis was performed with a Waters Acquity UPLC system coupled to a Waters Xevo TQ MS system (Waters Corporation, Milford, MA, USA). Compounds were separated on a Waters Acquity BEH phenyl column (100 by 2.1 mm; 1.7 µm) at 50°C using a 1% formic acid (in water) (solvent A) - acetonitrile (solvent B) gradient, starting with 100% solvent A for 1.5 min at a flow rate of 0.3 ml/min. The acetonitrile concentration was increased linearly to 2% over 2 min at a flow rate of 0.4 ml/min and then increased to 100% over 0.3 min at a flow rate of 0.5 ml/min and maintained for 0.2 min. The column was re-equilibrated for 2 min (the total run time was 6 min). ERG was analyzed in the ESI-positive mode, and the multiple-reaction-monitoring (MRM) transition m/z 230.1 > 127.1 (cone voltage = 18 V; collision energy =18 eV) was monitored. The source capillary was at 3.5 kV. The source and desolvation temperatures were 140°C and 400°C, respectively. The

desolvation and cone gas flows were 600 and 50 liters/h, respectively. A standard curve was generated for ERG quantification. Intracellular and extracellular ERG was expressed as pg/10⁵CFU for each time point, and the results are representative of at least 3 experiments, expressed as means ± standard deviations of the means. For MSH quantification, samples were treated with 0.02 M dithiothreitol (DTT) prior to analysis. Since no MSH standard is commercially available, we used liquid chromatography–electrospray ionization–high-resolution mass spectrometry (LC-ESI-HRMS) and the known exact m/z value for MSH ([M – H]⁻) of 485.1441 to detect MSH in the cell lysate of wild-type *M. smegmatis*, as previously described [158]. Briefly, LC-ESI-HRMS was performed with a Waters Synapt G2 MS (Waters Corporation, Milford, MA, USA). Compounds were separated on a Phenomenex Synergi Fusion column (250 x 2 mm, 4 µm) at 25 °C using a 0.1% formic acid (in water) (solvent A) / acetonitrile (solvent B) gradient: Starting with 100% solvent A for 6 min at a flow rate of 0.2 ml/min. The acetonitrile was increased linearly to 95% over 21 min and maintained for 3 min. The column was re-equilibrated for 7 min (total run time was 32 min). Mycothiol was analyzed in ESI negative and the MS instrument was operated in scan mode (cone voltage = 15 V). The source capillary was at 2.5 kV. The source and desolvation temperatures were 120 °C and 275 °C, respectively. The desolvation and cone gas flows were 650 and 50 L/h, respectively. Hercynine was quantified as well by LC-ESI-HRMS. Compounds were separated on a BEH Amide column (2.1 x 100mm; 1.7µm) in an ESI positive mode; m/z 198.1 [148]. The mobile phases constituted of 0.1% formic acid (solvent A) and 95% ACN (solvent B). Samples did not require DTT treatment prior hercynine quantification. Because hercynine standard was not available, it was expressed as well as peak area/10⁷ CFUs. Cysteine was quantified by UPLC-ESI-MS/MS. Compounds were separated on a BEH Amide column (2.1 x 150mm; 1.7µm). The mobile phase constituted of 0.1% formic acid (solvent A) and 95% ACN (solvent B). Samples were treated with 0.02M DTT prior analysis [159, 160].

- **Evaluation mycobacteria membrane integrity**

- Evaluation of the membrane of *M.smegmatis***

A volume of 10ml of growing cultures was pelleted and re-suspended in 1ml 150mM NaCl (Sigma Aldrich) and incubated for ~30 mins at room temperature. The suspension was mixed by pipetting every 15 mins. This was then centrifuged at 4000rpm room temperature and the pellet was re-suspended in NaCl and washed two more times. The pellet was then re-suspended in 1 ml of NaCl and 10 µl of the suspension was added in 5 ml polystyrene round-

bottom 12 X 75mm falcon tubes (BD Biosciences Discovery Labware-Two Oak Park, Bedford, MA 01730 USA) containing 987µl NaCl, 1 µl of propidium iodide (PI) and 1.5 µl of Syto9 LIVE/DEAD® BacLight™ bacterial Viability and counting kit (Molecular PROBES®; life technologies) [161]. The suspension (protected from light) was analysed by a flow cytometer (BD FACSCalibur). A total of 100000 events was acquired for each sample. Results were analysed using the software FlowJo (Version 6). Syto9 is a membrane permeable green fluorescence dye that stains every cell in a suspension by binding to the nucleic acids, while PI is a red fluorescence that stains only cells with disrupted membrane, because it cannot penetrate through intact membrane due to its high molecular weight [161]. Heat treated mycobacteria (2 hours at 80°C) were included as a control for the dead cell population [162, 163]. Fluorescence was collected in channel 1 (FL1) for Syto9 and channel 3 for PI. The forward scatter, side scatter and fluorescence were collected on a logarithmic scale.

-Evaluation of the membrane integrity of slow growing mycobacteria

M. bovis membrane integrity analysis was achieved using the Live/Dead BacLight bacterial viability and counting kit (Molecular Probes), as previously described [99, 161]. A volume of 10 ml of culture was pelleted and re-suspended in 1ml of 150mM NaCl. Cells were washed 2 to 3 times in this buffer for ~1 hour, and finally re-suspended in 1 ml of 150mM NaCl. 10µl of the suspension was added in BD falcon tubes containing 990µl of the running buffer (148mM NaCl + 22µM PI + 5µM Syto9). After a brief vortex, each sample (protected from light) was analysed by a BD FACSCalibur (Becton Dickinson Biosciences, San Jose, CA), using linear amplifiers to measure forward- and side-light scatter (FSC, SSC) and logarithmic amplifiers for all fluorescence measurements. A total of 100000 events were acquired for each sample. The BD FACSCalibur instrument settings optimized for BCG are shown in Table 2.1.

Table 2.1 FACSCalibur instrument setting for the analysis of *M. bovis*

Detector	Voltage	Amp Gain	Mode	Parameter
FSC ^a 488/10BP ^b	E01	4.75	Linear	FSC ^a
SSC ^c 488/10BP	455	6.06	Linear	SSC ^c
FL1 ^d 530/30BP	474		Log	Syto9
FL3 ^e 650LP ^f	630		Log	PI

^aForward Scatter (measures relative size), ^bBandpass Filter, ^cSide Scatter (measure relative granularity),

^dFluorescence 1, ^eFluorescence 3, ^fLongpass Filter

M. tuberculosis membrane integrity was analysed following the same procedure with a few modifications. One millilitre of growing *M. tuberculosis* culture was pelleted, washed and re-

suspended in 150mM NaCl. Hundred microliter of the cell suspension was added in BD Falcon tubes containing 977.4µl of the running buffer. Stained *M. tuberculosis* cells were analysed by a BD FACSJazz cell sorter (Becton Dickinson Biosciences, Belgium), using linear amplifiers to measure forward-light scatter (FSC) and logarithmic amplifiers for side-scatter and all fluorescence measurements. A total of 200000 events were acquired for each sample. The BD FACSJazz instrument settings optimized for *M. tuberculosis* are found in Table 2.2. As controls, dead cell and/or cells with damaged membranes were generated by heat treatment for 1h at 80⁰C [99, 163, 164]. Results are representative of the mean of 3 different cultures at each growth stage.

Table 2.2 FACSJazz instrument setting for the analysis of *M. tuberculosis*

Detector	Voltage	Mode	Parameter
PMT 1 ^a 488/10BP	56.9	Linear	FSC
PMT 2 ^b 488/10BP	23.78	Log	SSC
PMT 3 ^b 530/40BP	28.75	Log	Syto9
PMT5 ^b 692/40BP	46.46	Log	PI

^aPhotodiode, ^bPhotomultiplier Tube, FSC: forward scatter, SSC: size scatter, PI: propidium iodide

- **Investigation of ERG transporter**

In order to identify the transporter of ERG, the protein sequence of OCTN1, the ERG transporter in eukaryotes [128, 129, 165] was blasted against *H37Rv* proteome in NCBI Blast tool

(http://blast.ncbi.nlm.nih.gov/Blast.cgi?PROGRAM=blastp&PAGE_TYPE=BlastSearch&LINK_LOC=blasthome). Fifteen closely related proteins were identified. The gene coding for the proteins were searched in Uniprot (<http://www.uniprot.org/>). Available transposon mutants where these genes were deleted were identified in www.beiresources.org. Transposon mutants of four genes coding each for a transporter were available. The four transposon mutants are MT 3434 Transposon mutant 212, MT 1926 Transposon mutant 1015, and MT 1289 Transposon mutant 1643, MT 1953 Transposon mutant 2730. These transposon mutants were requested from the American tissue type culture (ATCC). Strains were grown and IE and EE were quantified in each strain.

2.2 Generation of *M. smegmatis* and *M.tuberculosis* mutants

- **Methods used to mutate genes**

Genes can be knocked out by chemical mutagenesis, transposon mutagenesis and homologous recombination (which can be through a one step or two-step selection method). Chemical mutagenesis involves the use of chemicals to disrupt the gene of interest, but this

method does not allow a rational selection of the target gene, and may lead to the disruption of many other genes.

Transposon mutagenesis involves the use of a transposon gene to disrupt another gene. A transposon gene carried by a phage that will infect the bacteria, will use a copy and cut mechanism to be inserted into a gene thereby disrupting it. Transposon mutagenesis is more advantageous than chemical mutagenesis because mutants can be distinguished from wild type by selectively growing them in an antibiotic rich medium because phages can be designed with an antibiotic marker, so that the transposon should mark its site of insertion. The other advantage is, a single mutation can be achieved by transposon mutagenesis, and the transposon can be useful in case of transcriptional or translational fusions [166-168]. Transposon mutagenesis cannot enable a rational selection of the target gene.

Homologous recombination mutagenesis on the other hand allows a rational selection of the target gene. Homologous recombination is an event that occurs in eukaryotes allowing allelic exchange between a pair of chromosomes thereby allowing exchange of genetic information. This event is mediated by the RecA protein when performed in bacteria where two homologous sequences (one is engineered with the mutated gene) undergo recombination leading to a mutant strain. Homologous recombination involves two methods: A one-step method where selection of the recombinant is done in one step usually because the gene of interest is replaced by an antibiotic resistance marker which enables discrimination of the mutants from the wild type by growing them in antibiotic containing media; generating marked mutants (gene disrupted or replaced by an antibiotic marker cassette). The two-step method involves the selection of the recombinant strains in two steps that is: a single cross over event is detected when all the included antibiotic markers are expressed. The second cross over event is identified when all the selectable markers present on the plasmid backbone are no longer expressed (except the one used to disrupt the gene in case of marked mutation). It is always difficult to perform homologous recombination in slow growing species like *M. tuberculosis*, but the two steps homologous recombination is more efficient than the one step method in slow growing mycobacteria like *M. tuberculosis*. A two-step homologous recombination can be designed for the generation of marked mutants (replacement of the gene by a marker) and unmarked mutants (replacement of the gene by either a truncated gene, or a point mutated gene or no gene at all). Unmarked mutagenesis allows performing many gene deletions on the same strain since the markers can be reused for subsequent mutagenesis, while in a marked mutation the number of deletions is limited due to the limited number of the marker cassettes. Furthermore, a marker can have a polar

effect on the transcription of the surrounding genes or an unknown physiological effect on the bacteria [169-173]. Therefore we made use of a two-step selection procedure to achieve genes deletion in this study (Figure 2.1).

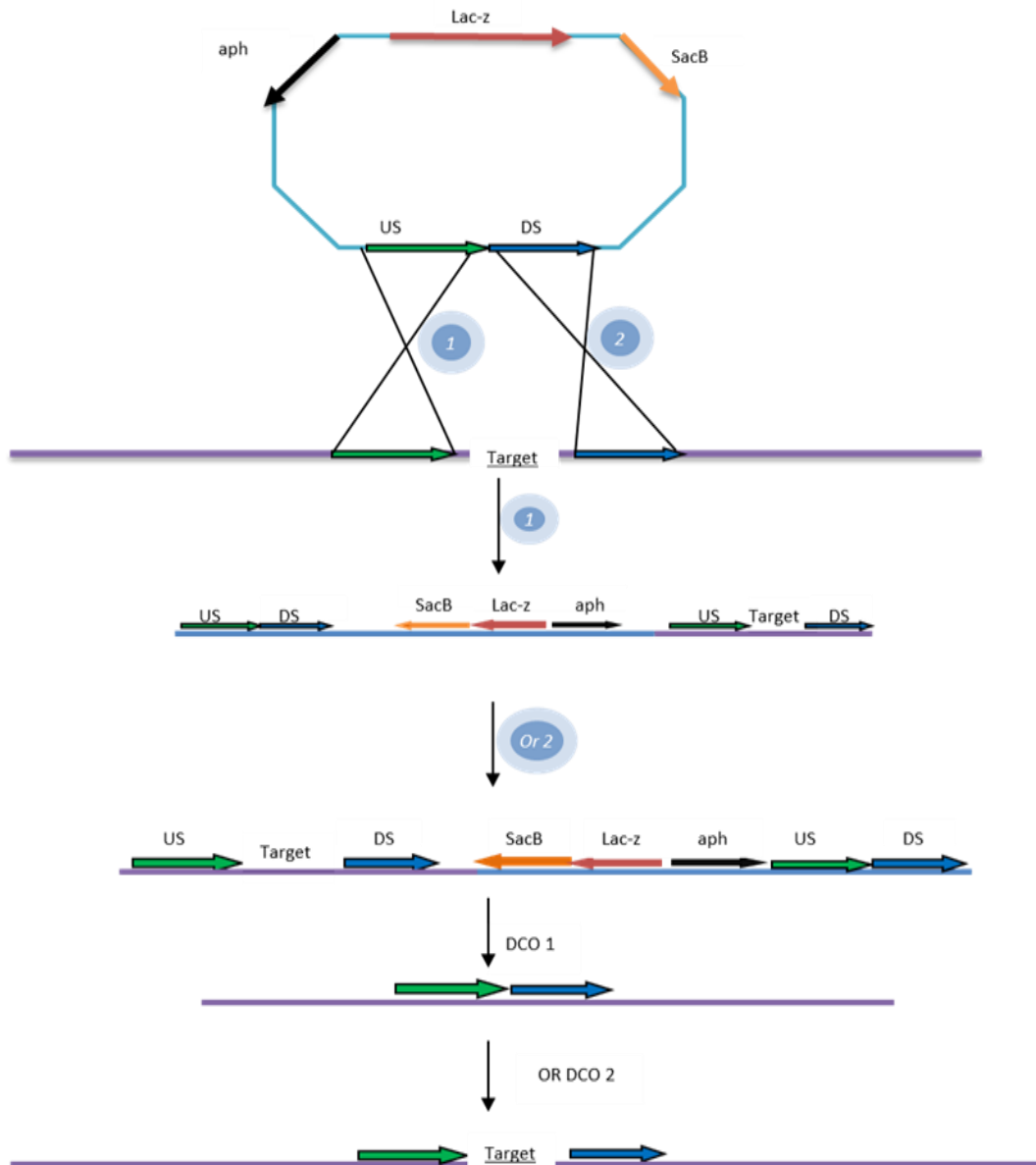


Figure 2.1 Two-step homologous recombination event

US: upstream, **DS:** downstream, **SacB:** gene that encode the protein characteristic for the sucrose sensitivity phenotype, **LacZ:** gene that encodes β thiogalactosidase characteristic for a blue phenotype in media containing X-galactose, **Kan:** gene coding for the kanamycin resistant protein, **DCO:** double cross over. The first homologous event can happen either at the upstream region (1) or at the downstream region (2). The second event is known as a double cross over which leads to the deletion of the target gene (DCO 1) or to the same unchanged genome (DCO 2).

- **Generation the $\Delta egtD$ and the $\Delta mshA/egtD$ *M. smegmatis* mutant strains**

An unmarked *egtD* (*MSMEG_6247*) deletion was generated by homologous recombination as described previously [170]. Briefly, upstream (US) and downstream (DS) fragments flanking *egtD* were amplified from *M. smegmatis mc²155* genomic DNA using the primers listed in Table 2.3. The enzyme used for the polymerase chain reaction (PCR) was Phusion polymerase (Thermo Scientific, Thermo Fisher Scientific Inc. 81 Wyman Street Waltham, MA USA 02451), the reaction set up is found in Table 2.4 and the thermo cycling conditions are found in Table 2.5. The resulting fragments were cloned individually into CloneJet™ Vector (Thermo scientific) and subsequently used to construct the suicide plasmid p2NILEgtD. The *sacB-lacZ* fragment from pGOAL17 or the *sacB-hyg-lacZ* fragment from pGOAL19 was cloned into the *PacI* site of p2NILEgtD to generate p2NILEgtD17 or p2NILEgtD19 respectively [170] (Table 2.5). p2NILEgtD17 or p2NILEgtD19 were electroporated into *M. smegmatis mc²155* and the $\Delta mshA$ mutant respectively [86] (kindly donated by Yossef Av gay and Adrie Steyn; see Table 2.6), and *egtD* deletion was achieved in each strain by a two-step allelic exchange (Figure S 1 in the additional information found in the appendix describes the entire process). The integrity of the allelic exchange substrates and complementation vector were confirmed by sequencing (Table 2.3) and the genotypes of the mutant strains were confirmed by Southern blotting and colony PCR (6247SF, 6247SR1, 6247SR2, Table 2.6).

Table 2.3 Primers used to generate the suicide plasmid and the complementation vector

Name	Sequences (5' to 3' direction)	Restriction enzymes	PCR product
6247 USF	<u>GCATATGGT</u> AGTTGGCCAGTGAGAG	NdeI	1923bp upstream <i>MSMEG_6247</i> including 18bp of its 5' end
6247 USR	<u>AAGCTTGA</u> ACTGCATCGCCAGTACA	HindIII	
6247 DSF	GATGCAT <u>G</u> GCGATAACCGACAACAG	Nsil I	1955bp downstream <i>MSMEG_6247</i> including 129bp of its 3' end
6247 DSR	<u>GCATATGCTC</u> ACCGAGGTGTCC	NdeI	
6247 CF	<u>AAGCTTCTC</u> GACATGACGCGAACAT	HindIII	4528bp product that includes 2398bp upstream <i>MSMEG_6247</i> to 1169bp downstream <i>MSMEG_6247</i>
6247 CR	<u>AAGCTTGAG</u> GCCGACCTGGACTATA	HindIII	
6247 SF	GTTCTCGGGACGGA ^{ACTT} G	NA	
6247 SR1	ACCGATCTGGTGAAGGACAC	NA	Screening primers, 279bp and 976bp for <i>mc²155</i> and 169bp for the mutant
6247 SR2	AACCCTACGACGACGATCC	NA	

SeqF	CAGACCGGCGAGCATGAA	NA	Sequencing primer
SeqR	AACAGCGTCATCGATTCCCTCG	NA	Sequencing primer
6247 S'1	GTTCGACGACGCGCCAC	NA	Sequencing primer
6247 S'2	CGCCCGTCGTCGTCGAC	NA	Sequencing primer
6247 S'3	GCGGGATCTTGCCCAGA	NA	Sequencing primer
6247 S'4	AGCGCAGCACGCCCCGCG	NA	Sequencing primer
6247 S'5	CCGACAGCGTGTCCCCC	NA	Sequencing primer
6247 S'6	CGGCGGGTCGAGCACCA	NA	Sequencing primer
6247 S'7	TCGGGGTTCAGAACTG	NA	Sequencing primer
6247SBF	GGGATCGTCGTCGTAGGGTT	NA	Sequencing primer
6247SBR	CGCACTCACTGGACAACGAA	NA	Sequencing primer

Table 2.4 Reaction set up of Phusion polymerase

Components	Final concentration
5X Phusion Buffer	1X
2.5mM dNTP	0.2mM
10µM forward primer	0.5µM
10µM Reverse primer	0.5µM
2u/µl Phusion polymerase	0.02u/µl
H ₂ O	make it up to final volume
DNA	100-200ng

Table 2.5 Thermo cycling conditions of Phusion polymerase

Temperature °C	Time	cycle
98	30s	1
98	10s	
59-72	30s	40
72	2mins	
72	10mins	1
4	+∞	1

Table 2.6 Plasmids and strains used in this study

Name	Description	Source/ Reference
Plasmids		
p2NIL	Cloning vector, kan ^r	[170]
p2NILegtD	p2NIL vector carrying 1955bp region downstream <i>egtD</i> and 1923bp region upstream <i>egtD</i>	This study
pGOAL17	Plasmid carrying <i>lacZ</i> and <i>sacB</i> genes as a <i>PacI</i> cassette; Ap ^r	[170]
pGOAL19	Plasmid carrying <i>hyg</i> , <i>lacZ</i> , and <i>sacB</i> genes as a <i>PacI</i> cassette; Ap ^r , Hyg ^r	[170]
p2NILegtD17	p2NILegtD containing the pGOAL17 <i>PacI</i> cassette	This study

p2NILegtD19	p2NILegtD containing the pGOAL19 <i>PacI</i> cassette	This study
pMV306	<i>E.coli- Mycobacterium</i> integrating shuttle vector, Hyg ^r	[174]
pMV306D	pMV306 carrying the region from 2398bp upstream of <i>egtD</i> to 1169bp downstream of <i>egtD</i>	This study
Strains		
<i>mc</i>²¹⁵⁵	<i>ept-1</i> (efficient plasmid transformation) mutant <i>mc</i> ²⁶	Laboratory stock
Δ<i>mshA</i>	Derivative of <i>mc</i> ²¹⁵⁵ carrying a transposon insertion in <i>mshA</i> , kan ^r	[86]; kindly donated by Yossef Av-Gay and Adrie Steyn
Δ<i>egtD</i>	Derivative of <i>mc</i> ²¹⁵⁵ carrying an unmarked deletion of <i>egtD</i>	This study
Δ<i>mshA</i>/Δ<i>egtD</i>	Derivative of Δ <i>mshA</i> carrying an unmarked deletion of <i>egtD</i>	This study
Δ<i>egtD</i> attB::<i>pMV306D</i>	Derivative of Δ <i>egtD</i> carrying pMV306D integrated at the attB locus; Hyg ^r	This study
Δ<i>mshA</i>/Δ<i>egtD</i> attB::<i>pMV306D</i>	Derivative of <i>mshA</i> / Δ <i>egtD</i> carrying pMV306D integrated at the attB locus; Hyg ^r	This study
DH5a	<i>E.coli</i> for routine cloning experiments	Laboratory stock

- **Generation of *M.tuberculosis* mutants**

Homology search was done to identify genes that code for enzymes involved in ERG biosynthesis in *M. tuberculosis*. This was achieved by aligning *M. smegmatis* ERG validated biosynthetic genes against *M. tuberculosis* genome as seen below (Figure 2.2).



Figure 2.2 Genomic alignment of the operon of genes coding for enzymes involved in ERG biosynthesis

Two-step allelic exchange mutagenesis was used to delete the genes involved in ERG biosynthesis as described above. The primers used to amplify the regions flanking each gene are listed in Table 2.7. Allelic exchange substrates were generated by cloning these fragments, along with selection markers into p2NIL vectors as described in Table 2.8

To obtain a marked construct for the deletion of *mshA*, a hygromycin cassette was amplified along with its promoter region from pMV306hyg^r [174] (primers in Table 2.7), cloned into the *SpeI* site between the US and DS regions of *mshA* in p2NIL. The *PacI* fragment of pGOAL17 was subsequently ligated to the p2NIL construct (Table 2.8). Mutants were

identified by colony PCR and confirmed by Southern blotting. PCR screening primers can be seen in Table 2.7 and Southern blotting probes and restriction enzymes are indicated in Table 2.9.

Table 2.7 Primers used in this study

Name	Sequence	Restriction site	Products
Construct Design			
A-USF	GCTGTACAGATACTACGACCCGGTTCCCA	BsrgI	2451bp US MT3807 including a 60bp flank
A-USR	GCACTAGTGTCGTCCGGGGCAGCGTTA	SpeI	
A-DSF	GCACTAGTCCGGCAGACGATTTCTCCGA	SpeI	2462bp DS MT3807 including a 81bp flank
A-DSR	GCAAGCTTGC GTT GATTTTCGACACCACTG	HindIII	
B-USF	GCTGTACACGCTATTACCACCACGGCA	BsrgI	2488bp US MT3806 including a 100bp flank
B-USR	GCACTAGTCATACTGGCAGCAAAGCTCG	SpeI	
B-DSF	GCACTAGTCCAGCTTCCGCAACTGGGAT	SpeI	2468bp DS MT3806 including a 74bp flank
B-DSR	GCAAGCTTCTCCATCAGCTCAGGACGAAC	HindIII	
C-USF	GCTGTACAAGATGGAGGCGCACTGCTT	BsrgI	2484bp US MT3805 including a 58bp flank
C-USR	GCACTAGTCCAGCACCAACGAAGAAACC	SpeI	
C-DSF	GCACTAGTACCTGGTGGAGGTAACCCAA	SpeI	2456bp DS MT3805 including 68bp flank
C-DSR	GCAAGCTTTGGAAGTCAAGCCAAACGAAG	HindIII	
D-USF	GCTGTACACTCGGCAATGGCTGGAAA	BsrgI	2452bp US MT3804 including a 110bp flank
D-USR	GCACTAGTCACTTGGGCGGTAACGATTT	SpeI	
D-DSF	GCACTAGTGACCGATGAAGCCGGTGACT	SpeI	2521bp DS MT3804 including a 46bp flank
D-DSR	GCAAGCTTGCATAACGGCACGGTGTACC	HindIII	
E-USF	GCTGTACAACCAACGGTGAATGGCAAGACTTC	BsrgI	2444bp US MT3803 including a 100bp flank
E-USR	GCACTAGTCCGCGCTGTCCAGG	SpeI	
E-DSF	GCACTAGTACAACACCGCCGATGACCT	SpeI	2367bp DS MT3803 including a 59bp flank
E-DSR	GCAAGCTTGCGCATACATCAGATGCTAACTCG	HindIII	
mshA-USF	GCTGTACACAACCTGTTCGACGGAGAAC	BsrgI	2597bp US MT0504 including a 40bp flank
mshA-USR	GCACTAGTTCGATCAACCCTGAACCGT	SpeI	
mshA-DSF	GCACTAGTTGATATCGGACCTGGTAGCG	SpeI	2532bp DS MT0504 including a 68bp flank
mshA-SR	GCAAGCTTTTCACATGCTGTTTGGCA	HindIII	
HF	ACTAGTTCAGGCGCCGGG	SpeI	
HR	ACTAGTCCGCTGGTAGCGGT	SpeI	1608bp
Screening			
A-SF	AGGGATCGTGATATGACGCT	NA	Set1: WT=617bp and $\Delta egtA=0$ bp
A-SR ₁	GCGATCATCGTCGGCCCCAA	NA	Set2: WT=1689bp and $\Delta egtA=1689-1152=537$ bp
A-SR ₂	TGATCACCATCGCGAACA	NA	
B-SF	GCGGGTACCGACTGAACTCA	NA	Set1: WT= 504bp and $\Delta egtB=0$ bp
B-SR ₁	CTGTCGCCGTCTCAGGTAGA	NA	Set 2: WT=1584bp and $\Delta egtB=1584-1104=479$ bp
B-SR ₂	GAATGGCACCGTCGAAGAAG	NA	
C-SF	TTCGTCCCGATGGTCTATGA	NA	Set1: WT=562bp; $\Delta egtC=0$ bp
C-SR ₁	GATTCGGCCGCCGGGCC	NA	
C-SR ₂	AACTCGACCAAAGTATCGGC	NA	Set2: WT=1128bp

			and $\Delta egtC=1128-570=558bp$
D-SF	ACCATCTTCGCTCACGGT	NA	Set1: WT=791bp
D-SR ₁	GGGCGTGAGGTTGCCGA	NA	and $\Delta egtD=0bp$
			Set2: WT=1400bp
D-SR ₂	GAAACTCTGGCGCGAACA	NA	and $\Delta egtD=1400-804=596bp$
E-SF	GGTGACTTTGGCCTGTCGCT	NA	Set 1:WT=861and
E-SR ₁	ACTCGCGCAGCTACATTG	NA	$\Delta egtE=0bp$
			Set2: WT= 1782bp
E-SR ₂	CGCCGAACTGTCATTGGCCC	NA	and $\Delta egtE=1782-996=786bp$
MshA-SF1	ATCAGCAAGCCAAGGAGC	NA	WT=0bp $\Delta mshA$, or
MshA-SR1	TCTCTCCGGCTTCACCGATCC	NA	$\Delta egtB/mshA=507bp$
MshA-SF2	CGAATATCCCGAGGCGATG	NA	
MshA-SR2	CCGAAACATTCCGATTGG	NA	WT=388bp $\Delta mshA$, or $\Delta egtB/mshA=0bp$
Complementation-1			
PF	AAGCTTCGCTATTACCACCACGGCA	Hind III	1093bp promoter region and <i>MT3807</i> yield 2392bp
A-GR	AAGCTTTCACGACGCCCCGTGCATCA	Hind III	
B-PR	GGTGAAGTCACATCACGATCCCTCC	NA	Fusion of <i>MT3806</i>
B-GF	TCGTGATGTGACTTCACCCGAGC	NA	to promoter (1093bp) to yield 2377bp
B-GR	AAGCTTTCAGATGTCCCACGCCA	Hind III	
C-PR	GACGACACATATCACGATCCCTCC	NA	Fusion of <i>MT3805</i> and promoter (1093bp)to yield 1795bp
C-GF	TCGTGATATGTGTCGTCACCTG	NA	
C-GR	AAGCTTTCATCGAGGTCCTTTCGCGC	Hind III	
D-PR	ACACTCTCATATCACGATCCCTCC	NA	Fusion of <i>MT3804</i>
D-GF	TCGTGATATGAGAGTGTCCGGTTG	NA	to promoter (1093bp)to yield 2059bp
D-GR	AAGCTTTCACCTGGCGGCCAGCGACA	Hind III	
E-PR	TTCTCCTCATATCACGATCCCTCCG	NA	Fusion of <i>MT3803</i>
E-GF	TCGTGATATGAGGAGAAGCGGCGCAAAC	NA	to promoter (1093)
E-GR	AAGCTTCTAACGTTCCGCCGCTGGTGC	Hind III	to yield 2272bp
mshA-CF	AAGCTTGGGACAACCTAATAAACG	Hind III	3536bp (from 1575US <i>MT0504</i> to 547DS <i>MT0504</i>)
mshA-CR	AAGCTTCTAACCGCCCAACTCCTTC	Hind III	
Complementation-3^A			
AF	<u>AAGCTT</u> <u>AGAAGGAGAAGTACCG</u> ATGACGCTTGCCGCCATGAC	Hind III	<i>egtA</i> (<i>Rv3704</i> ,
AR	GCATCGATTACACGACGCCCCGTGCATC	ClaI	<i>MT3807</i>)
BF	<u>AAGCTT</u> <u>AGAAGGAGAAGTACCG</u> GGTGACTTCACCCGAGCAGCT	HindIII	<i>egtB</i> (<i>Rv3703</i> ,
BR	GCATCGATTACAGATGTCCCACGCCAACC	ClaI	<i>MT3806</i>)
CF	<u>AAGCTT</u> <u>AGAAGGAGAAGTACCG</u> ATGTGTCGTCACCTGGGGTG	HindIII	<i>egtC</i> (<i>Rv3702</i> ,
CR	GCATCGATTACATCGAGGTCCTTTCGCGC		<i>MT3805</i>)
DF	<u>AAGCTT</u> <u>AGAAGGAGAAGTACCG</u> ATGAGAGTGTCCGGTTGCCAAC	HindIII	<i>egtD</i>
DR	GCATCGATTCACTTGGCGGCCAGCGACAG	ClaI	(<i>Rv3701</i> , <i>MT3804</i>)
EF	<u>AAGCTT</u> <u>AGAAGGAGAAGTACCG</u> ATGAGGAGAAGCGGCGCAAAC	HindIII	<i>egtE</i> (<i>Rv3700</i> ,
ER	GCATCGATTCTAACGTTCCGCCGCTGGTGC	ClaI	<i>MT3803</i>)
mshAF	<u>AAGCTT</u> <u>AGAAGGAGAAGTACCG</u> ATGGCAGGTGTGCGGCACGATG	Hind III	<i>mshA</i> (<i>RV0486</i> ,
mshAR	GCGTAACTCACGCGCCACCCCGCGAC	HpaI	<i>MT0504</i>)

^A Optimized Shine-Dalgarno sequence [175], underlined are the restriction sites

Table 2.8 Plasmids and strains used in this study

Name	Description	Source/ Reference
Plasmids		
p2NILA/G17	p2NIL plasmid and the PacI fragment of pGOAL17 carrying a 2451 bp upstream fragment and a 2462 bp downstream fragment of <i>egtA</i> (<i>Rv3704,MT3807</i>)	This study
p2NILB/G17	P2NIL plasmid and the PacI fragment of pGOAL17 carrying a 2488 bp US fragment and a 2462 bp DS fragment of <i>egtB</i> (<i>Rv3703,MT3806</i>)	This study
p2NILC/G17	p2NIL plasmid and the PacI fragment of pGOAL17 carrying a 2484 bp US fragment and a 2456 bp DS fragment of <i>egtC</i> (<i>Rv3702,MT3805</i>)	This study
p2NILD/G17	p2NIL plasmid and the PacI fragment of pGOAL17 carrying a 2452 bp US fragment and a 2521 bp DS fragment of <i>egtD</i> (<i>Rv3701,MT3804</i>)	This study
p2NILE/G17	P2NIL plasmid and the PacI fragment of pGOAL17 carrying a 2444 bp US fragment and a 2367 bp DS fragment of <i>egtE</i> (<i>Rv3700,MT3803</i>)	This study
p2NILmshAHyg/G17	p2NIL plasmid and the PacI fragment of pGOAL17 carrying a 2597 bp US fragment and a 2532 bp DS fragment of <i>mshA</i> (<i>Rv0486,MT0504</i>)	This study
pMVA	pMV306 integrating plasmid carrying region from 1093bp US to <i>MT3807</i> (<i>Rv3704</i>) ,Kan ^r	This study
pMV306hsp, kan^r	Mycobacteria integrating vector carrying the hsp60 promoter and a kanamycin resistance gene	Kindly donated by Samantha Sampson [175]
pMVB	pMV306 integrating plasmid carrying <i>MT3806</i> (<i>Rv3703</i>) joint to the 1093bp region US <i>MT3806</i> (<i>Rv3704</i>), Kan ^r	This study
pMVC	pMV integrating plasmid carrying <i>MT3805</i> (<i>Rv3702</i>) joint to the 1093bp region US <i>MT3805</i> (<i>Rv3704</i>), Kan ^r	This study
pMVD	pMV306 integrating plasmid carrying <i>MT3804</i> (<i>Rv3701</i>) joint to the 1093bp region US <i>MT3807</i> (<i>Rv3704</i>), Kan ^r	This study
pMVE	pMV306 integrating plasmid carrying <i>MT3803</i> (<i>Rv3700</i>) joint to the 1093bp region US <i>MT3807</i> (<i>Rv3704</i>), Kan ^r	This study
pMVmshA	pMV306 integrating plasmid carrying <i>region from 1545 US to 547bp DS MT0504</i> (<i>Rv0486</i>), Kan ^r	This study
pMVhspA	pMV306 integrating plasmid carrying <i>MT3807</i> (<i>Rv3704</i>) cloned downstream the hsp60 promoter ,Kan ^r	This study
pMVhspB	pMV306 integrating plasmid carrying <i>MT3806</i> (<i>Rv3703</i>) cloned downstream the hsp60 promoter ,Kan ^r	This study
pMVhspC	pMV306 integrating plasmid carrying <i>MT3805</i> (<i>Rv3702</i>) cloned downstream the hsp60 promoter ,Kan ^r	This study
pMVhspD	pMV306 integrating plasmid carrying <i>MT3804</i> (<i>Rv3701</i>) cloned downstream the hsp60 promoter ,Kan ^r	This study
pMVhspE	pMV306 integrating plasmid carrying <i>MT3803</i> (<i>Rv3700</i>) cloned downstream the hsp60 promoter ,Kan ^r	This study
pMVhsp mshA	pMV306 integrating plasmid carrying (<i>Rv0486,MT0504</i>)cloned downstream the hsp60 promoter ,Kan ^r	This study
pMVOP	pMV306 integrating plasmid carrying entire ERG operon	This Study
Strains		

<i>H37Rv</i>	<i>M. tuberculosis</i> laboratory strain	[102] , kindly donated by Catherine Vilcheze
<i>CDC1551</i>	<i>M. tuberculosis</i> clinical laboratory strain	Kindly donated by Adrie Steyn
Δ <i>egtA</i>	Derivative of CDC1551 carrying an unmarked deletion of <i>egtA</i>	This study
Δ <i>egtB</i> (H37Rv and CDC1551)	Derivatives of CDC1551 and H37Rv carrying an unmarked deletion of <i>egtB</i>	This study
Δ <i>egtC</i>	Derivative of CDC1551 carrying an unmarked deletion of <i>egtC</i>	This study
Δ <i>egtD</i>	Derivative of CDC1551 carrying an unmarked deletion of <i>egtD</i>	This study
Δ <i>egtE</i> (H37Rv and CDC1551)	Derivative of CDC1551 and H37Rv carrying an unmarked deletion of <i>egtE</i>	This study
Δ <i>mshA</i> , <i>hyg</i> ^r	Derivative of <i>CDC1551</i> carrying an marked deletion of <i>mshA</i>	This study
Δ <i>egtA</i> attB:: <i>pMVA</i> (<i>kan</i> ^r)	Derivative of Δ <i>egtA</i> carrying pMVA at the attB site	This study
Δ <i>egtApMVhspegtA</i> (<i>kan</i> ^r)	Derivative of Δ <i>egtA</i> carrying pMVhspA at the attB site	This study
Δ <i>egtB</i> attB:: <i>pMVB</i>	Derivative of Δ <i>egtB</i> carrying pMVB at the attB site	This study
Δ <i>egtBpMVhspegtB</i> (<i>kan</i> ^r)	Derivative of Δ <i>egtB</i> carrying pMVhspB at the attB site	This study
Δ <i>mshA/egtB</i> pMVhspegtB (<i>kan</i> ^r , <i>hyg</i> ^r)	Derivative of <i>mshA/ΔegtB</i> carrying pMVhspB at the attB site	This study
Δ <i>egtCpMVhspegtC</i> (<i>kan</i> ^r)	Derivative of Δ <i>egtC</i> carrying pMVhspC at the attB site	This study
Δ <i>egtD</i> attB:: <i>pMVD</i> (<i>kan</i> ^r)	Derivative of Δ <i>egtD</i> carrying pMVD	This study
Δ <i>egtDpMVhspegtD</i> (<i>kan</i> ^r)	Derivative of Δ <i>egtD</i> carrying pMVhspD	This study
Δ <i>egtE</i> pMVhspegtE (<i>kan</i> ^r)	Derivative of Δ <i>egtE</i> carrying pMVhspE	This study
Δ <i>mshA</i> attB:: <i>pMVmshA</i>	Derivative of Δ <i>mshA</i> carrying pMVmshA	This study
Δ <i>egtApMV OP</i> (<i>kan</i> ^r)	Derivative of Δ <i>egtA</i> carrying pMVOP	This study
Δ <i>egtBpMV OP</i> (<i>kan</i> ^r)	Derivative of Δ <i>egtB</i> carrying pMVOP	This study
Δ <i>egtDpMV OP</i> (<i>kan</i> ^r)	Derivative of Δ <i>egtD</i> carrying pMVOP	This study
Δ <i>MT1289</i> (<i>kan</i> ^r)	Derivative of CDC1551 carrying a transposon at <i>MT1289</i>	Kindly donated by the BEI resources
Δ <i>MT1953</i> (<i>kan</i> ^r)	Derivative of CDC1551 carrying a transposon at <i>MT1289</i>	Kindly donated by the BEI resources [176]

Table 2.9 Design of Southern blotting screening of *M. tuberculosis* mutants

Strains	probe	Restriction enzyme	Fragment sizes
Δ <i>egtA</i>	DS fragment of Δ <i>egtA</i> deletion construct	EspI	<i>H37Rv</i> = CDC1551= 4569bp, Δ <i>egtA</i> =10265-1158=9107bp
Δ <i>egtB</i>	US fragment of Δ <i>egtA</i> deletion construct	BamHI	<i>H37Rv</i> = CDC1551= 5318bp, Δ <i>egtB</i> =10218-1105=9113bp
Δ <i>egtC</i>	DS fragment of Δ <i>egtC</i> deletion construct	ApaBI (BstAPI)	<i>H37Rv</i> = CDC1551= 4089bp, Δ <i>egtC</i> =12424-576=11848
Δ <i>egtD</i>	<i>egtC</i> gene from the complementation construct	BclII	<i>H37Rv</i> = CDC1551= 2266bp, Δ <i>egtD</i> =7539-810=6729bp

$\Delta egtE$	DS fragment of $\Delta egtA$ deletion construct	NcoI	$H37Rv = CDC1551 = 4198bp$, $\Delta egtE = 8776-996 = 7780bp$
$\Delta mshA$	US fragment of the $\Delta mshA$ deletion construct	ClaI	$H37Rv = CDC1551 = 6361bp$, $\Delta mshA = 18469-1335+1608 = 15526bp$

- **Generation of complementation strains**

-Generation of the genetically complemented $\Delta egtD$ *attB::pMV306D* and $\Delta mshA/egtD$ *attB::pMV306D*

A complementation vector was generated by amplifying the region from 2398bp upstream of *egtD* to 1169bp downstream of *egtD* (primers in Table 2.3) using Long PCR polymerase (Thermo Scientific) (reaction set up found in Table 2.10, and thermo cycling conditions found in Table 2.11) and cloning it at the HindIII site of integrating vector pMV306 [174] (Table 2.4). The integrity of the vector was confirmed by sequencing (Primers in Table 2.3).

Table 2.10 Long Polymerase reaction set up

Components	volume
10X long PCR Buffer (15mM MgCl ₂)	1X
2.5mM dNTP	0.25mM
10 μ M forward primer	1 μ M
10 μ M Reverse primer	1 μ M
5u/ μ l long polymerase	0.05u/ μ l
H ₂ O	make it up to the final volume
DNA	100-200ng

Table 2.11 Long Polymerase thermo cycling

Temperature °C	Time	cycle
94	4mins	1
94	20s	
59 (0.5 decrease every cycle)	30s	
68	5mins	10
94	20S	
60	30S	
68	5mins	25
68	10mins	1
4	+∞	1

-Generation of *M.tuberculosis* complemented strains

Different sets of complementation constructs were generated for genes involved in ERG biosynthesis.

Firstly, complementation constructs were generated by amplifying the 1000bp region upstream of the ERG operon and fused to each gene of interest by overlap extension PCR

(Figure 2.3, Table 2.7, Table 2.8 and Table 2.12). This was based on the results obtained on http://www.fruitfly.org/seq_tools/promoter.html , which predicts promoter regions. Resulting fragments were then cloned to either the Pjet vector (Fermentas), or PgemTeasy (Promega) or Pdrive (Qiagen), and subsequently cloned into pMV306hsp [177] which is an integrating vector (Table 2.8). The resulting constructs were used to transform the mutants to achieve complementation. Due to insert toxicity to *E.coli*, Δ *egtC* complementation constructs were redesigned by amplifying instead the 583bp region upstream of the ERG operon and ligated it to the gene of interest. The sequence of forward primer in this case was: **AAGCTTAACTACCGGCGTGCAACA**.

The second complementation construct was designed by amplifying the entire operon from the first gene *egtA* to 100bp DS from *egtE* (primers are PF and E-GR in Table 2.7)

The third set of complementation constructs were generated by amplifying each gene and cloning it into the HindIII and ClaI sites of the pMV306hsp downstream of the hsp60 promoter (Table 2.8).

Two constructs were designed for the complementation of *mshA*.

The first construct was designed by cloning the region from 1545 US to 547bp DS *mshA* to the Hind III site of pMV306hsp (Table 2.8). The second construct was designed by cloning *mshA* downstream of the hsp60 promoter of pMV306hsp at the HindIII and HpaI site (Table 2.8)

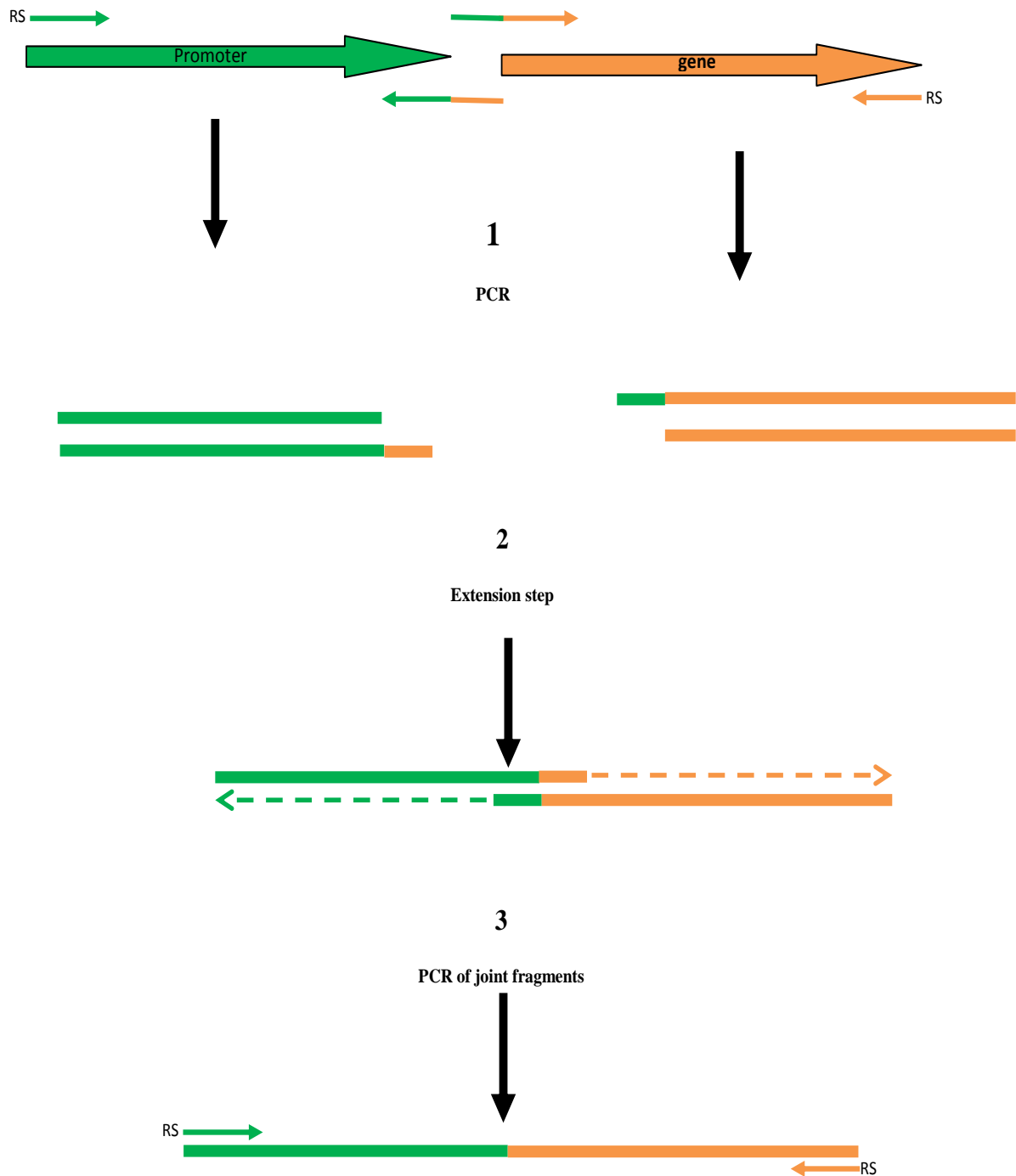


Figure 2.3 Illustration of the Joint PCR technique used to design the complementation constructs

1: primers flanking the promoter and the gene are designed. Either the reverse primer of the promoter or the forward primer of the gene or both is designed with and overhanged 10-40 bases end that is complementary (or identical) to the first few bases of the proximity of the fragment to be ligated. RS: restriction site, the promoter forward primer and the gene reverse primer are designed with a specific restriction enzyme site (at the extremity), not found in the gene, neither in the promoter but found at the multiple cloning site of the integration vector. The probe and the gene are amplified separately. 2: The two products from the previous step are brought together in a reaction and allowed to hybridize to each other, and then a polymerase will fill in the gap between two hybridized fragments thereby linking them. 3: The resulting joint fragment will be amplified using the forward primer of the promoter and the reverse primer of the gene.

Table 2.12 Joint PCR reaction set up

Step 1: Amplification of the promoter and the gene by Phusion polymerase (see Table 2.2)	
Step 2	
Reagents	Final concentration
5X Phusion HF or GC buffer	1X
2.5mM dNTPs	0.25mM
Amplified promoter product	≤200ng
Amplified gene product	≤200ng
Phusion polymerase	0.025u
H ₂ O	Up to 40ul
Thermo-cycling	98°C for 1mins and 60°C for 10mins
Step 3	
Total reaction product above	40µl
Forward primer of the promoter	0.4µM
Reverse primer of the gene	0.4µM
5X Phusion HF or GC buffer	0.2X
Phusion polymerase	0.025u
H ₂ O	Up to 50ul
Thermo-cycling	Phusion polymerase thermo-cycling conditions as described in Table 2.3

2.3 Genotyping of the mutants

Southern blotting was performed as previously described [178].

- **Genotyping of *M.smegmatis* mutants**

PstI was used to digest the genomic DNA while 6247SBF and 6247SBR primers (Table 2.3) were used to amplify the probe of interest that will hybridize to the target genomic region.

-Genomic DNA extraction

In order to extract genomic DNA, mycobacteria were allowed to grow on plates until they formed a thick layer of cells. These cells were scrapped using sterile loops into tubes containing 9ml of the extraction buffer (made up of 5% monosodium glutamic acid, 50mM Tris-HCl and 25mM EDTA) and glass beads (5mm diameter) Lysozymes (Roche Diagnostics Deutschland GmbH Sandhofer Straße 116; 68305 Mannheim, Germany) and RNaseA (Roche) were added to final concentration of 2.8mg/ml and 2.8µg/ml respectively and the suspension was vortexed for 2 mins and mixed by inversion every 30 mins at 37°C. A volume of 650µl of proteinase buffer and 150ul 10mg/ml proteinase K (Roche, Germany) were added in the suspension which was mixed by inversion and incubated at 45°C overnight.

The next day, 2.5ml phenol, 2.4 chloroform and 1ml isoamyl alcohol (Kimix) were added to the suspension, which was gently mixed every 30 mins at room temperature for 2 hrs and later centrifuged for 20 mins at room temperature at 4000rpm. The top phase was transferred into another tube containing 4.8ml chloroform and 200µl isoamyl alcohol. The resulting

suspension was centrifuged again for another 20 mins. The top phase was transferred into another tube containing 600µl sodium acetate. After adding 7ml ice cold isopropanol, the precipitated DNA was fished out of the solution using a glass rod. The precipitated DNA was immersed in 70% ethanol for 10mins, and then transferred to a clean eppendorf and allowed to dry. The resulting DNA was dissolved in nuclease free water or TE (1M Tris-HCl pH 8, 0.5M EDTA pH 8, Kimix; Unit 1, Shop 4, Ruco Park, Boston Cir, Cape Town, 7490) at room temperature overnight. Six micrograms of the genomic DNA was digested with pstI (40000-60000 U) in a 100µl reaction volume overnight. The digested sample was precipitated: by adding 1/10th volume of 3M sodium acetate and 2.5 volumes of ice cold ethanol and incubating overnight at -20°C. The next day, the sample was centrifuge at 4°C for 30 mins (10000rpm) and the supernatant discarded. Then the DNA pellet was washed with 500µl of 70% ice-cold ethanol and centrifuged again for another 30 mins at 4°C (10000rpm). The supernatant was discarded again and the DNA pellet was air-dried overnight.

The next day the pellet was re-suspended in 20µl loading dye containing 0.2ng/µl marker 10 (Roche, ranging from 938bp to 13900bp) and TE buffer (pH 8.0). A 10µl aliquot of this sample was separated on a 0.8% agarose gel using a 1X TAE buffer system (0.4 M Tris acetate, 0.001M EDTA) for 3 hours at a voltage of 65mV.

-Southern transfer of the DNA onto a membrane

Thereafter the gel was visualised to confirm complete digestion of the DNA. The DNA on the gel was thereafter denatured by incubating it for 30 mins at RT in 500ml of a denaturing buffer (1.5M NaCl, 0.54M NaOH). After the denaturing buffer was discarded, the gel was neutralized for 30 mins in a neutralization buffer (1.5M NaCl and 0.5M Tris-HCl, pH7.5). The digested DNA was then transferred onto a positively charged Hybond N1 membrane (GE Healthcare, UK) by capillary action according to the manufacturer's recommendations.

- Probe labelling, membrane hybridisation and detection

This was performed with the Amersham ECL Nucleic acid Labelling kit (GE Healthcare, UK) according to the manufacturer's instruction as follows: Approximately 200ng of the probe was rendered single stranded by heating it at 100°C for 5mins and snap freezing it for 5 mins. A volume of 15µl of Gluteraldehyde and 15µl of horse radish peroxidase were added to the probe and incubated at 37°C for 10 mins. The labelled probe was added to a plastic bag containing the hybridization buffer and the membrane (pre-hybridized at 42°C for at least an hour). Hybridization was allowed to occur overnight at 42°C in a water bath incubator. The membrane was washed twice in a pre-warmed 42°C wash buffer (36% urea, 0.4% SDS, 0.5X

SSC). Then the kit detection reagents were added into a plastic bag containing the washed membrane. The membrane was then exposed to an X-ray film which was later developed.

- **Genotyping of *M.tuberculosis* mutants**

Extracted and digested genomic DNA (4-6µg) was separated on a 1% agarose gel, then the DNA was depurinated in 250mM HCl for 10 mins at RT then rinsed in dH₂O.

-Southern transfer of DNA onto the membrane

Then DNA was denatured by incubating the gel at RT for 30mins in the denaturing buffer (0.5MNaOH, 1.5mNaCl) and neutralised in the neutralization buffer (0.5MTris/HCl Ph7.5, 1.5MNaCl) for another 30mins. Southern transfer was performed using the positively charged nylon membranes (Roche Diagnostic GmbH Mannheim, Germany) overnight in 20XSSC (3M NaCl, 300mM sodium citrate, pH 7). The membranes were washed in 2X SSC the next day and baked for 2hrs at 80°C between 2 Wattman papers.

-Probe labelling

The DIG High Prime DNA labelling and detection kit II and the DIG wash and block Buffer set (Roche) were used for the labelling of the probe. An amount of 150-200ng of probe DNA was denatured at 100°C for 10mins and snapped cooled on ice for 5mins and then was added in 1X DIG High prime and incubated for 24-48hr at 37°C for the labelling reaction to occur. The reaction was stopped at 65°C for 10mins.

-Prehybridization and hybridization of the membrane

The membranes were pre-hybridized at 65°C for 30-60mins (optimal hybridization temperature is equal to the melting temperature of the probes minus forty two) in the pre-hybridization buffer supplied with the detection kit in a shaking water bath. Then the individual denatured probes were added in the hybridization buffer of each membrane that was preheated at 65°C. The pre-hybridization buffer was replaced with the individual hybridization buffers and the sealed membranes were incubated at 65°C overnight without air bubbles. Then next day, the membranes were washed in a high stringency buffer (2XSSC/0.1%SDS) preheated to 65°C at RT for 5mins twice, then in a preheated low stringency buffer (0.5XSSC/0.1%SDS) twice for 15mins at 65°C in a shaking water bath. Then the membranes were incubated with shaking at RT for 2 mins in 1X maleate buffer, then for 30mins to 3hr in the blocking solution. The membranes were then incubated for 30mins in the blocking solution containing the specific antibody, washed twice in 1X washing buffer at RT for 15mins and then equilibrated with the detection buffer for 3mins.

-Detection

Finally each membrane was placed in hybridization bags, 1-3ml CSPD (chemiluminescent substrate for alkaline phosphatase) was applied to each membrane, air bubbles were removed and the membranes were heat sealed in the bag. Following, incubation at RT for 5mins, excess fluid was removed, and the membrane were sealed again and these were incubated at 37°C for 10mins. The bands were then detected by the ChemiDoc™ MP System (BioRad; 2000 Alfred Nobel Drive, Hercules, California 94547, USA).

2.4 Drug susceptibility testing of mutants

This was achieved by the broth micro-dilution assay. A two-fold serial dilution of the drug was performed across a V-bottom 96 well plate (Cellstar® Greiner Bio-One GmbH) in a volume of 50µl. An equal volume of exponential mycobacterial culture diluted to 10⁴ CFU/ml was aliquoted in every well except the first row of wells, which served as the negative control (Figure 2.4). After incubation for 3-4 days for *M. smegmatis* or 8 days for *M. tuberculosis*, resazurin or alamar blue (Sigma Aldrich; St. Louis, MO, USA) was added in every well to a final concentration of 0.001% to determine growth which is indicated by a pink coloration (Figure 2.4). Alternatively, growth was assessed visually by looking for a white pellet at the bottom of the well. The MIC was reported as the range between the concentration of the well where 99% of the growth is inhibited and the well just before it (where growth is obvious) (Figure 2.4). Results are representative of 2 to 6 independent experiments.

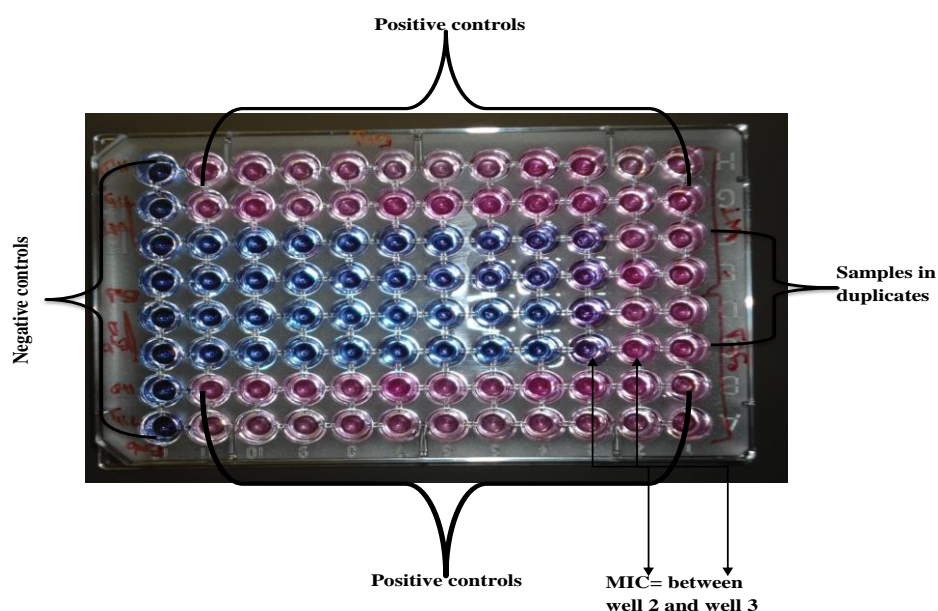


Figure 2.4 Illustration of broth micro-dilution

Cells of the first two and last two columns except the first row represent positive controls where no drugs were added, while the blue first row represents the negative control where drugs were added but the culture were not.

2.5 Growth curve of mutants

- **Growth curve of *M. smegmatis* mutants**

All strains were maintained as frozen stocks at -80°C . Frozen stocks were used to inoculate 10ml (*M. smegmatis*) of starter cultures which were incubated overnight in a shaking incubator at 37°C . These were then sub-cultured in 200ml of culture media to an OD_{600} (optical density at 600 nm wavelength) of 0.05. The subcultures were incubated in sterile 1L Erlenmeyer flasks in a shaking incubator at 37°C for approximately 48 hours. Every 3 hours, a 500 μl aliquot of each culture was taken and the OD_{600} measured using a spectrophotometer (ULTROSPEC 4051, LKB BIOCHROM LTD, Science park, Cambridge cb4 4bh, England). Where appropriate, culture was diluted to obtain a reading below 1 in order to be within the concentration range that will give a reliable reading.

- **Growth curve of *M. tuberculosis* mutants**

Frozen stocks of each strain were used to inoculate ~5ml of a starter culture that was incubated at 37°C for approximately 7 days in tissue culture flasks. A 35ml of culture was then inoculated to a starting OD_{600} of ~0.05. The OD_{600} was recorded every second day for a period of 25 days. Results are representative of 3 independent experiments.

Chemical complementation of the mutants was achieved by supplementing the culture media of the mutants with ERG to a final concentration of ~1mg/ml. Results are representative of 3 independent experiments for all tested mutants except $\Delta egtD$ which is represented by 2 independent experiments because the third biological replicate got contaminated before it entered stationary phase.

We also evaluated the growth rate of each mutant using the MGIT (mycobacterial growth indicator tubes) system. Tubes containing BBL MGIT medium (Becton, Dickinson and Company) were supplemented with 800 μl OADC and 100 μl (103-104) of diluted cultures were added to each vial and growth was monitored by the MGIT fluorescence reader. This experiment was repeated nine times.

2.6 Oxidative, acidic and nitrosative stress susceptibility testing of mutants

- **Testing of *M. smegmatis* mutants**

M. smegmatis was grown to an OD_{600} of 1 and exposed to 2mM, 0.6 mM of Luperox® Tert-Butyl hydroperoxide (TBHP, 70% in water, Sigma Aldrich) and Cumene hydroperoxide (CuOOH in DMSO, Sigma Aldrich) respectively for 2 hours. Cell viability was assessed by colony forming unit (CFU) counts before and after exposure to oxidative stress.

To assess response to nitrosative stress, mycobacteria were grown to an OD₆₀₀ of 0.5 and exposed to 5mM Diethylaminetriamine nitric oxide adduct (DETA/NO, Sigma Aldrich) for 3 hours, and CFU counts were assessed before and after exposure.

- **Testing of *M. tuberculosis* mutants**

Exponentially growing mycobacterial cultures were washed in phosphate buffered saline (PBS, Sigma Aldrich). The washed cultures were used to inoculate 5ml of acidified PBS (pH~4.5, prepared fresh for every experiment) to an OD₆₀₀ of ~0.2-0.3. Each culture was serially diluted and plated on the day of exposure, the third day and the fifth day [191][193]. The percentage survival was evaluated as the CFU of each time point divided by the initial CFU multiply by 100. Results are representative of 3 to 4 independent experiments.

On the other hand, early to mid-exponential mycobacteria were washed in PBS and re-inoculated in PBS to an OD₆₀₀ of ~0.2-0.3 and exposed to either 1mM DETA-NO [194], to 1mM CuOOH or 500µM pyrogallol (PRG). Cultures were serially diluted and plated before exposure, 24 and 48 hours after exposure.

2.7 SDS-PAGE analysis of the mutants

Mycobacteria were grown on 7H11 agar plates for 9 days. Cells were scraped off the plates and re-suspended in Middlebrook 7H9 liquid medium. The suspension was centrifuged and the pellet re-suspended in cold (4°C) lysis buffer (10mM Tris-HCL, 0.1% Tween-80 and complete protease inhibitor cocktail). Cells were homogenized using the FastPrep-24 (MP Biomedicals, LLC; 3 Hutton Center Drive; Suite 100; Santa Ana, CA92707 USA) (6m/s) in tubes containing 0.1mm beads (Biospec Products Inc; Bartlesville, UK) 6 times for 20 seconds, with 1 minute intermittent cooling steps on ice [179]. Total protein was quantified using the RCDC protein assay kit (Bio-Rad Laboratories, Hercules, CA 94547) according to the manufacturer's instructions. Five micograms of total protein from each strain was treated with 2-mercaptoethanol and SDS and separated on an SDS-PAGE gel containing of 4% stacking gel (0.124 M Tris-HCl, 0.1%SDS, 0.05% Ammonium persulfate, 0.09% TEMED (N,N,N',N'-tetramethylethylenediamine) , 4% Acrylamide, 0.1% Bis-acrylamide) and 15% separating gel (0.375 M Tris-HCl, 0.1%SDS, 15% Acrylamide, 0.375% Bis-acrylamide, 0.05% ammonium persulfate, 0.581M TEMED). The running buffer (pH~8.3) contained 25mM Tris, 192mM glycine and 0.1% SDS. Bands were visualized with the aid of the Coomassie brilliant blue (CBB) solution (2.5% CBB, 45% methanol, 10% acetic acid) and the identity of the 15KDa *MSMEG_0447* (Ohr) was confirmed by mass spectrometry using

the Thermo Scientific EASY-nLC II connected to a LTQ Orbitrap Velos mass spectrometer (Thermo Scientific, Bremen, Germany).

CHAPTER 3: THE ROLE
OF ERGOTHIONEINE IN
Mycobacterium smegmatis

CHAPTER 3: THE ROLE OF ERGOTHIONEINE IN *Mycobacterium smegmatis*

The aim of this study was to evaluate the role of ERG in a non-pathogenic mycobacterium which is a well-documented model for *M. tuberculosis* research. This study has been published in the Journal Of Antimicrobial Agent And Chemotherapy; see reference [99].

Mycobacterium smegmatis is a fast-growing mycobacteria closely related to *M. tuberculosis*. Since *M. smegmatis* is non-pathogenic (does not require a biosafety level 3 laboratory) and grows faster than *M. tuberculosis* (doubling time 3hrs versus 24hrs), it is often used as the model organism for studying mycobacterial physiology [180, 181]. In this study we aimed to evaluate the role of ERG in mycobacteria by generating strains of *M. smegmatis* deficient in ERG alone or both ERG and MSH.

The enzyme EgtD catalyses the methylation of histidine in ERG biosynthesis (Figure 1.8). The gene coding for that enzyme (*egtD*) was deleted in the wild type *mc²155* and the MSH-deficient mutant $\Delta mshA$ by two-step allelic exchange mutagenesis. The susceptibility of the mutants to oxidative stress, nitrosative stress and antibiotics was subsequently evaluated. In addition, ERG secretion was investigated by liquid chromatography tandem mass spectrometry (LC-MS) and flow cytometry.

Our first aim in this study was to prove that EgtD is essential for ERG biosynthesis

Our second aim was to show that ERG protects *M. smegmatis* from toxic compounds, ROS and NOS.

It has been discussed in the previous chapter that ERG redox potential is lower than that of many other thiols. This makes it more stable and therefore do not require enzymatic recycling as other thiols. Therefore it is more likely to be found extracellularly.

Our third aim then, was to show that ERG is secreted by *M. smegmatis*

3.1 *M. smegmatis* secretes ERG

Investigation of extracellular ERG was prompted by a previous observation that ERG was detected in the buffer fluid surrounding resting cell preparations of *M. smegmatis* [157]. ERG was detected both in the culture media and in the cell lysate of *M. smegmatis* at the three time points investigated (Table 3.1).

Table 3.1 Ergothioneine concentration (pg per 10^5 CFU) in *mc^2155* and $\Delta mshA$

Strain	OD ₆₀₀ ~0.5		OD ₆₀₀ ~1		OD ₆₀₀ >2	
	IE	EE	IE	EE	IE	EE
<i>mc^2155</i>	4.07±0.66	17.03±3.5	1.74±0.30	7.6±1.45	0.83±0.80	12.66±2.65
$\Delta mshA$	7.50±3.5	44.30±4.0	6.3±2.61	39 ±10.5	1.62±0.48	37.61±2.55

Legend: **IE:** intracellular ERG, **EE:** extracellular ERG, the majority of ERG is extracellular and ERG is higher in the MSH-deficient mutant, data representative of 3 biological replicates

Furthermore, the percentage of extracellular ERG was significantly higher than intracellular ERG at all three time points. In order to confirm that the ERG detected in the media was not due to leakage from cells with disrupted cell membranes, the membrane integrity of the cells within the population was determined by flow cytometry (Figure 3.1).

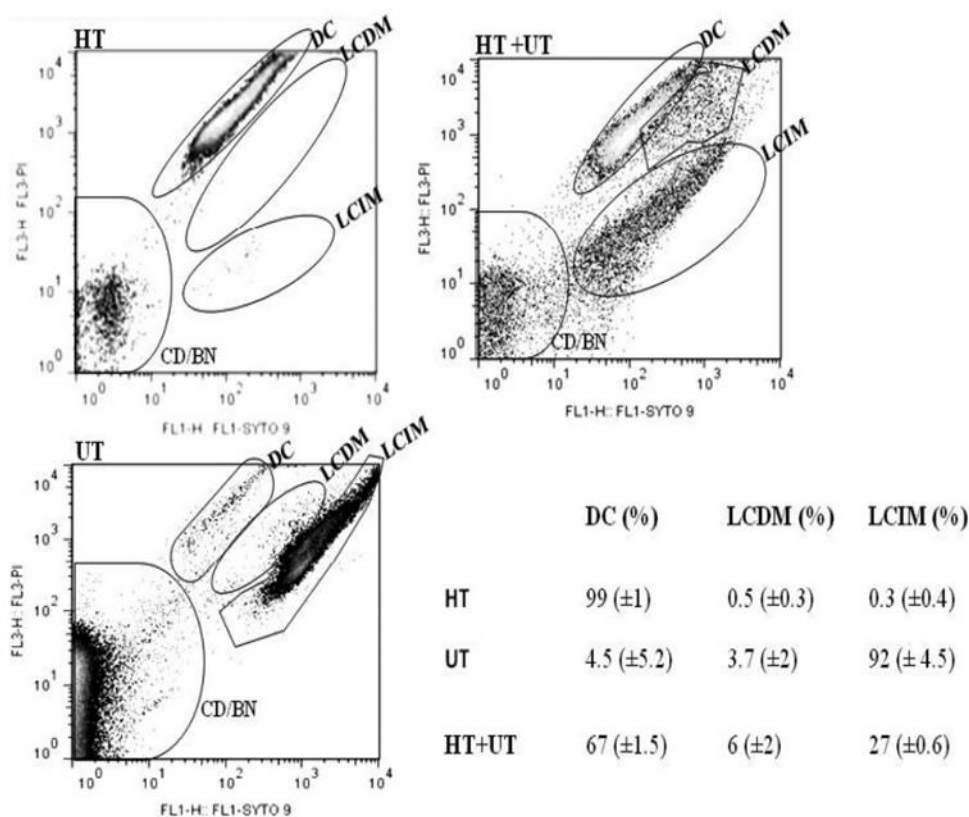


Figure 3.1 Characterization of *M. smegmatis* membrane integrity by flow cytometry

UT: untreated sample. HT: heat treated sample, DC: dead cells, CD/BN: cellular debris and background noise, LCDM: live cells with damaged membrane, LCIM: live cells with intact membrane, HT+UT: mixture of an

equal ratio of the UT and HT samples. The program Flowjo (version 6) was used to analyse the population distribution of mycobacteria, which was represented by a pseudocolor plot. Using automatic and manual gating options, we could count the number of events per population and therefore estimate the representative percentage of each population. When the untreated sample was stained with SYTO-9 and propidium iodide (PI), the analyses indicated that an average of 92% of the population is LCIM, while 3.7% is LCDM and 4.5% are DC. In the heat treated sample, an average of 99% of the population was indicated to be dead, while 0.5 % was LCDM and 0.3% was LCIM. When an equal amount of the treated (HT) and untreated (UT) cells were mixed, 67% of the population was indicated as dead, while 27% was LCIM and 27% was LCDM. This shows that this technique was sensitive enough to detect cells with damaged membranes even in a population mixture, implicating consistency of the result showing that in an actively growing wild type *M. smegmatis* culture of OD 600 ~0.5, the membrane integrity of ~92% of the cells is still intact (Table 3.2).

Dual nucleic acid staining was performed using the membrane permeable dye SYTO-9 and the non-permeable propidium iodide (PI), that is able to enter cells and displace SYTO-9 only when the membrane is damaged [182]. Cells were gated into three populations corresponding to their membrane integrity on the basis of PI and SYTO-9 intensities. Cells with the highest PI fluorescence and the lowest SYTO-9 fluorescence represent dead cells (DC) in the population, and heat treatment of *M. smegmatis* results in 99% of the cells gating into this subpopulation. The population with the lowest PI fluorescence and the highest SYTO-9 fluorescence represent living cells with intact membranes (LCIM), and this was absent following heat treatment of *M. smegmatis*. A third intermediate population was observed, and is thought to represent cells in the population which are live but have damaged membranes (LCDM), as described previously [161] (Figure 3.1).

Analysis of *M. smegmatis* grown to an OD₆₀₀ ~ 0.5, 1 and >2 revealed that approximately 92%, 87% and 86% of the culture population was made of LCIM respectively, while the minority was made of the population of LCDM and DC (Table 3.2).

Table 3.2 Estimation of the different mycobacterial population in *mc²155* culture at different growth stage by Flow cytometry

OD ₆₀₀	DC (%)	LCDM (%)	LCIM (%)
~0.5	4.5±5.2	3.7±2	92±4.5
~1	2.6±0.84	10.1±2.17	87.22±2.06
>2	2.5±1.6	11.2±2.5	86.3±4.02

The majority of cells have an intact membrane during every growth stage; data are representative of 3 biological replicates

To further confirm the membrane integrity of the cells within the population, the culture medium was assayed for MSH, which is not normally present extracellularly [91, 183]. MSH was analysed by LC-ESI-HRMS in the cell lysate of wild-type *M. smegmatis* as previously described (Figure 3.2 A&B) [158].

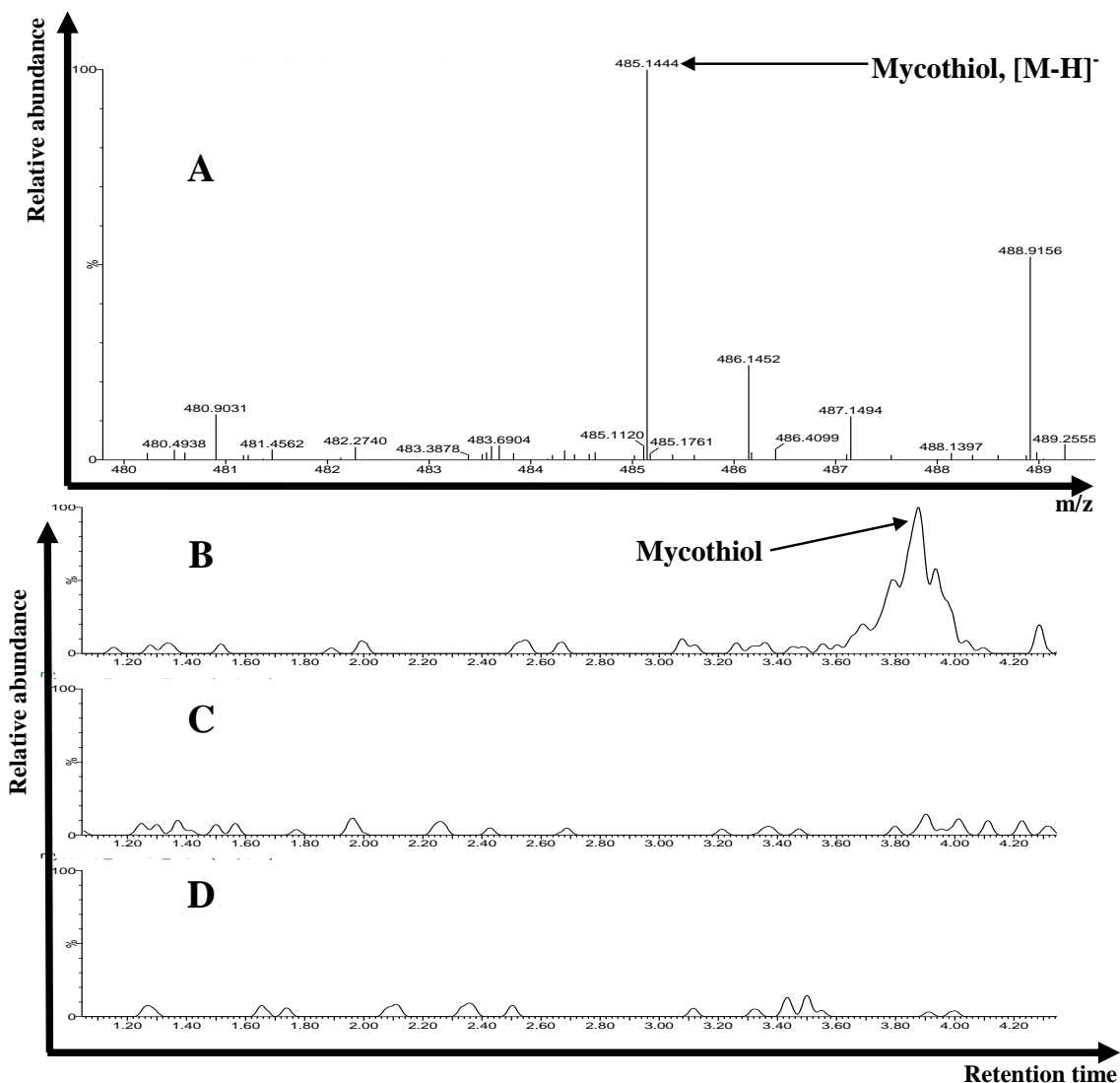


Figure 3. 2 Detection of mycothiol in *M. smegmatis*

Figure 3.2A: The ESI negative mass spectrum (of the peak at 3.87 min; Figure 3.2B) of the cell lysate of the wild type. Analysis was performed using LC-ESI-HRMS. Accurate mass measurement (m/z 485.1444) was performed within 0.6 ppm of the calculated exact mass (m/z 485.1441) of the deprotonated mycothiol ion [158], which strongly indicates the presence of mycothiol. Figure 3.2B, 3.2C, and 3.2D: The extracted ion chromatograms at m/z 485.144. Mycothiol was detected (retention time of 3.87 min) of the cell lysate of the wild type (Figure 3.2B), but not in its culture media (Figure 3.2C). As a negative control the cell lysate of the $\Delta mshA$ mutant was analysed (Figure 3.2D).

The identity of the ion was verified by its absence in the $\Delta mshA$ mutant, which is MSH-deficient (Figure 3.2 D). No MSH was detected in the culture media from wild-type *M. smegmatis* (Figure 3.2 C), supporting the flow cytometry data. Therefore, while a small percentage of ERG present in the media may originate from cells with disrupted membranes, the observation that the largest proportion of ERG (~81% at OD_{600} 0.5 and 1) is found in the

media whilst the majority of cells display an intact membrane (~90% at OD₆₀₀ 0.5 and 1), implies that ERG is secreted by *M. smegmatis*.

ERG exists as a thione in solution at neutral pH, and as a result it is relatively resistant to oxidation [184]. It is therefore better suited to function extracellularly than MSH, since it does not require an enzyme to maintain it in the reduced form [132]. While MSH is not detected extracellularly, a study utilizing MSH-deficient mutants demonstrated that *M. smegmatis* is able to actively transport MSH into cells [183] and *MSMEG_1642* was proposed as a possible MSH transporter. Since ERG is unable to diffuse across membranes [128, 185], an ERG transporter would also be required in *M. smegmatis*. In humans the OCTN1 transporter is required for ERG transport into cells and involves co-transport of Na⁺ [128]. This leads us to speculate that the ERG transporter in mycobacteria may be a member of the monovalent cation: proton antiporter family or the H⁺/Na⁺ translocating F-type, V-type and A-type ATPase superfamily, which both utilise Na⁺ as a substrate [186]. Since ERG has anti-inflammatory properties [141], the potential secretion of this molecule by *M. tuberculosis* may play a role in modulating the immune response by the host during infection and therefore warrants further investigation.

A previous study found that the ERG concentration is higher in the MSH-deficient mutant of *M. smegmatis*, suggesting that ERG compensates for the loss of MSH in this organism [100]. Our analysis revealed a similar trend with a 2-5 fold increase in intracellular and extracellular ERG levels observed for the $\Delta mshA$ *M. smegmatis* mutant (Table 3.1), which appears to be lower than was previously reported, but this may be due to the different methods for thiol quantification. The previous study used a method based on the HPLC separation and fluorescent detection of thiols conjugated to monobromobimane (mBBr) [187, 188], whereas we used UPLC-ESI-MS/MS to quantify ERG.

3.2 EgtD is essential for ERG biosynthesis

The gene *egtD* was successfully deleted in *mc²155* and $\Delta mshA$ *M. smegmatis* mutant. The genotype of the mutants was confirmed by colony PCR (Figure 3.3), and by Southern blotting (Figure 3.4).

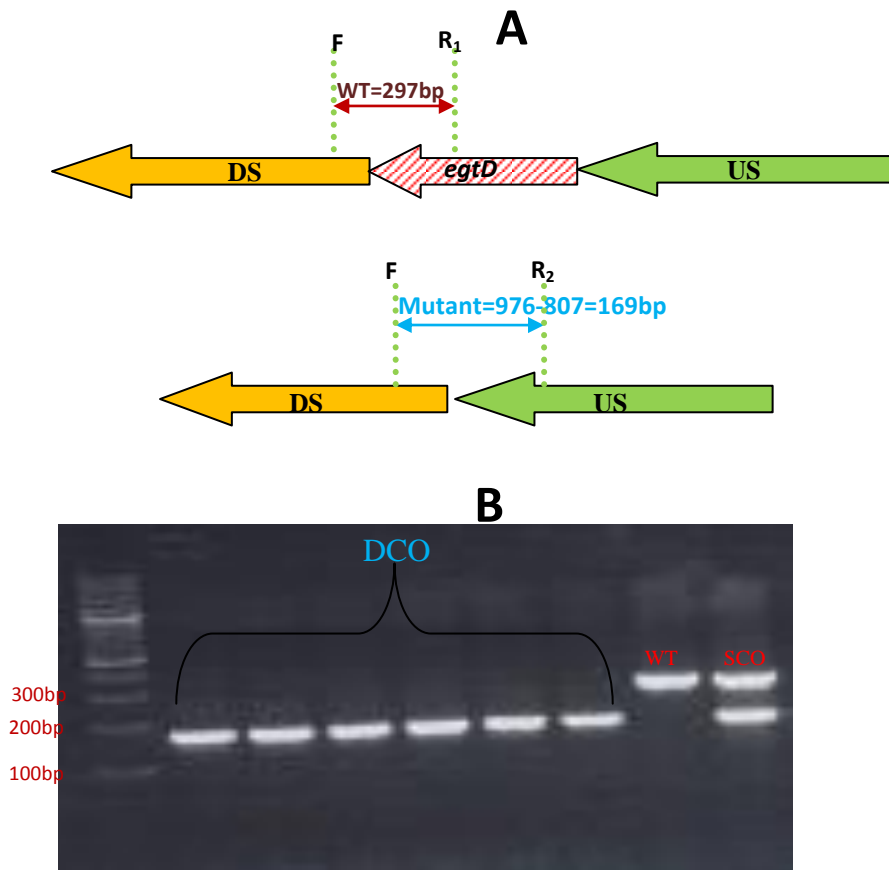


Figure 3.3 Colony PCR of the $\Delta egtD$ mutant

A: Map indicating the fragment sizes expected after PCR screening to confirm deletion of *egtD* (F: forward primer, R: reverse primer, US: upstream region, DS: downstream region); B: PCR screening of *egtD* deletion, WT: wild type band 297bp, SCO: single cross over; consists of the wild type band 297bp and the mutant band 169bp; DCO: double cross over, indicating deletion by the 169bp band

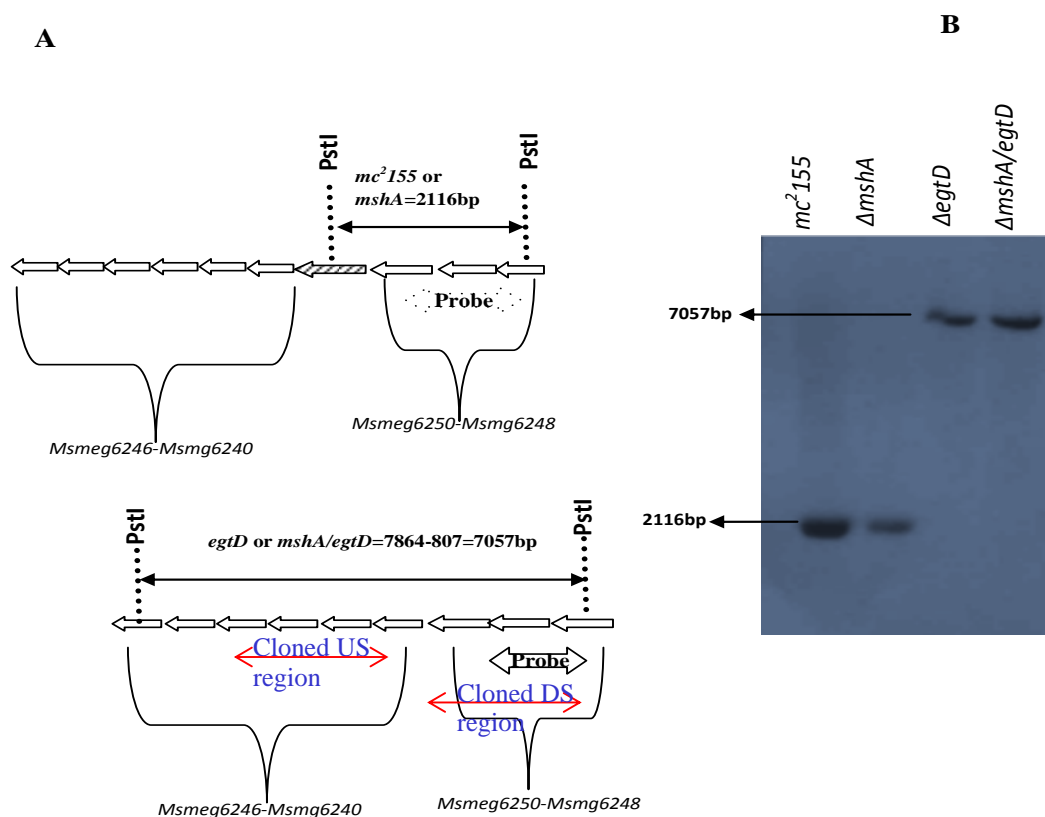


Figure 3.4 Validation of *egtD* deletion by Southern blotting

Southern blotting of digested genomic DNA of the different strain was performed as previously described [178]

A: Restriction map of the wild-type and mutant strains. *Pst*I cuts within *egtD* and on the a the downstream region in the wild type strain, while in the mutant strain *Pst*I cuts within the cloned DS region and outside the cloned US region to rule out illegitimate homologous recombination.

B: Southern blotting of the fragment restricted by *Pst*I, the band (2116bp) in the first and second lanes represents the wild type and the Δ *mshA* mutant which have an intact *egtD* gene, while the 7057bp for Δ *mshA/egtD* and Δ *egtD* strains indicates the deletion of *egtD* and the loss of the *Pst*I site.

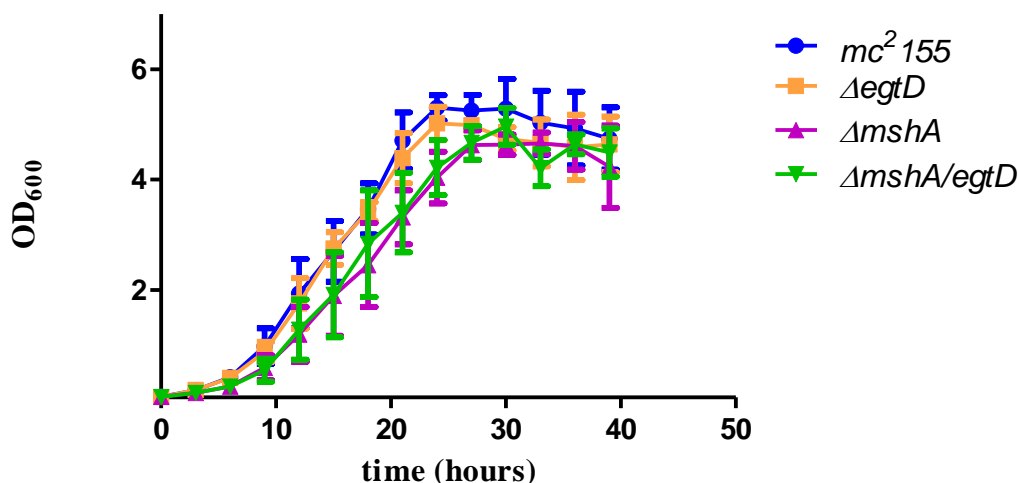
Our primary concern when targeting *egtD* was the potential compensation by other methyltransferases found in mycobacteria [189]. However when EgtD was blasted against *M. tuberculosis* proteome, very few proteins share similarities with it, and the percentage coverage and similarity is lower than 50%. Indicating already that EgtD-deficiency may not be compensated for. In addition, it was shown that EgtD as opposed to other methyltransferase, is highly specific to histidine, N-monomethylhistidine and N, N-dimethylhistidine [155]. It does not bind to other substrates indicating how important is EgtD for ERG biosynthesis. And we could show as well in this study that EgtD is indeed essential for ERG biosynthesis since the EgtD-deficient mutants lack ERG as well. Loss of ERG biosynthesis in the Δ *egtD* single and Δ *mshA/egtD* double mutants and restoration of ERG biosynthesis in the complemented strains was confirmed by UPLC-ESI-MS/MS (Table 3.3).

Table 3.3 ERG concentration (pg/10⁵ CFU) in *M. smegmatis* mutants at OD₆₀₀~ 1

Fraction	<i>mc</i> ² <i>155</i>	Δ <i>mshA</i>	Δ <i>egtD</i>	Δ <i>mshA/egtD</i>	Δ <i>egtDc</i> *	Δ <i>mshA/egtDc</i> *
Intracellular	1.74±0.3	6.3±2.6	0	0	0.88±0.3	2.2±0.5
Extracellular	7.6±1.5	39±10.5	0	0	4.3±2	16±5.1

* Δ *egtDc*: complemented Δ *egtD*, Δ *mshA/egtDc*: Δ *mshA/egtD* where *egtD* has been complemented; data are representative of three biological replicates

It was previously indicated that the Δ *mshA* mutant has a longer lag phase, however no growth defect was associated with the deletion of *egtD* in the wild-type strain (Figure 3.5); and the extended lag phase [107] and sensitivity to the inoculum size [100] observed previously for the Δ *mshA* mutant, was slightly exacerbated by the loss of ERG in this mutant.

**Figure 3. 5** Growth curves of *M. smegmatis* strains

Starter cultures were used to inoculate main cultures to an OD₆₀₀ of 0.05, and growth was monitored by OD₆₀₀ readings every 3 hours for ~48hours

Since the ERG level in the Δ *mshA* mutant is elevated relative to the wild type strain, we compared the level of MSH in the ERG-deficient single mutant and the wild type via LC-ESI-HRMS. Relative comparison of the MSH peak area revealed no significant difference in the MSH levels between the two strains (Table 3.4, Figure 3.6). Therefore, while the ERG level is elevated in the MSH-deficient mutant, the MSH level is unchanged in the ERG-deficient mutant. This implies that the wild type MSH level may be adequate to compensate for the loss of intracellular ERG or that compensation occurs by another mechanism or there is no compensation.

Table 3.4 Relative abundance of MSH expressed by the peak area of the extracted ion chromatogram m/z 485.

<i>mc²155</i>	398.55 ± 19.36
Δ <i>egtD</i>	458.86 ± 23.04

Data are representative of three biological replicates

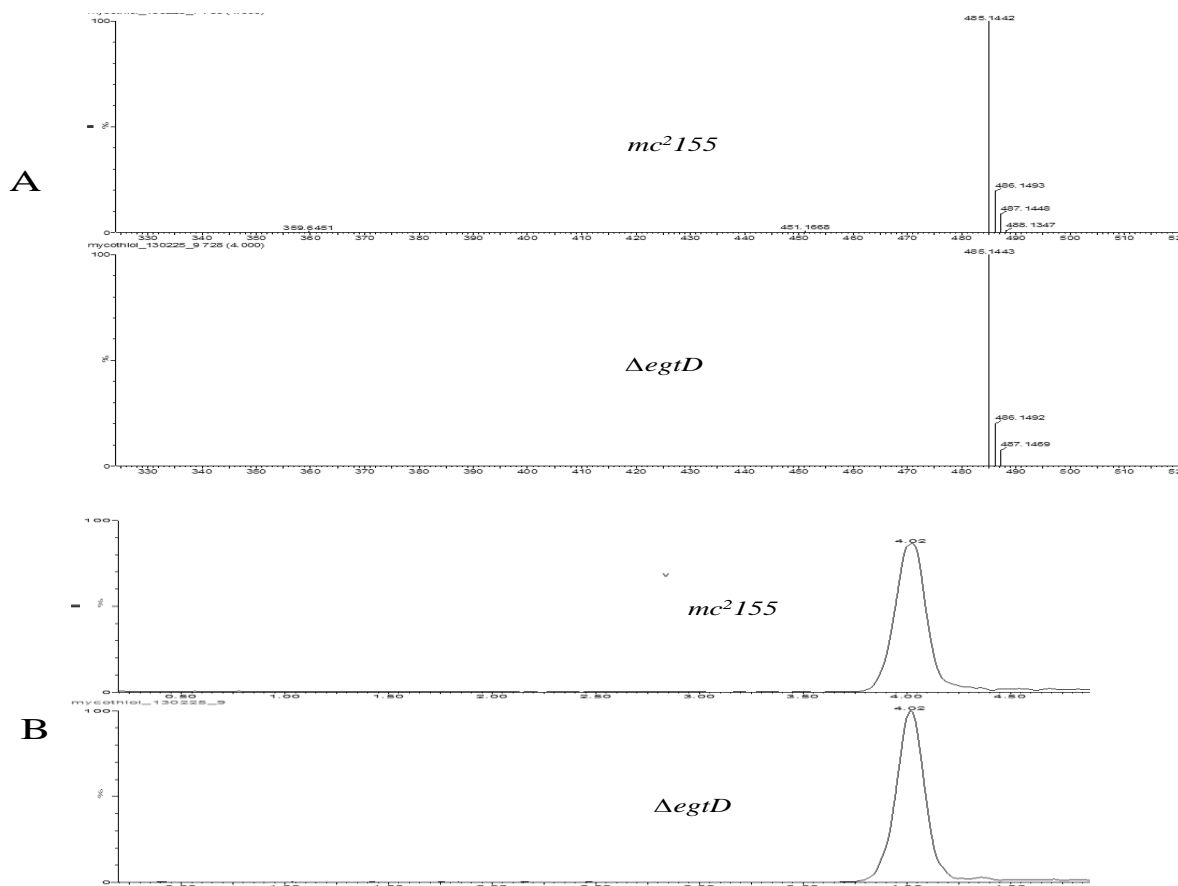
**Figure 3.6** Relative quantification of mycothiol by LC-ESI-HRMS

Figure 2.8A: The ESI negative mass spectrum (of the peak at 3.87 min) of the cell lysate of the wild type and of the ERG-deficient single mutant. Figure 2.8B: The extracted ion chromatograms at m/z 485.144 of the cell lysate of the wild type and of the ERG-deficient single mutant

3.3 ERG does not protect *M. smegmatis* from antibiotics

In order to determine whether the absence of ERG in *M. smegmatis* alters its sensitivity to antibiotics, we investigated the susceptibility of the different strains to antibiotics by a broth micro-dilution method [190]. Besides a slight ethionamide resistance in the ERG-deficient mutants, the susceptibility of the Δ *egtD* mutant and the Δ *mshA*/ Δ *egtD* mutant to isoniazid, ethambutol and kanamycin did not differ significantly from their respective parental strains (Table 3.5), demonstrating that ERG does not protect *M. smegmatis* from these compounds.

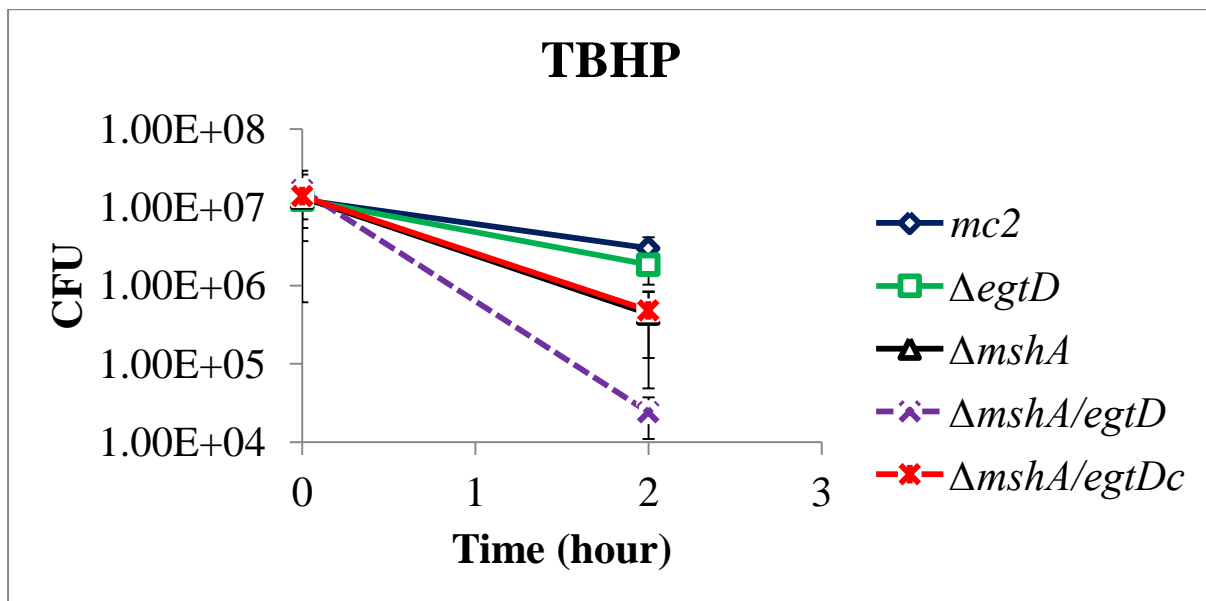
Table 3.5 Anti-tuberculosis drugs MIC ($\mu\text{g/ml}$) of *M. smegmatis* strains

Strains	Kanamycin	Isoniazid	Ethionamide	Rifampicin	Ethambutol
<i>mc</i> ² <i>155</i>	0.5-1	5-20	12.5-25	0.3-0.6	0.4-0.75
Δ <i>mshA</i>	ND	312-625	375-400	0.3-0.6	0.4-0.75
Δ <i>egtD</i>	0.5-1	5-20	25-50	0.3-0.6	0.4-0.75
Δ <i>egtDc</i>	ND	ND	12.5-25	ND	ND
Δ <i>mshA</i> / Δ <i>egtD</i>	ND	312-625	400-425	0.3-0.6	0.4-0.75

Legend: ND: not determined; ERG deficiency do not affect mycobacteria deficiency to current anti-tuberculosis drugs; data are representative of three biological replicates

3.4 ERG protects *M. smegmatis* from oxidative stress

A marginal increase in susceptibility to TBHP and CuOOH was observed for both the Δ *mshA* and the Δ *egtD* single mutants, while a distinct increase in susceptibility was observed for the Δ *mshA*/ Δ *egtD* double mutant (Figure 3.7).



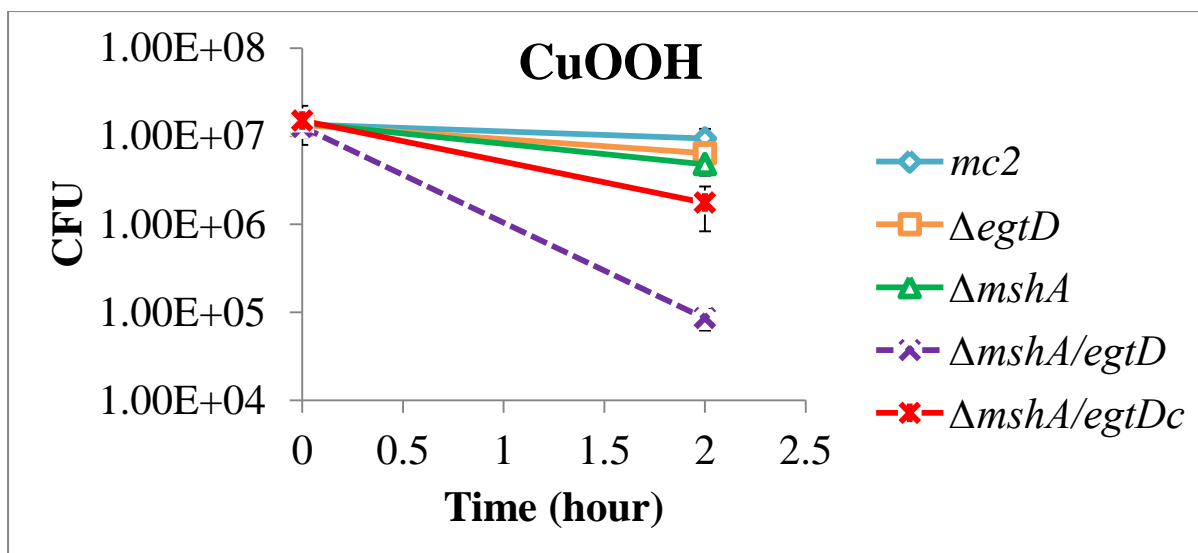


Figure 3.7 Survival of *M. smegmatis* mutants during in vitro oxidative stress

Mycobacteria were grown to the exponential phase and exposed to oxidative stress generated by either 2mM TBHP or 0.6mM CuOOH. The data were analysed by using GraphPad Prism version 5.01 and are represented as means with standard errors of the means. Two-way analysis of variance followed by a Bonferroni test was performed. The double mutant ($\Delta mshA\ egtD$) was more sensitive to oxidative stress than any other strain used in this study, it was significantly ($p < 0.01$) sensitive to oxidative stress generated by CuOOH (bottom panel) relative to the wild type and the $\Delta egtD$ mutant. The same trend was observed when bacteria were exposed to TBHP (top panel, $p > 0.05$).

This demonstrates that both ERG and MSH are involved in protecting *M. smegmatis* against peroxide, and that the loss of either low molecular weight thiol is potentially compensated for by the presence of the other. This compensation appears, at least in the MSH-deficient mutant, to involve increasing the amount of the remaining thiol molecule [100]. A previous study demonstrated that *MSMEG_0447*, annotated as Ohr (organic hydroperoxide resistance protein) is highly induced in the $\Delta mshA$ mutant, and that over-expression of Ohr in *M. smegmatis* increases resistance to CuOOH [100]. We therefore investigated the Ohr expression level in all strains using SDS-PAGE (Figure 3.8).

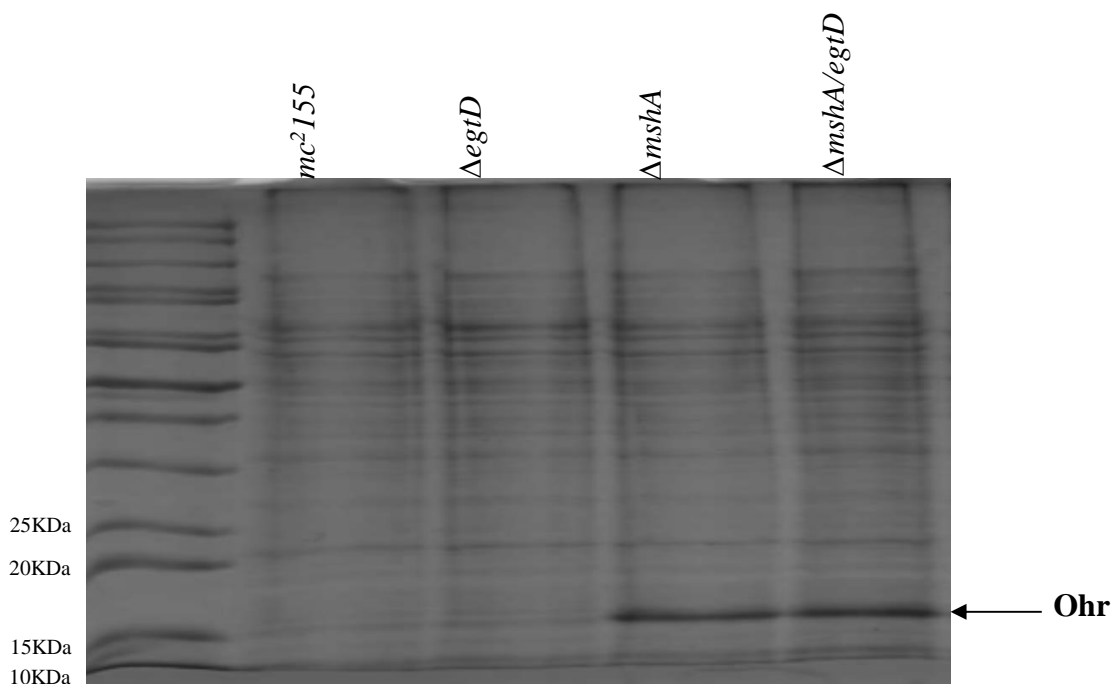


Figure 3. 8 SDS PAGE of *M. smegmatis* cell extract

The different *M. smegmatis* strains were grown on 7H11 solid culture for 11 days, and proteins were extracted and analysed as previously described [100, 179]. Relative intensities of protein fragment bands at 15KDa between the different strains were determined using the UN-SCAN-IT automated digitizing system (V 5.1, Silk Scientific Corporation) and showed at least a 7-fold increase in band intensity in the $\Delta mshA$ and $\Delta mshA/egtD$ mutants. A similar banding pattern was observed when mycobacteria were grown in liquid culture to an $OD_{600} \sim 0.8$ (Figure not shown). The identity of the 15KDa fragment was revealed to be *MSMEG_0447* (Ohr) by mass spectrometry using the Thermo Scientific EASY-nLC II connected to a LTQ Orbitrap Velos mass spectrometer (Thermo Scientific, Bremen, Germany). Quantification revealed a slight increase in the expression of Ohr in the MSH/ERG-deficient double mutant relative to the MSH-deficient single mutant. As was shown previously, Ohr is over-expressed in the *mshA* *M. smegmatis* mutant, but Ohr remained over-expressed in this same strain even when *egtD* was deleted. The wild type and $\Delta egtD$ mutant do not exhibit an over-expression of Ohr.

Ohr expression was elevated in the $\Delta mshA$ and $\Delta mshA/egtD$ mutants relative to the wild type strain and $\Delta egtD$ mutant. This indicates that the Ohr expression level is not influenced by the loss of ERG. In addition, the increased sensitivity of the ERG/MSH-deficient double mutant to peroxides, despite the elevated Ohr level suggests that ERG also plays a role in protecting *M. smegmatis* against peroxide. Despite the increased sensitivity of the MSH-deficient *M. tuberculosis* $\Delta mshA$ mutant to oxidative stress, it survives during the mouse-model of infection [102]. Considering the fact that *M. smegmatis* Ohr has no homolog in *M. tuberculosis* [100], we speculate that ERG may compensate for the loss of MSH in this organism and the lack of phenotype of the MSH-deficient *M. tuberculosis* mutant in the

mouse model is potentially due to compensation by ERG; however this remains to be demonstrated.

3.5 ERG does not protect *M. smegmatis* from nitrosative stress

The sensitivity of ERG-deficient mutants to nitrosative stress was not different to their parent strains (Figure 3.9). MSH-deficient mutants were slightly resistant to nitrosative stress generated by DETA/NO. A previous study showed that MSH-deficient mutants were not sensitive to nitrosative stress generated by sodium nitrite in a broth dilution assay [108], while another study demonstrated that MSH-deficient mutants were sensitive to nitrosative stress generated by a gaseous nitric oxide donor [106]. This therefore indicates that, the susceptibility of MSH-deficient *M. smegmatis* mutants to nitrosative stress is variable, depending on the nitric oxide donor, the method and the exposure time. However these variables were not optimized in this study.

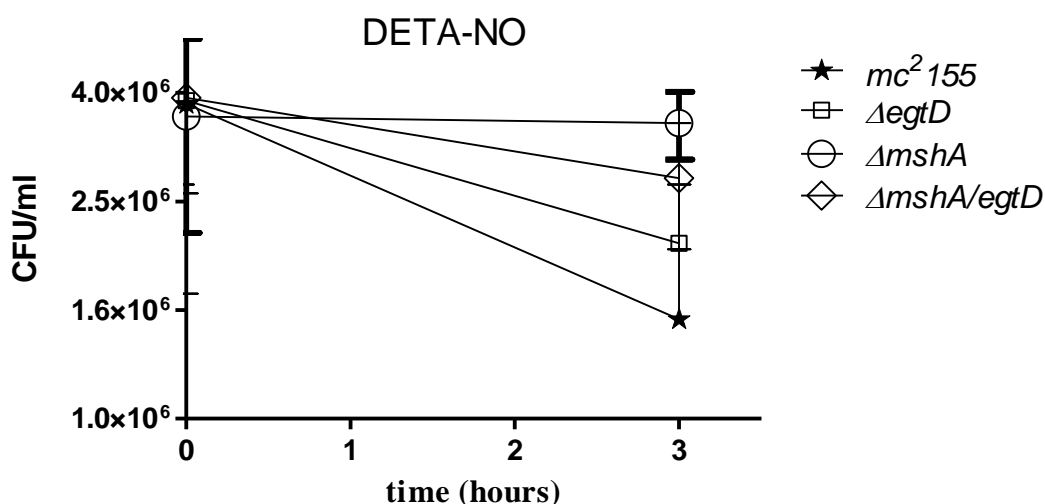


Figure 3.9 Survival of *M. smegmatis* strains to nitrosative stress generated by DETA/NO

Strains were grown to an early log phase ($OD_{600} \sim 0.5$) and exposed to nitrosative stress for 3 hours. Results are representative of at least 2 biological replicates. The data were analysed by using GraphPad Prism version 5.01 and are represented as means with standard errors of the means. Two-way analysis of variance followed by a Bonferroni test was performed. Mycothiol deficient mutants ($\Delta mshA$, $\Delta mshA/egtD$) were slightly resistant to nitrosative stress ($P < 0.05$).

3.6 Conclusion

The protective role of ERG in eukaryotes has been well documented [150]. However, little is known of its role in microorganisms. Its anti-oxidative role was reported in fungi [145] and in bacteria [144]. However in *M. smegmatis* it was reported that the MSH-deficient mutants produce more ERG [100], and then we demonstrated that ERG protects *M. smegmatis* from oxidative stress [99]. This study investigated the role of ERG in *M. smegmatis*. In order to

achieve that, we deleted the gene that code for the enzyme that catalyses the first step of ERG biosynthesis (*egtD*, the methylation of histidine) via a homologous recombination based cloning technique. This gene was deleted in a wild type strain of *M. smegmatis* (*mc²155*) and a MSH-deficient mutant strain of *M. smegmatis* (Δ *mshA*) generating ERG-deficient mutants (Table 3.3). This indicates that the enzyme EgtD is essential for ERG biosynthesis in *M. smegmatis*, and that it cannot be compensated for by any other enzyme.

The susceptibility of the ERG-deficient mutants to antibiotics was evaluated, and no significant change in the susceptibility of the mutants was observed (Table 3.5), indicating that ERG does not protect *M. smegmatis* from the antibiotics tested in this study. Investigation of the ERG-deficient mutants' susceptibility to nitrosative stress indicated as well that ERG does not protect *M. smegmatis* from nitrosative stress in the tested conditions (Figure 3.9).

However, the viability of the ERG/MSH-deficient double mutant was significantly affected by oxidative stress (Figure 3.7). The investigation of the expression of Ohr in the double mutant indicated that it was still up-regulated in this strain (Figure 3.8). Therefore, though Ohr may protect MSH-deficient *M. smegmatis* from oxidative stress as previously shown [100], the absence of ERG in this strain renders it more susceptible to oxidative stress, indicating the anti-oxidative role of ERG in *M. smegmatis*.

In this study we were also able to quantify extracellular ERG by UPLC/MS and could demonstrate that the majority (>80%) of biosynthesized ERG was found extracellular (Table 3.1). To rule out a possible leakage from damaged cells as being the reason for an elevated extracellular ERG, we investigated the membrane integrity of *M. smegmatis* cells before ERG quantification. We were able to show by flow cytometry that the majority of cells of exponentially growing culture of *M. smegmatis* possess an intact membrane (Table 3.2). Further, this enabled us to conclude that ERG is secreted by *M. smegmatis*.

This study indicates the protective role of ERG in mycobacteria, and has prompted us to further investigate its role in *M. tuberculosis*, the causative agent of tuberculosis aiming to validate it as a potential novel drug target against tuberculosis.

CHAPTER 4: THE ROLE
OF ERGOTHIONEINE IN
Mycobacterium.
tuberculosis

CHAPTER 4: THE ROLE OF ERGOTHIONEINE IN *M.tuberculosis*

The investigation of the role of ERG in *M. smegmatis*, detailed in the preceding section, revealed that ERG protects *M. smegmatis* from oxidative stress. Since *M. tuberculosis* is known to encounter oxidative stress within the host [191], ergothioneine biosynthesis may represent a novel target for the development of anti-TB drugs. In addition, we observed that inhibiting ERG biosynthesis does not affect its susceptibility to the current anti-tuberculosis drugs, suggesting compounds targeting this pathway would be compatible with the current first line drugs. We therefore sought to further validate ERG biosynthesis as a novel drug target by investigating its role in the pathogenic organism *M. tuberculosis*. This is important since *M. smegmatis* and *M. tuberculosis* differ in their proteomic and genomic profiles, which points to differences in their physiology [148].

Approach:

We have shown that ERG is secreted by *M. smegmatis*, and ERG secretion was recently also reported in *Streptomyces coelicolor* [159]. We therefore sought to investigate ERG secretion in the slow growing mycobacteria *M. bovis* BCG (Bacille Calmette Guerin), *M. tuberculosis* H37Rv and *M. tuberculosis* CDC1551 strain.

In vitro enzymatic assays demonstrated that five enzymes are involved in ERG biosynthesis namely EgtA, EgtB, EgtC, EgtD and EgtE [148]. We attempted to evaluate the role of each of these enzymes in the production of ERG and in the physiology of *M. tuberculosis* by generating targeted deletion mutants for each gene individually and characterising the resulting mutants. In addition, since we have shown in previous studies that ERG compensates for MSH in the *M. smegmatis* $\Delta mshA$ mutant [99], we investigated the compensatory anti-oxidative role of ERG in *M. tuberculosis* as well. This was achieved by generating a MSH-deficient *M. tuberculosis* mutant by deleting *mshA* and an ERG/MSH-deficient double mutant by deleting *egtB* and *mshA* in *M. tuberculosis*.

The aims of this study were:

- To investigate and demonstrate ERG secretion in slow growing mycobacteria.
- To evaluate the role of each enzyme involved in ERG biosynthesis in the physiology of *M. tuberculosis* and the production of ERG.

- To investigate the anti-oxidative role of ERG.
- To determine if ERG and MSH compensate each others.
- To validate ERG biosynthesis as a potential TB drug target.

4.1 Slow growing mycobacteria secrete ERG

Approximately 76% and 58% of ERG is found in the extracellular medium of exponential and stationary *M. bovis* cultures respectively (Table 4.1), while analysis of *M. bovis* membrane integrity indicates that approximately 70% and 58% of cells have intact membrane during exponential phase and stationary phase respectively (Table 4.2, Figure 4.1). This implies that although a small percentage of extracellular ERG (EE) may result from leakage through the membrane of dead cells and live cells with damaged membrane, the majority of extracellular *M. bovis* ERG results from secretion. This was also observed in *M. tuberculosis* H37Rv, as approximately 81 and 90% of ERG was extracellular in exponential and stationary *M. tuberculosis* H37Rv cultures respectively, while analysis of the membrane integrity indicated that approximately 91% and 52% of H37Rv cells had intact membrane during exponential and stationary phase respectively (Table 4.1, 4.3 and Figure 4.1). As for *M. tuberculosis* CDC1551 approximately 73% and 15% of ERG was extracellular during exponential and stationary phase respectively while the analysis of the membrane integrity indicates approximately 91% and 83% of CDC1511 had intact membrane respectively (Table 4.1 and 4.4).

Table 4.1 ERG concentration in *M.tuberculosis* and *M. bovis* (BCG) in pg/10⁵ CFU

Strains	OD ₆₀₀ ~1		OD ₆₀₀ >2	
	IE	EE	IE	EE
<i>M. bovis</i>	3.93 ± 0.59	12.02 ± 1.30	10.47 ± 1.72	14.76 ± 1.21
<i>M. tuberculosis</i> (H37Rv)	4.10 ± 1.94	17.00 ± 3.06	1.82 ± 0.43	17.24 ± 2.69
<i>M. tuberculosis</i> (CDC1551)	2.63 ± 1.65	7.20 ± 5.63	10.31 ± 12.34	1.81 ± 1.37
ΔMT1289	0.75 ± 0.82	3.17 ± 4.49	1.99 ± 2.8	4.60 ± 3.43
ΔMT1953	1.55 ± 0.40	15.42 ± 15.79	0.14 ± 0.10	1.93 ± 1.36

Table 4.2 Subpopulation ratio (%) of BCG cultures analysed by flow cytometry

	LCDM	DC	LCIM
OD ₆₀₀ ~1	7.91 ± 2.50	30.4 ± 0.87	61.69 ± 2.34
OD ₆₀₀ >2	6.49 ± 0.37	36 ± 6.10	57.5 ± 5.87
Heat treated cells	20.27 ± 1.56	60.28 ± 1.70	19.45 ± 1.46

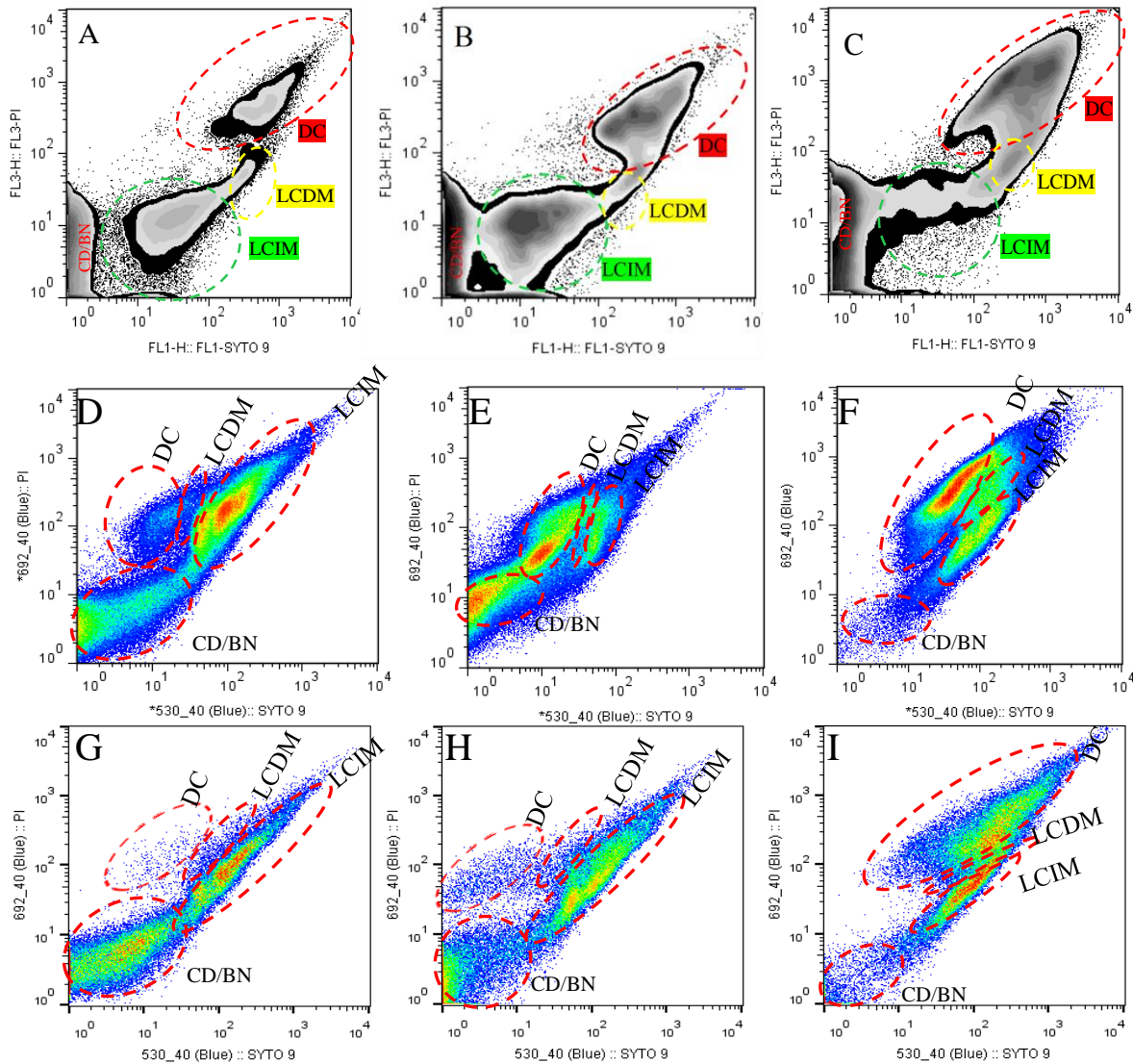


Figure 4.1 Population distribution of *M. bovis* (first row), *M. tuberculosis* H37Rv (2nd row) and *M. tuberculosis* CDC 1551 culture (3rd row)

FlowJo (version 7.6.4 and version 10.07 r2) software (Tree Star, Inc.) was used to visualise and analyse the flow cytometric data. Exponential (Figure 4.1A), stationary (Figure 4.1B) and heat treated (Figure 4.1C) *M. bovis* BCG cultures, stained with PI and Syto9, are shown as zebra plots. *M. tuberculosis* H37Rv and *M. tuberculosis* CDC1551 exponential (Figure 4.1D and 4.1G), stationary (Figure 4.1E and 4.1H) and heat treated cultures (Figure 4.1F and I) are shown as pseudo-colour plots. The fluorescence intensities defining the population distribution differs between *M. tuberculosis* and *M. bovis* since they are different mycobacteria species. A sub-population with relatively high PI and high Syto 9 intensities was defined as the sub-population of dead cells (DC) in *M. bovis* (Figure 4.1A, B, C) while the sub-population of DC in *M. tuberculosis* (H37Rv and CDC 1551) had a relatively high PI and low Syto 9 intensities (Figure 4.1D, E, F, G, H, I). The *M. bovis* sub-population with a relatively low PI and Syto 9 intensities was defined as live cells with intact membrane (LCIM) while in *M. tuberculosis* the sub-population with a relatively high Syto9 and low PI intensities represent LCIM. The intermediate sub-population in both species represents live cells with damaged membrane (LCDM). LCIM constitute the major sub-population in exponential *M. bovis* culture (Figure 4.1A, ~61.69%), exponential *M. tuberculosis* H37Rv culture (Figure 4.1D, 90.85%) and *M. tuberculosis* CDC1551 (Figure 4.1G, 91.14%) while in heat treated cultures LCIM constitute the minority (Figure 4.1C, Figure 4.1F and Figure 4.1I). As opposed to *M. tuberculosis* CDC1551 that has few dead cells, approximately one third of the population is dead during stationary phase in *M. tuberculosis* H37Rv and *M. bovis*.

Table 4.3 Subpopulation ratio (%) of *H37Rv* cultures analysed by flow cytometry

	LCDM	DC	LCIM
OD ₆₀₀ ~1	3.33 ± 1.70	5.82 ± 0.75	90.85 ± 2.21
OD ₆₀₀ >2	14.11 ± 1.91	34.21 ± 18.70	51.70 ± 17.4
Heat treated cells	11.29 ± 1.53	61.57 ± 0.97	27.13 ± 1.70

Table 4.4 Subpopulation ratio (%) of CDC1551 cultures analysed by flow cytometry

	LCDM	DC	LCIM
OD ₆₀₀ ~1	6.35 ± 0.25	2.5 ± 0.5	91.14 ± 0.61
OD ₆₀₀ >2	9.85 ± 3.95	7.01 ± 0.90	83.13 ± 4.80
Heat treated cells	6.83 ± 0.70	60.81 ± 0.73	32.35 ± 0.57

It was previously shown that *M. smegmatis* secretes ERG [99], and in this study we could show that *M. bovis* and *M. tuberculosis* secretes ERG as well. Mycothiol and ERG are the only thiols known to be synthesized by mycobacteria. The anti-oxidative role of MSH in mycobacteria has been shown. However, MSH cannot be secreted by mycobacteria but can be imported [91, 183]. This makes ERG the only thiol known to be secreted by mycobacteria. It was previously speculated that MSH constitute the major thiol in actinomycetes [131], but subsequent studies revealed that MSH-deficient mutants have a high level of ERG relative to the wild type strain [99, 100] and we have shown that ERG is not only found intracellularly but also extracellularly making ERG a major thiol in mycobacteria. In addition, the anti-oxidative role of ERG has been shown in eukaryotes [150], fungi [145] and more recently in *M. smegmatis* [99]. This suggests that ERG can play an anti-oxidative role in slow growing mycobacteria as well. Therefore ERG may protect mycobacteria from extracellular and intracellular oxidative stress as opposed to MSH which plays just an intracellular anti-oxidative role. Ergothioneine is very stable, resists auto-oxidation and does not require enzymatic recycling [132, 184] and therefore will function more efficiently in the extracellular medium than MSH. In addition, it has been shown that *M. tuberculosis* redox homeostasis is highly perturbed when it encounters intracellular oxidative stress leading to intracellular damage. Therefore, *M. tuberculosis* would alleviate the exogenous ROS generated by macrophages to prevent influx by secreting ROS detoxifying enzymes (SOD and catalase) and ERG [191]. Hence ERG secretion may constitute the primary defence mechanism of *M. tuberculosis* during infection. On the other hand, it was shown that ERG could prevent inflammatory response in higher eukaryotes by suppressing IL-8 [141]. This indicates the ability of ERG to modulate the immune system and therefore suggests a role for

secreted ERG during infection by *M. tuberculosis* since this will be able to modulate the immune system, which may suit its survival in macrophages. It is worth noting that CDC1551 membrane integrity indicates that ~ 17% of cells have a damaged membrane during stationary growth while only 15% of ERG is extracellular (Table 4.4 and Table 4.1). Therefore CDC1551 may not secrete ERG during stationary growth or may secrete a low level of ERG during stationary phase. It is tempting to speculate that this may explain why it was observed that infection with CDC1551 induced a higher cytokine production (TNF- α , IL-10, IL-6 and IL-12) relatively to H37Rv [192] and that the high EE in H37Rv hampers the immune system by lowering cytokine production making H37Rv more virulent than CDC1551 [192].

In attempt to identify an ERG transporter, ERG was quantified in mutants carrying a transposon on a gene coding for an ortholog of OCTN1 (ERG transporter in humans). Four transposons mutants were investigated namely $\Delta MT3434$, $\Delta MT2926$, $\Delta MT1289$, $\Delta MT1953$. The mutant $\Delta MT3434$ failed to grow, while the level of ERG was unchanged in $\Delta MT2926$ (data not shown). Though the extracellular level of ERG was still high in $\Delta MT1289$ and $\Delta MT1953$, the intracellular level of ERG was significantly lower than the wild type level in both strains (Table 4.1). This was pronounced in $\Delta MT1953$ as IE during stationary phase of this strain was 74-fold lower than the wild type level. The proteins MT1953 and MT1289 are both integral component of the membrane. The protein MT1289 (Rv1250) is an uncharacterized MFS-type transporter while MT1953 (Rv1902c) known as nanT is a hypothetical sugar transporter [59, 193]. The results obtained in this study indicate that these proteins may be involved in ERG metabolism, however their specific function is not known and further investigation is required.

deleted it in CDC1551 and in the $\Delta egtB$ mutant of CDC155 by a homologous recombination based method. This indicates that this gene is not essential in *M. tuberculosis* and that MSH, neither ERG, is essential for *M. tuberculosis* growth in vitro (in cultures supplemented with OADC). However, strains lacking either MSH or both MSH and ERG grew very slowly on solid culture (4-8 weeks for visible colonies to appear on plates) and are very sensitive to the decrease of catalase concentration in the culture media. They fail to grow in the absence of OADC (because of the absence of catalase) or in low level of OADC (data not shown). Caution must be taken when making the solid culture that the OADC supplemented is not added when the media is too hot, as this may cause degradation of catalase and therefore decrease its concentration in the media; hence affecting the growth of these mutants.

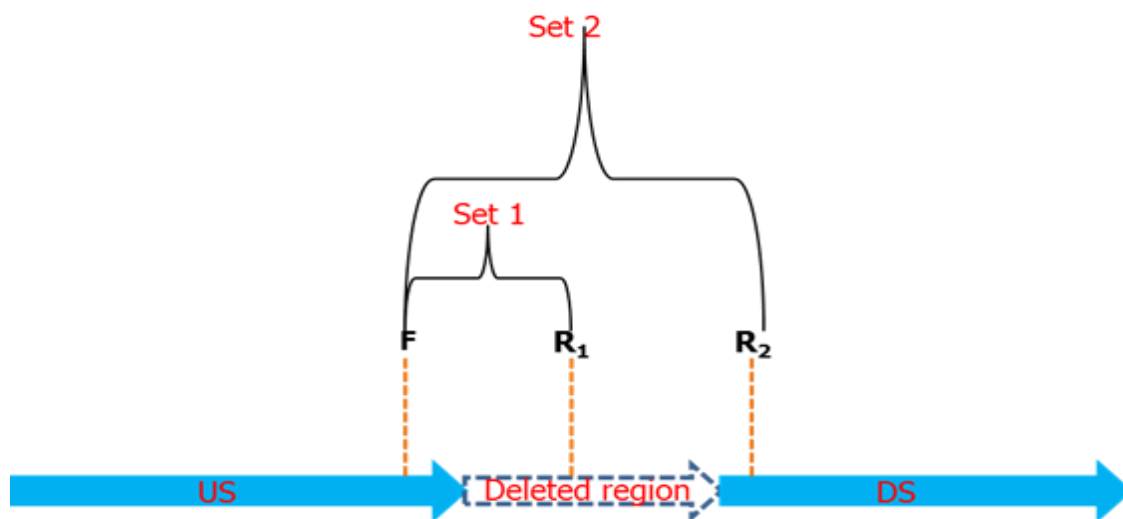


Figure 4.3 Screening PCR design of the unmarked mutants

When amplified with primer set 1, only wild type and SCO will get amplified since they both have a copy of the gene, while the mutant will not be amplified since the gene has been deleted. When amplified with primer set 2, the wild type, the SCO and the mutant will be amplified, since the reverse primer R_2 hybridizes outside the deleted region. However the mutant band will be smaller than the wild type band, since the gene has been deleted.

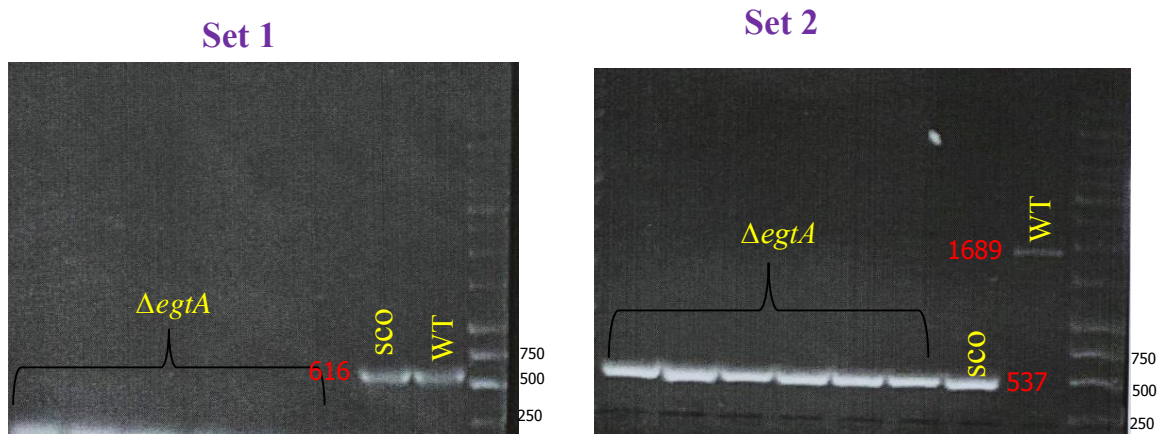


Figure 4.4 Screening PCR of *egtA* mutant generated in CDC1551

A 537bp region of *egtA* was completely deleted from CDC1551, therefore when screened with primer set 1; only primer dimers were observed in the mutants while a 616bp fragment could be amplified in the SCO and WT. When screened with primer set 2, the WT with the intact gene has a 1682bp fragment while the mutant and the SCO have a smaller fragment of 537bp which is 1682bp minus the deleted 537bp.

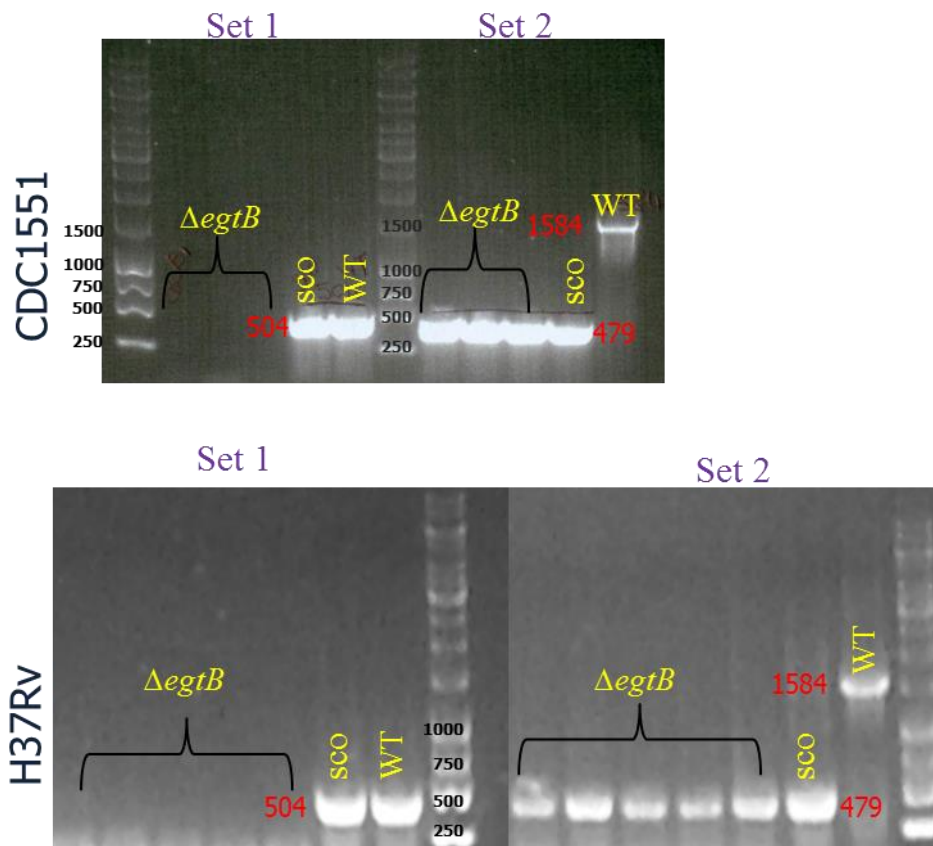


Figure 4.5 Screening PCR of *egtB* mutant generated in CDC155 and H37Rv

A 1105bp region of *egtB* was completely deleted from CDC1551 and H37Rv, therefore when screened with primer set 1; the mutants could not be amplified while a 504bp fragment could be amplified in the SCO and WT. When screened with primer set 2, the WT with the intact gene has a 1584bp fragment while the mutant and the SCO have a smaller fragment of 479bp which is 1584bp minus the deleted 1104bp.

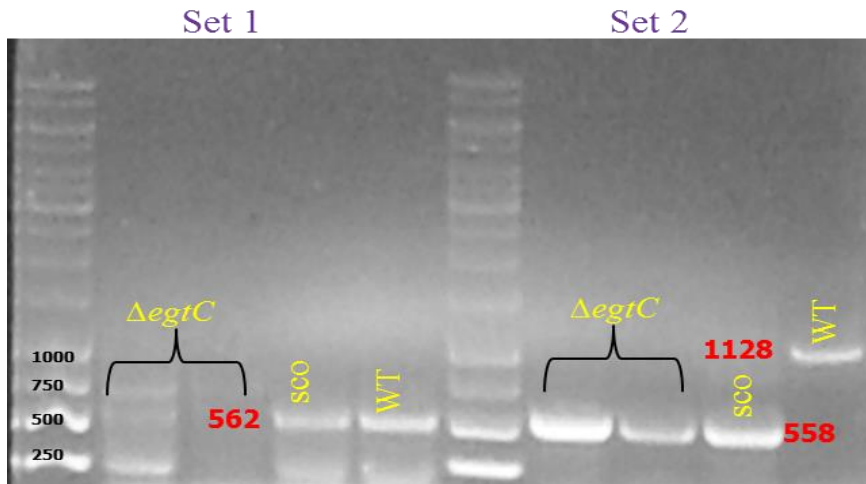


Figure 4.6 Screening PCR of *egtC* mutant generated in CDC155

A 570bp region of *egtC* was completely deleted from CDC1551, therefore when screened with primer set 1; the mutants could not be amplified while a 562bp fragment could be amplified in the SCO and WT. When screened with primer set 2, the WT with the intact gene has an 1128bp fragment while the mutant and the SCO have a smaller fragment of 558bp which is 1128bp minus the deleted 570bp

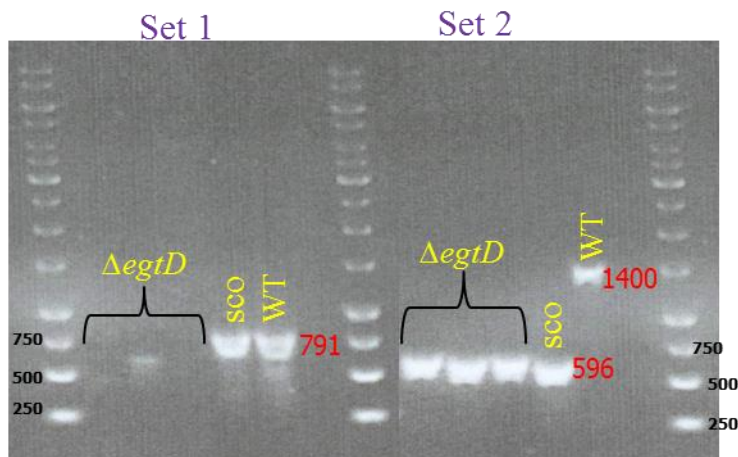


Figure 4.7 Screening PCR of *egtD* mutant generated in CDC155

An 804bp region of *egtD* was completely deleted from CDC1551, therefore when screened with primer set 1; the mutants could not be amplified while a 791bp fragment could be amplified in the SCO and WT. When screened with primer set 2, the WT with the intact gene has a 1400bp fragment while the mutant and the SCO have a smaller fragment of 596bp which is 1400bp minus the deleted 804bp

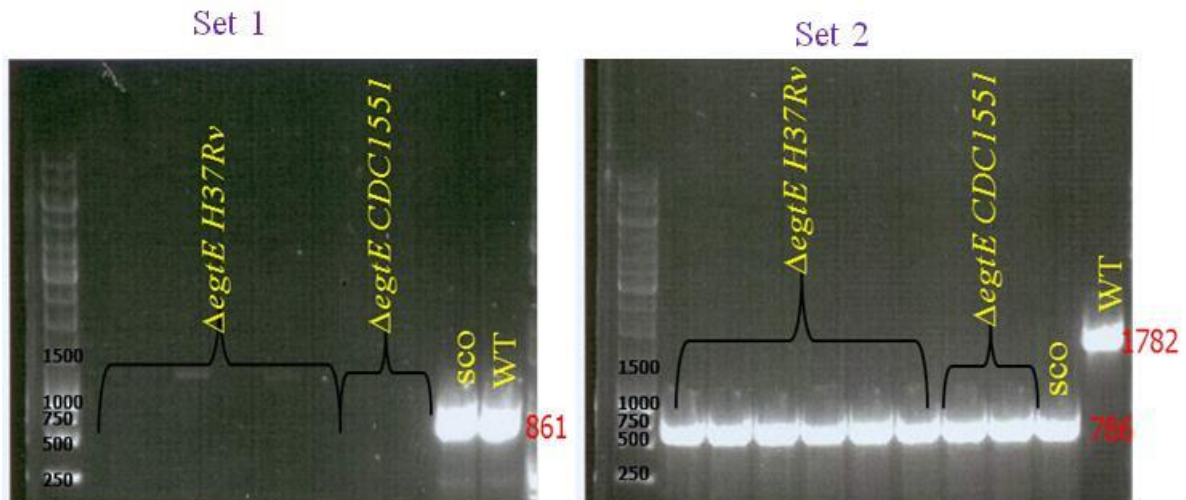


Figure 4.8 Screening PCR of *egtE* mutant generated in H37Rv and CDC155

A 996bp region of *egtE* was completely deleted from H37Rv and CDC1551, therefore when screened with primer set 1; the mutants could not be amplified while an 861bp fragment could be amplified in the SCO and WT. When screened with primer set 2, the WT with the intact gene has a 1782bp fragment while the mutant and the SCO have a smaller fragment of 786bp which is 1782bp minus the deleted 996bp.

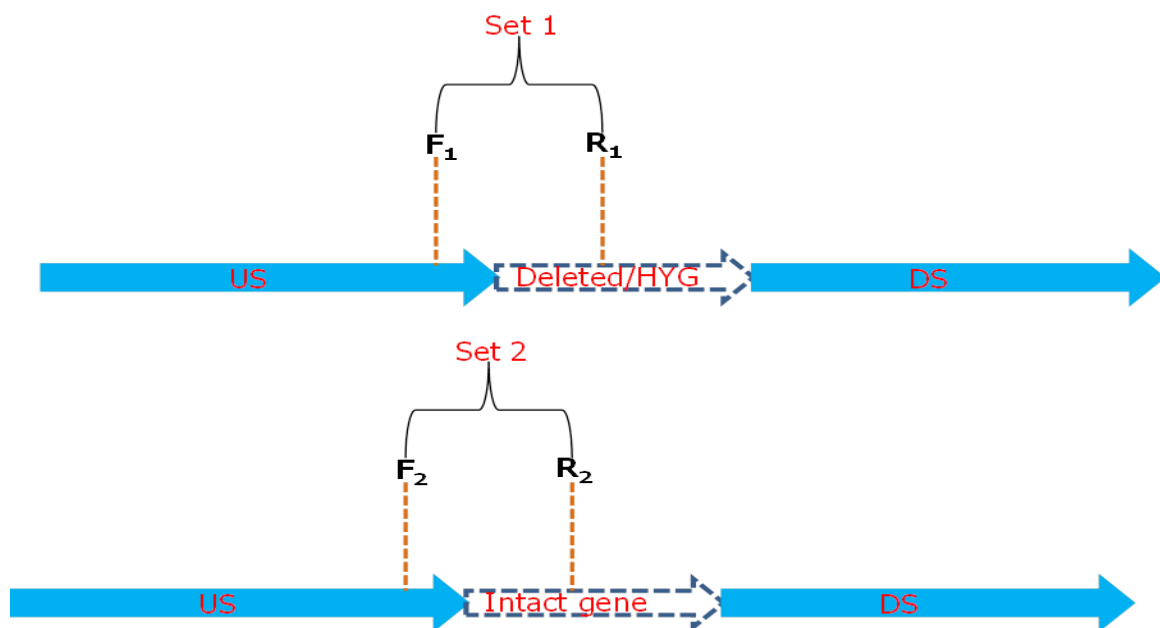


Figure 4.9 Screening PCR design of the marked mutants

When amplified with primer set 1, only mutants and SCOs will get amplified since they both have the hygromycin cassette, while the wild type will not be amplified since the gene has been deleted. When amplified with primer set 2, the wild type and the SCO will be amplified but not the mutant, since the reverse primer R_2 hybridizes in the deleted region.

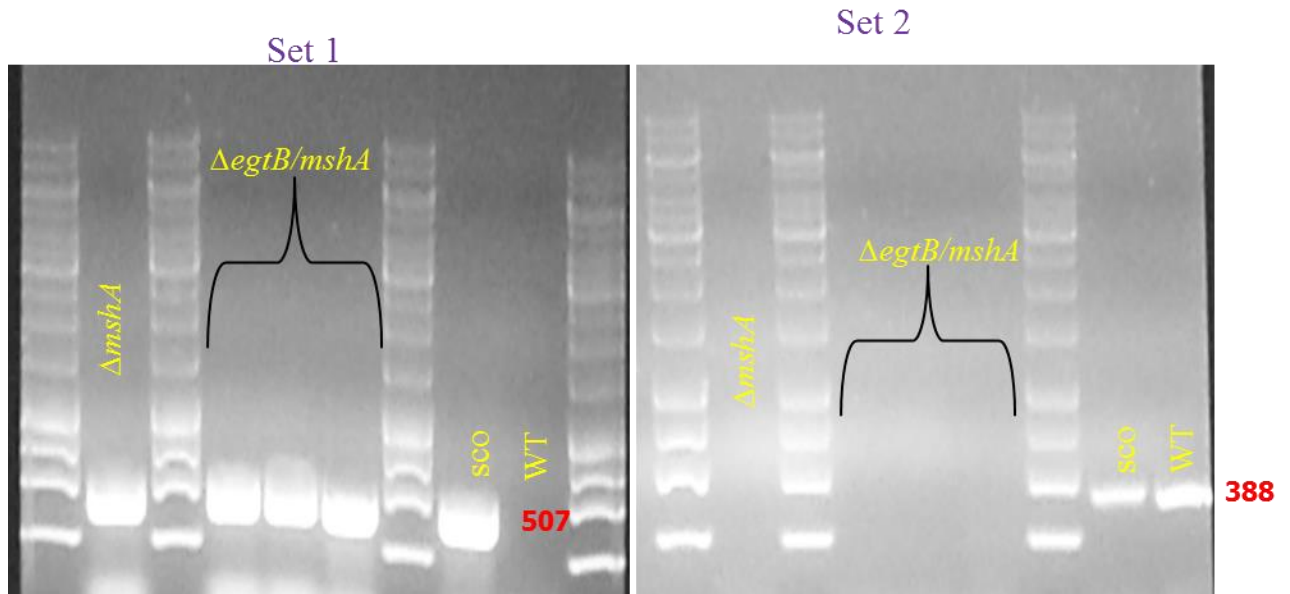


Figure 4.10 Screening PCR of $\Delta mshA$, $\Delta egtB/mshA$ mutant generated in CDC1551

A 1335bp region of *mshA* was completely deleted and replaced with hygromycin cassette with its promoter. When amplified by primer set 1 that hybridizes outside the deleted region and within the hygromycin cassette, only the mutant and the SCO that still has the construct are amplified giving a 507bp band. Then when amplified with primer set 2 that hybridizes in the intact gene, only the wild type and the SCO are amplified giving a 388bp fragment.

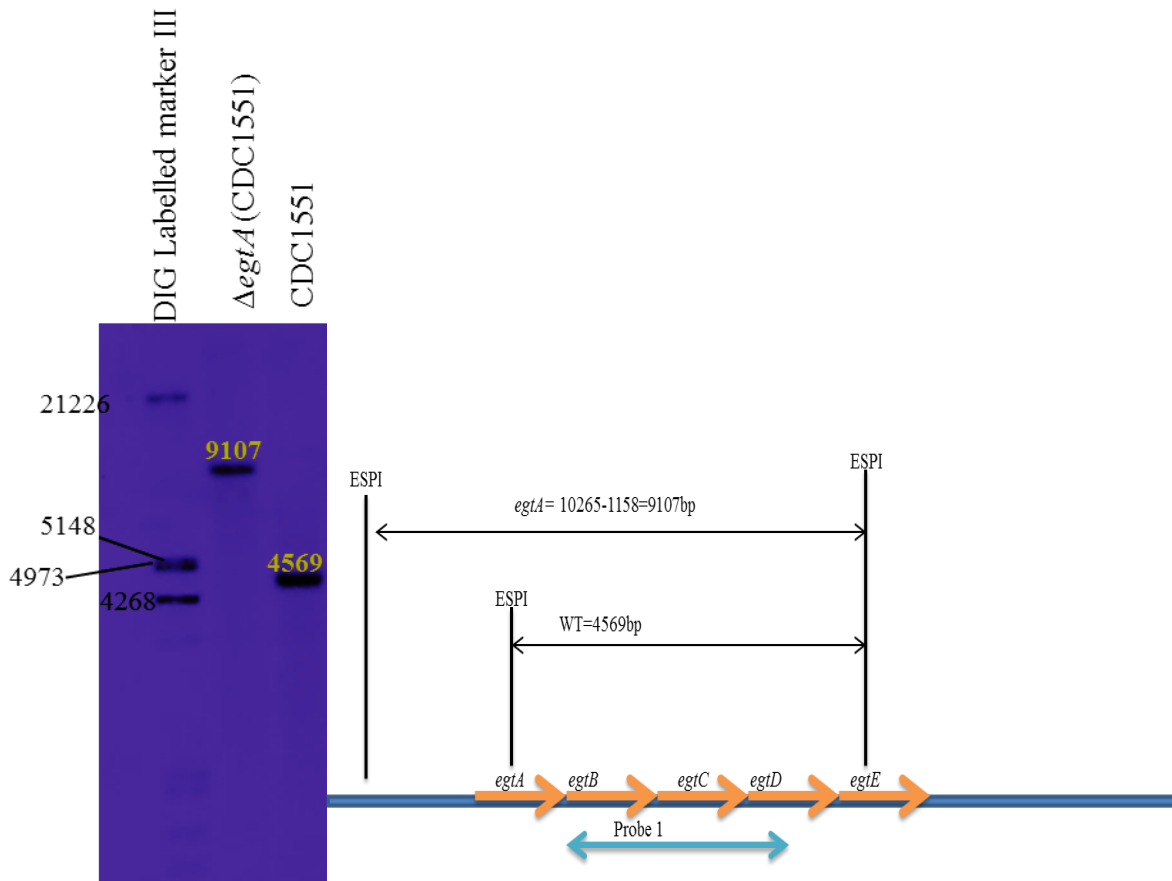
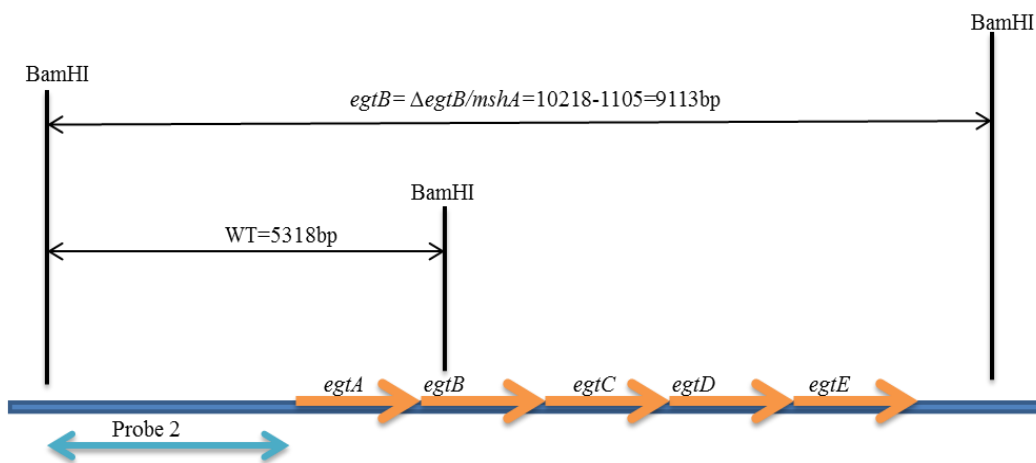


Figure 4.11 Southern blotting analysis of the CDC1551 Δ *egtA* mutant

Right panel describes the Southern blot design; the genomic DNA of the wild type and the mutant was digested with ESPI. ESPI cuts within *egtA*, *egtE* and outside the operon. A DNA fragment that hybridizes to the digested region that will enable distinction of the wild type from the mutant was used as the probe (table 3.5). The mutant band on the left panel is longer than that of the wild type (9107bp for the mutant and 4569bp for the wild type) as the ESPI site found within *egtA* does not exist in the mutant since it has been deleted as illustrated in the right panel.



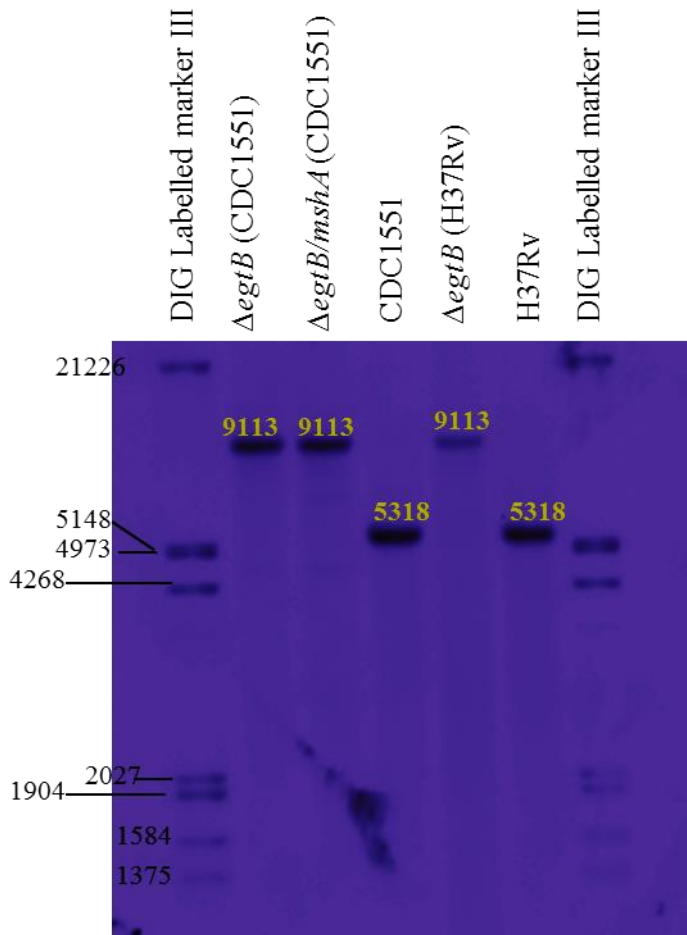


Figure 4.12 Southern blotting analysis of *egtB* deletion in H37Rv $\Delta egtB$, CDC1551 $\Delta egtB$ and the *mshA/egtB* mutants

Top panel describes the Southern blot design; the genomic DNA of the wild type and the mutants was digested with BamHI. BamHI cuts within *egtB*, and outside the operon. A DNA fragment that hybridizes to the digested region to enable distinction of the wild type from the mutant was used as the probe (table 3.5). The mutants' band on the bottom panel is longer than that of the wild type (9113bp for the mutant and 5318bp for the wild type) as the BamHI site found within *egtB* does not exist in the mutants since it has been deleted as illustrated in the top panel.

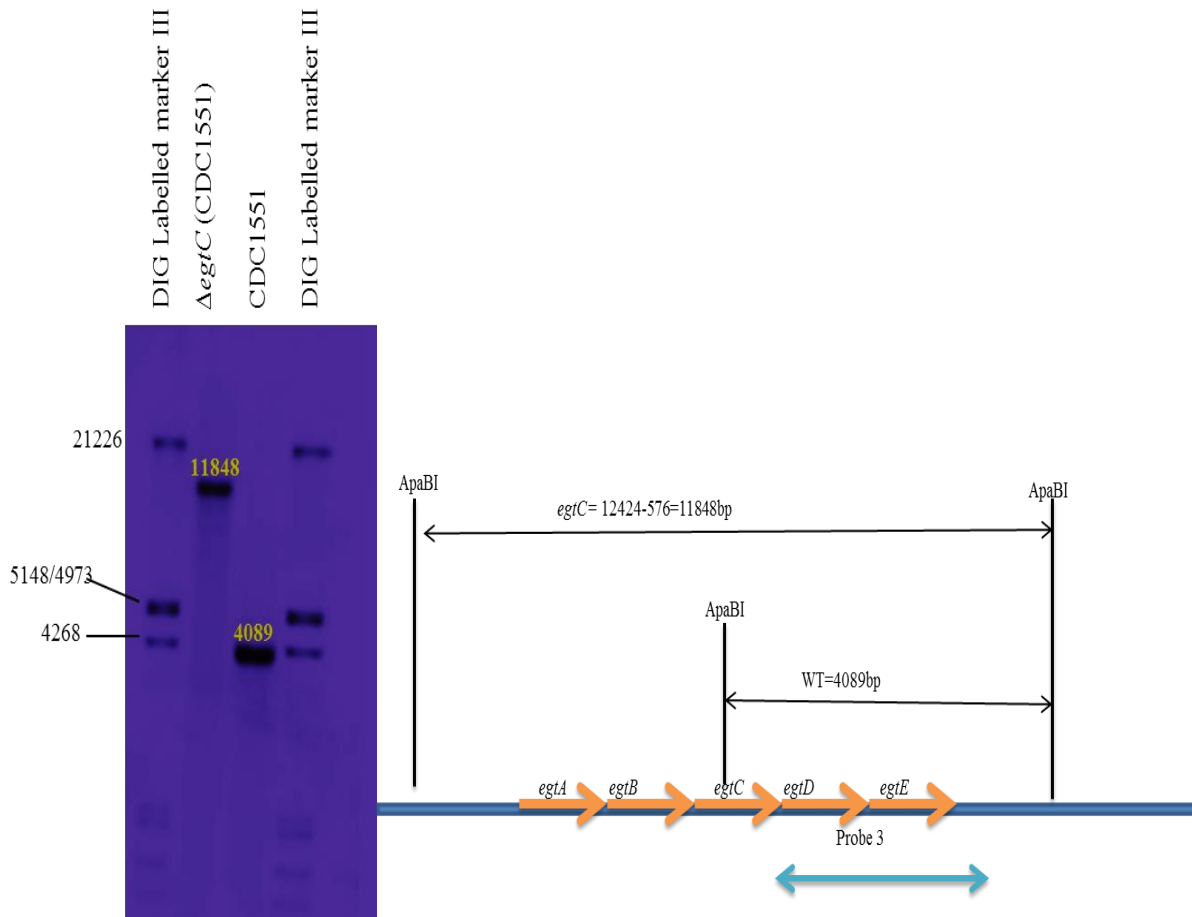


Figure 4.13 Southern blotting analysis of *egtC* deletion in the CDC1551 Δ *egtC* mutant

Right panel describes the Southern blot design; the genomic DNA of the wild type and the mutant was digested with ApaBI. ApaBI cuts within *egtC*, and outside the operon. A DNA fragment that hybridizes to the region to enable distinction of the wild type from the mutant was used as the probe (table 3.5). The mutant band on the probe (table 3.5) is longer than that of the wild type (11848bp for the mutant and 4089bp for the wild type) as the ApaBI site found within *egtC* does not exist in the mutant since it has been deleted as illustrated in the right panel.

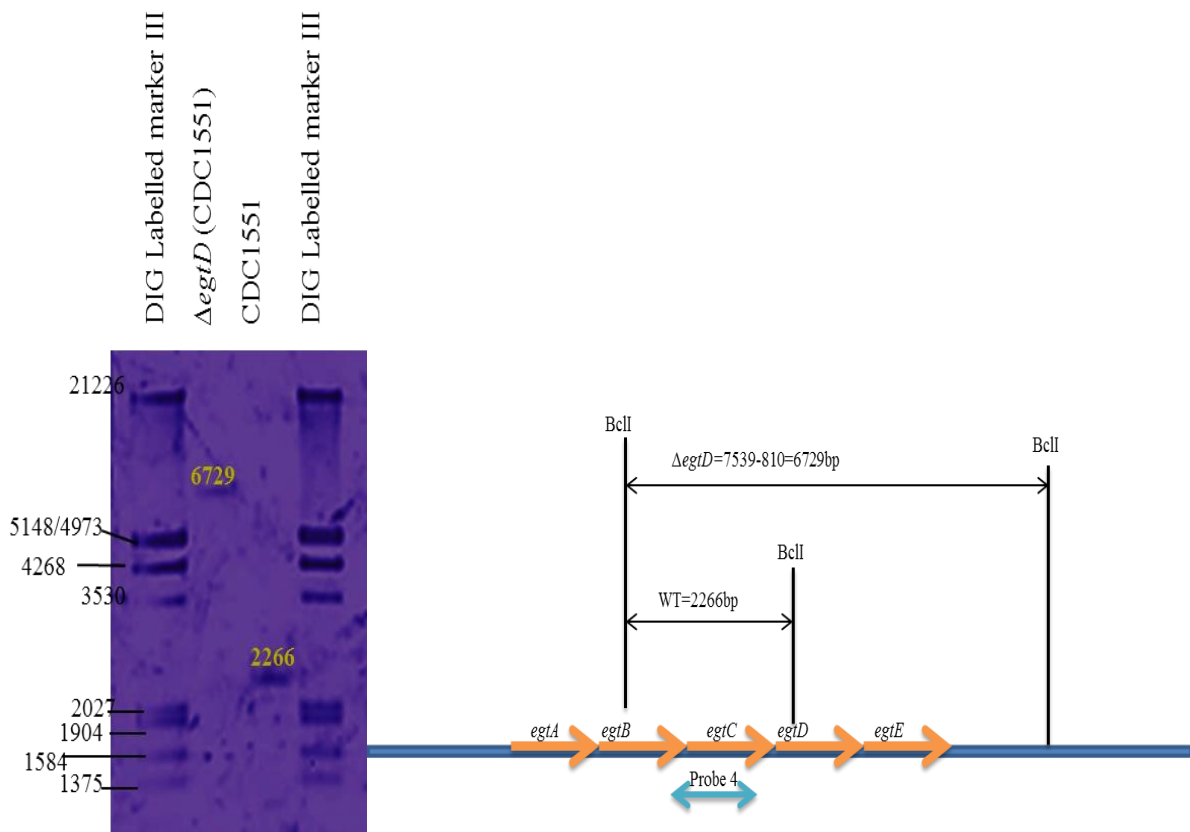


Figure 4.14 Southern blotting analysis of *egtD* deletion in the CDC1551 Δ *egtD* mutant

Right panel describes the Southern blot design; the genomic DNA of the wild type and the mutant was digested with *Bcl*I. *Bcl*I cuts within *egtC*, and outside the operon. A DNA fragment that hybridizes to the digested region to enable distinction of the wild type from the mutant was used as the probe (table 3.5). The mutant band on the left panel is longer than that of the wild type (6729bp for the mutant and 2266bp for the wild type) as the *Bcl*I site found within *egtD* does not exist in the mutant since it has been deleted as described in the right panel.

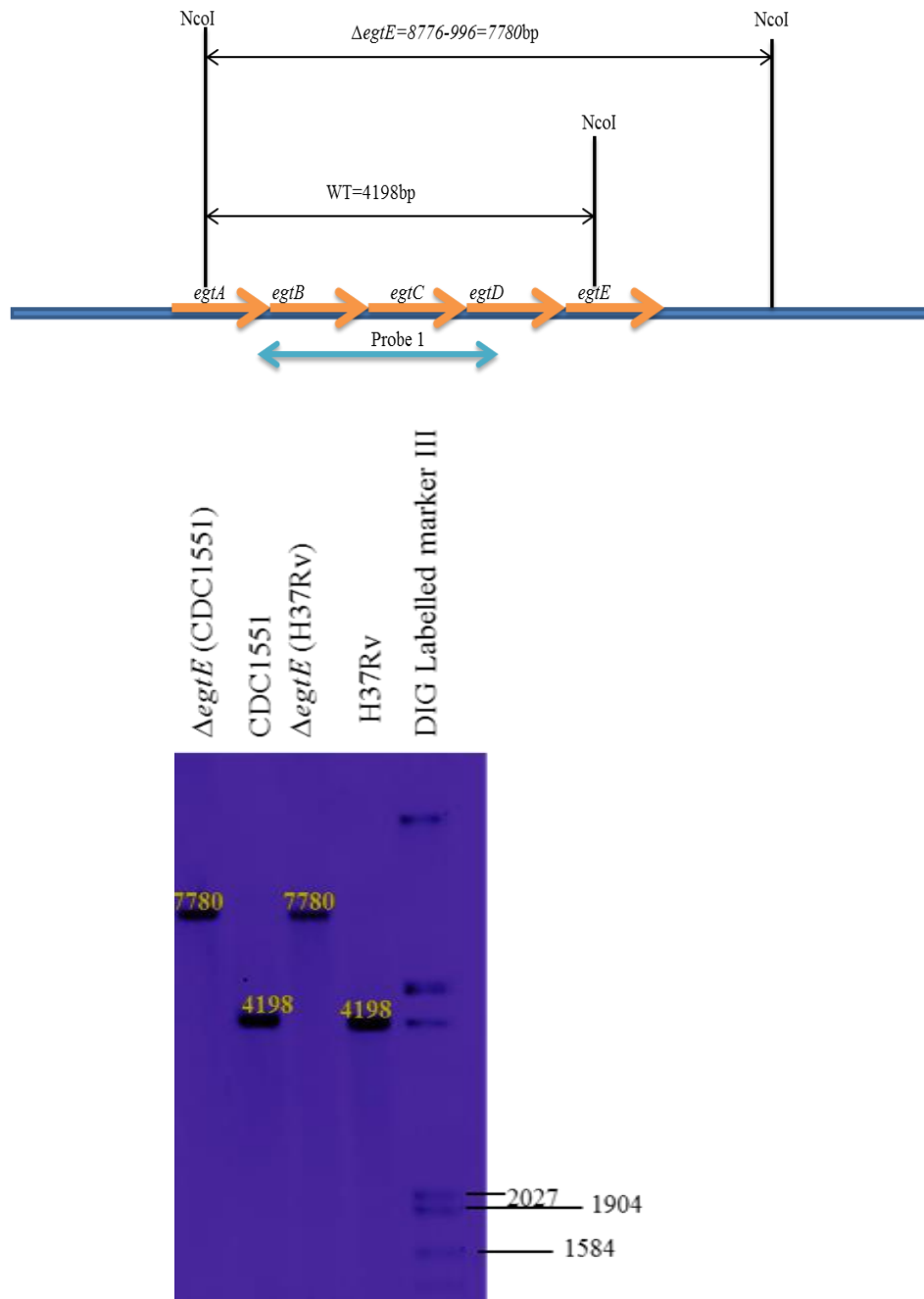


Figure 4.15 Southern blotting analysis of *egtE* deletion in H37Rv $\Delta egtE$ and CDC1551 $\Delta egtE$

Top panel describes the Southern blot design; the genomic DNA of the wild type and the mutants was digested with NcoI. NcoI cuts within *egtE*, and outside the operon. A DNA fragment that hybridizes to the digested region to enable distinction of the wild type from the mutant was used as the probe (table 3.5). The mutants' band on the bottom panel is longer than that of the wild type (7780bp for the mutants and 4198bp for the wild type) as the NcoI site found within *egtB* does not exist in the mutants since it has been deleted as described in the top panel.

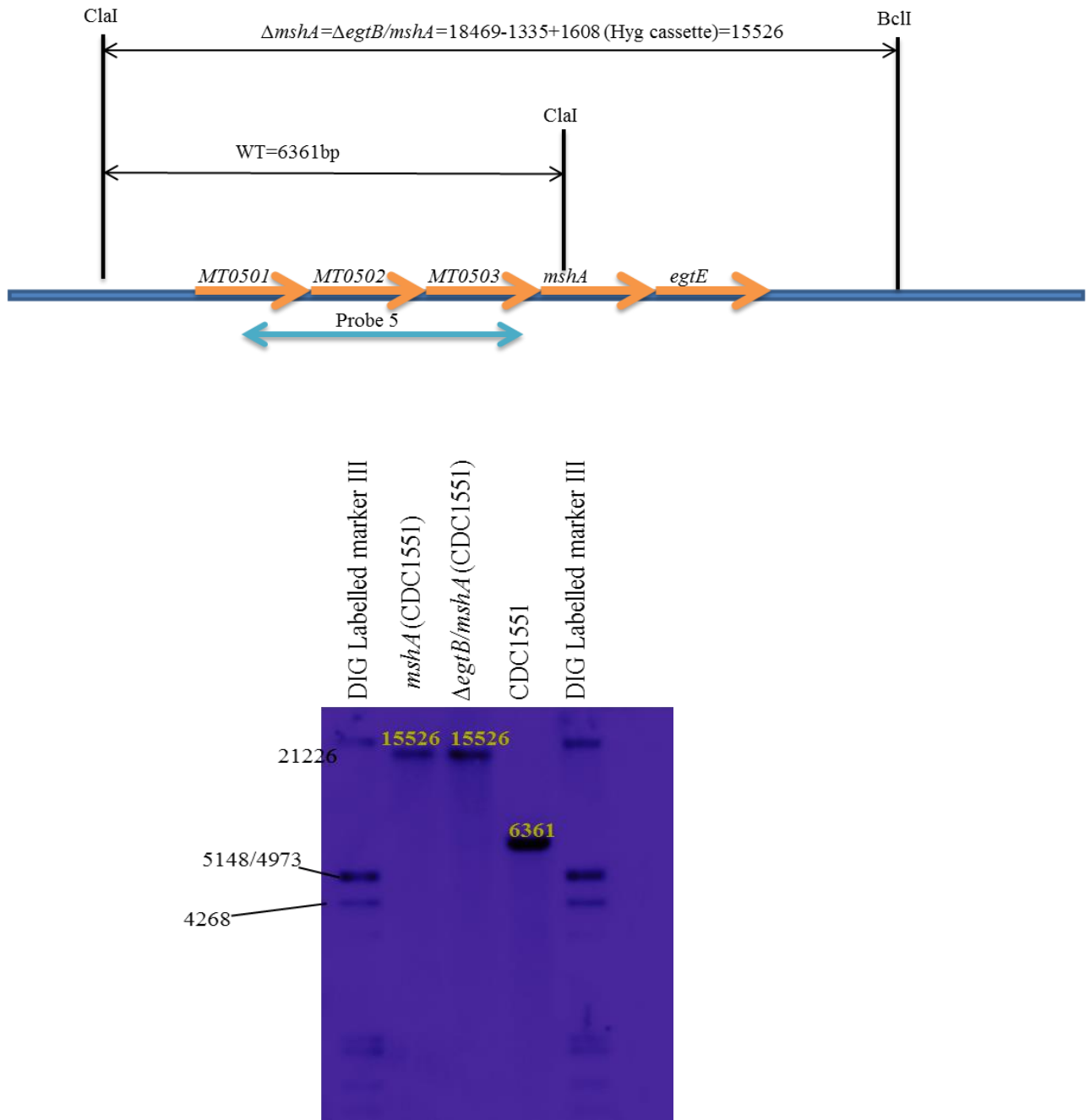


Figure 4.16 Southern blotting analysis of *mshA* deletion in CDC1551 $\Delta mshA$ and the *mshA/egtB* mutant

Top panel describes the Southern blot design; the genomic DNA of the wild type and the mutants was digested with ClaI. ClaI cuts within *mshA*, and outside the operon. A DNA fragment that hybridizes to the digested region to enable distinction of the wild type from the mutant was used as the probe (table 3.5). The mutants' band on the bottom panel is longer than that of the wild type (15526bp for the mutant and 6361bp for the wild type) as the ClaI site found within *mshA* does not exist in the mutants since it has been deleted as illustrated in the top panel.

4.3 Deletion of ERG biosynthetic genes does not affect *M. tuberculosis* susceptibility to current anti-tuberculosis drugs

In this study, two mutants were generated in H37Rv namely H37Rv $\Delta egtE$ and $\Delta egtB$ and 7 mutants in CDC1551 namely $\Delta egtA$, $\Delta egtB$, $\Delta egtC$, $\Delta egtD$, $\Delta egtE$, $\Delta mshA$ and $\Delta egtB/mshA$. The susceptibility of the CDC1551 mutants to RIF, ETH, EMB and INH were investigated. Deleting either *egtA*, *egtB*, *egtC*, *egtD* or *egtE* in CDC1551 did not affect its susceptibility to the antibiotics tested, as was previously shown in *M. smegmatis* [99]. Therefore ERG does play a role in protecting mycobacteria from current anti-tuberculosis drugs (Table 4.5). However MSH deficiency affects mycobacterial susceptibility to antibiotics, as they are resistant to INH and ETH. As was previously shown in *M. smegmatis* [99], the loss of ERG in the MSH-deficient mutants does not alter their susceptibility to current anti-tuberculosis drugs (Table 4.5). Thus, ERG and MSH do not compensate each other in the protection of mycobacteria against current anti-tuberculosis drugs. It was speculated that MSH protects *M. tuberculosis* from the bactericidal effect of RIF as the $\Delta mshB$ mutants that produced low but detectable level of MSH were more sensitive to RIF [104]. However, in this study, MSH deficiency was achieved by deleting *mshA* in CDC1551 and the susceptibility of the resulting mutant to RIF was not affected. This implies that the previous observed phenotype was associated to the lack of MshB and not of MSH.

Table 4.5 Drugs MIC ($\mu\text{g/ml}$) of mutants generated in this study

RIF	ETH	INH	EMB	Strains
0.98E-03_1,95E-03	0,39_0,78	0,012_0,02	0,39_0,78	<i>CDC1551</i>
0.49E-03_0.98E-03	0,78_1,56	0,012_0,02	0,19_0,39	$\Delta egtA$
1,95E-03_3,91E-03	0,39_0,78	0,012_0,02	0,39_0,78	$\Delta egtB$
0.98E-03_1,95E-03	0,78_1,56	0,012_0,02	0,39_0,78	$\Delta egtC$
0.98E-03_1,95E-03	0,78_1,56	0,012_0,02	0,19_0,39	$\Delta egtD$
0.98E-03_1,95E-03	0,39_0,78	0,012_0,02	0,39_0,78	$\Delta egtE$
1,95E-03_3,91E-03	125-250	0.06-0.12	0.39-0.78	$\Delta egtB/mshA$
1,95E-03_3,91E-03	125-250	0.06-0.12	0.78-1.56	$\Delta mshA$
ND	3.9-7.8	0.015-0.03	ND	$\Delta mshAc^*$

*complemented $\Delta mshA$ with pMVhsp*mshA*

4.4 The enzyme EgtE is not essential for ERG biosynthesis

The genes *egtE* and *egtB* were individually deleted in H37Rv and CDC1551 while *egtA*, *egtB*, *egtC*, *egtD* and *egtE* were individually deleted in CDC1551. The gene *mshA* was deleted in CDC1551 and in the $\Delta egtB$ mutant of CDC1551. Thus, nine mutant strains were generated in *M. tuberculosis*. In order to confirm the function of each enzyme on ERG biosynthesis, ERG was quantified in each mutant. The $\Delta egtB$ mutant is ERG deficient in both CDC1551 and H37Rv, the $\Delta egtD$ mutant of CDC1551 is ERG deficient as well. The $\Delta egtA$ mutant of CDC1551 has lost 78% of IE and completely lost EE. The $\Delta egtC$ mutant of CDC1551 has

lost 30% of IE and 45% of EE while the $\Delta egtE$ mutant has an increased level of ERG; ~1.5-fold increase of IE in the CDC1551 $\Delta egtE$ mutant, ~4-fold increase of IE and ~3-fold increase of EE in the H37Rv mutant (Table 4.6). In addition the level IE was ~3-fold higher in the $\Delta mshA$ mutant indicating compensation of MSH by ERG (Table 4.6). It was shown that transcription of integrated genes under their native promoter is problematic, since they are integrated at a different site of the genome (*attB* site). This is pronounced when the gene is not the first in the operon [197]. This was observed in this study as well, since complementation with the endogenous promoter was successful only with the $\Delta egtA$ mutant ($\Delta egtA^+$ in Table 4.6).

Table 4.6 ERG level in mutants generated in this study (pg/10⁵CFUs)

Strains	IE				EE			
	1	2	3	Average	1	2	3	Average
H37Rv	0.83	0.51	2.26	1.20 ± 0.76	4.92	8.16	0	4.6 ± 3.35
$\Delta egtE$ (H37Rv)	7.63	0.44	6.10	4.73 ± 3.09	13.45	6.70	17.90	12.68 ± 4.6
$\Delta egtB$ (H37Rv)	0.18	0	0.18	0.1 ± 0.08	0	0	0	0
CDC1551	0.77	2.35	4.77	2.6 ± 1.64	13.76	7.84	0	7.19 ± 5.63
$\Delta egtA$ (CDC1551)	1.05	0.69	0	0.58 ± 0.43	0	0	0	0
$\Delta egtB$ (CDC1551)	0	0	0	0	0	0	0	0
$\Delta egtC$ (CDC1551)	1.44	3.14	0.90	1.8 ± 0.95	11.76	0	0	3.92 ± 5.54
$\Delta egtD$ (CDC1551)	0	0	0	0	0	0	0	0
$\Delta egtE$ (CDC1551)	1.18	7.16	3.44	3.93 ± 2.46	0	13.09	0	4.36 ± 6.17
$\Delta mshA$ (CDC1551)	1.97	12.46	5.04	6.50 ± 4.4	14.53	4.30	11.82	10.21 ± 4.33
$\Delta egtB$ - <i>mshA</i> (CDC1551)	0	0	0	0	0	0	0	0
$\Delta egtAc$ (CDC1551)	4.59	30.92	4.3	13.27 ± 12.47	28.07	107.66	35.73	57.16 ± 35.84
$\Delta egtBc$ (CDC1551)	0.82	0.47	0.198	0.50 ± 0.25	0	0	0	0
$\Delta egtCc$ (CDC1551)	2.90	4.36	1.12	2.80 ± 1.3	0	47.20	0	15.73 ± 22.25
$\Delta egtDc$ (CDC1551)	2.84	6.07	0.83	3.25 ± 2.15	9.50	4.80	0	4.77 ± 3.88
$\Delta mshAc$ (CDC1551)	4.48	1.90	1.20	2.52 ± 1.14	0	22.88	0	7.63 ± 10.78
$\Delta egtBop$ (CDC1551)	2.35	0.77	1.11	1.41 ± 0.68	0	0	0	0
$\Delta egtA^+$ (CDC1551)	2.60	1.13	0.23	1.32 ± 0.97	17.782	19.96	5.76	14.5 ± 6.2
$\Delta egtB^+$ (CDC1551)	0	0	0.22	0.075 ± 0.1	0	0	0	0
$\Delta egtD^+$ (CDC1551)	0	0	0.19	0.064 ± 0.09	0	0	0	0

c: mutants complemented with genes expressed under the hsp60 promoter, **op:** mutant complemented by the entire operon, **+**: mutants complemented by the gene fused to a 1000bp US the operon; IE: intracellular ERG, EE: extracellular ERG. Results are representative of three independent extractions and three independent quantifications

The enzyme EgtD catalyses the methylation of histidine to hercynine during ERG biosynthesis (Figure 1.8). Therefore, deletion of *egtD* will obstruct the production of hercynine which is what we observed (Table 4.7). To verify if the low level of ERG in all the mutants except $\Delta egtE$ was due to a polar effect on *egtD*, we quantified the level hercynine, an intermediate in ERG biosynthesis. The $\Delta egtB$ mutant which is ERG-deficient still produce hercynine (Table 4.7), indicating that the deletion of *egtB* does not affect the expression of *egtD* and that the enzyme EgtB is essential for ERG biosynthesis as well. However, when the $\Delta egtB$ mutant was complemented under hsp60 promoter or the endogenous promoter,

hercynine was below detection limit. This may be due to some unknown metabolic regulations. The mutant $\Delta egtA$ and $\Delta egtC$ also produced hercynine indicating that deletion of these genes did not affect *egtD* expression (Table 4.7). Since $\Delta MT1289$ and $\Delta MT1953$ had a very low level of ERG (Table 4.1), hercynine was quantified in them as well, and results indicate that hercynine is also produced in these mutants (Table 4.7).

Table 4.7 Hercynine level during exponential growth of mutants generated in this study (Area/10⁷CFUs)

Strains	IH	EH
H37Rv	3.15 ± 1.42	0
$\Delta egtE$ (H37Rv)	1.61 ± 1.30	0
$\Delta egtB$ (H37Rv)	0.68 ± 0.53	0
CDC1551	4.32 ± 1.54	0
$\Delta egtA$ (CDC1551)	12.36 ± 6.57	0
$\Delta egtB$ (CDC1551)	0.93 ± 0.38	0
$\Delta egtC$ (CDC1551)	2.18 ± 1.42	0
$\Delta egtD$ (CDC1551)	0	0
$\Delta egtE$ (CDC1551)	1.50 ± 0.94	0
$\Delta mshA$ (CDC1551)	8.96 ± 11.36	0
$\Delta egtB$ - <i>mshA</i> (CDC1551)	3.63 ± 3.17	0
$\Delta MT1289$ (CDC1551)	5.62 ± 2.24	0
$\Delta MT1953$ (CDC1551)	2.15 ± 1.76	0
$\Delta egtAc$ (CDC1551)	3.37 ± 4.11	0
$\Delta egtBc$ (CDC1551)	0	0
$\Delta egtCc$ (CDC1551)	3.54 ± 3.62	0
$\Delta egtDc$ (CDC1551)	29.46 ± 30.27	13.35 ± 6.89
$\Delta mshAc$ (CDC1551)	4.24 ± 1.35	0
$\Delta egtBop$ (CDC1551)	5.00 ± 4.33	0
$\Delta egtA^+$ (CDC1551)	42.68 ± 36.38	0
$\Delta egtB^+$ (CDC1551)	0	0
$\Delta egtD^+$ (CDC1551)	0	0

c: mutants complemented with genes expressed under the *hsp60* promoter, **op:** mutant complemented by the entire operon, **+**: mutants complemented by the gene fused to a 1000bp US the operon; IH: intracellular hercynine, EH: extracellular hercynine. Data are representative of three independent extractions and three independent quantifications.

It is worth noting that, the level of hercynine in the mutants is not the same (Table 4.7), this is may be due to differential metabolic regulations in these strains as a result of different levels of ERG or other intermediates in the pathway in these strains. To date, the mechanism of regulation of this pathway has not been investigated in mycobacteria.

In addition, hercynine is not detected in the extracellular medium (Table 4.7) except in the complemented $\Delta egtD$. This is an indication that either hercynine is not secreted, or it is secreted at a very low level during exponential phase of growth. To verify this, we quantified hercynine in stationary cultures of the CDC1551, $\Delta MT1289$ and $\Delta MT1953$. Hercynine was detected at a concentration of 5.16 ± 3.3 , 33 ± 19 , 11 ± 4.3 respectively in the extracellular medium, while it was detected at a concentration of 2.27 ± 0.92 , 6.42 ± 1.75 and 1.58 ± 0.35 area/10⁷ CFUs respectively in the cell lysate. Since these data indicates that extracellular hercynine constitute $\geq 70\%$ of total hercynine in these strains, it is less likely that the

extracellular hercynine observed is due to leakage through damaged cells because we have shown that approximately 17% of CDC1551 mycobacterial cells have a damaged membrane during stationary growth (Table 4.4). It is possible that hercynine is secreted at a very low level (below detection limit) during exponential phase but is secreted at a detectable level during stationary phase. Since the complemented strain is not genetically identical to the wild type, secretion of hercynine may be regulated differently in these two strains. We have shown that CDC1551 may not secrete ERG during stationary phase. Therefore it is possible that when ERG is being secreted during exponential phase hercynine is not and when hercynine is secreted during stationary phase, ERG is not in CDC1551. However, due to the large variation between biological replicates, more quantification experiments are needed to confirm this assertion.

We previously showed that deleting *egtD* in *M. smegmatis* abolished ERG biosynthesis [99], therefore this result is consistent in mycobacteria. This indicates that EgtD is the only methyltransferase involved in ERG biosynthesis and cannot be compensated for by any other enzymes. The enzyme EgtD catalyses the methylation of histidine by a proximity and orientation effect in a successive reaction. It consists of two domains, the methyltransferase domain and the substrate binding domain. The histidine binding pocket primarily recognises the imidazole ring and the carboxylate group of histidine accounting for its methylation selectivity and specificity [155]. Similarly, it has been shown that EgtB binding is specific to γ -glutamyl cysteine (GGC) and any mutation on its residue (D416) may affect its sulphur donor specificity [154]. This indicates that EgtB is the only enzyme that catalyses the third step of ERG biosynthesis. Similarly searches revealed no homolog of EgtB in *M. tuberculosis* or enzymes that can perform the same function. Therefore EgtB is specific to ERG biosynthesis. To further confirm that this finding is not strain specific *egtB* was deleted in H37Rv as well and this led to the loss of ERG biosynthesis in this strain (Table 4.6). This is supported by some studies that identified ERG producing organisms that possess only have EgtB and EgtD but not EgtA, EgtC and EgtE. In addition the expression of *egtD* and *egtB* are positively correlated [153]. Furthermore, the first two steps of ERG biosynthesis in *N.crassa* are catalysed by NcEgt-1 which is an enzyme that contains domains found in EgtD and EgtB, thereby playing the catalytic role of both enzymes in the fungus *N.crassa* [145]. These results support the previous speculation that EgtB and EgtD are the key enzymes in ERG biosynthesis across species [151].

Mycobacterial nitrogen metabolism has been explored to identify new drug targets. Glutamine synthetases (GS) are the key enzymes in this metabolism. These enzymes are inhibited by L-methionine-S,R-sulphoximine (MSO) which is known to inhibit mycobacterial growth in vitro and in vivo [198, 199]. There are four glutamine synthetases in *M. tuberculosis* (GlnA1, GlnA2, GlnA3 and Gln4) whose activities are regulated by other enzymes. Few examples of the GS regulatory enzymes are adenylyl transferase (GlnE), gamma-glutamylcysteine synthase (GshA or EgtA), UDP-N-acetylmuramoylalanine-D-glutamate ligase (MurD) and glutamate racemase (MurI) [200]. It has been shown that EgtA (GshA) is inhibited weakly by MSO and strongly by D,L-buthionine-S-R-sulphoximine (BSO) indicating that EgtA shares functional similarities with the GS [200]. Therefore, it is more likely that EgtA is partially compensated for by one of these enzymes which play similar functions. A low level of ERG was detected in the $\Delta egtA$ mutant of *S.coelicolor* as well and it was suggested that EgtB could use cysteine instead of GGC as a substrate in the absence of EgtA (since it catalyses the synthesis of GGC) [159]. However, it was previously shown that cysteine is a poor substrate of EgtB [148] which make that speculation questionable.

The enzyme Rv1061 (MT1091) is a glutamine amidotransferase hypothetical protein that shares 87% similarity with the amidohydrolase EgtC. It is more likely this enzyme compensates for the loss of EgtC in the $\Delta egtC$ mutants, which explains the detectable low level of ERG in this mutant. A validation of this assertion will be to delete *Rv1061* in the $\Delta egtC$ mutant and measure the level of ERG in the resulting double mutant.

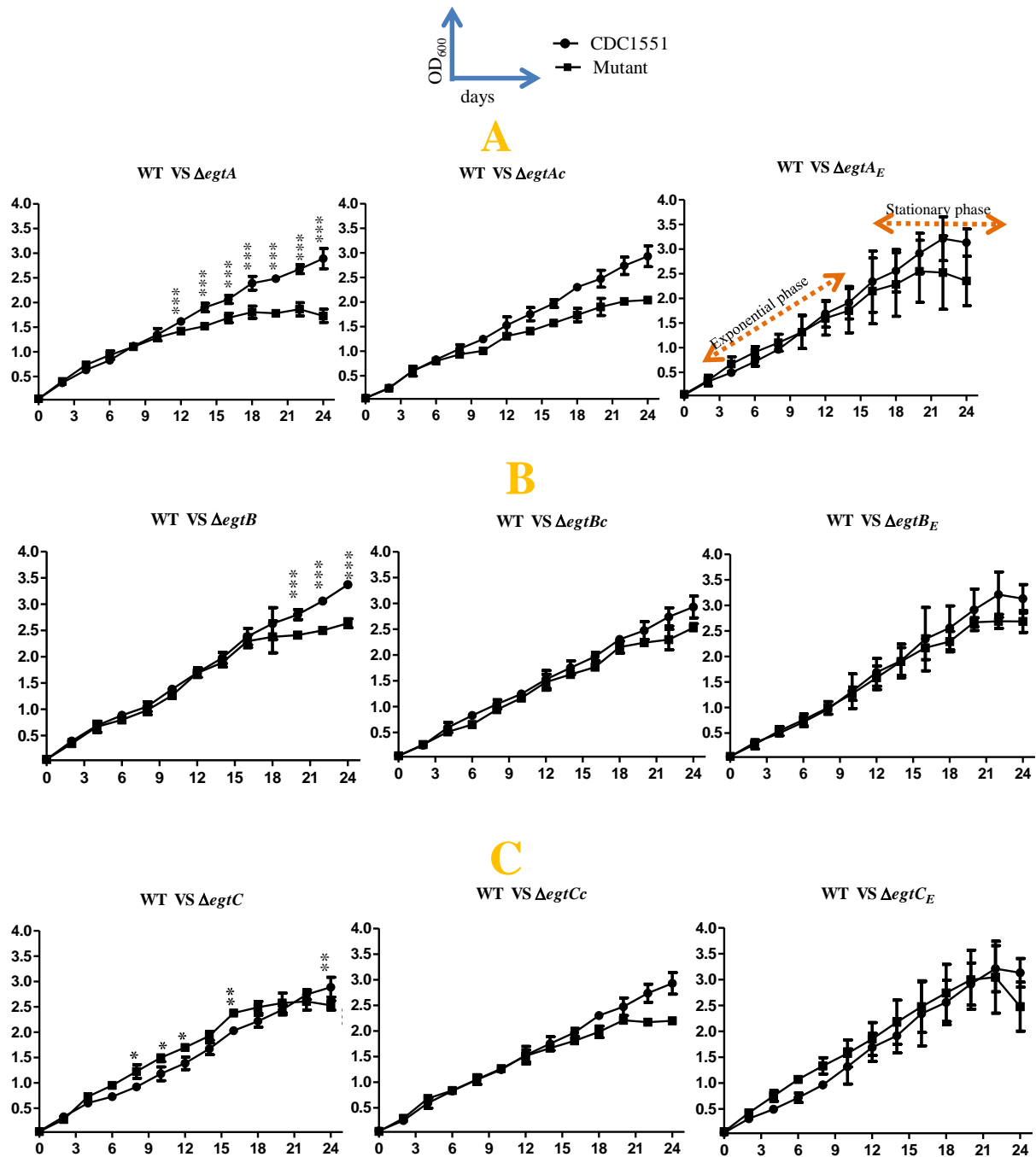
The first attempt of the recombinant production of soluble EgtE was unsuccessful; and the function of EgtE in ERG biosynthesis was assigned by homology, when an enzyme of similar activity from *Erwinia tasmaniensis* was assayed [148]. Recently it was shown that EgtE could catalyse the formation of ERG only in the presence of a reducing agent [149]. In this study the level of ERG was higher in the CDC1551 $\Delta egtE$ mutant and in the H37Rv $\Delta egtE$ mutant (Table 4.6). It was shown that PLP alone could induce the formation of ERG in the absence of EgtE [201]. Therefore, EgtE is not essential for ERG biosynthesis. It is possible that there is a spontaneous production of ERG in the presence of PLP with or without EgtE. On the other hand EgtE is a homologue of enzymes involved in Fe-S metabolism namely Rv1464/MT1511 (71%) and Rv3025c/ MT3109 (52%); known as cysteine desulfurases. Cysteine desulfurases are PLP-dependent enzymes which are the central components of the multiprotein systems ISC (iron-sulfur cluster) and SUF (sulphur metabolism). These systems are required for the Fe-S cluster biogenesis. Iron-sulfur proteins are involved in many critical

biological processes such as RNA modification, DNA repair and others. In gram negative bacteria, it is believed that the SUF system is active only under oxidative stress and iron limitation conditions, while the ISC system is a housekeeping system. Proteins involved in this system are encoded by gene clustered in the same operon (the *iscRSUA-hscBA-fdx* operon or the *sufABCDSE* operon) [202-204]. However in gram positive bacteria such as *M. tuberculosis*, only one cysteine desulfurase is found in the ISC operon which is Rv3025c (IscS). Phenotypic experiments revealed that IscS is involved in Fe-S metabolism and may be active under oxidative stress conditions (as seen with components of the SUF system) since *M. tuberculosis* mutants lacking Rv3025c (IscS) are sensitive to oxidative stress [202]. The propensity of the SUF system to be active only under oxidative stress conditions and iron depletion may be dependent on the ability of mycobacteria to produce or regulate the level of ERG and/or MSH which are known antioxidants. Since we definitely know that it is a PLP dependent cysteine desulfurase that catalyses the last step of ERG biosynthesis, it is possible that IscS (Rv3025c) catalyses that step and/or the production of IscS is elevated in the $\Delta egtE$ mutant to compensate for the loss of the cysteine desulfurase EgtE resulting in the increased level of ERG in the $\Delta egtE$ mutants. However, it is worth noting that Rv1464 shares a 71% homology with EgtE, and it is a hypothetical protein denoted as a cysteine desulfurase as well. This enzyme is situated in the *Rv1460-Rv1461-Rv1462-Rv1463-Rv1464-Rv1465-Rv1466* operon in *M. tuberculosis*, which is thought to encode the major Fe-S cluster biogenesis machinery in this organism. In addition, it was shown recently that the gene coding for this enzyme was highly expressed when H37Rv was treated by an intracellular ROS generating molecule (ATD-3169) [191]. This enzyme may also have the ability to compensate for the loss of EgtE during ERG biosynthesis. Therefore in the absence of EgtE, there is probably a defect in the Fe-S metabolism causing the up-regulation of another cysteine desulfurase Rv3025c (IscS) or/and Rv1464 and consequently an increase production of ERG. However, this remained to be shown. One way to investigate this interplay between these enzymes would be to quantify ERG in the $\Delta iscS$ mutant.

4.5 ERG is necessary for growth during the stationary phase

The $\Delta egtE$ mutant growth was not different from the wild type (Figure 4.17E). However, this strain does not exhibit any visual aggregation in comparison with the wild type and other strains, even after incubation for up to 60 days (Figure 4.17). To verify if this particular phenotype was unique to the $\Delta egtE$ mutant of the CDC1551, the $\Delta egtE$ *M. tuberculosis* H37Rv mutant was incubated for about a month and clumping was observed from approximately the third week of incubation. To further investigate if this unique phenotype

was associated with the metabolism of the detergent Tween 80 in the culture media, or to the structure of the membrane of the CDC1551 $\Delta egtE$ mutant, it was incubated without Tween 80 which resulted in aggregation of the mycobacteria; indicating that the absence of a visual aggregation of the $\Delta egtE$ mutant may not be due to an alteration of its membrane structure. However, the membrane structure of this mutant must be investigated by electron microscopy.



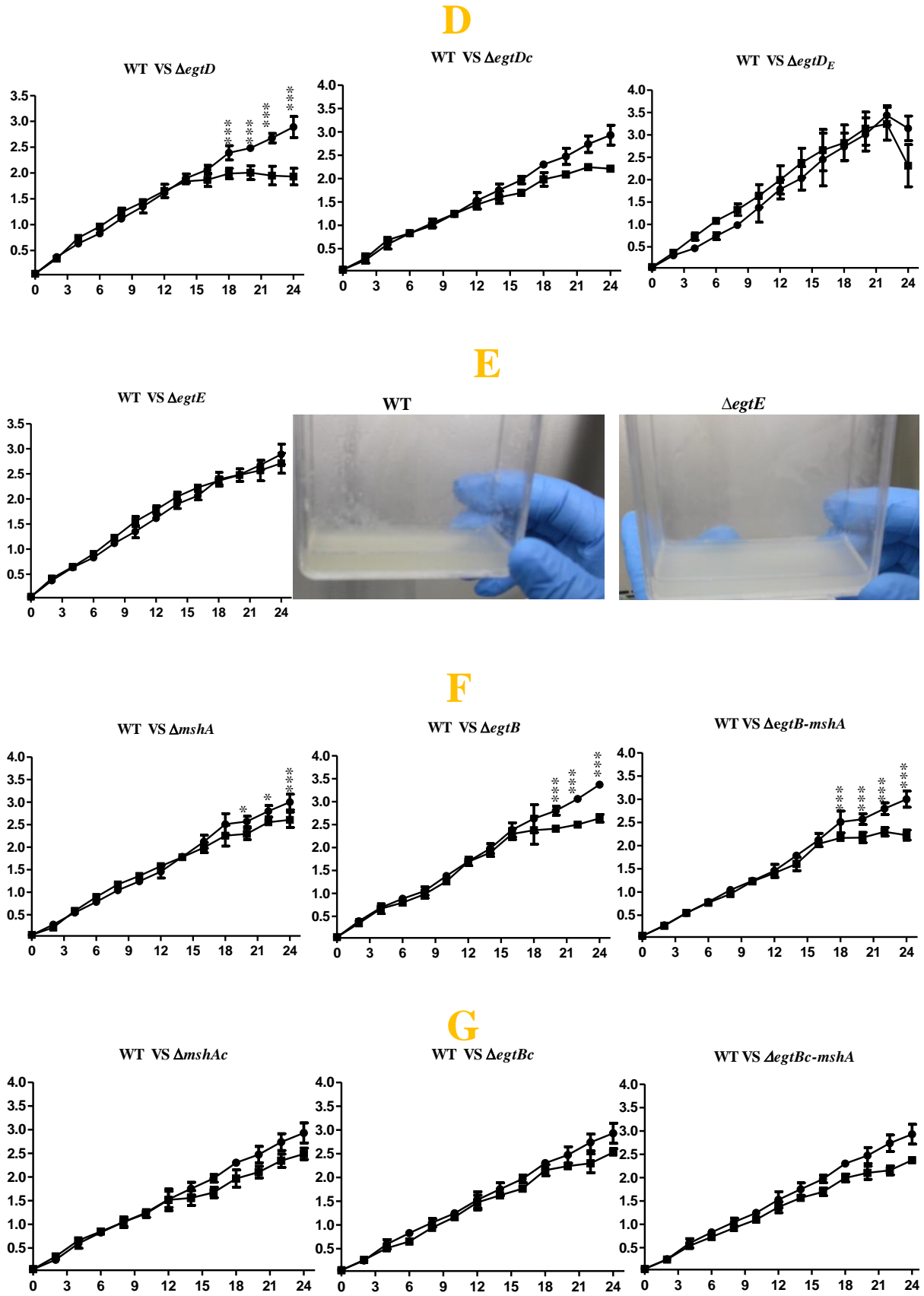


Figure 4.17 Growth curve of CDC1551 *M. tuberculosis* mutants

Cultures were inoculated to and OD₆₀₀ of approximately 0.05 and the OD₆₀₀ was measured every second day. Data are representative of three independent experiments (except $\Delta egtD_E$) and are represented as mean and SD (standard deviation). *** (P<0.001), ** (P<0.01), * (P<0.05), WT: wild type, VS: versus

Figure 4.17A Growth curves of the $\Delta egtA$ mutant (left panel), Figure 4.17B Growth curves of the $\Delta egtB$ mutant (left panel), Figure 4.17C Growth curves of the $\Delta egtC$ mutant (left panel), Figure 4.17D Growth curves of the $\Delta egtD$ mutant (left panel); genetic complements (middle panel) and chemical complements (right panel) relative to the wild type. Figure 4.17E Growth curve of the $\Delta egtE$ mutant (left panel), culture granularity after 60 days of the wild type (middle panel) and the mutant (right panel). Figure 4.17F Growth curves of the $\Delta mshA$, $\Delta egtB$ and $\Delta egtB$ - $mshA$ and Figure 4.17G Growth curves the genetically complemented $\Delta mshA$, $\Delta egtB$ and $\Delta egtB$ - $mshA$ (only $egtB$)

During in vitro growth, mycobacteria exhibit three main growth phases. The lag phase where the metabolism of the mycobacteria is slow; this stage is observed in *M. tuberculosis* when bacteria starting inoculum is less than 0.05, but in this study, we could not start the cultures at an OD₆₀₀ lower than 0.05 because some of the mutants failed to grow at a lower inoculum. The exponential phase (characterized by a high metabolic level) and finally the stationary phase (where mycobacteria growth slows down as they become metabolically less active) which can lead to the death phase (Figure 4.17A). Under electron microscopy, mycobacteria appear as corded aggregates throughout every growth stage. However during the stationary phase these cords are bigger more compact and round, probably due to an increase in their hydrophobicity which stands out when the culture is observed visually [205] (Figure 4.17E). On the other hand, Tween 80 is a detergent known to induce homogenous growth of mycobacteria [206]. The exact biochemical mechanism of action of Tween 80 is not known, but it was observed that the polar C-mycosidic glycopeptidolipids (GLPs) of the Mycobacterium avium-Mycobacterium intracellulare complex (MAC) superficial L₁ layer decreases with an increase Tween 80 concentration [207]. However, the dispersing ability of Tween 80 is not effective during stationary phase as mycobacteria aggregate more during that stage. It has been speculated that Tween 80 slowly hydrolyses in culture media. It has also been speculated that lipases from mycobacteria may accelerate hydrolysis of Tween 80 to an un-esterified oleic acid [208]. On the other hand, it was shown that *Traustochytrium aurium* was able to use Tween 80 as a carbon source or directly incorporate the Oleate of Tween into its fatty acid content [206]. Irrespective, we can deduce that Tween 80 decreases in bacterial culture over time which explains the increase in the mycobacterial aggregation. The enzyme EgtE belongs to a family of enzymes known as the cysteine desulfurase family, whose main function is basically to cleave the sulphur residue of cysteine in order to transfer it to another amino acid [209]. However, it has been shown that desulfurization of cysteine or methionine leads to a change of the configuration of fatty acids which can lead to their degradation [210]. Therefore, EgtE may be involved in the degradation of the oleic acid of Tween 80, which

explains why the $\Delta egtE$ mutant does not aggregate as much as the wild type during stationary phase because the level of Tween 80 in the $\Delta egtE$ culture is possibly higher. However, it should be noted that EgtE could be compensated for by other cysteine desulfurases and that the H37Rv $\Delta egtE$ mutant does not exhibit that phenotype. There is no data indicating that these cysteine desulfurases are secreted, it is possible that EgtE is the only secreted cysteine desulfurase in CDC1551, that's why it could directly affect the extracellular level of Tween 80. However, the opposite could be true in the case of H37Rv; this assertion is supported by previous studies that demonstrated that the crude lipid fraction of CDC1551 was different to that of H37Rv and it is worth noting this was shown with mycobacteria grown in 7H9 containing the same percentage (0.05%) of Tween 80 we used in this study [192]. More experiments need to be done to confirm this assertion. Gas or liquid chromatographic measurement of the unsaturated oleic acid in the stationary culture of the wild type and of the $\Delta egtE$ mutant will be useful to confirm degradation of Oleate by EgtE. In this case the extracellular Tween 80 lipid will be isolated by the phenol chloroform method as previously described [211].

On the other hand, ERG-deficient mutants and the MSH-deficient mutant grew poorly from late exponential phase to stationary phase.

The $\Delta egtA$ mutant grew poorly from day 14 throughout the stationary phase ($P < 0.001$ each time point) and genetic complementation of *egtA* under the control of the *hsp60* promoter, ameliorated the growth of this mutant while chemical complementation of this mutant restored its growth to the wild type level (Figure 4.17A). The $\Delta egtB$ mutant grew poorly from day 18 throughout the stationary phase ($P < 0.001$) and genetic complementation of *egtB* under the control of the *hsp60* promoter, ameliorated the growth of this mutant while chemical complementation restored its growth to wild type level (Figure 4.17B). Strangely, the $\Delta egtC$ mutant grew better than the wild type from day 8 to 12 ($P < 0.05$), then grew normally 2 days later, but then grew better than the wild type again on day 16 ($P < 0.01$) and grew normally from day 18 to 22. However, on the 24th day, the wild type grew better than it. Genetic complementation of *egtC* under the *hsp60* promoter partially restored its phenotype to the wild type level, while chemical complementation of this mutant completely restored its growth phenotype to the wild type level (Figure 4.17C). The $\Delta egtD$ mutant had a growth defect from day 18 throughout the stationary phase ($P < 0.001$ throughout). Genetic complementation of *egtD* under the *hsp60* promoter ameliorated the growth of this mutant while chemical complementation restored its growth to the wild type level (Figure 4.17D)

The $\Delta mshA$ mutant had a growth defect only from day 18 to 22 ($P < 0.05$), and at day 26 ($P < 0.01$) (Figure 4.17F), but genetic complementation aggravated the phenotype as the complement showed a growth defect from day 16 throughout the stationary phase (Figure 4.17G).

The $\Delta egtB$ - $mshA$ grew poorly relatively to the wild type from day 18 throughout the stationary phase ($P < 0.001$) (Figure 4.17F). Results indicate that the effect of the deletion of *egtB* and *mshA* in CDC1551 is additive. Genetic complementation *egtB* in this mutant ameliorated its growth phenotype (Figure 4.17G). With the exception of the $\Delta egtE$ mutant which is not an ERG-deficient mutant (Table 4.6), all the ERG-deficient strains grew poorly during stationary phase. The MSH-deficient $\Delta mshA$ mutant also grew poorly during stationary phase but not as much as the ERG deficient mutants.

The stationary phase is characterized mainly by depletion of nutrients, and the metabolism of the mycobacteria gradually shuts down while they enter a dormant state and stop multiplying [212]. Dormancy in other hand is characterized by a slow replication rate or complete replication shut down of mycobacteria residing within necrotic cells known as granuloma. Their metabolic shut down has been proposed to more driven by conditions such as nutrient limitation and low oxygen tension found within the granuloma [213]. Therefore these results suggest that ERG potentially protects *M. tuberculosis* during dormancy in latent tuberculosis. These results are supported by recent studies that showed that an ERG-deficient $\Delta egtD$ H37Rv mutant viability decreased after three weeks of incubation in a nutrient deprived media [214]. The ability of chemical complementation to ameliorate the stationary growth defect suggests either that this effect is as a result of a function of EE, or that ERG can also be imported. Previous work showed that ERG-deficient *M. smegmatis* mutants did not have any growth defect [99] while ERG-deficient *Streptomyces coelicolor* grew poorly during stationary phase [159]. Organic hydroperoxide is known to be overproduced in the MSH-deficient *M. smegmatis* mutant [100], however there is no ortholog of Ohr in *M. tuberculosis* and the Ohr ortholog in *Streptomyces coelicolor* is not overproduced in the MSH-deficient mutants neither in the ERG-deficient mutant. This implies that *M. smegmatis* uses other protective molecules during harsh conditions and therefore does not require ERG for its survival during dormancy. On the other hand, MSH-deficient mutants present a slight growth defect but not as aggravated as in the ERG-deficient mutants. Furthermore, complementation worsens its growth defect. It has been observed that MSH-deficient *M. smegmatis* and *M. tuberculosis* mutants produce more ERG than the wild type strain ([99, 100]; Table 3.3, Table 4.6) which explains why the ERG-deficient mutants grew more poorly than the MSH-

deficient mutant as the high level of ERG in the MSH-deficient mutant may enable it to grow better during stationary phase. That's why, complementation of MSH which implies restoration of ERG and MSH more or less to the wild type level in this strain, aggravated the growth defect phenotype. As opposed to *M. tuberculosis*, it was shown that the MSH-deficient *S. coelicolor* grew as poorly as the ERG-deficient strain during stationary phase [159]. This is explained by the fact that *S.coelicolor* MSH-deficient mutant produces the same amount of ERG as the wild type as opposed to *M. tuberculosis* and *M. smegmatis* [159]. In addition, MSH deficiency was obtained in *S.coelicolor* by deleting *mshC* causing an accumulation of the metabolites whose reaction are catalysed by MshC which are cysteine and GlcN-Ins. However, excess cysteine is toxic to bacteria, inhibiting growth [215]. This is because cysteine forms complexes with redox-active transition metals which consecutively enhance the production of ROS [216]. However, in this study MSH-deficient mutants were obtained by deleting *mshA* instead of *mshC* hence there is no accumulation of cysteine in this strain.

It is worth noting that the $\Delta egtC$ mutant grew better than the wild type during the exponential phase but gradually grew poorly during the stationary phase (Figure 4.17C). This is an indication that the accumulated intermediary metabolite in this strain may favour the growth of this strain during the exponential phase. On the other hand, it is possible that the absence of the enzyme EgtC may have induced the overproduction of another enzyme that lead to an enhance growth phenotype. A mass spectrometry analysis of the cell extract of this mutant to identify any potential up-regulated protein that may have caused this phenotype will bring more clarification. On the other hand, LC-MS analysis of the cell extract of this mutant may enable to identify the accumulated compound that may have caused this phenotype. However, whatever mechanism is involved, it was not good enough to enable that strain to also grow better during the stationary phase, as the growth of the mutant gradually decreased to the wild type level from day 18 and it began to grow less than wild type from day 24.

Since we know mycobacteria have the tendency to aggregate more during stationary phase, we investigated if aggregation may have affected the viability of the mutants. This was achieved by monitoring the viability of the mutants using the MGIT system. The MGIT system is a method used to evaluate the drug susceptibility of *M. tuberculosis* strains. It is based on the growth unit of the tested strain when the growth unit of the control sample is 400. Mycobacteria are inoculated into MGIT tubes containing 7H9 supplemented with OADC and the oxygen-quenched fluorochrome, tris 4, 7-diphenyl-1, 10-phenanthroline

ruthenium chloride pentahydrate, embedded in silicone at the bottom of the tube. But there is no Tween 80 in this culture media to prevent aggregation. As the mycobacteria grow, they release CO₂ and consume O₂ which causes the release of the fluorochrome whose fluorescence is detected by the MGIT 960 instrument and reported as growth units [217, 218]. When the growth unit of the mutants were compared to the wild type from the day they all became positive to the day of the last reading, there was no significance difference (Figure 4.18); indicating that aggregation or the absence of Tween80 does not affect the viability of the mutants.

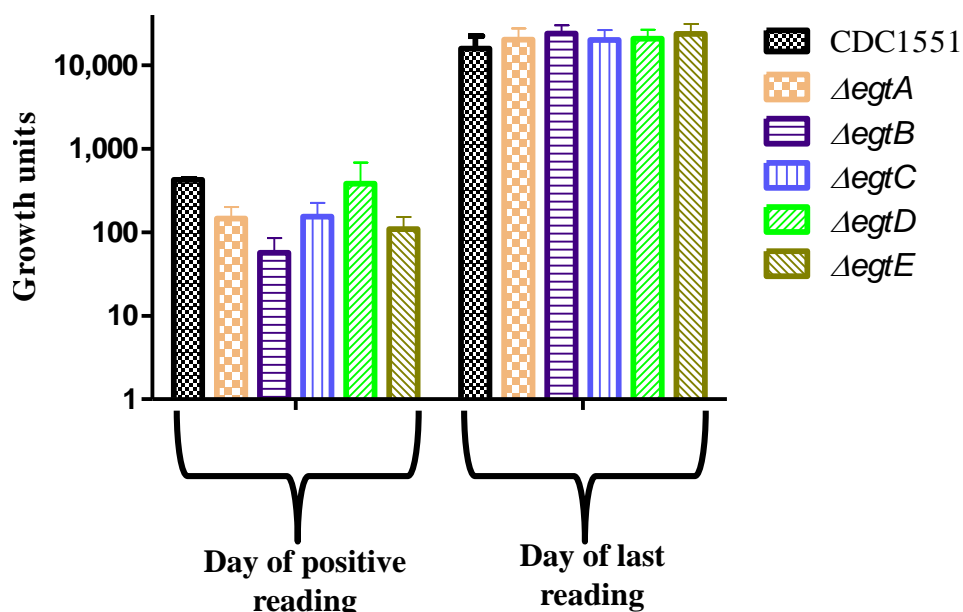


Figure 4.18 Evaluation of the mutants' viability when grown without Tween80

MGIT vials were inoculated with 10^3 - 10^4 CFUs and incubated at 37°C in the MGIT 960 instrument which recorded the growth units.

In view of this, we can conclude that ERG and MSH enable mycobacteria to survive during stationary growth. However, *M. tuberculosis* needs more ERG than MSH during this stage. It would be interesting to investigate the survival of ERG-deficient mutants during dormancy.

4.6 ERG deficiency does not affect *M. tuberculosis* susceptibility to in vitro stress

Oxidative stress and nitrosative stress are the major stresses that mycobacteria encounter upon infection. However, it has been shown that MSH protects *M. smegmatis* from oxidative stress [104], but there is no published data indicating the role of MSH in *M. tuberculosis* during nitrosative stress. In this study, we investigated the role of ERG, its biosynthetic enzymes and MSH during nitrosative stress and oxidative stress.

The susceptibility to nitrosative stress of the mutants tested in this study was not affected ($P>0.05$); However, the $\Delta egtB$ mutant was resistant to nitric oxide 24 hrs post-exposure ($P<0.01$) but became sensitive 48hrs later (Figure 4.19). This indicates that neither ERG nor MSH, protect *M. tuberculosis* from nitrosative stress.

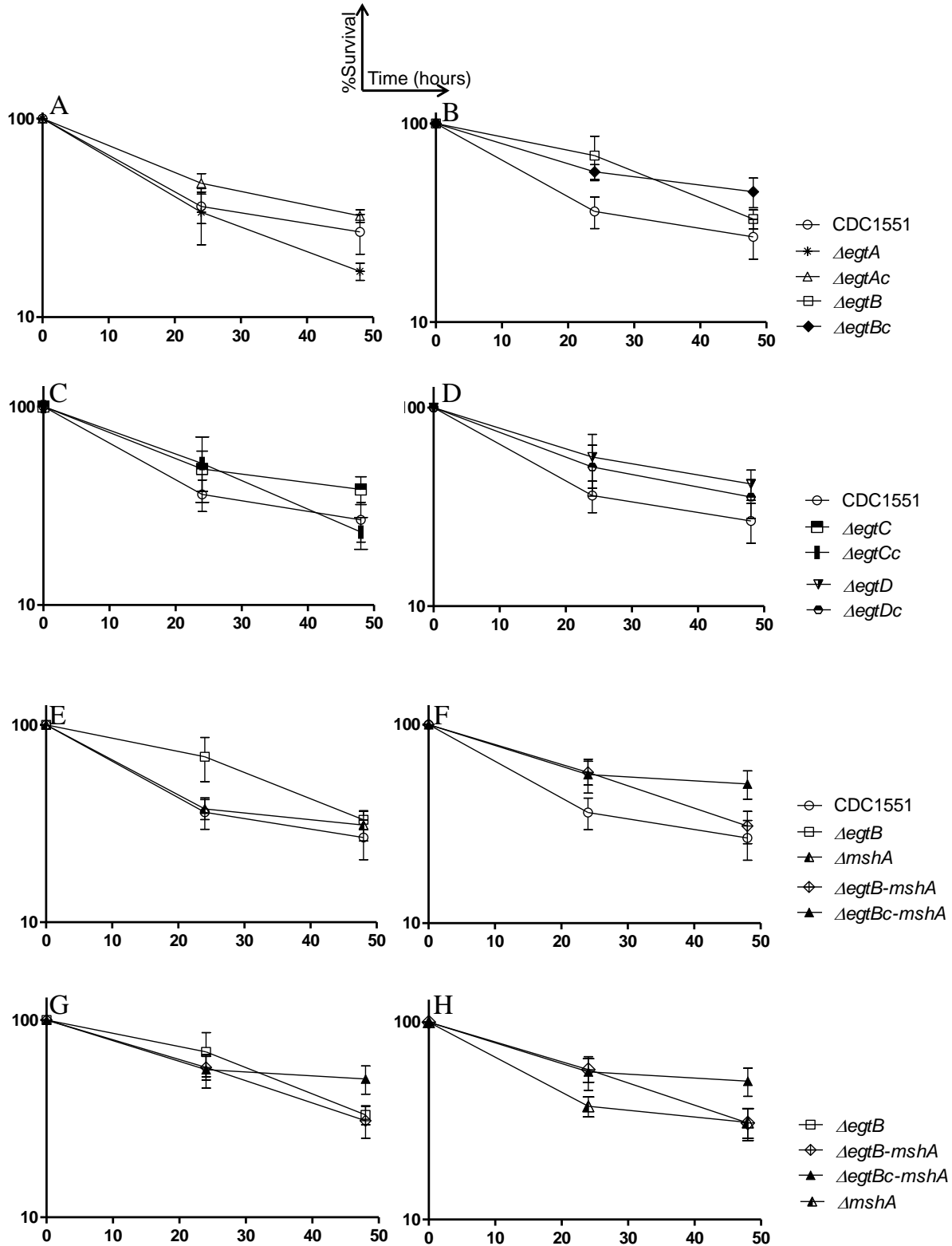


Figure 4.19 Susceptibility of *M. tuberculosis* mutants to nitrosative stress generated by DETA-NO

CFUs were counted before exposure and 24 and 48 hours post-exposure. Data are plotted as percentage survival calculated from CFUs counts before exposure. Data are representative of three to four independent experiments and are represented as mean and SEM (standard error of the mean). Figure 4.19A describes $\Delta egtA$, Figure 4.19B describes $\Delta egtB$ ($p < 0.01$), Figure 4.19C describes $\Delta egtC$, Figure 4.19D describes $\Delta egtD$, Figure 4.19E describes $\Delta egtB$ and $\Delta mshA$ and Figure 4.19F describes $\Delta egtB-mshA$ susceptibility to nitrosative stress relative to the wild

type. Figure 4.19G describes $\Delta egtB$ - $mshA$ susceptibility to nitrosative stress relative to $\Delta egtB$. Figure 4.19H describes $\Delta egtB$ - $mshA$ susceptibility to nitrosative stress relative to $\Delta mshA$

Mutants were not sensitive to oxidative stress generated by 1mM CuOOH (Figure 4.20). However, when PRG was used to generate oxidative stress, the $\Delta egtA$ mutant was more sensitive to the wild type 3 hours post-exposure ($P < 0.05$), then its phenotype was restored to the wild type level 24hrs later (Figure 4.21A). Attempts to complement this phenotype were unsuccessful either with the hsp60 promoter (Figure 4.21A) or with the endogenous promoter (data not shown). The susceptibility of the other tested mutants to PRG was not affected (Figure 4.21).

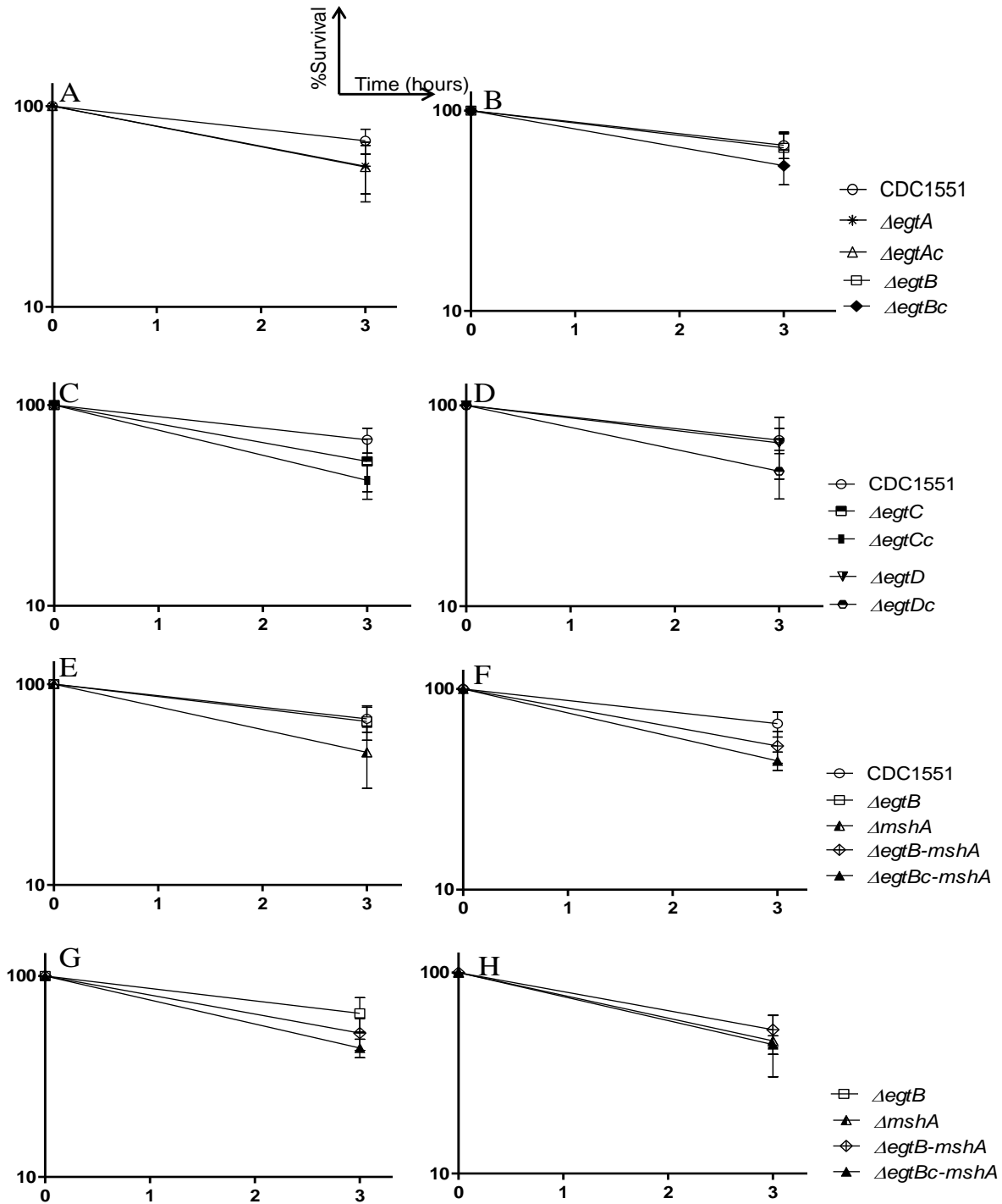


Figure 4.20 Susceptibility of *M. tuberculosis* mutants to oxidative stress generated by CuOOH

CFUs were counted before exposure and 3 hours post-exposure. Data are plotted as percentage survival calculated from CFUs counts before exposure. Data are representative of three to four independent experiments and are represented as mean and SEM (standard error of the mean). Figure 4.20A describes $\Delta egtA$, Figure 4.20B describes $\Delta egtB$, Figure 4.20C describes $\Delta egtC$, Figure 4.20D describes $\Delta egtD$, Figure 4.20E describes $\Delta egtB$ and $\Delta mshA$ and Figure 4.20F describes $\Delta egtB-mshA$ susceptibility to CuOOH relative to the wild type while Figure 4.20G describes $\Delta egtB-mshA$ susceptibility to CuOOH relative to $\Delta egtB$ and Figure 4.20H describes $\Delta egtB-mshA$ susceptibility to CuOOH relative to $\Delta mshA$

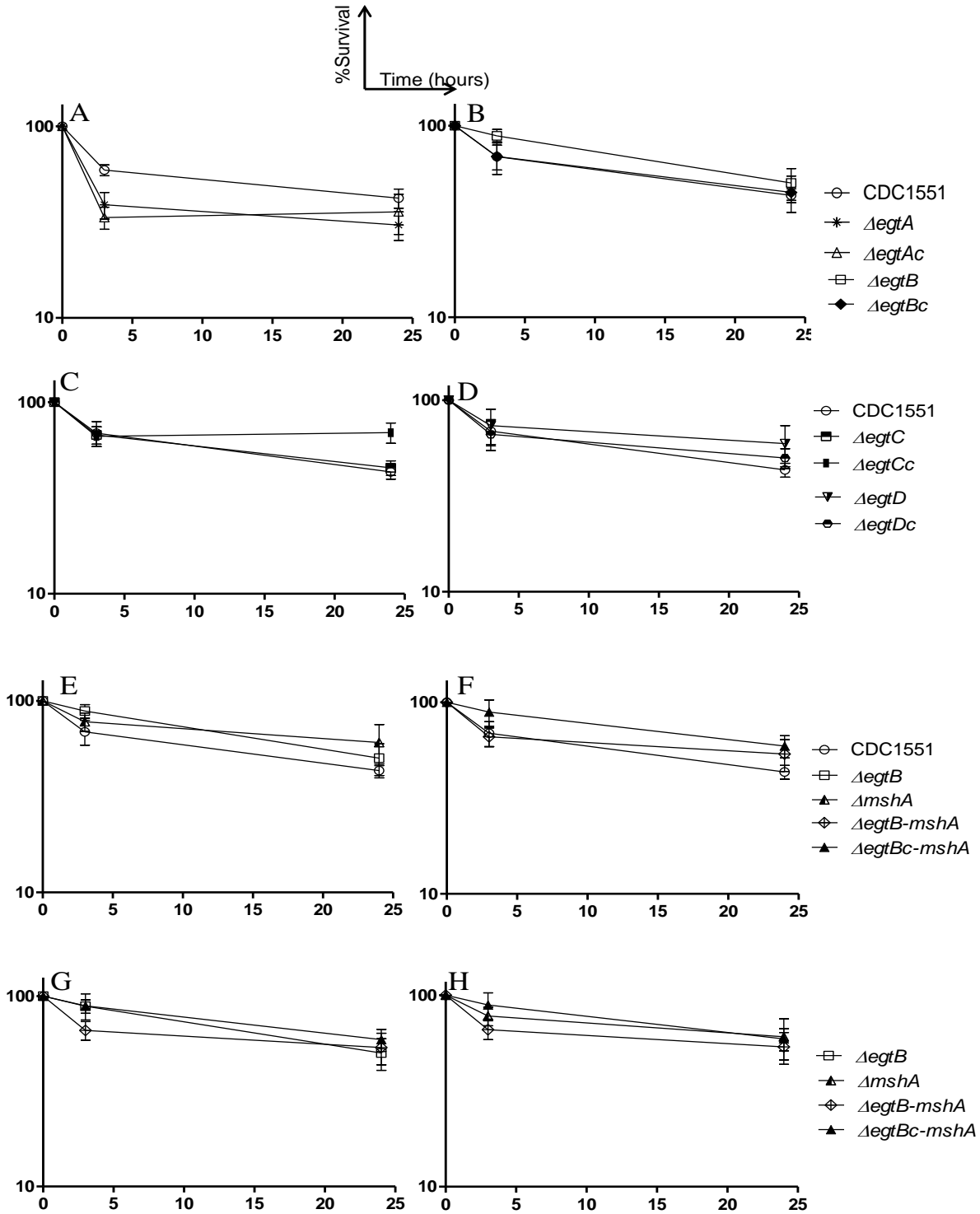


Figure 4.21 Susceptibility of *M. tuberculosis* mutants to oxidative stress generated by PRG

CFUs were counted before exposure and 3 hours post-exposure. Data are plotted as percentage survival calculated from CFUs counts before exposure. Data are representative of three to four independent experiments and are represented as mean and SEM (standard error of the mean). Figure 4.21A describes $\Delta egtA$ ($P < 0.05$), Figure 4.21B describes $\Delta egtB$, Figure 4.21C describes $\Delta egtC$, Figure 4.21D describes $\Delta egtD$, Figure 4.21E describes $\Delta egtB$ and $\Delta mshA$, and Figure 4.21F describes $\Delta egtB-mshA$ susceptibility to PRG relative to the wild type. While Figure 4.21G describes $\Delta egtB-mshA$ susceptibility to PRG relative to $\Delta egtB$ and Figure 4.21H describes $\Delta egtB-mshA$ susceptibility to PRG relative to $\Delta mshA$.

In addition, the susceptibility of every mutant to acidic stress was not altered as well (Figure 4.22).

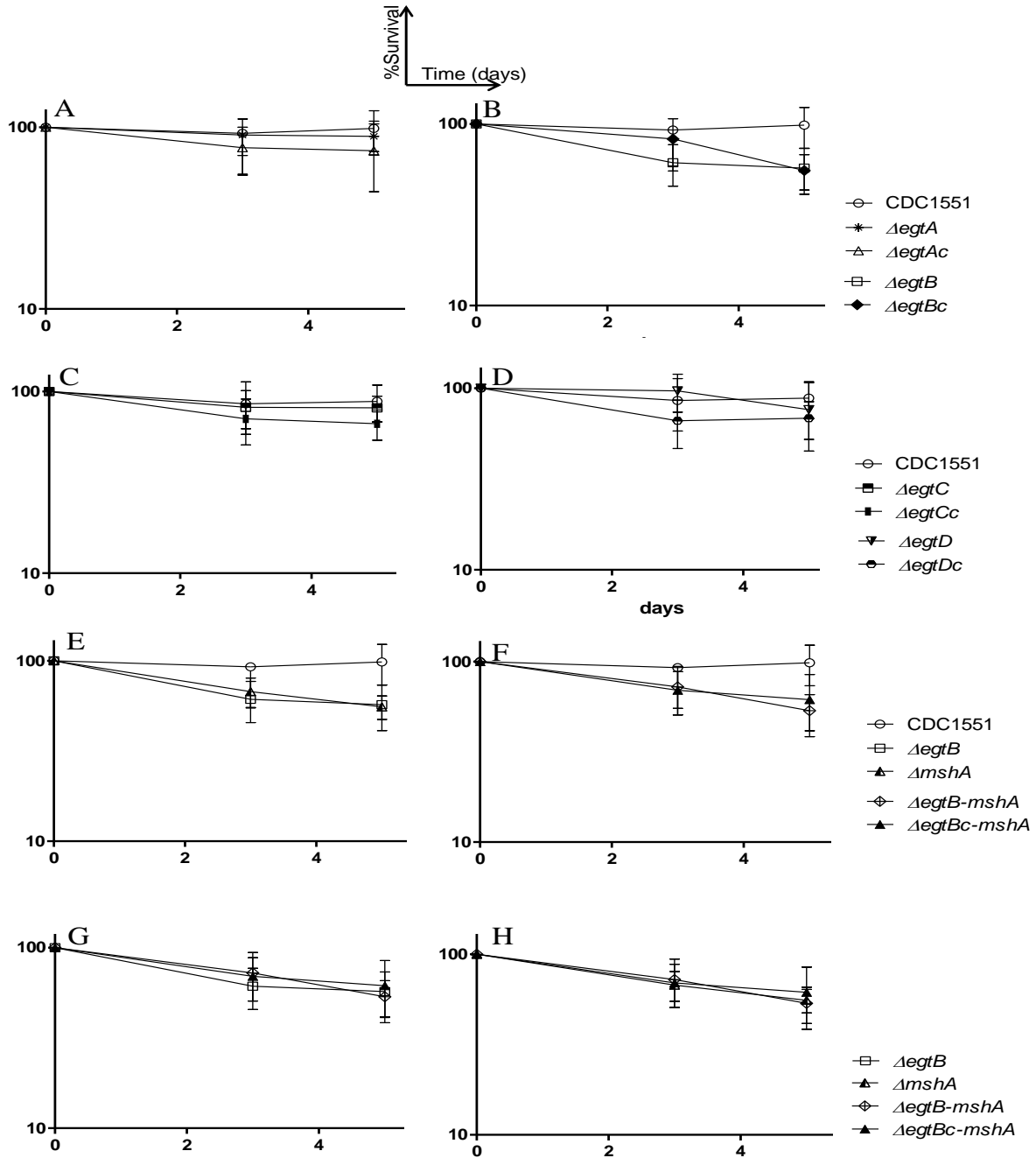


Figure 4.22 Susceptibility of *M. tuberculosis* mutants to acidic stress (pH~4.5)

CFUs were counted before exposure, 3 and 5 days post-exposure. Data are plotted as percentage survival calculated from CFUs counts before exposure. Data are representative of three to four independent experiments and are represented as mean and SEM (standard error of the mean). Figure 4.22A describes $\Delta egtA$ ($p < 0.01$), Figure 4.22B describes $\Delta egtB$, Figure 4.22C describes $\Delta egtC$, Figure 4.22D describes $\Delta egtD$, Figure 4.22E describes $\Delta egtB$ and $\Delta mshA$ and Figure 4.22F describes $\Delta egtB-mshA$ susceptibility to acidic stress relative to the wild type. Figure 4.22G describes $\Delta egtB-mshA$ susceptibility to acidic stress relative to $\Delta egtB$. Figure 4.22H describes $\Delta egtB-mshA$ susceptibility to acidic stress relative to $\Delta mshA$.

Acidification of macrophages during maturation is a mechanism used by the host to fight invading mycobacteria. However, it has been shown that *M.tuberculosis* is able to escape this defence mechanism by neutralizing the acidic effect [219]. In order to evaluate if ERG or ERG biosynthetic genes and/or MSH are involved in this process, we exposed the mutants generated in this study to an acidified medium. This study indicates that neither MSH, nor ERG protects mycobacteria from acidic stress. However, it was shown that MSH-deficient *M. smegmatis* mutants were sensitive to acidic stress (pH~4) [108]. It may be due to the strain difference; it could be that *M. tuberculosis* evolves a different survival mechanism under acidic stress as compared to *M. smegmatis*. The difference in the result may also be due to the method of testing. The authors exposed the mycobacteria to acidified 7H9 medium while we exposed the mycobacteria to acidified PBS medium. Since it was shown that mycobacteria are more sensitive to acidic stress in acidified 7H9 medium relative to other media, to perform an acidic stress experiment that better reflects the in vivo condition, it is recommended to use a buffer that will not influence interpretation of the data [220], which in this case was PBS.

It has been shown that MSH-deficient $\Delta mshB$ mutants are sensitive to oxidative stress generated by 0.5mM CuOOH [104]. But the susceptibility of the $\Delta mshA$ mutants to oxidative stress has never been investigated [102]. In this study it was shown that the $\Delta mshA$ mutant which totally lacks MSH as opposed to the $\Delta mshB$ mutant which still produces low level of MSH [102, 104], was not sensitive to oxidative stress. Therefore the $\Delta mshB$ mutants were sensitive to oxidative stress generated by CuOOH either because of other biological consequences resulting from *mshB* deletion or because a different strain was used (Erdman strain instead of the CDC1551 strain) or because mycobacteria were plated on 7H9 agar media instead of 7H11 which is known to contain more nutrients and therefore will maximize growth recovery. Further, none of the ERG-deficient mutants (except the $\Delta egtA$ mutant) were sensitive to oxidative stress generated either by CuOOH or by PRG. It was previously shown that bacterial sensitivity to oxidative stress differs depending on the compound used to generate the oxidative stress. *S.coelicolor* $\Delta egtA$ mutant was sensitive to oxidative stress generated by CuOOH and hydrogen peroxide but not to diamide [159]. In addition, it is worth noting that it was previously shown that MSH-deficient *M. smegmatis* mutants were sensitivitive to oxidative stress generated by hydrogen peroxide and TBHP but not by the aromatic compound CuOOH [108]. It is possible that the ERG-deficient single mutants and the MSH-deficient mutant generated in this study are not sensitive to oxidative stress generated by aromatic compounds since PRG is also an aromatic compound. In *M. smegmatis*

(Chapter 3); ERG and MSH single mutants were not sensitive to oxidative stress generated by CuOOH ; however the ERG/MSH-deficient double mutant was [99]. So to investigate if that was the case as well in *M. tuberculosis*, we generated an ERG/MSH-deficient double mutant by deleting *mshA* in the $\Delta egtB$ mutant, but unexpectedly, this mutant was not sensitive to oxidative stress neither to nitrosative stress nor to acidic stress (Figure 4.19F-H, 4.20F-H, 4.21F-H, and 4.22F-H). To understand this contradiction, we first had to look at the difference between the double mutant that was generated in *M. smegmatis* and the double mutant generated in this study. The double mutant in *M. smegmatis* was obtained by deleting *egtD* in the $\Delta mshA$ mutant, whereas in this study the double mutant was obtained by deleting *mshA* in the $\Delta egtB$ mutant. The enzyme EgtD catalyses the methylation of histidine in the first step of ERG biosynthesis to produce hercynine while EgtB is an iron (II)-dependent enzyme that catalyses oxidative sulfurization of hercynine by GGC (synthesized by EgtA) (Figure 1.8). Therefore, deletion of *egtB* will abolish that reaction and may cause accumulation of gamma glutamyl-cysteine (GGC). However, it was shown that GGC plays the same role as glutathione in the detoxification of ROS and RNS in eukaryotes [221-223]. Therefore the potential accumulation of GGC in $\Delta egtB$ protects it from nitrosative and oxidative stress. Hence, the ERG/MSH-deficient double mutant could still survive under oxidative stress probably because of the protective effect of excess GGC. We have shown that neither MSH nor ERG , nor both protect *M. smegmatis* from nitrosative stress (Chapter 3) [99] which concurs what we saw in this study and may explain why neither the double mutant nor the single mutants were sensitive to nitrosative stress. Since ERG does not protect mycobacteria from nitrosative stress, the protective effect of accumulated GGC in the $\Delta egtB$ mutant could not be neutralized by the lack of ERG; making this mutant resistant to nitrosative stress (Figure 4.19B; $P < 0.01$). The same trend was observed in the double mutant (Figure 4.19F-H) though it was not significant ($P > 0.05$). It is not known how exactly that happens, but the discovery of gamma glutamyl transferase in *M. smegmatis*, the evaluation of its activity and the discovery of glutathione biosynthetic enzymes in *M. smegmatis*, indicate that GGC definitely plays a protective role in mycobacteria as well [224-226].

The $\Delta egtA$ mutant in this study was sensitive to oxidative stress generated by PRG but not to oxidative stress generated by CuOOH (Figure 4.21A & 4.20A); in accordance with previous findings [159]. However, they showed that the $\Delta egtA$ mutant of *S.coelicolor* was sensitive to oxidative stress generated by CuOOH which was not observed in this study. The discrepancy in the result may be due to the difference on the methods used to evaluate mutant sensitivity to oxidative stress. They used the disk-agar diffusion assay while we investigated the survival

after exposure to stress by CFU counts. They concluded that the sensitivity of the $\Delta egtA$ mutant was due to the lack of ERG or the toxic effect of the accumulated cysteine. The results obtained in this study enabled us to deduce that the susceptibility of the $\Delta egtA$ mutant is not solely due to the lack of ERG as the other ERG-deficient mutants were not sensitive. EgtA is known as GGC synthetase, it catalyses the ligation of cysteine to glutamate to form GGC in ERG biosynthesis (Figure 1.8). So, when EgtA is abolished, there is more likely accumulation of cysteine (Table 4.8) and glutamate and a decrease in the level of GGC.

Table 4.8 Cysteine concentration in the cell extract of the CDC1551 mutants pg/10⁷ CFUs

Strains	1	2*	average
CDC1551	0	0	0
$\Delta egtA$	17.12	3.87	10.50 ± 6.62
$\Delta egtB$	7.08	0	3.54 ± 3.54
$\Delta egtC$	5.60	0	2.80 ± 2.80
$\Delta egtD$	5.14	0	2.56 ± 2.56
$\Delta egtE$	0	0	0
$\Delta egtAc$	0	0	0

*Data are representative of two independent experiments and two independent quantifications; cysteine was below detection limit in all samples during the second quantification except in the $\Delta egtA$ mutant which contains a higher level of cysteine as seen in the first replicate

Hence, this mutant may be sensitive because of the toxic effect of the accumulated cysteine [215] and/or the low level of GGC (which is known to protect against oxidative stress) and/or the low level of ERG in this mutant. A similar trend was observed when this strain was exposed to nitrosative stress; it became slightly sensitive 24 hrs later (Figure 4.19A, P>0.05). One baffling observation is the inability to complement this mutant susceptibility to oxidative stress generated by PRG (Figure 4.21A) while its phenotype is complemented during nitrosative stress (Figure 4.19A). There was no data indicating complementation of the $\Delta egtA$ mutant *S.coelicolor* as well [159]. Nevertheless, since we know that ERG production was restored in this mutant (Table 4.6), then the lack of complementation during oxidative stress may be due to the chemical properties of PRG. Pyrogallol is a compound used to evaluate the antioxidant capacity of foods, beverages and human fluids. It is induced by free radicals and ROS (to yield a quinone derivative and peroxides) and is inhibited by antioxidants. Pyrogallol has three hydroxyl groups that enable it to chelate metals and to be oxidized [227]. Since it is known that that gene expression can be altered by metal chelation [228, 229], it is more likely that complementation was not observed because of the metal chelating ability of PRG which inhibited the expression of the complemented gene. Another plausible explanation of the lack of complementation is the possible residual effect of accumulated cysteine in the $\Delta egtA$ mutant. To further understand why the ERG-deficient mutants are resistant to oxidative stress generated by CuOOH, we quantified MSH in the mutants generated in this study. Every

ERG-deficient mutant (except $\Delta egtB$ and $\Delta egtC$) had a high level of MSH relative their wild type counterpart (Table 4.9). The CDC1551 $\Delta egtB$, $\Delta egtC$ and the $\Delta egtE$ mutants had a relatively low level of MSH, the H37Rv $\Delta egtB$ and $\Delta egtE$ mutants had more or less an unchanged level of MSH (Table 4.9).

Table 4.9 MSH level during exponential growth of the mutants generated in this study (Area/10⁷ CFUs)

H37Rv	2.75 ± 1.65
$\Delta egtE$ (H37Rv)	3.26 ± 1.07
$\Delta egtB$ (H37Rv)	2.86 ± 0.83
CDC1551	2.64 ± 0.29
$\Delta egtA$ (CDC1551)	3.60 ± 0.61
$\Delta egtB$ (CDC1551)	1.13 ± 0.35
$\Delta egtC$ (CDC1551)	1.97 ± 1.16
$\Delta egtD$ (CDC1551)	3.69 ± 1.02
$\Delta egtE$ (CDC1551)	0.685 ± 0.07
$\Delta mshA$ (CDC1551)	0
$\Delta egtB$ - $mshA$ (CDC1551)	0
$\Delta MT1289$ (CDC1551)	4.32 ± 0.37
$\Delta MT1953$ (CDC1551)	5.33 ± 1.77
$\Delta mshAc$ (CDC1551)	3.79 ± 1.2
$\Delta egtAc$ (CDC1551)	7.46 ± 2.99
$\Delta egtBc$ (CDC1551)	2.34 ± 0.16
$\Delta egtCc$ (CDC1551)	4.13 ± 0.62
$\Delta egtDc$ (CDC1551)	5.03 ± 2.90
$\Delta egtBop$ (CDC1551)	2.63 ± 0.13

e: mutants complemented with genes expressed under the hsp60 promoter, **op**: mutant complemented by the entire operon, **+**: mutants complemented by the gene fused to a 1000bp US the operon; IH: intracellular hercynine, EH: extracellular hercynine. Data are representative of two independent extractions and two independent quantifications.

The $\Delta egtE$ mutants produce a low to normal level of MSH because they produce a relatively high level of ERG. The $\Delta egtC$ mutant produces a low to normal level of MSH because it still produces 70% of ERG (table 4.6). The $\Delta egtB$ mutant produces a low level of MSH because though it is ERG-deficient, it is likely to have excess GGC which protects it and therefore does not need MSH. The $\Delta egtA$ and $\Delta egtD$ mutants known to be ERG-deficient (Table 4.6) produce a high level of MSH. This is seen as well in the $\Delta MT1289$, $\Delta MT1953$ mutants known to produce a very low level of ERG (Table 4.1, Table 4.9). These results indicate that MSH compensates for the loss of ERG. In addition, we have shown as well that the MSH-deficient mutants produce more ERG (Table 4.6). Therefore, since ERG and MSH are the only known thiols in *M. tuberculosis*, they compensate for each other to protect *M. tuberculosis* during infection. Therefore a drug or drug combination that targets both thiols in a therapy can be effective against TB; however the drug target should be carefully decided as choosing the wrong target (EgtB) may cause resistance instead.

4.7 Conclusion

Ergothioneine is known to play an anti-oxidative role in many organisms including higher eukaryotes [230-232]. However it is important to determine whether it plays the same role in *M. tuberculosis* the causative agent of TB. Moreover, it is important to assess other potential roles of this compound in *M. tuberculosis* since we know it is not synthesized in higher eukaryotes. Understanding the role of ERG will enable us to validate its biosynthesis as a TB drug target. However, to be able to validate the right drug target, we have to study the role of each enzyme involved in the production of ERG and in the physiology of the mycobacteria. In this study, to reach that goal, we deleted each gene coding for the enzymes involved in ERG biosynthesis. And we investigated the physiological effect due to the abolishment of each enzyme. In addition, based on past studies indicating ERG secretion in *M. smegmatis* (Chapter 3,[99]), we investigated ERG secretion as well in slow growing mycobacteria (*M. bovis*, *M. tuberculosis* (CDC1551 and H37Rv). We could show that slow growing mycobacteria secrete ERG as well. This is a unique feature because MSH that has been previously described as the major thiol in mycobacteria is not secreted [80, 183]. However, it is worth therefore investigating why ERG and not MSH is secreted by microorganisms. Mycothiol as opposed to ERG requires enzymatic recycling when oxidized [90]. The oxidized form of ERG (ERG disulphide) is very unstable at physiological pH (stable only in acid pH), and rapidly degrades to yield free ERG [184]. This feature makes ERG a more stable thiol as opposed to MSH, therefore it is more suitable to function both intracellular and extracellular. However, it is possible that ERG does not only play an anti-oxidative role in the extracellular environment. It was previously shown that ERG modulates the immune system in order to inhibit the inflammatory response [141]. Therefore, it is more likely that mycobacteria, more precisely pathogenic mycobacteria secrete ERG to promote their survival within the host. To support this assertion, CDC1551 was shown in this study to have a lower percentage of EE relative to the H37Rv strain which is in accordance with previous studies that showed that the CDC1551 strain was less virulent relative to H37Rv and induced a higher level of cytokine production during infection [192]. Furthermore, we have shown in this study that not every gene involved in ERG biosynthesis is essential for ERG production. EgtA and EgtC are partially compensated for by other enzymes probably a glutamine synthetase and Rv1061 respectively. However, we have found that EgtE is not essential for ERG biosynthesis, as the level of the ERG in the mutant deficient in this enzyme was higher than the wild type. It could be due to a spontaneous production of ERG in the presence of PLP, or the catalysis of another PLP dependent cysteine desulfurase, either Rv1464/MT1511

or Rv3025c/ MT3109 since there are data indicating the anti-oxidative role of these enzymes [191, 202]. In addition, we have shown in this study that ERG enables *M. tuberculosis* to survive during stationary phase of growth, as every mutant except the $\Delta egtE$ mutant (which is not ERG-deficient) grew poorly during stationary phase. This is an indication of the potential role of ERG during dormancy which is also characterized by a metabolic shutdown of mycobacteria. Therefore, may highlight the role of ERG in mycobacteria in latent TB. However, we were unable to demonstrate the anti-oxidative role of ERG in this study. Based on previous information on *M. smegmatis*, we predicted that ERG could be compensated for by MSH or other anti-oxidants and therefore characterized an ERG/MSH-deficient double mutant, however this mutant may have accumulated GGC making it resistant to oxidative stress and nitrosative stress due to the anti-oxidative role of GGC [222, 233]. In addition, it was observed that the $\Delta egtB$ and the $\Delta egtC$ mutants generated in this study do not produce a high level of MSH as opposed to the $\Delta egtA$ and $\Delta egtD$ mutants. This probably is because the $\Delta egtC$ mutant still produce a high level of ERG (only ~30% of ERG is loss in this strain) and therefore do not require compensation by MSH, while the $\Delta egtB$ mutant is protected by the accumulated GGC and hence do not require compensation as well. The relatively high level of ERG in the MSH-deficient mutant ($\Delta mshA$) and the relatively high level of MSH in the ERG-deficient mutants ($\Delta egtA$ and $\Delta egtD$) generated in this study suggest the anti-oxidative role of ERG in *M. tuberculosis*; then MSH and ERG compensate for each other in the protection of *M. tuberculosis*. In view of this, future studies are discussed in the next chapter.

CHAPTER 5:
FUTURE/CURRENT
STUDIES

CHAPTER 5: FUTURE/CURRENT STUDIES

5.1 Final conclusion

In this study, we have investigated the role of ERG biosynthetic enzymes in the production and physiology of *M. tuberculosis* and have shown that ERG is secreted across many species. In addition, we could show that ERG plays an anti-oxidative role in *M. smegmatis*. This study is the first to evaluate the role of each enzyme involved in ERG biosynthesis by generating mutants deficient in the respective enzymes. It is the first study to show and report ERG secretion in mycobacteria. The key messages from this work are:

1. Ergothioneine appears to be the only thiol to be secreted by mycobacteria
2. Ergothioneine protects mycobacteria from oxidative stress; therefore secreted ERG may play an important role during infection of the host by *M. tuberculosis*.
3. Ergothioneine may play a key role during latent TB when mycobacteria are dormant as mycobacteria deficient in ERG struggle to grow during stationary phase. This could be a therapeutic benefit of drugs that target ERG biosynthesis since latent TB is not yet curable because latent bacilli are resistant to the first line drug Isoniazid [32].
4. The enzyme EgtB is not a good drug target in ERG biosynthesis as targeting that enzyme may induce resistance instead of susceptibility in the mycobacteria
5. The enzyme EgtA and EgtD could be a good drug targets if effects other than inhibition of ERG production are taken into account.
6. The enzyme EgtC is compensated for by another enzyme therefore may not be a good drug target since mutant deficient in EgtC has lost only ~ 30% of ERG
7. The proteins MT1289 and MT1953 are involved in the metabolism of ERG, but their specific function is yet unknown
8. The enzyme EgtE is not essential for ERG biosynthesis as deleting this enzyme causes an increased production of ERG.
9. Mycothiol and ERG compensate each other to protect *M. tuberculosis* since mutants deficient in one produce more of the other.

However, more studies need to be done to investigate the role of the ERG in mycobacteria in order to validate its biosynthesis as a potential TB drug target.

This study opens a new avenue of research for a new drug target against TB. Ergothioneine biosynthesis could be a new drug target against MDR, XDR, TDR and latent TB. This study contributes to the global fight against TB.

5.2 Future studies: Quantification of ERG in the $\Delta iscS$ (*Rv3025c*) mutant

Since the $\Delta egtE$ mutant produces more ERG relative than the wild type, it is important to investigate which enzyme alternatively catalyses the last step of ERG biosynthesis. We will attempt to do that by quantifying ERG in the $\Delta iscS$ mutant which is known to be sensitive to oxidative stress. If data indicate that the $\Delta iscS$ mutant is ERG-deficient or has a decreased level of ERG, then we will have to investigate the expression level or protein level of IscS and Rv1464 in the $\Delta egtE$ mutants.

5.3 Future studies: Investigation of the role of ERG during dormancy

In view of the data that indicate that ERG is essential to mycobacteria when their metabolism shuts down, it is very important to investigate the role of ERG during dormancy. In this study we will use published models of dormancy to evaluate the role of ERG. Mutants will be cultured in conditions known to induce dormancy; low oxygen (5%), high CO₂ (10%), low nutrient (10% Dubos medium) and acidic pH (5.0) [234]. Viability of the mutants relative to the wild type will be evaluated over time with and without treatment with current anti-tuberculosis drugs.

5.4 Future studies: Generation and characterization of $\Delta egtA$ -*mshA* and $\Delta egtD$ -*mshA* *M. tuberculosis* CDC1551 mutants

Since we were not able to conclude that ERG protects *M. tuberculosis* from oxidative stress because of the protective effect of GGC in the $\Delta egtB$ -*mshA* mutant We have transformed the $\Delta egtA$ and $\Delta egtD$ mutants with the deletion construct of *mshA*, that will enable us to generate double mutants via homologous recombination. We will further investigate the anti-oxidative role of ERG in these mutants. Their susceptibility to current anti-tuberculosis drugs, oxidative stress, nitrosative stress and acidic stress will be investigated. Then, the survival of the most susceptible double mutant will be investigated ex-vivo (macrophage infection experiment) and in-vivo (mouse model of infection).

5.5 Future studies: Cytokine expression profile determination upon infection with ERG-deficient mutants

Since it is known that ERG modulates the immune response and that the CDC1551 and H37Rv modulate the immune response differently during infection, it will be interesting to compare the cytokine expression profile of those strains with and without ERG during

infection. In other words compare the cytokine expression profile of the ERG-deficient strain ($\Delta egtD$ in CDC1511 versus $\Delta egtD$ in H37Rv generated in this study) and of the wild type strains (CDC1551 versus H37Rv). It was worth noting that the protein EgtD is negatively regulated by phosphorylation with PknD which is a protein kinase. Since it is known that protein kinases are involved in the regulation of stress responses and pathogenicity, results from this experiment may indicate the role of ERG in the pathogenesis of tuberculosis [214].

5.6 Future studies: Investigation of ERG transporter

In this study, we have quantified ERG in potential mutants of ERG transporter; results obtained in this study did not allow us to deduce the ERG transporter. Therefore, more investigations are needed. The second attempt will be to use commercially available antibodies directed against eukaryote ERG transporter OCTN1 to identify ERG transporter in *M. tuberculosis*.

5.7 Future studies: Investigation of ERG import

We have shown that ERG is secreted, but we don't know if it is imported as was seen with MSH. This study will aim to supplement an ERG-deficient mutant culture with various concentrations of ERG and quantify IE and EE at various time points post supplementation. Ribonucleic acid (RNA) will be extracted at these time points and the expression profile of this strain will be determined by RNA-sequencing. If a potential ERG importer is identified, mutant deficient in this will be generated and using ^{14}C labelled ERG we will validate ERG importer by an uptake experiment.

5.8 Future studies: Investigation of the role of EgtE in cellular aggregation

We have observed in this study that the $\Delta egtE$ CDC1551 mutant do not form visual aggregates as opposed to other strains at stationary phase. To further investigate this observation, cells were spotted on solid culture to compare the granularity pattern of the mutant to the wild type. Secondly, the membrane structure the mutant is compared to the wild by electron microscopy. Thirdly, the biofilm formation pattern of the mutant is compared to the wild type. Fourthly, the mycolic acid content of the membrane of the mutant is compared to the wild type. Lastly, the mutant will be grown in the detergent taloxypol to investigate if the absence of aggregation is observed using a different detergent.

5.9 Future studies: Deletion of *egtA*, *egtC* and *egtD* in H37Rv and characterization of the mutants

In this study, we generated an ΔegB and $\Delta egtE$ mutant in H37Rv, to further investigate the role of each enzyme in ERG biosynthesis in H37Rv, *egtA*, *egtC* and *egtD* will be deleted individually and the resulting mutants will be characterized. Results obtained will validate what was obtained in CDC1551 or will enable us to determine the physiological differences between CDC1551 and H37Rv.

5.10 Future studies: Generation of $\Delta mshA$, $\Delta egtA$ -*mshA*, $\Delta egtB$ -*mshA*, $\Delta egtC$ -*mshA* and $\Delta egtD$ -*mshA* in H37Rv and characterization of the mutants

This study will also enable us to validate results obtained in case of CDC1551 in this study.

5.11 Future studies: Evaluation of total thiols content of ERG single and ERG/MSH double deficient mutants

It was previously stated that MSH is the major thiol when the cell lysate of MSH-deficient mutants were evaluated for total thiols using the Ellman's reagent by measuring spectrophotometrically at 412 nm [102]. However, it is more likely that ERG measurement was missed in that assay, since ERG due its unique structure, does not react positively to many thiol assays [184]. So it will be important to know the total thiol content of the extracellular medium and cell lysate of the ERG-deficient mutants as well as the ERG/MSH-deficient mutant. A suitable assay should be carefully designed.

5.12 Future studies: Measurement of the oxidative stress level of ERG single and ERG/MSH double deficient mutants by flow cytometry

It was shown that mycobacteria ROS level could be measured by flow cytometry when stained with dihydroethidium [235]. It will be interesting to investigate the ROS level in the most susceptible ERG/MSH-deficient mutant and in the ERG and MSH-deficient single mutants in order to shed more light on the role of ERG and MSH in *M. tuberculosis*.

5.13 Future studies: Investigation of the susceptibility of ERG and ERG/MSH deficient mutants to vitamin C

It was previously shown that vitamin C has a sterilizing effect and functions as a pro-oxidant or anti-oxidant depending on the culture medium. It was shown that when a MSH-deficient mutant was treated with 4mM vitamin C, its viability decreased dramatically over time [235]. So, it will be interesting to know the effect of vitamin C on the ERG-deficient mutants and the ERG/MSH double mutant. The MIC of the mutants to vitamin C will also be investigated.

Appendix: Additional information and references

ADDITIONAL INFORMATION

- RESTRICTION ENZYME DIGESTION, AGAROSE GEL ELECTROPHORESIS AND LIGATION

The PCR product was run on a 1% agarose gel. The gel was made as follows: 1-3 gram of SeaKem® LE Agarose (Whitehead Scientific) was added in ~100-300ml 1X TEA buffer (Buffer of Tris Base, acetic acid and EDTA at a pH of 8). This was boiled in a microwave, allowed to cool and poured in an electrophoresis tray. Then, an appropriate amount of fluorescent DNA stain (Novel juice, BiochomBiotec) was added to each sample or the more efficient GR green (Inqaba Biotec) was added directly into the gel (1ul per 100 ml of agarose gel) and the ladder (O gene ruler 1kb DNA, Inqaba Biotec). This was run at a voltage of 100-150 volts depending on the gel tray size in 1X TAE buffer. The gel was visualised in a dark room under UV irradiation or using the fluorescence detection light box. The band of interest was excised from the gel using a scalpel surgical blade. This gel piece was placed in a 1.5-2ml tube and a specific volume of DNA binding solution was added. The gel was allowed to dissolve at 55-60°C. The higher the volume of the DNA binding solution the quicker the gel would dissolve. The dissolved gel solution was transferred into a column and the column was washed twice with a wash solution and the DNA was finally eluted with a low salt solution or nuclease free water. This was done according to the manufacturer instructions on the kit I used (GeneJet Gel extraction kit (Therrmo Scienitifc) or Zymoclean Gel DNA recovery Kit (Zymoresearch)).

The concentration of DNA was estimated using a spectrophotometer (Thermo Scientific) by measuring the absorbance at 260nm and/or by visual comparison of the sample band intensity on the gel to the band intensity of a ladder of known concentration.

The extracted DNA fragment was then ligated to PgemTeasy. Ligation throughout this study was optimised to the following protocol:

Using the Rapid DNA ligation kit, a specific amount of Insert DNA and the vector (3:1 ratio) were added into a reaction containing 2.5-5% polyethylglycol (PEG), 1X ligation buffer and 1-2ul of ligase. This was left at room temperature or at 22°C for 10-45 mins depending on how big the insert and the vector are. Then the ligation reaction mix was purified using the gel recovery kit of Zymoresearch or Thermo Scientific. Five microliter of the ligation mixture

was used to transform 50µl of *Escherichia coli* electrical competent cells using a gene pulsar II (Biorad) with the following settings: Resistance of 200Ω, Voltage of 2.5V, capacitance 25µF or 100-300µl of chemical competent *E.coli* cells by heat shock. If *E.coli* chemical competent cells were used, purification of the ligation product was not necessary, half or the entire reaction was added into the competent cells and these were incubated on ice for 30 mins then heat shocked for 5 mins at 45 degrees and cool immediately for 1 mins on ice. After electroporation, the cells were quickly re-suspended in 1ml of LB- broth media (Sigma Aldrich) and incubated for an hour at 37°C and plated on LB-agar solid culture containing the specific selective antibiotic and incubated overnight. Electrical *E. coli* competent cells were obtained as follow: *E.coli* was grown to and OD₆₀₀ of 0.8, then it was washed several times with ice cold 10% glycerol to remove completely any salt that may interfere with electroporation. Then, it was re-suspended in 10% glycerol, snapped freeze in liquid nitrogen and stored at -80°C.

Chemical competent cells were obtained as follows:

Exponentially growing *E.coli* cultures were pelleted and re-suspended in 100mM MgCl₂ and incubated on ice for 20-30mins and then these were pelleted again and re-suspended in 100mM CaCl₂-15% glycerol snapped free in liquid nitrogen and store at -80°C.

Colony forming units were then picked from the plate that were incubated overnight and were used to inoculate cultures from which plasmids were extracted and screened by restriction enzyme digestion (RED). Expected bands are determined using the program known as GENTle. The desired fragments were excised from Pgem Teasy by RED, using the enzymes that correspond to the restriction sites (RS) introduced into the primers used to amplify the inserts. The excised fragments were ligated to a subsequent vector that was digested with the same enzyme to ensure compatibility during ligation.

Similar procedures were followed to design every construct in this study, and the final desired construct was used to transform the mycobacteria.

- **EXPERIMENTAL PROCEDURE TO OBTAIN DELETION MUTANTS**

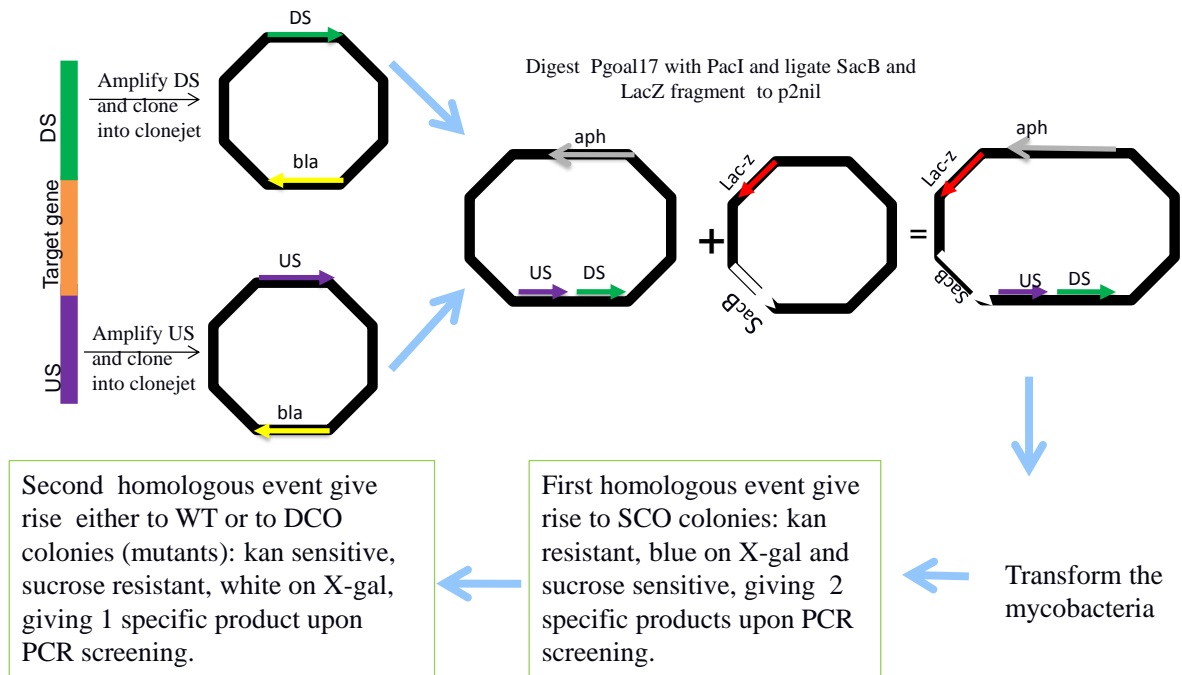
Once the deletion constructs were designed, they were used to delete the gene of interest as follows:

Mycobacteria were rendered competent and were transformed with 4-6µg of the purified construct. *M. smegmatis* was rendered competent as previously described with *E.coli*, while *M. tuberculosis* was rendered competent by washing the exponential culture in 10% glycerol containing 0.05% Tween 80. As opposed to *M. smegmatis* and *E.coli*, *M. tuberculosis* was rendered competent at 37°C not 4°C. Competent mycobacteria were electroporated directly

and were snap frozen as in the case of *E.coli*, neither were they stored. They were prepared fresh for every electroporation

Mycobacteria were electroporated using the following settings: Resistance of 1000 Ω , Voltage of 2.5V, capacitance 25 μ F. The electroporated cells were re-suspended in 7H9 and incubated overnight at 37°C. These were plated on 7H11 containing kanamycin at concentration 50 μ g/ml and X-gal (~0.08mg/ml) and incubated for 2 to 4 weeks protected from light.

Blue colonies (SCO) were picked, and a few were streaked on plates without antibiotics, and others were inoculated in liquid cultures containing kanamycin. These were incubated for 1 to 2 weeks. A loop full of cells was scrapped off the plate and re-suspended in 7H9 and clumping was disrupted by vortexing and/or triturating. Then this was serially diluted and plated on 7H11 plates containing 5% sucrose and X-gal. Three to four weeks later, white colonies were picked and suspended into 20 to 100 μ l (depending on the size of the colony) of sterile distilled water. Then 2-5 μ l of suspension was spotted on kanamycin plates and sucrose plates separately. The rest was boiled at 100 degree for 20 mins to 1 hour. The boiled culture was used as template for the screening PCR. Colonies were confirmed to be mutants when the PCR result indicated deletion and when the corresponding colony could not grow on kanamycin plates but grew on sucrose plates. SCO blue colonies that were inoculated in kanamycin media were either kept as back up stocks or were used to inoculate another liquid culture without kanamycin. This culture was allowed to grow for 1-2 weeks, and the culture was pelleted, re-suspended in a smaller volume and serially diluted and plated on sucrose plates to allow for DCO as well. The entire cloning process is described in the figure below.



FigureS 1 Gene deletion process

Kan: kanamycin, X-gal: 5-bromo-4-chloro-3-indolyl- β -D-galactopyranoside, aph: kanamycin resistance gene, *sacB*: code for levan sucrase, Lac-z: gene coding for the β -galactosidase which break down X-gal to yield a blue product; bla: ampicillin resistance gene; US: upstream, DS: downstream, WT: wild type, SCO: single cross over, DCO: double cross over

References

1. Kaufmann, S.H.E. (2003). A short history of Robert Koch's fight against tuberculosis: those who do not remember the past are condemned to repeat it. *Tuberculosis (Edinb)* 83, 86-90.
2. Garnier, T., Eiglmeier, K., Camus, J., Medina, N., Mansoor, H., Pryor, M., Duthoy, S., Grondin, S., Lacroix, C., Monsempe, C., Simon, S., Harris, B., Atkin, R., Doggett, J., Mayes, R., Keating, L., Wheeler, P.R., Parkhill, J., Barrell, B.G., Cole, S.T., Gordon, S.V. and Hewinson, R.G. (2003). The complete genome sequence of *Mycobacterium bovis*. *Proc. Natl. Acad. Sci. U.S.A.* 100, 7877-7882.
3. Porter, R.S., Kaplan, J.L. and Homeier, B.P. (2009-2010). The Merck Manual — Home Health Handbook. *Merck* , .
4. Aparicio, J.P., Capurro, A.F. and Castillo-Chavez, C. (2000). Transmission and dynamics of tuberculosis on generalized households. *J. Theor. Biol.* 206, 327-341.
5. Feng, Z., Castillo-Chavez, C. and Capurro, A.F. (2000). A model for tuberculosis with exogenous reinfection. *Theor Popul Biol* 57, 235-247.
6. Horna-Campos, O.J., Sánchez-Pérez, H.J., Sánchez, I., Bedoya, A. and Martín, M. (2007). Public transportation and pulmonary tuberculosis, Lima, Peru. *Emerging Infect. Dis.* 13, 1491-1493.
7. Pienaar, E., Fluitt, A.M., Whitney, S.E., Freifeld, A.G. and Viljoen, H.J. (2010). A model of tuberculosis transmission and intervention strategies in an urban residential area. *Computational Biology and Chemistry* 34, 86 - 96.
8. Parrish, N.M., Dick, J.D. and Bishai, W.R. (1998). Mechanisms of latency in *Mycobacterium tuberculosis*. *Trends Microbiol.* 6, 107-112.
9. van Rie, A., Warren, R., Richardson, M., Victor, T.C., Gie, R.P., Enarson, D.A., Beyers, N. and van Helden, P.D. (1999). Exogenous reinfection as a cause of recurrent tuberculosis after curative treatment. *N. Engl. J. Med.* 341, 1174-1179.
10. Sonnenberg, P., Murray, J., Glynn, J.R., Shearer, S., Kambashi, B. and Godfrey-Faussett, P. (2001). HIV-1 and recurrence, relapse, and reinfection of tuberculosis after cure: a cohort study in South African mineworkers. *Lancet* 358, 1687-1693.
11. CDC (2009). Plan to combat extensively drug-resistant tuberculosis: recommendations of the Federal Tuberculosis Task Force. *MMWR Recomm Rep* 58, 1-43.
12. World Health Organization (WHO), S.T.P. (2010/2011). Tuberculosis: Global Facts. *Media centre* , .

13. WHO Geneva, 2. (2014). Global tuberculosis report 2014. [www.who.int/tb/publications/global_report/\(http://www.who.int/tb/publications/global_report/en/\)](http://www.who.int/tb/publications/global_report/), .
14. WHO, S.T.P. (2012). " Annual meeting of childhood TB subgroup", 11th November 2012. <http://www.stoptb.org> , .
15. Velayati, A.A., Masjedi, M.R., Farnia, P., Tabarsi, P., Ghanavi, J., Ziazarifi, A.H. and Hoffner, S.E. (2009). Emergence of new forms of totally drug-resistant tuberculosis bacilli: super extensively drug-resistant tuberculosis or totally drug-resistant strains in Iran. *Chest* 136, 420-425.
16. Matee, M., Mtei, L., Lounasvaara, T., Wieland-Alter, W., Waddell, R., Lyimo, J., Bakari, M., Pallangyo, K. and von Reyn, C.F. (2008). Sputum microscopy for the diagnosis of HIV-associated pulmonary tuberculosis in Tanzania. *BMC Public Health* 8, 68.
17. Petrović, S. (2005). [Diagnostic value of certain methods for isolation of *Mycobacterium tuberculosis* in children with suspected pulmonary tuberculosis]. *Med. Pregl.* 58, 231-235.
18. Monkongdee, P., McCarthy, K.D., Cain, K.P., Tasaneeyapan, T., Nguyen, H.D., Nguyen, T.N.L., Nguyen, T.B.Y., Teeratakulpisarn, N., Udomsantisuk, N., Heilig, C. and Varma, J.K. (2009). Yield of acid-fast smear and mycobacterial culture for tuberculosis diagnosis in people with human immunodeficiency virus. *Am. J. Respir. Crit. Care Med.* 180, 903-908.
19. Chakravorty, S., Sen, M.K. and Tyagi, J.S. (2005). Diagnosis of extrapulmonary tuberculosis by smear, culture, and PCR using universal sample processing technology. *J. Clin. Microbiol.* 43, 4357-4362.
20. Rodrigues, C.S., Shenai, S.V., Almeida, D., Sadani, M.A., Goyal, N., Vadher, C. and Mehta, A.P. (2007). Use of bactec 460 TB system in the diagnosis of tuberculosis. *Indian J Med Microbiol* 25, 32-36.
21. Morcillo, N., Scipioni, S., Vignoles, M. and Trovero, A. (1998). [Rapid diagnosis and susceptibility of *Mycobacterium tuberculosis* to antibiotics using MGIT system]. *Rev. Argent. Microbiol.* 30, 155-162.
22. Vinton, P., Miharshahi, S., Johnson, P., Jenkin, G.A., Jolley, D. and Biggs, B. (2009). Comparison of QuantiFERON-TB Gold In-Tube Test and tuberculin skin test for identification of latent *Mycobacterium tuberculosis* infection in healthcare staff and association between positive test results and known risk factors for infection. *Infect Control Hosp Epidemiol* 30, 215-221.
23. Johnson, J.L., Nyole, S., Okwera, A., Whalen, C.C., Nsubuga, P., Pekovic, V., Huebner, R., Wallis, R.S., Mugenyi, P.N., Mugerwa, R.D. and Ellner, J.J. (1998). Instability of tuberculin and *Candida* skin test reactivity in HIV-infected Ugandans. The Uganda-Case

- Western Reserve University Research Collaboration. *Am. J. Respir. Crit. Care Med.* 158, 1790-1796.
24. Janis, E.M., Allen, D.W., Glesby, M.J., Carey, L.A., Mundy, L.M., Gopalan, R. and Chaisson, R.E. (1996). Tuberculin skin test reactivity, anergy, and HIV infection in hospitalized patients. Longcope Firm of the Osler Medical Housestaff. *Am. J. Med.* 100, 186-192.
 25. Golberg, B. (1957). Tuberculosis and other pulmonary diseases at an Indonesian chest clinic. *Tubercle* 38, 157 - 163.
 26. Bunsow, E., Ruiz-Serrano, M.J., López Roa, P., Kestler, M., Viedma, D.G. and Bouza, E. (2013). Evaluation of GeneXpert MTB/RIF for the detection of *Mycobacterium tuberculosis* and resistance to rifampin in clinical specimens. *Journal of Infection.* , .
 27. Nakiyingi, L., Nankabirwa, H. and Lamorde, M. (2013). Tuberculosis diagnosis in resource-limited settings: Clinical use of GeneXpert in the diagnosis of smear-negative PTB: a case report. *Afr Health Sci* 13, 522-524.
 28. Folgueira, L., Delgado, R., Palenque, E. and Noriega, A.R. (1993). Detection of *Mycobacterium tuberculosis* DNA in clinical samples by using a simple lysis method and polymerase chain reaction. *J. Clin. Microbiol.* 31, 1019-1021.
 29. Seyd, M.R., Gulraiz, A., Sikandar, H. and Farzana Mahdi (2009). Molecular diagnosis of tuberculosis: a new primer design. *Iranian journal of clinical infectious diseases* 2, 105-108.
 30. Janin, Y.L. (2007). Antituberculosis drugs: ten years of research. *Bioorg. Med. Chem.* 15, 2479-2513.
 31. Wayne, L.G. and Sramek, H.A. (1994). Metronidazole is bactericidal to dormant cells of *Mycobacterium tuberculosis*. *Antimicrob. Agents Chemother.* 38, 2054-2058.
 32. Chao, M.C. and Rubin, E.J. (2010). Letting sleeping dos lie: does dormancy play a role in tuberculosis?. *Annu. Rev. Microbiol.* 64, 293-311.
 33. Ma, Z., Lienhardt, C., McIlleron, H., Nunn, A.J. and Wang, X. (2010). Global tuberculosis drug development pipeline: the need and the reality. *Lancet* 375, 2100-2109.
 34. Raybon, J.J., Pray, D., Morgan, D.G., Zoekler, M., Zheng, M., Sinz, M. and Kim, S. (2011). Pharmacokinetic-pharmacodynamic modeling of rifampicin-mediated Cyp3AII induction in steroid and xenobiotic X receptor humanized mice. *J. Pharmacol. Exp. Ther.* 337, 75-82.
 35. Yenny, Nafrialdi, Djoerban, Z. and Setiabudy, R. (2011). Pharmacokinetic interaction between efavirenz and rifampicin in healthy volunteers. *Int J Clin Pharmacol Ther* 49, 162-168.

36. Dye, C., Bourdin Trunz, B., Lönnroth, K., Roglic, G. and Williams, B.G. (2011). Nutrition, diabetes and tuberculosis in the epidemiological transition. *PLoS ONE* 6, e21161.
37. Bacakoğlu, F., Başoğlu, O.K., Cok, G., Sayiner, A. and Ateş, M. (2001). Pulmonary tuberculosis in patients with diabetes mellitus. *Respiration* 68, 595-600.
38. Stevenson, C.R., Critchley, J.A., Forouhi, N.G., Roglic, G., Williams, B.G., Dye, C. and Unwin, N.C. (2007). Diabetes and the risk of tuberculosis: a neglected threat to public health?. *Chronic Illn* 3, 228-245.
39. Dooley, K.E. and Chaisson, R.E. (2009). Tuberculosis and diabetes mellitus: convergence of two epidemics. *Lancet Infect Dis* 9, 737-746.
40. Kurashima, A., Mori, T., Tomono, Y., Abe, S., Nagaoka, M. and Abe, M. (2010). [A new anti-mycobacterial agent, rifabutin]. *Kekkaku* 85, 743-756.
41. Hidaka, T. (1999). [Current status and perspectives on the development of rifamycin derivative antibiotics]. *Kekkaku* 74, 53-61.
42. Mayer, G. (2006). Innate (non-specific) immunity Immunology — Chapter One: Innate (non-specific) Immunity. *Immunology*,.
43. Dahlberg, M., Dahlgren, C., Hellstrand, K. and Movitz, C. (2008). A new chemiluminescence paradox: selective inhibition of isoluminol-amplified activity in phagocytes by peptides from annexin AI. *Luminescence* 23, 139-143.
44. Herrero, C., Hu, X., Li, W.P., Samuels, S., Sharif, M.N., Kotenko, S. and Ivashkiv, L.B. (2003). Reprogramming of IL-10 activity and signaling by IFN-gamma. *J. Immunol.* 171, 5034-5041.
45. Hoffbrand, A.V., Pettit, J.E. and Moss, P.A.H. (2005). Essential Haematology (4th ed.). London: Blackwell Science ISBN 0-632-05153-1, .
46. Delves, P.J., Martin, S.J., Burton, D.R. and Roitt, I.M. (2006). Roitt's Essential Immunology (11th ed.). Malden, MA: Blackwell Publishing ISBN 1-4051-3603-0, .
47. Meyer, K.C. (2004). Neutrophils, myeloperoxidase, and bronchiectasis in cystic fibrosis: green is not good. *J. Lab. Clin. Med.* 144, 124-126.
48. Klebanoff, S.J. and Rosen, H. (1978). The role of myeloperoxidase in the microbicidal activity of polymorphonuclear leukocytes. *Ciba Found. Symp.* , 263-284.
49. Michele, T.M., Ko, C. and Bishai, W.R. (1999). Exposure to antibiotics induces expression of the *Mycobacterium tuberculosis* sigF gene: implications for chemotherapy against mycobacterial persisters. *Antimicrob. Agents Chemother.* 43, 218-225.
50. Hu, Y.M., Butcher, P.D., Sole, K., Mitchison, D.A. and Coates, A.R. (1998). Protein synthesis is shutdown in dormant *Mycobacterium tuberculosis* and is reversed by oxygen or heat shock. *FEMS Microbiol. Lett.* 158, 139-145.

51. Via, L.E., Lin, P.L., Ray, S.M., Carrillo, J., Allen, S.S., Eum, S.Y., Taylor, K., Klein, E., Manjunatha, U., Gonzales, J., Lee, E.G., Park, S.K., Raleigh, J.A., Cho, S.N., McMurray, D.N., Flynn, J.L. and Barry, C.E.3. (2008). Tuberculous granulomas are hypoxic in guinea pigs, rabbits, and nonhuman primates. *Infect. Immun.* 76, 2333-2340.
52. Rao, S.P.S., Alonso, S., Rand, L., Dick, T. and Pethe, K. (2008). The protonmotive force is required for maintaining ATP homeostasis and viability of hypoxic, nonreplicating *Mycobacterium tuberculosis*. *Proc. Natl. Acad. Sci. U.S.A.* 105, 11945-11950.
53. Cooper, A.M., Segal, B.H., Frank, A.A., Holland, S.M. and Orme, I.M. (2000). Transient loss of resistance to pulmonary tuberculosis in p47(phox^{-/-}) mice. *Infect. Immun.* 68, 1231-1234.
54. MacMicking, J.D., North, R.J., LaCourse, R., Mudgett, J.S., Shah, S.K. and Nathan, C.F. (1997). Identification of nitric oxide synthase as a protective locus against tuberculosis. *Proc. Natl. Acad. Sci. U.S.A.* 94, 5243-5248.
55. Lee, P.P.W., Chan, K., Jiang, L., Chen, T., Li, C., Lee, T., Mak, P.H.S., Fok, S.F.S., Yang, X. and Lau, Y. (2008). Susceptibility to mycobacterial infections in children with X-linked chronic granulomatous disease: a review of 17 patients living in a region endemic for tuberculosis. *Pediatr. Infect. Dis. J.* 27, 224-230.
56. Poole, L.B. and Ellis, H.R. (1996). Flavin-dependent alkyl hydroperoxide reductase from *Salmonella typhimurium*. 1. Purification and enzymatic activities of overexpressed AhpF and AhpC proteins. *Biochemistry* 35, 56-64.
57. Bryk, R., Lima, C.D., Erdjument-Bromage, H., Tempst, P. and Nathan, C. (2002). Metabolic enzymes of mycobacteria linked to antioxidant defense by a thioredoxin-like protein. *Science* 295, 1073-1077.
58. Lee, S.P., Hwang, Y.S., Kim, Y.J., Kwon, K.S., Kim, H.J., Kim, K. and Chae, H.Z. (2001). Cyclophilin a binds to peroxiredoxins and activates its peroxidase activity. *J. Biol. Chem.* 276, 29826-29832.
59. Cole, S.T., Brosch, R., Parkhill, J., Garnier, T., Churcher, C., Harris, D., Gordon, S.V., Eiglmeier, K., Gas, S., Barry, C.E.3., Tekaia, F., Badcock, K., Basham, D., Brown, D., Chillingworth, T., Connor, R., Davies, R., Devlin, K., Feltwell, T., Gentles, S., Hamlin, N., Holroyd, S., Hornsby, T., Jagels, K., Krogh, A., McLean, J., Moule, S., Murphy, L., Oliver, K., Osborne, J., Quail, M.A., Rajandream, M.A., Rogers, J., Rutter, S., Seeger, K., Skelton, J., Squares, R., Squares, S., Sulston, J.E., Taylor, K., Whitehead, S. and Barrell, B.G. (1998). Deciphering the biology of *Mycobacterium tuberculosis* from the complete genome sequence. *Nature* 393, 537-544.
60. Mongkolsuk, S. and Helmann, J.D. (2002). Regulation of inducible peroxide stress responses. *Mol. Microbiol.* 45, 9-15.

61. Deretic, V., Philipp, W., Dhandayuthapani, S., Mudd, M.H., Curcic, R., Garbe, T., Heym, B., Via, L.E. and Cole, S.T. (1995). *Mycobacterium tuberculosis* is a natural mutant with an inactivated oxidative-stress regulatory gene: implications for sensitivity to isoniazid. *Mol. Microbiol.* 17, 889-900.
62. Mongkolsuk, S., Praituan, W., Loprasert, S., Fuangthong, M. and Chamnongpol, S. (1998). Identification and characterization of a new organic hydroperoxide resistance (ohr) gene with a novel pattern of oxidative stress regulation from *Xanthomonas campestris* pv. phaseoli. *J. Bacteriol.* 180, 2636-2643.
63. Gutierrez, C. and Devedjian, J.C. (1991). Osmotic induction of gene osmC expression in *Escherichia coli* K12. *J. Mol. Biol.* 220, 959-973.
64. Atichartpongkul, S., Loprasert, S., Vattanaviboon, P., Whangsuk, W., Helmann, J.D. and Mongkolsuk, S. (2001). Bacterial Ohr and OsmC paralogues define two protein families with distinct functions and patterns of expression. *Microbiology* 147, 1775-1782.
65. Lesniak, J., Barton, W.A. and Nikolov, D.B. (2002). Structural and functional characterization of the *Pseudomonas* hydroperoxide resistance protein Ohr. *EMBO J.* 21, 6649-6659.
66. Lesniak, J., Barton, W.A. and Nikolov, D.B. (2003). Structural and functional features of the *Escherichia coli* hydroperoxide resistance protein OsmC. *Protein Sci.* 12, 2838-2843.
67. Saikolappan, S., Das, K. and Dhandayuthapani, S. (2015). Inactivation of the organic hydroperoxide stress resistance regulator OhrR enhances resistance to oxidative stress and isoniazid in *Mycobacterium smegmatis*. *J. Bacteriol.* 197, 51-62.
68. Ochsner, U.A., Hassett, D.J. and Vasil, M.L. (2001). Genetic and physiological characterization of ohr, encoding a protein involved in organic hydroperoxide resistance in *Pseudomonas aeruginosa*. *J. Bacteriol.* 183, 773-778.
69. Rincé, A., Giard, J.C., Pichereau, V., Flahaut, S. and Auffray, Y. (2001). Identification and characterization of gsp65, an organic hydroperoxide resistance (ohr) gene encoding a general stress protein in *Enterococcus faecalis*. *J. Bacteriol.* 183, 1482-1488.
70. Shea, R.J. and Mulks, M.H. (2002). ohr, Encoding an organic hydroperoxide reductase, is an in vivo-induced gene in *Actinobacillus pleuropneumoniae*. *Infect. Immun.* 70, 794-802.
71. Dubbs, J.M. and Mongkolsuk, S. (2012). Peroxide-sensing transcriptional regulators in bacteria. *J. Bacteriol.* 194, 5495-5503.
72. Muttucumaru, D.G.N., Roberts, G., Hinds, J., Stabler, R.A. and Parish, T. (2004). Gene expression profile of *Mycobacterium tuberculosis* in a non-replicating state. *Tuberculosis (Edinb)* 84, 239-246.

73. Park, H., Guinn, K.M., Harrell, M.I., Liao, R., Voskuil, M.I., Tompa, M., Schoolnik, G.K. and Sherman, D.R. (2003). Rv3133c/dosR is a transcription factor that mediates the hypoxic response of *Mycobacterium tuberculosis*. *Mol. Microbiol.* 48, 833-843.
74. Schnappinger, D., Ehrt, S., Voskuil, M.I., Liu, Y., Mangan, J.A., Monahan, I.M., Dolganov, G., Efron, B., Butcher, P.D., Nathan, C. and Schoolnik, G.K. (2003). Transcriptional Adaptation of *Mycobacterium tuberculosis* within Macrophages: Insights into the Phagosomal Environment. *J. Exp. Med.* 198, 693-704.
75. Sherman, D.R., Voskuil, M., Schnappinger, D., Liao, R., Harrell, M.I. and Schoolnik, G.K. (2001). Regulation of the *Mycobacterium tuberculosis* hypoxic response gene encoding alpha -crystallin. *Proc. Natl. Acad. Sci. U.S.A.* 98, 7534-7539.
76. Voskuil, M.I., Visconti, K.C. and Schoolnik, G.K. (2004). *Mycobacterium tuberculosis* gene expression during adaptation to stationary phase and low-oxygen dormancy. *Tuberculosis (Edinb)* 84, 218-227.
77. Boon, C. and Dick, T. (2002). *Mycobacterium bovis* BCG response regulator essential for hypoxic dormancy. *J. Bacteriol.* 184, 6760-6767.
78. Hingley-Wilson, S.M., Lougheed, K.E.A., Ferguson, K., Leiva, S. and Williams, H.D. (2010). Individual *Mycobacterium tuberculosis* universal stress protein homologues are dispensable in vitro. *Tuberculosis (Edinb)* 90, 236-244.
79. Fahey, R.C., Brown, W.C., Adams, W.B. and Worsham, M.B. (1978). Occurrence of glutathione in bacteria. *J. Bacteriol.* 133, 1126-1129.
80. Newton, G.L., Arnold, K., Price, M.S., Sherrill, C., Delcardayre, S.B., Aharonowitz, Y., Cohen, G., Davies, J., Fahey, R.C. and Davis, C. (1996). Distribution of thiols in microorganisms: mycothiol is a major thiol in most actinomycetes. *J. Bacteriol.* 178, 1990-1995.
81. Wang, W. and Ballatori, N. (1998). Endogenous glutathione conjugates: occurrence and biological functions. *Pharmacol. Rev.* 50, 335-356.
82. Mwanakasale, V., Songolo, P. and Daka, V. (2013). Challenges in the control of Human African Trypanosomiasis in the Mpika district of Zambia. *BMC Res Notes* 6, 180.
83. Tovar, J., Cunningham, M.L., Smith, A.C., Croft, S.L. and Fairlamb, A.H. (1998). Down-regulation of *Leishmania donovani* trypanothione reductase by heterologous expression of a trans-dominant mutant homologue: effect on parasite intracellular survival. *Proc. Natl. Acad. Sci. U.S.A.* 95, 5311-5316.
84. Dumas, C., Ouellette, M., Tovar, J., Cunningham, M.L., Fairlamb, A.H., Tamar, S., Olivier, M. and Papadopolou, B. (1997). Disruption of the trypanothione reductase gene of *Leishmania* decreases its ability to survive oxidative stress in macrophages. *EMBO J.* 16, 2590-2598.

85. Krieger, S., Schwarz, W., Ariyanayagam, M.R., Fairlamb, A.H., Krauth-Siegel, R.L. and Clayton, C. (2000). Trypanosomes lacking trypanothione reductase are avirulent and show increased sensitivity to oxidative stress. *Mol. Microbiol.* 35, 542-552.
86. Newton, G.L., Koledin, T., Gorovitz, B., Rawat, M., Fahey, R.C. and Av-Gay, Y. (2003). The glycosyltransferase gene encoding the enzyme catalyzing the first step of mycothiol biosynthesis (mshA). *J. Bacteriol.* 185, 3476-3479.
87. Newton, G.L., Av-Gay, Y. and Fahey, R.C. (2000). N-Acetyl-1-D-myo-inosityl-2-amino-2-deoxy-alpha-D-glucopyranoside deacetylase (MshB) is a key enzyme in mycothiol biosynthesis. *J. Bacteriol.* 182, 6958-6963.
88. Sareen, D., Steffek, M., Newton, G.L. and Fahey, R.C. (2002). ATP-dependent L-cysteine:1D-myo-inosityl 2-amino-2-deoxy-alpha-D-glucopyranoside ligase, mycothiol biosynthesis enzyme MshC, is related to class I cysteinyl-tRNA synthetases. *Biochemistry* 41, 6885-6890.
89. Koledin, T., Newton, G.L. and Fahey, R.C. (2002). Identification of the mycothiol synthase gene (mshD) encoding the acetyltransferase producing mycothiol in actinomycetes. *Arch. Microbiol.* 178, 331-337.
90. Newton, G.L., Buchmeier, N. and Fahey, R.C. (2008). Biosynthesis and functions of mycothiol, the unique protective thiol of Actinobacteria. *Microbiol. Mol. Biol. Rev.* 72, 471-494.
91. Newton, G.L., Av-Gay, Y. and Fahey, R.C. (2000). A novel mycothiol-dependent detoxification pathway in mycobacteria involving mycothiol S-conjugate amidase. *Biochemistry* 39, 10739-10746.
92. Steffek, M., Newton, G.L., Av-Gay, Y. and Fahey, R.C. (2003). Characterization of *Mycobacterium tuberculosis* mycothiol S-conjugate amidase. *Biochemistry* 42, 12067-12076.
93. Zhao, Q., Wang, M., Xu, D., Zhang, Q. and Liu, W. (2015). Metabolic coupling of two small-molecule thiols programs the biosynthesis of lincomycin A. *Nature* 518, 115-119.
94. Van Laer, K., Buts, L., Foloppe, N., Vertommen, D., Van Belle, K., Wahni, K., Roos, G., Nilsson, L., Mateos, L.M., Rawat, M., van Nuland, N.A.J. and Messens, J. (2012). Mycoredoxin-1 is one of the missing links in the oxidative stress defence mechanism of Mycobacteria. *Mol. Microbiol.* 86, 787-804.
95. Villadangos, A.F., Van Belle, K., Wahni, K., Dufe, V.T., Freitas, S., Nur, H., De Galan, S., Gil, J.A., Collet, J., Mateos, L.M. and Messens, J. (2011). *Corynebacterium glutamicum* survives arsenic stress with arsenate reductases coupled to two distinct redox mechanisms. *Mol. Microbiol.* 82, 998-1014.
96. Newton, G.L., Leung, S.S., Wakabayashi, J.I., Rawat, M. and Fahey, R.C. (2011). The DinB superfamily includes novel mycothiol, bacillithiol, and glutathione S-transferases. *Biochemistry* 50, 10751-10760.

97. Loi, V.V., Rossius, M. and Antelmann, H. (2015). Redox regulation by reversible protein S-thiolation in bacteria. *Front Microbiol* 6, 187.
98. Chi, B.K., Roberts, A.A., Huyen, T.T.T., Bäsell, K., Becher, D., Albrecht, D., Hamilton, C.J. and Antelmann, H. (2013). S-bacillithiolation protects conserved and essential proteins against hypochlorite stress in firmicutes bacteria. *Antioxid. Redox Signal.* 18, 1273-1295.
99. Sao Emani, C., Williams, M.J., Wiid, I.J., Hiten, N.F., Viljoen, A.J., Pietersen, R.D., van Helden, P.D. and Baker, B. (2013). Ergothioneine is a secreted antioxidant in *Mycobacterium smegmatis*. *Antimicrob. Agents Chemother.* 57, 3202-3207.
100. Ta, P., Buchmeier, N., Newton, G.L., Rawat, M. and Fahey, R.C. (2011). Organic Hydroperoxide Resistance Protein and Ergothioneine Compensate for Loss of Mycothiol in *Mycobacterium smegmatis* Mutants. *J. Bacteriol.* 193, 1981-1990.
101. Sareen, D., Newton, G.L., Fahey, R.C. and Buchmeier, N.A. (2003). Mycothiol is essential for growth of *Mycobacterium tuberculosis* Erdman. *J. Bacteriol.* 185, 6736-6740.
102. Vilchèze, C., Av-Gay, Y., Attarian, R., Liu, Z., Hazbón, M.H., Colangeli, R., Chen, B., Liu, W., Alland, D., Sacchettini, J.C. and Jacobs, W.R.J. (2008). Mycothiol biosynthesis is essential for ethionamide susceptibility in *Mycobacterium tuberculosis*. *Mol. Microbiol.* 69, 1316-1329.
103. Newton, G.L., Ta, P. and Fahey, R.C. (2005). A mycothiol synthase mutant of *Mycobacterium smegmatis* produces novel thiols and has an altered thiol redox status. *J. Bacteriol.* 187, 7309-7316.
104. Buchmeier, N.A., Newton, G.L., Koledin, T. and Fahey, R.C. (2003). Association of mycothiol with protection of *Mycobacterium tuberculosis* from toxic oxidants and antibiotics. *Mol. Microbiol.* 47, 1723-1732.
105. Catherine, V., Yossef, A., S. Whitney, B., Michelle, H.L., John, R.W. and Richard, J. Glynne and William R. Jacobs, Jr (2011). Coresistance to Isoniazid and Ethionamide Maps to Mycothiol Biosynthetic Genes in *Mycobacterium bovis*. *Antimicrob. Agents Chemotherapy* vol. 55 no. 9 4422-4423, .
106. Miller, C.C., Rawat, M., Johnson, T. and Av-Gay, Y. (2007). Innate protection of *Mycobacterium smegmatis* against the antimicrobial activity of nitric oxide is provided by mycothiol. *Antimicrob. Agents Chemother.* 51, 3364-3366.
107. Rawat, M., Newton, G.L., Ko, M., Martinez, G.J., Fahey, R.C. and Av-Gay, Y. (2002). Mycothiol-deficient *Mycobacterium smegmatis* mutants are hypersensitive to alkylating agents, free radicals, and antibiotics. *Antimicrob. Agents Chemother.* 46, 3348-3355.

108. Rawat, M., Johnson, C., Cadiz, V. and Av-Gay, Y. (2007). Comparative analysis of mutants in the mycothiol biosynthesis pathway in *Mycobacterium smegmatis*. *Biochem. Biophys. Res. Commun.* 363, 71-76.
109. DeBarber, A.E., Mdluli, K., Bosman, M., Bekker, L.G. and Barry, C.E.3. (2000). Ethionamide activation and sensitivity in multidrug-resistant *Mycobacterium tuberculosis*. *Proc. Natl. Acad. Sci. U.S.A.* 97, 9677-9682.
110. Wengenack, N.L. and Rusnak, F. (2001). Evidence for isoniazid-dependent free radical generation catalyzed by *Mycobacterium tuberculosis* KatG and the isoniazid-resistant mutant KatG (S315T). *Biochemistry* 40, 8990-8996.
111. Vilchèze, C., Wang, F., Arai, M., Hazbón, M.H., Colangeli, R., Kremer, L., Weisbrod, T.R., Alland, D., Sacchettini, J.C. and Jacobs, W.R.J. (2006). Transfer of a point mutation in *Mycobacterium tuberculosis* inhA resolves the target of isoniazid. *Nat. Med.* 12, 1027-1029.
112. Zhang, Y., Dhandayuthapani, S. and Deretic, V. (1996). Molecular basis for the exquisite sensitivity of *Mycobacterium tuberculosis* to isoniazid. *Proc. Natl. Acad. Sci. U.S.A.* 93, 13212-13216.
113. Turner, E., Kleivit, R., Hopkins, P.B. and Shapiro, B.M. (1986). Ovothiol: a novel thiohistidine compound from sea urchin eggs that confers NAD(P)H-O₂ oxidoreductase activity on ovoperoxidase. *J. Biol. Chem.* 261, 13056-13063.
114. Turner, E., Kleivit, R., Hager, L.J. and Shapiro, B.M. (1987). Ovothiols, a family of redox-active mercaptohistidine compounds from marine invertebrate eggs. *Biochemistry* 26, 4028-4036.
115. Ariyanayagam, M.R. and Fairlamb, A.H. (2001). Ovothiol and trypanothione as antioxidants in trypanosomatids. *Mol. Biochem. Parasitol.* 115, 189-198.
116. Holler, T.P. and Hopkins, P.B. (1995). Ovothiols. *Meth. Enzymol.* 252, 115-123.
117. Tanret MC (1909). Sur une base nouvelle retirée du seigle ergote, l'ergothioneine. *Comptes rendus de l'Académie des Sciences* 149, 222-224.
118. Ey, J., Schömig, E. and Taubert, D. (2007). Dietary sources and antioxidant effects of ergothioneine. *J. Agric. Food Chem.* 55, 6466-6474.
119. Melville, D.B., Eich, S. and Luwig, M.L. (1957). The biosynthesis of ergothioneine. *J. Biol. Chem.* 224, 871-877.
120. Melville, D.B., Otken, C.C. and Kovalenko, V. (1955). On the origin of animal ergothioneine. *J. Biol. Chem.* 216, 325-331.

121. Kawano, H., Otani, M., Takeyama, K., Kawai, Y., Mayumi, T. and Hama, T. (1982). Studies on ergothioneine. VI. Distribution and fluctuations of ergothioneine in rats. *Chem. Pharm. Bull.* 30, 1760-1765.
122. Nikodemus, D., Lazic, D., Bach, M., Bauer, T., Pfeiffer, C., Wiltzer, L., Lain, E., Schömig, E. and Gründemann, D. (2011). Paramount levels of ergothioneine transporter SLC22A4 mRNA in boar seminal vesicles and cross-species analysis of ergothioneine and glutathione in seminal plasma. *J. Physiol. Pharmacol.* 62, 411-419.
123. Shires, T.K., Brummel, M.C., Pulido, J.S. and Stegink, L.D. (1997). Ergothioneine distribution in bovine and porcine ocular tissues. *Comp. Biochem. Physiol. C, Pharmacol. Toxicol. Endocrinol.* 117, 117-120.
124. Briggs, I. (1972). Ergothioneine in the central nervous system. *J. Neurochem.* 19, 27-35.
125. Crossland, J., Mitchell, J. and Woodruff, G.N. (1966). The presence of ergothioneine in the central nervous system and its probable identity with the cerebellar factor. *J. Physiol. (Lond.)* 182, 427-438.
126. Dong, K.K., Damaghi, N., Kibitel, J., Canning, M.T., Smiles, K.A. and Yarosh, D.B. (2007). A comparison of the relative antioxidant potency of L-ergothioneine and idebenone. *J. Cosmet Dermatol* 6, 183-188.
127. Lamhonwah, A. and Tein, I. (2006). Novel localization of OCTN1, an organic cation/carnitine transporter, to mammalian mitochondria. *Biochem. Biophys. Res. Commun.* 345, 1315-1325.
128. Gründemann, D., Harlfinger, S., Golz, S., Geerts, A., Lazar, A., Berkels, R., Jung, N., Rubbert, A. and Schömig, E. (2005). Discovery of the ergothioneine transporter. *Proc. Natl. Acad. Sci. U.S.A.* 102, 5256-5261.
129. Grigat, S., Harlfinger, S., Pal, S., Striebinger, R., Golz, S., Geerts, A., Lazar, A., Schömig, E. and Gründemann, D. (2007). Probing the substrate specificity of the ergothioneine transporter with methimazole, hercynine, and organic cations. *Biochem. Pharmacol.* 74, 309-316.
130. Hand, C.E., Taylor, N.J. and Honek, J.F. (2005). Ab initio studies of the properties of intracellular thiols ergothioneine and ovoidiol. *Bioorg. Med. Chem. Lett.* 15, 1357-1360.
131. Hand, C.E., Taylor, N.J. and Honek, J.F. (2005). Ab initio studies of the properties of intracellular thiols ergothioneine and ovoidiol. *Bioorg. Med. Chem. Lett.* 15, 1357-1360.
132. Hartman, P.E. (1990). Ergothioneine as antioxidant. *Meth. Enzymol.* 186, 310-318.
133. Hand, C.E. and Honek, J.F. (2005). Biological chemistry of naturally occurring thiols of microbial and marine origin. *J. Nat. Prod.* 68, 293-308.

134. Melville, D. (1959). "Ergothioneine," *Vitamins and Hormones*. 7, 155-204.
135. Zhu, B., Mao, L., Fan, R., Zhu, J., Zhang, Y., Wang, J., Kalyanaraman, B. and Frei, B. (2010). Ergothioneine Prevents Copper-Induced Oxidative Damage to DNA and Protein by Forming a Redox-Inactive Ergothioneine-Copper Complex. *Chem. Res. Toxicol.* , .
136. Song, T., Chen, C., Liao, J., Ou, H. and Tsai, M. (2010). Ergothioneine protects against neuronal injury induced by cisplatin both in vitro and in vivo. *Food Chem. Toxicol.* 48, 3492-3499.
137. Markova, N.G., Karaman-Jurukovska, N., Dong, K.K., Damaghi, N., Smiles, K.A. and Yarosh, D.B. (2009). Skin cells and tissue are capable of using L-ergothioneine as an integral component of their antioxidant defense system. *Free Radic. Biol. Med.* 46, 1168-1176.
138. Mann, T. and Leone, E. (1953). Studies on the metabolism of semen. VIII. Ergothioneine as a normal constituent of boar seminal plasma; purification and crystallization; site of formation and function. *Biochem. J.* 53, 140-148.
139. Haag, F.M. and Macleod, J. (1959). Relationship between nonprotein sulfhydryl concentration of seminal fluid and motility of spermatozoa in man. *J. Appl. Physiol.* 14, 27-30.
140. Shukla, Y., Kulshrestha, O.P. and Khuteta, K.P. (1981). Ergothioneine content in normal and senile human cataractous lenses. *Indian J. Med. Res.* 73, 472-473.
141. Rahman, I., Gilmour, P.S., Jimenez, L.A., Biswas, S.K., Antonicelli, F. and Aruoma, O.I. (2003). Ergothioneine inhibits oxidative stress- and TNF-alpha-induced NF-kappa B activation and interleukin-8 release in alveolar epithelial cells. *Biochem. Biophys. Res. Commun.* 302, 860-864.
142. Taubert, D., Lazar, A., Grimberg, G., Jung, N., Rubbert, A., Delank, K., Perniok, A., Erdmann, E. and Schömig, E. (2006). Association of rheumatoid arthritis with ergothioneine levels in red blood cells: a case control study. *J. Rheumatol.* 33, 2139-2145.
143. Taubert, D., Grimberg, G., Jung, N., Rubbert, A. and Schömig, E. (2005). Functional role of the 503F variant of the organic cation transporter OCTN1 in Crohn's disease. *Gut* 54, 1505-1506.
144. Hartman, Z. and Hartman, P.E. (1987). Interception of some direct-acting mutagens by ergothioneine. *Environ. Mol. Mutagen.* 10, 3-15.
145. Bello, M.H., Barrera-Perez, V., Morin, D. and Epstein, L. (2012). The *Neurospora crassa* mutant *NcΔEgt-1* identifies an ergothioneine biosynthetic gene and demonstrates that ergothioneine enhances conidial survival and protects against peroxide toxicity during conidial germination. *Fungal Genet. Biol.* 49, 160-172.

146. Fu, P. and MacMillan, J.B. (2015). Spithioneines A and B, Two New Bohemamine Derivatives Possessing Ergothioneine Moiety from a Marine-Derived *Streptomyces spinoverrucosus*. *Org. Lett.* 17, 3046-3049.
147. Askari, A. and Melville, D.B. (1962). The reaction sequence in ergothioneine biosynthesis: hercynine as an intermediate. *J. Biol. Chem.* 237, 1615-1618.
148. Seebeck, F.P. (2010). In vitro reconstitution of Mycobacterial ergothioneine biosynthesis. *J. Am. Chem. Soc.* 132, 6632-6633.
149. Song, H., Hu, W., Naowarajna, N., Her, A.S., Wang, S., Desai, R., Qin, L., Chen, X. and Liu, P. (2015). Mechanistic studies of a novel C-S lyase in ergothioneine biosynthesis: the involvement of a sulfenic acid intermediate. *Sci Rep* 5, 11870.
150. Cheah, I.K. and Halliwell, B. (2012). Ergothioneine; antioxidant potential, physiological function and role in disease. *Biochim. Biophys. Acta* 1822, 784-793.
151. Jones, G.W., Doyle, S. and Fitzpatrick, D.A. (2014). The evolutionary history of the genes involved in the biosynthesis of the antioxidant ergothioneine. *Gene* 549, 161-170.
152. Pfeiffer, C., Bauer, T., Surek, B., Schämig, E. and Grändemann, D. (2011). Cyanobacteria produce high levels of ergothioneine. *Food Chemistry* 129, 1766-1769.
153. Galagan, J.E., Sisk, P., Stolte, C., Weiner, B., Koehrsen, M., Wymore, F., Reddy, T., Zucker, J.D., Engels, R., Gellesch, M., Hubble, J., Jin, H., Larson, L., Mao, M., Nitzberg, M., White, J., Zachariah, Z.K., Sherlock, G., Ball, C.A. and Schoolnik, G.K. (2010). TB database 2010: Overview and update. *Tuberculosis* 90, 225-235.
154. Goncharenko, K.V., Vit, A., Blankenfeldt, W. and Seebeck, F.P. (2015). Structure of the Sulfoxide Synthase EgtB from the Ergothioneine Biosynthetic Pathway. *Angew. Chem. Int. Ed. Engl.* 54, 2821-2824.
155. Jeong, J., Cha, H.J., Ha, S., Rojviriyaya, C. and Kim, Y. (2014). Structural insights into the histidine trimethylation activity of EgtD from *Mycobacterium smegmatis*. *Biochem. Biophys. Res. Commun.* , .
156. Kato, Y., Kubo, Y., Iwata, D., Kato, S., Sudo, T., Sugiura, T., Kagaya, T., Wakayama, T., Hirayama, A., Sugimoto, M., Sugihara, K., Kaneko, S., Soga, T., Asano, M., Tomita, M., Matsui, T., Wada, M. and Tsuji, A. (2010). Gene knockout and metabolome analysis of carnitine/organic cation transporter OCTN1. *Pharm. Res.* 27, 832-840.
157. Genghof, D.S. and Van Damme, O. (1968). Biosynthesis of ergothioneine from endogenous hercynine in *Mycobacterium smegmatis*. *J. Bacteriol.* 95, 340-344.
158. Holsclaw, C.M., Muse, W.B.3., Carroll, K.S. and Leary, J.A. (2011). Mass Spectrometric Analysis of Mycothiol levels in Wild-Type and Mycothiol Disulfide Reductase Mutant *Mycobacterium smegmatis*. *Int J Mass Spectrom* 305, 151-156.

159. Nakajima, S., Satoh, Y., Yanashima, K., Matsui, T. and Dairi, T. (2015). Ergothioneine protects *Streptomyces coelicolor* A3 (2) from oxidative stresses. *J. Biosci. Bioeng.* ,
160. Volohonsky, G., Tuby, C.N.Y.H., Porat, N., Wellman-Rousseau, M., Visvikis, A., Leroy, P., Rashi, S., Steinberg, P. and Stark, A. (2002). A spectrophotometric assay of gamma-glutamylcysteine synthetase and glutathione synthetase in crude extracts from tissues and cultured mammalian cells. *Chem. Biol. Interact.* 140, 49-65.
161. Lehtinen, J., Nuutila, J. and Lilius, E. (2004). Green fluorescent protein-propidium iodide (GFP-PI) based assay for flow cytometric measurement of bacterial viability. *Cytometry A* 60, 165-172.
162. Tell, L.A., Foley, J., Needham, M.L. and Walker, R.L. (2003). Comparison of four rapid DNA extraction techniques for conventional polymerase chain reaction testing of three *Mycobacterium* spp. that affect birds. *Avian Dis.* 47, 1486-1490.
163. Kremer, L., Guérardel, Y., Gurcha, S.S., Locht, C. and Besra, G.S. (2002). Temperature-induced changes in the cell-wall components of *Mycobacterium thermoresistibile*. *Microbiology* 148, 3145-3154.
164. IqbalL, S., IqbalL, R., Mumtaz Khan, M., Hussain, I., Akhtar A And † And Iffat Shabbir (2003). Comparison of Two Conventional Techniques used for the diagnosis of tuberculosis cases. *International journal of agriculture and biology* 5, 545-547.
165. Gründemann, D. (2012). The ergothioneine transporter controls and indicates ergothioneine activity-a review. *Prev Med* 54 Suppl, S71-4.
166. Lampe, D.J., Akerley, B.J., Rubin, E.J., Mekalanos, J.J. and Robertson, H.M. (1999). Hyperactive transposase mutants of the Himar1 mariner transposon. *Proc. Natl. Acad. Sci. U.S.A.* 96, 11428-11433.
167. Bardarov, S., Kriakov, J., Carriere, C., Yu, S., Vaamonde, C., McAdam, R.A., Bloom, B.R., Hatfull, G.F. and Jacobs, W.R.J. (1997). Conditionally replicating mycobacteriophages: a system for transposon delivery to *Mycobacterium tuberculosis*. *Proc. Natl. Acad. Sci. U.S.A.* 94, 10961-10966.
168. Rubin, E.J., Akerley, B.J., Novik, V.N., Lampe, D.J., Husson, R.N. and Mekalanos, J.J. (1999). In vivo transposition of mariner-based elements in enteric bacteria and mycobacteria. *Proc. Natl. Acad. Sci. U.S.A.* 96, 1645-1650.
169. Atlagic, D., Kiliç, A.O. and Tao, L. (2006). Unmarked gene deletion mutagenesis of *gtfB* and *gtfC* in *Streptococcus mutans* using a targeted hit-and-run strategy with a thermosensitive plasmid. *Oral Microbiol. Immunol.* 21, 132-135.
170. Parish, T. and Stoker, N.G. (2000). Use of a flexible cassette method to generate a double unmarked *Mycobacterium tuberculosis tlyA plcABC* mutant by gene replacement. *Microbiology* 146 (Pt 8), 1969-1975.

171. Parish, T., Gordhan, B.G., McAdam, R.A., Duncan, K., Mizrahi, V. and Stoker, N.G. (1999). Production of mutants in amino acid biosynthesis genes of *Mycobacterium tuberculosis* by homologous recombination. *Microbiology* 145 (Pt 12), 3497-3503.
172. Pelicic, V., Reyrat, J.M. and Gicquel, B. (1996). Generation of unmarked directed mutations in mycobacteria, using sucrose counter-selectable suicide vectors. *Mol. Microbiol.* 20, 919-925.
173. Pelicic, V., Reyrat, J.M. and Gicquel, B. (1996). Positive selection of allelic exchange mutants in *Mycobacterium bovis* BCG. *FEMS Microbiol. Lett.* 144, 161-166.
174. Stover, C.K., de la Cruz, V.F., Fuerst, T.R., Burlein, J.E., Benson, L.A., Bennett, L.T., Bansal, G.P., Young, J.F., Lee, M.H. and Hatfull, G.F. (1991). New use of BCG for recombinant vaccines. *Nature* 351, 456-460.
175. Le Dantec, C., Winter, N., Gicquel, B., Vincent, V. and Picardeau, M. (2001). Genomic sequence and transcriptional analysis of a 23-kilobase mycobacterial linear plasmid: evidence for horizontal transfer and identification of plasmid maintenance systems. *J. Bacteriol.* 183, 2157-2164.
176. Lamichhane, G., Zignol, M., Blades, N.J., Geiman, D.E., Dougherty, A., Grosset, J., Broman, K.W. and Bishai, W.R. (2003). A postgenomic method for predicting essential genes at subsaturation levels of mutagenesis: application to *Mycobacterium tuberculosis*. *Proc. Natl. Acad. Sci. U.S.A.* 100, 7213-7218.
177. Andreu, N., Zelmer, A., Fletcher, T., Elkington, P.T., Ward, T.H., Ripoll, J., Parish, T., Bancroft, G.J., Schaible, U., Robertson, B.D. and Wiles, S. (2010). Optimisation of bioluminescent reporters for use with mycobacteria. *PLoS ONE* 5, e10777.
178. Warren, R.M., Sampson, S.L., Richardson, M., Van Der Spuy, G.D., Lombard, C.J., Victor, T.C. and van Helden, P.D. (2000). Mapping of IS6110 flanking regions in clinical isolates of *Mycobacterium tuberculosis* demonstrates genome plasticity. *Mol. Microbiol.* 37, 1405-1416.
179. Geiler-Samerotte, K.A., Dion, M.F., Budnik, B.A., Wang, S.M., Hartl, D.L. and Drummond, D.A. (2011). Misfolded proteins impose a dosage-dependent fitness cost and trigger a cytosolic unfolded protein response in yeast. *Proc. Natl. Acad. Sci. U.S.A.* 108, 680-685.
180. Muttucumaru, D.G.N. and Parish, T. (2004). The molecular biology of recombination in Mycobacteria: what do we know and how can we use it?. *Curr Issues Mol Biol* 6, 145-157.
181. Reyrat, J.M. and Kahn, D. (2001). *Mycobacterium smegmatis*: an absurd model for tuberculosis?. *Trends Microbiol.* 9, 472-474.
182. Stocks, S.M. (2004). Mechanism and use of the commercially available viability stain, BacLight. *Cytometry A* 61, 189-195.

183. Bzymek, K.P., Newton, G.L., Ta, P. and Fahey, R.C. (2007). Mycothiol import by *Mycobacterium smegmatis* and function as a resource for metabolic precursors and energy production. *J. Bacteriol.* 189, 6796-6805.
184. Heath, H. and Toennies, G. (1958). The preparation and properties of ergothioneine disulphide. *Biochem. J.* 68, 204-210.
185. Paul, B.D. and Snyder, S.H. (2010). The unusual amino acid L-ergothioneine is a physiologic cytoprotectant. *Cell Death Differ.* 17, 1134-1140.
186. Wolfe, L.M., Mahaffey, S.B., Kruh, N.A. and Dobos, K.M. (2010). Proteomic definition of the cell wall of *Mycobacterium tuberculosis*. *J. Proteome Res.* 9, 5816-5826.
187. Fahey, R.C. and Newton, G.L. (1987). Determination of low-molecular-weight thiols using monobromobimane fluorescent labeling and high-performance liquid chromatography. *Meth. Enzymol.* 143, 85-96.
188. Newton, G.L., Dorian, R. and Fahey, R.C. (1981). Analysis of biological thiols: derivatization with monobromobimane and separation by reverse-phase high-performance liquid chromatography. *Anal. Biochem.* 114, 383-387.
189. Kumar, A., Kumar, S. and Taneja, B. (2014). The structure of Rv2372c identifies an RsmE-like methyltransferase from *Mycobacterium tuberculosis*. *Acta Crystallogr. D Biol. Crystallogr.* 70, 821-832.
190. Wallace, R.J.J., Nash, D.R., Steele, L.C. and Steingrube, V. (1986). Susceptibility testing of slowly growing mycobacteria by a microdilution MIC method with 7H9 broth. *J. Clin. Microbiol.* 24, 976-981.
191. Tyagi, P., Dharmaraja, A.T., Bhaskar, A., Chakrapani, H. and Singh, A. (2015). *Mycobacterium tuberculosis* has diminished capacity to counteract redox stress induced by elevated levels of endogenous superoxide. *Free Radic. Biol. Med.* 84, 344-354.
192. Manca, C., Tsenova, L., Barry, C.E.3., Bergtold, A., Freeman, S., Haslett, P.A., Musser, J.M., Freedman, V.H. and Kaplan, G. (1999). *Mycobacterium tuberculosis* CDC1551 induces a more vigorous host response in vivo and in vitro, but is not more virulent than other clinical isolates. *J. Immunol.* 162, 6740-6746.
193. Camus, J., Pryor, M.J., Médigue, C. and Cole, S.T. (2002). Re-annotation of the genome sequence of *Mycobacterium tuberculosis* H37Rv. *Microbiology* 148, 2967-2973.
194. Sasseti, C.M., Boyd, D.H. and Rubin, E.J. (2003). Genes required for mycobacterial growth defined by high density mutagenesis. *Mol. Microbiol.* 48, 77-84.
195. Zhang, Y.J., Ioerger, T.R., Huttenhower, C., Long, J.E., Sasseti, C.M., Sacchettini, J.C. and Rubin, E.J. (2012). Global Assessment of Genomic Regions Required for Growth in *Mycobacterium tuberculosis*. *PLoS Pathog.* 8, e1002946.

196. Buchmeier, N. and Fahey, R.C. (2006). The *mshA* gene encoding the glycosyltransferase of mycothiol biosynthesis is essential in *Mycobacterium tuberculosis* Erdman. *FEMS Microbiol. Lett.* 264, 74-79.
197. Murry, J., Sasseti, C.M., Moreira, J., Lane, J. and Rubin, E.J. (2005). A new site-specific integration system for mycobacteria. *Tuberculosis (Edinb)* 85, 317-323.
198. Harth, G. and Horwitz, M.A. (1997). Expression and efficient export of enzymatically active *Mycobacterium tuberculosis* glutamine synthetase in *Mycobacterium smegmatis* and evidence that the information for export is contained within the protein. *J. Biol. Chem.* 272, 22728-22735.
199. Harth, G. and Horwitz, M.A. (1999). An inhibitor of exported *Mycobacterium tuberculosis* glutamine synthetase selectively blocks the growth of pathogenic mycobacteria in axenic culture and in human monocytes: extracellular proteins as potential novel drug targets. *J. Exp. Med.* 189, 1425-1436.
200. Harth, G., Maslesa-Galić, S., Tullius, M.V. and Horwitz, M.A. (2005). All four *Mycobacterium tuberculosis* *glnA* genes encode glutamine synthetase activities but only GlnA1 is abundantly expressed and essential for bacterial homeostasis. *Mol. Microbiol.* 58, 1157-1172.
201. Khonde, P.L. and Jardine, A. (2015). Improved synthesis of the super antioxidant, ergothioneine, and its biosynthetic pathway intermediates. *Org. Biomol. Chem.* 13, 1415-1419.
202. Rybniker, J., Pojer, F., Marienhagen, J., Kolly, G.S., Chen, J.M., van Gumpel, E., Hartmann, P. and Cole, S.T. (2014). The cysteine desulfurase IscS of *Mycobacterium tuberculosis* is involved in iron-sulfur cluster biogenesis and oxidative stress defence. *Biochem. J.* 459, 467-478.
203. Takahashi, Y. and Nakamura, M. (1999). Functional assignment of the ORF2-iscS-iscU-iscA-hscB-hscA-fdx-ORF3 gene cluster involved in the assembly of Fe-S clusters in *Escherichia coli*. *J Biochem* 126, 917-926.
204. Takahashi, Y. and Tokumoto, U. (2002). A third bacterial system for the assembly of iron-sulfur clusters with homologs in archaea and plastids. *J. Biol. Chem.* 277, 28380-28383.
205. Caceres, N., Vilaplana, C., Prats, C., Marzo, E., Llopis, I., Valls, J., Lopez, D. and Cardona, P. (2013). Evolution and role of corded cell aggregation in *Mycobacterium tuberculosis* cultures. *Tuberculosis (Edinb)* 93, 690-698.
206. Taoka, Y., Nagano, N., Okita, Y., Izumida, H., Sugimoto, S. and Hayashi, M. (2011). Effect of Tween 80 on the growth, lipid accumulation and fatty acid composition of *Thraustochytrium aureum* ATCC 34304. *J. Biosci. Bioeng.* 111, 420-424.

207. Masaki, S., Sugimori, G., Okamoto, A., Imose, J. and Hayashi, Y. (1991). Effect of Tween 80 on formation of the superficial L1 layer of the *Mycobacterium avium-Mycobacterium intracellulare* complex. *J. Clin. Microbiol.* 29, 1453-1456.
208. Sattler, T.H. and Youmans, G.P. (1948). The Effect of "Tween 80," Bovine Albumin, Glycerol, and Glucose on the Growth of *Mycobacterium tuberculosis* var. hominis (H37Rv). *J. Bacteriol.* 56, 235-243.
209. Zheng, L., White, R.H., Cash, V.L., Jack, R.F. and Dean, D.R. (1993). Cysteine desulfurase activity indicates a role for NIFS in metallocluster biosynthesis. *Proc. Natl. Acad. Sci. U.S.A.* 90, 2754-2758.
210. Ferreri, C., Chatgililoglu, C., Torreggiani, A., Salzano, A.M., Renzone, G. and Scaloni, A. (2008). The reductive desulfurization of Met and Cys residues in bovine RNase A is associated with trans lipids formation in a mimetic model of biological membranes. *J. Proteome Res.* 7, 2007-2015.
211. Christie, W.W. (1985). Rapid separation and quantification of lipid classes by high performance liquid chromatography and mass (light-scattering) detection. *J. Lipid Res.* 26, 507-512.
212. Smeulders, M.J., Keer, J., Speight, R.A. and Williams, H.D. (1999). Adaptation of *Mycobacterium smegmatis* to stationary phase. *J. Bacteriol.* 181, 270-283.
213. Gengenbacher, M. and Kaufmann, S.H.E. (2012). *Mycobacterium tuberculosis*: success through dormancy. *FEMS Microbiol. Rev.* 36, 514-532.
214. Richard-Greenblatt, M., Bach, H., Adamson, J., Pena-Diaz, S., Wu, L., Steyn, A.J.C. and Av-Gay, Y. (2015). Regulation of Ergothioneine Biosynthesis and its effect on *Mycobacterium tuberculosis* Growth and Infectivity. *J. Biol. Chem.* , .
215. Kari, C., Nagy, Z., Kovács, P. and Hernádi, F. (1971). Mechanism of the growth inhibitory effect of cysteine on *Escherichia coli*. *J. Gen. Microbiol.* 68, 349-356.
216. Zechmann, B., Tomasić, A., Horvat, L. and Fulgosi, H. (2010). Subcellular distribution of glutathione and cysteine in cyanobacteria. *Protoplasma* 246, 65-72.
217. Hanna, B.A., Ebrahimzadeh, A., Elliott, L.B., Morgan, M.A., Novak, S.M., Rusch-Gerdes, S., Acio, M., Dunbar, D.F., Holmes, T.M., Rexer, C.H., Savthyakumar, C. and Vannier, A.M. (1999). Multicenter evaluation of the BACTEC MGIT 960 system for recovery of mycobacteria. *J. Clin. Microbiol.* 37, 748-752.
218. Heifets, L., Linder, T., Sanchez, T., Spencer, D. and Brennan, J. (2000). Two liquid medium systems, mycobacteria growth indicator tube and MB redox tube, for *Mycobacterium tuberculosis* isolation from sputum specimens. *J. Clin. Microbiol.* 38, 1227-1230.

219. Crowle, A.J., Dahl, R., Ross, E. and May, M.H. (1991). Evidence that vesicles containing living, virulent *Mycobacterium tuberculosis* or *Mycobacterium avium* in cultured human macrophages are not acidic. *Infect. Immun.* 59, 1823-1831.
220. Vandal, O.H., Nathan, C.F. and Ehrt, S. (2009). Acid resistance in *Mycobacterium tuberculosis*. *J. Bacteriol.* 191, 4714-4721.
221. Quintana-Cabrera, R. and Bolaños, J.P. (2013). Glutathione and γ -glutamylcysteine in the antioxidant and survival functions of mitochondria. *Biochem. Soc. Trans.* 41, 106-110.
222. Quintana-Cabrera, R., Fernandez-Fernandez, S., Bobo-Jimenez, V., Escobar, J., Sastre, J., Almeida, A. and Bolaños, J.P. (2012). γ -Glutamylcysteine detoxifies reactive oxygen species by acting as glutathione peroxidase-1 cofactor. *Nat Commun* 3, 718.
223. Huseby, N., Asare, N., Wetting, S., Mikkelsen, I.M., Mortensen, B., Sveinbjørnsson, B. and Wellman, M. (2003). Nitric oxide exposure of CC531 rat colon carcinoma cells induces gamma-glutamyltransferase which may counteract glutathione depletion and cell death. *Free Radic. Res.* 37, 99-107.
224. Kumar, S., Ojha, V., Ganguly, N.K. and Kohli, K.K. (1990). Presence of gamma glutamyl transferase in *Mycobacterium smegmatis*. *Biochem. Int.* 20, 539-548.
225. Kumar, S., Ganguly, N.K. and Kohli, K.K. (1994). Effect of isoniazid on glutathione biosynthesis and degradation in *Mycobacterium smegmatis*. *Folia Microbiol. (Praha)* 39, 571-575.
226. Kumar, S., Ganguly, N.K. and Kohli, K.K. (1992). Inhibition of cellular glutathione biosynthesis by rifampicin in *Mycobacterium smegmatis*. *Biochem. Int.* 26, 469-476.
227. Atala, E., Velásquez, G., Vergara, C., Mardones, C., Reyes, J., Tapia, R.A., Quina, F., Mendes, M.A., Speisky, H., Lissi, E., Ureta-Zañartu, M.S., Aspée, A. and López-Alarcón, C. (2013). Mechanism of pyrogallol red oxidation induced by free radicals and reactive oxidant species. A kinetic and spectroelectrochemistry study. *J Phys Chem B* 117, 4870-4879.
228. Xu, X., Sutak, R. and Richardson, D.R. (2008). Iron chelation by clinically relevant anthracyclines: alteration in expression of iron-regulated genes and atypical changes in intracellular iron distribution and trafficking. *Mol. Pharmacol.* 73, 833-844.
229. Saletta, F., Suryo Rahmanto, Y., Noulsri, E. and Richardson, D.R. (2010). Iron chelator-mediated alterations in gene expression: identification of novel iron-regulated molecules that are molecular targets of hypoxia-inducible factor-1 alpha and p53. *Mol. Pharmacol.* 77, 443-458.
230. Akanmu, D., Cecchini, R., Aruoma, O.I. and Halliwell, B. (1991). The antioxidant action of ergothioneine. *Arch. Biochem. Biophys.* 288, 10-16.

231. Aruoma, O.I., Whiteman, M., England, T.G. and Halliwell, B. (1997). Antioxidant action of ergothioneine: assessment of its ability to scavenge peroxynitrite. *Biochem. Biophys. Res. Commun.* 231, 389-391.
232. Genghof, D.S., Inamine, E., Kovalenko, V. and Melville, D.B. (1956). Ergothioneine in microorganisms. *J. Biol. Chem.* 223, 9-17.
233. Mukherjee, A., Roy, G., Guimond, C. and Ouellette, M. (2009). The gamma-glutamylcysteine synthetase gene of *Leishmania* is essential and involved in response to oxidants. *Mol. Microbiol.* 74, 914-927.
234. Deb, C., Lee, C., Dubey, V.S., Daniel, J., Abomoelak, B., Sirakova, T.D., Pawar, S., Rogers, L. and Kolattukudy, P.E. (2009). A novel in vitro multiple-stress dormancy model for *Mycobacterium tuberculosis* generates a lipid-loaded, drug-tolerant, dormant pathogen. *PLoS ONE* 4, e6077.
235. Vilchèze, C., Hartman, T., Weinrick, B. and Jacobs, W.R.J. (2013). *Mycobacterium tuberculosis* is extraordinarily sensitive to killing by a vitamin C-induced Fenton reaction. *Nat Commun* 4, 1881.